ACRYLIC POLYAMPHOLYTE SOLUTIONS FOR PROTEIN SEPARATIONS

by

Costas S. Patrickios

M.S. in Chemical Engineering Practice
Massachusetts Institute of Technology, 1990

Diploma in Chemical Engineering
National Technical University of Athens, Greece, 1988

Submitted to the
Department of Chemical Engineering
in partial fulfillment of the requirements for the degree of

Doctor of Philosophy

at the

Massachusetts Institute of Technology

February, 1994

Signature of Author ______________________________
Department of Chemical Engineering
September 29, 1993

Certified by ______________________________
Professor T. Alan Hatton
Thesis Advisor

and ______________________________
Professor Peter T. Lansbury, Jr.
Thesis Advisor

Accepted by ______________________________
Professor Robert E. Cohen
Chairman, Departmental Committee on Graduate Students

ACRYLIC POLYAMPHOLYTE SOLUTIONS FOR PROTEIN SEPARATIONS

by

Costas S. Patrickios

Submitted to the Department of Chemical Engineering
on September 29, 1993, in partial fulfillment of the
requirements for the degree of
Doctor of Philosophy

Abstract

AB diblock, ABC triblock and random low-molecular-weight methacrylic polyampholytes were synthesized by Group Transfer Polymerization (GTP). The solution behavior of these novel copolymers was investigated by a variety of methods including static and dynamic light-scattering, Gel Permeation Chromatography (GPC) in tetrahydrofuran, aqueous GPC, anion-exchange chromatography, steady-state pyrene fluorescence, hydrogen-ion titration and turbidimetric titration. The triblock copolymers formed micelles at intermediate pH values as a result of the presence of the hydrophobic block. While the random copolymers did not precipitate at any pH, the triblocks precipitated strongly around the isoelectric pH. It was determined that, at pH 8.5, the anion-exchange affinity of the block polyampholytes was high and that of the random was low probably due to the statistical distribution of the negatively charged residues.

The utilization of aqueous solutions of the triblock polyampholytes for protein separation by coprecipitation and anion-exchange displacement chromatography was explored. Protein partitioning in two-phase aqueous polymer systems formed by a random polyampholyte and poly(vinyl alcohol) was also performed. In coprecipitation, it was observed turbidimetrically that the polyampholyte interacted with the protein of opposite charge without any influence from the protein of the same charge polarity that was also present in the mixture. In anion-exchange displacement chromatography, successful separation and concentration of two very similar proteins, β-lactoglobulins A and B, was achieved at the appropriate conditions. For the separation of ovalbumin and chymotrypsinogen by partitioning, a maximum selectivity of 10 was measured.

While homopolyelectrolytes can be used also for protein separation, polyampholytes offer the opportunity of polymer precipitation at the isoelectric point and recycling after the completion of the separation process. This constitutes an attractive process-scale advantage.

Thesis Supervisor: T. Alan Hatton
Title: Chevron Professor of Chemical Engineering
Director, School of Chemical Engineering Practice

Acknowledgments

I would like to express my gratitude and appreciation to my thesis advisor, Professor T. Alan Hatton, for his support and technical guidance during these years. I am particularly greatful to Alan for his generosity with my expenses in my many research trips including those to New York, Delaware and to the AIChE and ACS conferences. Also I am very obliged for his positive response and understanding during these thesis-typing/editing days. I thank my coadvisor Professor Peter T. Lansbury, Jr. from the Chemistry Department for his ever-availability and particularly for his advice in several Chemistry issues that came up in the beginning of my work.

Financial support from the Biotechnology Process Engineering Center (BPEC) at MIT is greatfully acknowledged.

I thank my thesis committee members Dr Walter R. Hertler from Du Pont, Professor Steven M. Cramer from RPI and Professors Daniel Blankschtein, Robert E. Cohen and Charles L. Cooney from Chemical Engineering at MIT for their interest in my work. I am particularly indebted to Wally Hertler for his valuable help in polymer synthesis as well as for his subsequent continuous involvement. I hope that my work will contribute in establishing the usefulness of Group Transfer Polymerization that Webster and Hertler invented and explored. I also thank Shawn Glattfelter and Martha Heyman from Wally's lab for their help in polymer synthesis. I am greatful to Steve Cramer for providing know-how, labspace and materials for studying the polyampholytes in their most important application, ion-exchange displacement chromatography of proteins. Steve's enthusiasm for research will always be remembered.

I express my gratitude to Nicholas L. Abbott for his guidance during my first year in our group as well as his continuous help and involvement until he left Boston three months ago. I consider myself very lucky that I enjoyed the privilege of a guru of Nick's caliber.

I want to thank Dr Robert P. Foss, formerly of Du Pont, for his help with the random polyampholytes as well as his guidance in setting up the apparatus for Group Transfer Polymerization at MIT.

Although not an engineer or chemist, equally important and helpful during all these years was Carol Phillips. I want to express my love and appreciation to her.

I want to thank all the colleagues from our group, old and new. From the ones that are gone I particularly want to thank Minos Leodidis. Minos was one of the main reasons that I joined the group. Thanks also go to Ganesh Venkataraman, Patricia Hurter and Brian Kelley. From the new ones I thank Pascalis Alexandridis for his help in different issues, the many discussions we have and the papers we exchange. I also want to thank Gerald Priolaeu and Ed Browne.

I would like to thank my students, Christine J. Jang and Justin A. Strittmatter. Part of this thesis is the result of their work. Also, I would like to thank Professor Sunil Nath from IIT for continuing the polyampholyte-protein interaction studies and obtaining some interesting and useful results.

Many thanks go to the many friends in the Department. Particularly to Abdul Barakat for our long conversations and friendship. Also thanks go to Stathis

Avgoustiniatos, Peter Kofinas, Alex Koulouris, Cliff Rutt, Gautam Nayar, Leo Lue, Brian Laffey and Mike Pomianek. Thanks also go to all the Greek friends: Babis Papadopoulos, Jorge Papadimitriou, Costas Boussios and Thanassis Tjavaras.

Thanks also go to the RPI group. Particularly to Shishir Gadam for our collaboration. Also to Amitava Kundu and Suresh Vunnum for their friendship and advice. Also I thank Joseph Gerstner for his valuable suggestions in my work there. I would like to thank my roommates in Troy, Guhan Jayaraman and Harish Iyer for their friendship and hospitality and also for our scientific discussions.

I want to thank my family in Cyprus for their support and encouragement during all the years of my graduate and undergraduate studies.

I would like to thank my companion Edna Yamasaki whose love and invaluable support helped me through my thesis and I wish her to finish her PhD soon.

TABLE OF CONTENTS

LIST OF FIGURES

LIST OF TABLES

SCHEMES

Chapter 1.

Introduction.

A plethora of new materials have been developed over the past twenty-five years, leading to significant advances in many areas, including the aerospace industry, optoelectronics and, with biocompatibility an important issue, the biomedical field. The recent advances in biotechnology permitting the production of therapeutic and diagnostic proteins on a commercial scale, and to increased demand for industrial biocatalysts, have highlighted the need for more selective protein separation and purification procedures. In this area, too, new materials development can play an important role, as solid support materials for chromatographic operations, for instance, or as solution modifiers to effect the separation of proteins selectively. It is this latter problem that is the subject of this thesis: a new family of synthetic ampholytic polymers has been synthesized and shown to have potential applications in protein separation processes such as ion-exchange displacement chromatography and coprecipitation. The results of this work are reported here.

In the sections that follow, a brief summary of the most important novel polymeric materials is given, the revolution in packing materials of High Performance Liquid Chromatography (HPLC) for biomolecule separation is discussed and the utilization of ampholytes in novel protein separations summarized. Finally, our polymers and the techniques by which they were synthesized are described, followed by a brief discussion of the contents of subsequent chapters in the thesis.

1.1 New Polymers

Novel polymeric materials with important applications include liquid crystalline polymers, thermoplastic elastomers, thermally stable polymers, flame resistant polymers, chemically resistant polymers, degradable polymers, electrically conducting polymers, photoconducting polymers [1] and non-linear optical polymers [2,3]. Kevlar (du Pont trade name of an aromatic polyamide), for example, is a liquid crystalline polymer which exhibits exceptional mechanical properties. Compared to steel, this novel polymer has much higher tensile strength and much lower density. It is used in tire cord as well as in lightweight bullet-proof vests. Thermoplastic elastomers are ABA triblock copolymers based on monomers with substantially different structure, such as butadiene and styrene, and are physically cross-linked through the aggregation of the A (polystyrene) blocks. Although they exhibit elastic behavior due to the physical cross-linking, they still maintain the flow properties of thermoplastics. Thermally stable polymers are polymers with ladder or semiladder structure such as poly(*p*-phenylene). These materials maintain their properties up to temperatures as high as 600°C and are used in aerospace applications. Flame resistant materials include inflammable polymers such as poly(vinyl chloride) and self-extinguising polymers such as polyurethanes and polycarbonates. Fluoropolymers are chemically resistant polymers that are used as gaskets, sealants and valves and may also be used in artificial organs and other prosthetic devices. Degradable polymers include polyketoesters and polyketoamines which were originally developed as a result of the increased ecological awareness and later found application in positive resist technology for the manufacture of integrated circuits and also in controlled release in agriculture and medicine. Electrically conducting polymers include polyacetylene and poly(sulfur nitride) which, in the presence of dopants, become highly conducting. These materials are important in the development of light-weight batteries. Photoconducting polymers are materials such as poly(N-vinyl-carbazole), that conduct electricity to a small degree under the influence of light and are used in the photocopying industry [1]. Non-linear optical materials are π-electron polymers, such as poly(diacetylene) and polypyrrole, that are under intense investigation for the development of photonics (the optical analogue of electronics) which will make possible optical computing, optical radar and high-speed communication [2,3].

1.2 Materials for HPLC of Biomolecules

HPLC of biomolecules was introduced 17 years ago by Regnier and coworkers who used surface-modified spherical silica to separate proteins and nucleic acids [4,5]. Since then, HPLC has found wide acceptance in the analysis and preparative purification of proteins. During the past five years, Regnier and colleages have developed a new type of chromatographic packing material, the perfusive material, the novelty of which lies in the presence of a bimodal distribution of pores [6]. The first family of pores is that of the diffusive pores (1000 Å) which contribute most of the surface area and they are the same as those found in the conventional HPLC packing material. The second family of pores is that of the convective pores (5000 Å) which reduce significantly intraparticle solute transport and, consequently, band spreading [6]. The new packing material can achieve separations one order of magnitude faster than conventional HPLC materials. Most recently, Regnier and coworkers are developing a new type of packing material which is chemically derivatized such that it specifically recognizes and retains the protein of interest.

1.3 New Protein Separation Techniques Mediated by Ampholytes

Figure 1.1 illustrates three methods for protein separation that utilize synthetic ampholytes: (a) isoelectric focusing, (b) chromatofocusing and (c) ampholyte displacement chromatography. The "carrier ampholytes" utilized in these techniques are essentially mixtures of ampholytes covering a spectrum of compositions and isoelectric points [7]. They are random oligomers of amines, aminoacids and dipeptides with a molecular weight of approximately 500 (ten times smaller than the ones developed in this thesis). These species have high buffering capacity and conductivity at the isoelectric point [7].

In isoelectric focusing (Figure 1.1(a)), an electric field is applied accross the gel which causes the migration of the ampholytes to locations in the gel that are determined by their isoelectric points. Thus, a pH gradient is created, which, unlike that in electrophoresis, is time independent. The protein sample is applied and each protein species migrates to the region where the pH is equal to its isoelectric point.

A very recent development in isoelectric focusing involves a gel that contains copolymerized ampholytes of composition that varies along the direction of the applied electric field [8]. In this way the ampholytes that create the pH gradient are already in the right position. The materials for the synthesis of such gels are commercially available by Pharmacia and are called Immobilines.

In chromatofocusing (Figure 1.1(b)), a weak anion-exchange column is used. First, the column is equilibrated at high pH, and subsequently eluted with a low pH ampholyte solution. A transient and almost linear pH gradient is created as a result of the buffering capacity of the column and of the ampholytes. The proteins are eluted close to the pH that corresponds to their isoelectric point.

While in isoelectric focusing and chromatofocusing they are utilized for the establishment of a pH gradient, in ampholyte displacement chromatography (Figure 1.1(c)) the carrier ampholytes are used to elute the protein sample which is adsorbed on an ion-exchange column [7]. This is essentially what it is done in Chapter 7 of this thesis. However, the column affinity of the carrier ampholytes (designed specifically for isoelectric focusing and chromatofocusing) is low. This leads to the requirement of a high (60g/l) ampholyte concentration for elution. Moreover, the obtained protein bands are diffuse and do not form a displacement train [9]. As illustrated in this thesis, many of these limitations can be overcome by using block polymeric ampholytes, rather than the traditional low-molecular-weight random ampholytes.

1.4 Our Materials

A limiting factor in the development of new materials is the existence of the appropriate chemistry. For example, thermoplastic elastomers were developed only several years after the advent of anionic polymerization [10]. With the invention of Group Transfer Polymerization (GTP) in 1983 [11] new synthetic horizons opened by offering the ability to polymerize methacrylates and acrylates in a controlled fashion.

There is a large number of methacrylate monomers that are commercially available; many of these are listed in Table 1.1, and most might be polymerized by GTP to give homopolymers, random and block copolymers of well-defined size. Table 1.2 lists multifunctional methacrylates which can be used for the synthesis of star polymers and gels. Another attractive feature of GTP is that, unlike anionic polymerization that requires very low temperatures (-78°C), it takes place at room temperature.

There are several limitations of GTP. The strictest is that proton donating monomers, such as alcohols and acids, can not be used for polymerization, as is also true for anionic polymerization. Another limitation arises from the contamination of GTP monomers by proton donating impurities. This can be resolved sometimes by simple purification techniques, such as distillation or treatment with agents like calcium hydride. However, when the proton donating impurities are very inert (e.g. higher aliphatic alcohols) more reactive purifying agents must be used. Trialkyl aluminum is an example whose high reactivity may result in free radical polymerization of the monomer. Therefore, treatment with trialkyl aluminum must be carried out at low temperature and in the absence of oxygen. Another limitation for GTP is the sluggishness observed in the polymerization of some monomers with bulky groups that cause steric hindrances. Such an example is *t*-butyl methacrylate, which needs to be polymerized at low temperatures (below -20°C).

We wished to prepare polymers for utilization in existing bioseparation processes. To be able to interact electrostatically with the charged biomolecules or the charged matrix, these materials should be polyelectrolytes. They should also be polyampholytes so that they can be precipitated and recycled. To maximize the extent of electrostatic interactions, the charged components of the polyampholytes should be segregated. Therefore, we had to synthesize block polyampholytes and for the synthesis we elected to use GTP. Because of the versatility of GTP we included a third block made of methyl methacrylate to enhance the hydrophobic interactions and make precipitation more extensive. This resulted also in micellization of the block polyampholytes. Another opportunity that GTP offered was the ability to synthesize random polyampholytes of the same size and composition as the block polyampholytes and compare their performance.

In the following Chapter, the synthesis and solution properties of the polyampholytes are presented. Chapters 3 and 4 describe the polymer characterization in size exclusion and anion-exchange columns, respectively. In Chapters 5 and 6 the interaction of the polyampholytes with proteins is studied and the potential of this interaction for protein separation is discussed. In Chapter 7 the block polyampholytes are used to separate proteins by anion-exchange displacement chromatography. In Chapter 8 the utilization of random polyampholytes for protein partitioning in two-phase aqueous polymer systems is explored. In Chapter 9 the formation of two-phase aqueous polymer systems by block polyampholytes is studied. In Chapter 10 the findings of this work are summarized and recommendations for future work are given.

1.5 Literature Cited

(1) Stevens, M. P. *Polymer chemistry: An Introduction*; Oxford Univ. Press: New York, 1990, 2nd Ed.; p 95-137.

(2) Dalton, L. R.; Sapochak, L. S.; Yu, L. P. Recent Advances in Nonlinear Spectroscopy and Nonlinear Optical Materials. *J. Phys. Chem.* **1993,** *97,* 2871-2883.

(3) Dalton, L. R. Fresh Start for Photonics. *Nature* **1992,** *359,* 269-270.

(4) Hashimoto, T. Macroporous Synthetic Hydrophilic Resin-Based Packings for the Separation of Biopolymers. *J. Chromatogr.* **1991,** *544,* 249-255.

(5) Regnier, F. E. High-Performance Liquid Chromatography of Biopolymers. *Science* **1983,** *222,* 245-252.

(6) Regnier, F. E. Perfusion Chromatography. *Nature* **1991,** *350,* 634-635.

(7) Righetti, P. G. *Isoelectric Focusing: Theory, Methodology and Applications*; Elsevier: Amsterdam, 1983, p 1-50, 141-146.

(8) Righetti, P. G. *Immobilized pH Gradients: Theory and Methodology*; Elsevier: Amsterdam, 1990.

(9) Young, J. L.; Webb, B. A. Two Methods for the Separation of Human α-Fetoprotein and Albumin. *Anal. Biochem.* **1978,** *88,* 619-623.

(10) McGrath, J. E. An Introductory Overview of Block Copolymers. *Block Copolymers: Science and Technology*; Meier, D. J., Ed.; MMI Symposium Series, Harwood: New York, 1983; Vol. 3, p 1-16.

(11) Maugh, T. H. New Way to Catalyze Polymerization. *Science* **1983,** *222,* 39.

Table 1.1 Group Transfer Polymerizable monomethacrylates.

N-ALKYL	ISO-ALKYL	UNSATURATED	ETHER	AMINO	FLUOROSUBSTITUTED	OTHERS
methyl	iso-propyl	vinyl	2-methoxyethyl	dimethylaminoethyl	2-fluoroethyl	trimethylsilyl
ethyl	iso-butyl	allyl	2-ethoxyethyl	diethylaminoethyl	2,2,2-trifluoroethyl	trimethylsilylmethyl
n-propyl	sec-butyl	crotyl	3-methoxybutyl	t-butylaminoethyl	1H,1H,3H-tetrafluoropropyl	2-trimethylsiloxyethyl
n-butyl	t-butyl	propargyl	2-n-butoxyethyl	2-(1-aziridinyl)ethyl	hexafluoroiso-propyl	3-(trimethoxysilyl)propyl
n-amyl	iso-amyl	phenyl	2-(2-methoxyethoxy)ethyl	2-N-morpholinoethyl	1H,1H,3H-hexafluorobutyl	ethylthioethyl
n-hexyl	t-amyl	benzyl	2-(2-ethoxyethoxy)ethyl	2-(N-carbazolyl)ethyl	1H,1H,4H-hexafluorobutyl	2,3-epithiopropyl
n-heptyl	neo-pentyl	2-phenylethyl	ethoxytriethylene glycol	2-(9-carbazoyl)ethyl	1H,1H-heptafluorobutyl	tributyltin
n-octyl	2-ethylbutyl	3-phenylpropyl	methoxypolyethylene glycol 200		1H,1H,5H- octafluoropentyl	2-ferrocenyl
n-nonyl	2-ethylhexyl	p-nonylphenyl	methoxypolyethylene glycol 400		pentafluorophenyl	
n-decyl	cyclopentyl	2-naphthyl	methoxypolyethylene glycol 1000		1H,1H,7H-dodecafluoro-1-heptyl	
n-undecyl	cyclohexyl	dicyclopentenyl	2,3-epoxypropyl		1H,1H-pentadecafluorooctyl	
n-lauryl	3,3,5-trimethyl-cyclohexyl	cinnamyl	2-phenoxyethyl		2-(N-ethylperfluorooctane sulfonamido)ethyl	
n-tridecyl	4-t-butyl-cyclohexyl	9-anthrylmethyl	2-benzyloxyethyl		1H,1H,9H-hexadecafluorononyl	
n-tetradecyl	isobornyl		dicyclopentenyloxyethyl		1H,1H,2H,2H-heptadecafluorodecyl	
1-hexadecyl	1-adamantyl		furfuryl			
n-octadecyl	3,5-dimethyl-1-adamantyl		tetrahydrofurfuryl			
behenyl			tetrahydropyranyl			

Table 1.2 Group Transfer Polymerizable multimethacrylates.

DIMETHACRYLATES		TRIMETHACRYLATES	TETRAMETHACRYLATES
ethylene glycol	bisphenol A	glyceryl	pentaerythritol
1,4-butanediol	diethylene glycol	1,1,1-trimethylolethane	zirconium
1,5-pentanediol	dipropylene glycol	1,1,1-trimethylolpropane	
1,6-hexanediol	triethylene glycol		
1,10-decanediol	polyethylene glycol 200		
1,12-dodecanediol	polyethylene glycol 400		
1,2-propanediol	polyethylene glycol 600		
1,3-propanediol	polyethylene glycol 1000		
neopentyl glycol	ethoxylated bisphenol A		
1,4-cyclohexanediol			
hydrogenated bisphenol A			

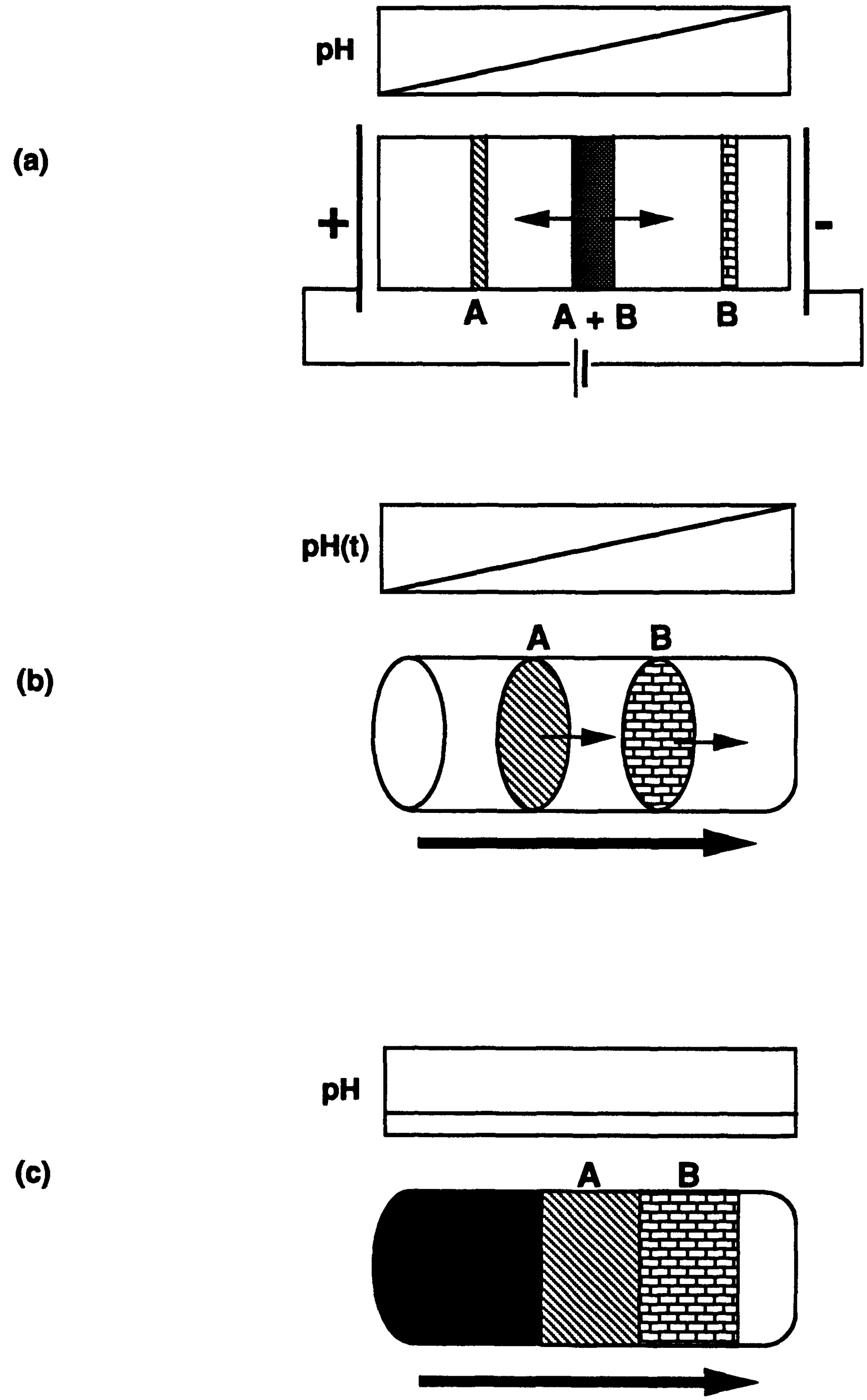

Figure 1.1 Protein separations mediated by ampholyte solutions: (a) isoelectric focusing, (b) chromatofocusing and (c) ampholyte displacement chromatography.

Chapter 2.

Synthesis and Solution Behavior of Random and Block Methacrylic Polyampholytes.

In this chapter we describe the Group Transfer Polymerization (GTP) synthesis of the polymers that are the subject of investigation in this thesis. Various solution characterization techniques are also presented, including determination of isoelectric points, titration, solubility, light-scattering and fluorescence. The motivation for the development of the block polyampholytes was the hypothesis that they would perform better in the various protein separation processes than their random counterparts which we first encountered in protein partitioning experiments (Chapter 8). Besides their potential importance for protein separation applications, these polymers are the first ABC triblock polyampholytes to be synthesized by GTP and they are among the very few ABC triblock copolymers to be studied in solution. A very interesting property that the triblock polyampholytes possess is their rich phase-behavior with respect to pH. At intermediate values of pH they form micelles, around the isoelectric pH they precipitate and at extreme values of pH they exist as single chains. The ability that is given to vary polymer solubility as well as micellar stability by pH manipulations may have significant impact for future applications of these polyampholytes, not limited to protein separation processes.

2.1 Introduction

Random and block copolymers can exhibit contrasting behaviors both in the bulk and in solution. For example, in the bulk, the modulus of a random copolymer undergoes a sharp decrease at a single temperature defined by the copolymer composition. In contrast, the modulus of the corresponding block copolymer undergoes one decrease at the glass transition temperature of each component block and, between the decreases, it assumes a plateau value, defined by the copolymer composition [1]. In solution, the fluorescence quenching of a block copolymer of 9-vinylphenanthrene and methacrylic acid in water, a selective solvent, is more efficient than that of the corresponding random copolymer because of the larger size of the hydrophobic phenanthrene microdomain, which results in more efficient binding of the quencher and longer range energy migration [2]. At interfaces, Monte Carlo simulations show that random copolymers orient along the interface, while diblocks tend to assume a configuration perpendicular to the interface [3,4]. These are only some of the many examples of different behavior between random and block copolymers.

We are interested in polyampholyte-mediated protein separation methods such as ion-exchange displacement chromatography [5-7], precipitation [8,9] and aqueous two-phase partitioning [10]. Recently, we partitioned proteins between the phases of a two-phase aqueous polymer system comprising a random acrylic polyampholyte and poly(vinyl alcohol) [11]. Utilization of block instead of random polyampholytes in these applications may have a dramatic effect on the performance of these separation processes, as the properties of the block copolymers are expected to be different from those of the random. For instance, in displacement chromatography, we expect to have enhanced performance because the block architecture will strengthen the separation driving force which is the electrostatic interaction between the polyampholyte and the chromatography column. The localization of the similar charges within a block will generate an electric field which will be stronger than that for the random copolymer. Another implication of the strengthening of the electrostatic interactions by block copolymer architecture is that, at the isoelectric point of the polymer, the interpolyampholyte attractions will be stronger leading to a more extensive precipitation. The ability to precipitate the polymer is very crucial in industrial applications because it will facilitate recycling. Random acrylic polyampholytes do precipitate when they are of relatively high molecular weight, typically above 15,000 Da, but they do not when they are of much lower molecular weight [12].

Reports on the synthesis and characterization of block polyampholytes are very few and not systematic. On the other hand, there are more than 200 reports for random polyampholytes [13], which were chemically synthesized for the first time in the 1950's [14-20]. The dual charge nature of these polymers and their resulting isoelectric points make them attractive non-biological models for proteins. We summarize here some of the most recent studies on random polyampholytes. McCormick and Salazar [21] reported on a viscosity study of random polyampholytes based on sodium 2-acrylamide-2-methylpropanesulfonate, 2-acrylamide-2-methylpropanedimethylammonium chloride and acrylamide. Annaka and Tanaka [22] studied the swelling of random polyampholyte gels based on acrylic acid, methacrylamidopropyltrimethylammonium chloride and N,N'-methylenebisacrylamide, and observed multiple phases in the gels with an acid to base molar ratio close to two. The swelling of random polyampholyte gels of sodium styrenesulfonate, methacrylamidopropyltrimethylammonium chloride, acrylamide, and N,N'-methylenebisacrylamide was studied by Baker et al. [23]. Ebersole et al. [24] developed a piezoelectric cell growth sensor which detects the pH change in the cell broth through the solubility change of a random polyampholyte, based on acrylic acid, methyl methacrylate and dimethylaminoethyl methacrylate, which is also present in the broth. Higgs and Joanny [25] developed a scaling theory for random polyampholytes at the isoelectric point. Higgs and Orland [26] performed Monte Carlo simulations on an alternating polyampholyte at the isoelectric point. Kantor and colleages [27] employed Monte Carlo simulations and analytical arguments to study the conformations of random polyampholytes at both zero and nearly-zero net charge. Kamiyama and Israelachvili [28] measured the adsorption and surface force of gelatin, a proteinaceous polyampholyte, adsorbed on mica, at different pH and salt concentration. Most recently, Corpart and Candeau [29] studied the viscosity and salt-dependence of precipitation of random polyampholytes carrying sulfonate and quaternary amine groups.

Stille's group in 1972 was the first to synthesize block polyampholytes, via anionic polymerization [30,31]. These copolymers, based on 2-vinylpyridine and methacrylic acid (MAA) or acrylic acid, were evaluated for their salt-rejecting properties in dynamic reverse osmosis membranes. Following this study, Varoqui et al. [32] synthesized a diblock polyampholyte based on styrenesulfonic acid and 2-vinylpyridine for study of the intramolecular complexation of the anionic poly(styrene sulfonate) block with the cationic poly(2-vinylpyridinium) block. Miyaki and coworkers [33-38] synthesized charge-mosaic membranes which are cross-linked pentablock polyampholytes, the second block comprising quaternary ammonium residues, the fourth block styrenesulfonate, and the other three blocks being neutral cross-linkable isoprene blocks. The charge-mosaic membranes could find application in desalination. Most recently, Bekturov and coworkers [39,40] studied the precipitation and polymer complexation of two diblock polyampholytes of high molecular weight (600 kDa) comprising methacrylic acid and 1-methyl-4-pyridinium chloride residues.

Inclusion of an uncharged, hydrophobic block in a block polyampholyte leads to an ABC triblock polymer structure. Water-soluble methacrylic ABC triblock polymers appear to be a new class of polymers and they are expected to exhibit a richer solution behavior than the corresponding diblocks. The literature on ABC triblock polymers is modest, and primarily concerns studies of morphology and film properties [41]. Recently, Sdranis and Kosmas [42] have provided a theoretical consideration of solution properties of non-ionic ABC triblock polymers. Most recently, Wu and Slater [43] calculated the static structure factor and shape of ABC triblock polyampholytes (one of the blocks being non-hydrophobic and neutral) reptating in a gel in the presence of an electric field.

The most straightforward way to prepare acrylic triblock polyampholytes is to use a living polymerization method with sequential addition of monomers. Because group transfer polymerization (GTP) is convenient and amenable to a wide variety of functional and non-functional methacrylates [44,45], we chose to use this process to prepare block polymers containing DMAEMA and MAA. Möller and coworkers [46] have reported the preparation by GTP of diblock polymers comprising DMAEMA and MMA or decyl methacrylate. Since carboxylic acids cause termination of GTP, it is necessary to use an ester of MAA, which, after polymerization by GTP, can easily be converted to the free carboxylic acid. Three protected monomers which have been used in GTP to prepare precursors to MAA-containing polymers are *t*-butyl methacrylate, trimethylsilyl methacrylate (TMSMA), and tetrahydropyranyl methacrylate (THPMA). Poly(*t*-butyl methacrylate) is converted to poly(methacrylic anhydride) and isobutylene at 180-200°C, but in the presence of a catalytic amount of strong acid, thermolysis to poly(MAA) occurs at 90-140°C (Scheme 1) [47]. Deprotection with trimethylsilyl iodide at 50°C has also been reported [48]. In detailed kinetic studies of GTP of *t*-butyl methacrylate, it was reported that deactivation occurred above -20°C [49]. This was confirmed by Choi et al. [50], who used GTP to prepare ABA triblock polymers with *t*-butyl methacrylate A blocks. Stereochemical studies by Wei and Wnek [51] show that GTP of *t*-butyl methacrylate leads to lower syndiotacticity than does GTP of either methyl methacrylate or TMSMA. THPMA has recently been reported to undergo GTP to give random copolymers [52, 53], block copolymers, and homopolymer [54] with narrow molecular weight distribution (MWD).

For our synthesis of polyampholytes by GTP, we elected to use TMSMA and THPMA. TMSMA is a very attractive precursor to poly(MAA) because of its commercial availablilty, and the ease of methanolysis or hydrolysis of poly(TMSMA) with, or without, mild acid catalysis (Scheme 2). However, the reactivity of the trimethylsilyl ester toward nucleophilic GTP catalysts results in significant slowing of polymer growth. Thus, it is generally desirable to (i) add supplementary amounts of catalyst during the polymerization of TMSMA, (ii) leave TMSMA until the last block in block copolymerizations, and (iii) use alternative monomers for the synthesis of polymers of molecular weight higher than about 10,000 Da. For polymers of higher molecular weight THPMA is a better choice. This monomer, however, is not commercially available. Although several procedures have been reported for the synthesis of THPMA [55,56], careful purification is required to remove traces of methacrylic acid which interfere with GTP [52,55]. Poly(THPMA) is smoothly converted to poly(MAA) by heating at 140°C under vacuum for several hours (Scheme 3).

This report describes the synthesis by GTP of low molecular weight methacrylic polyampholytes, most of which are triblock copolymers and two of which are random terpolymers. The polymer solution characterization includes molecular weight determination by GPC, structural characterization by light scattering, water-solubility determination as a function of pH and salt concentration, isoelectric point determination, hydrogen-ion titration and a fluorescence study.

2.2 Experimental Section

2.2.1 Materials

Solvent. Tetrahydrofuran was distilled from sodium and benzophenone immediately prior to use.

Initiator. 1-Methoxy-1-trimethylsiloxy-2-methyl-1-propene was prepared by the method of Ainsworth [57], distilled in a spinning band column, and stored under nitrogen.

Monomers. Commercially available monomers were purified by passage over a column of basic alumina under an argon atmosphere to remove inhibitors and protonic impurities, except for trimethylsilyl methacrylate, which was used as received. Tetrahydropyranyl methacrylate was prepared by the reaction of MAA with 3,4-dihydro-2*H*-pyran (Aldrich Chemical Co.) using crosslinked poly(4-vinylpyridine hydrochloride) (Fluka Chemie AG) as catalyst by the method of Hertler [55]. Two distillations over calcium hydride provided tetrahydropyranyl methacrylate of sufficient purity for GTP.

Catalyst. Tetrabutylammonium biacetate [58] was prepared in a dry box by addition of one equivalent of acetic acid to a solution of tetrabutylammonium acetate (Fluka Chemie AG) in THF. The resulting precipitated tetrabutylammonium biacetate was collected by filtration and dissolved in freshly distilled propylene carbonate to give a 0.1 M stock solution of catalyst for GTP. The use of propylene carbonate, rather than THF, as solvent avoids the use of 6 molar equivalents of water required to solubilize tetrabutylammonium biacetate in THF [58].

2.2.2 Methods

Polymerizations. Polymerization reactions were performed in a 250 mL three-necked flask fitted with an addition funnel, two rubber septa, and a magnetic stirrer. A thermocouple was inserted through one septum. The second septum was used for injection by syringe of solvent, catalyst, and initiator. All glassware and syringes were stored overnight at 120°C in an oven, and the glassware was assembled while hot, heated at 100°C with a heat gun, and allowed to cool to room temperature under a flow of argon. The syringes and syringe needles were cooled in nitrogen-blanketted bell-jars. All transfers of liquid were performed with syringes. First, 40 mL of THF were transferred to the reactor, and the amount of monomer corresponding to the first block, typically about 15 mL, was transferred to the addition funnel. Catalyst solution, typically 1 mL, corresponding to 1 mole% of initiator, was injected. Then, the initiator, typically 2 mL, was injected, followed immediately by dropwise addition of the monomer at a feed rate of 1mL/min. The polymerization exotherm was monitored by a digital thermometer. When the temperature fell to near room temperature, addition of the next monomer was begun. The concentration of polymer after the addition of all of the monomers was typically 50% w/w. Since the polymerization of MMA, DMAEMA, and THPMA is much faster than that of TMSMA, TMSMA was the last block for all but one of the reactions. During the polymerization of the TMSMA, after all of the TMSMA had been added, additional 3 or 4 1-mL aliquots of catalyst solution were periodically injected to obtain satisfactory polymerization rates (as evidenced by increasing or steady temperature). In the case of random polymerizations, the three monomers were mixed and loaded into the addition funnel. At the end of the polymerizations the living chain ends were quenched by addition of 5 mL of methanol. The complete consumption of monomers was confirmed by ^{1}H NMR which indicated absence of the peaks characteristic of the hydrogens adjacent to a double bond.

Removal of the Protecting Groups. The tetrahydropyranyl functionality was removed by heating the neat polymer in a vacuum oven at 140°C for 48 hours. The extent of deprotection was followed by the decrease in weight resulting from loss of dihydropyran. The weight loss was just as expected from stoichiometry. The trimethylsilyl functionality was removed by refluxing the polymerization reaction mixture at 60°C after the addition of a 5-fold molar excess of methanol, 5-fold molar excess of water, and 0.5 mole% of dichloroacetic acid, all of the percentages referring to TMSMA. The completion of the reaction was confirmed by titration.

Molecular Weight Determination. Molecular weights and molecular weight distributions were determined by gel permeation chromatography using a series of four Waters Ultrastyragel columns (10000, 1000, 500, 100 Å) on a Hewlett-Packard 1090 HPLC system connected to a refractometer. The mobile phase was THF at a flow rate of 1 mL/min. Four narrow molecular weight poly(MMA) standards (Mp = 2700, 9800, 17500, and 33500 Da) were used for calibration. The logarithm of Mp was determined to vary linearly with retention time. The correlation coefficient was equal to 1.000.

Isoelectric Point Determinations. The isoelectric points were determined by two methods. First, neutral polymer powder was equilibrated with deionized water and the pH of the resulting 10% w/w suspension was measured. This is called the isoionic pH and, for the spectrum of the compositions of our polyampholytes and the high polymer concentration in the suspension, it is practically the same as the isoelectric pH [59]. In the second method, the midpoint of the pH range of precipitation during the titration of 1% w/w solutions of polymers in 0.1M KCl was used as an indication of the isoelectric point.

Hydrogen-Ion Titrations. A Model 825 MP Fisher Accumet pH meter with a miniature glass electrode and a microreference electrode with a glass barrel was used for the measurement of the pH. Titration of 5 mL of 1% w/w solutions of polymer in 0.02, 0.1 and 0.5M KCl was performed from pH 2 to 12 at room temperature (23±1°C).

Solubility Determinations. Different amounts of acid or base, as calculated from the experimental titration curves, were added to basic (typically pH = 8) and acidic (typically pH = 5) 10% w/w copolymer stock solutions to adjust the pH at different values within the range 5 to 8. The samples were vortexed, centrifuged for one hour at 4,000rpm, and allowed to equilibrate for at least one day. The polymer concentrations in the supernatant phase were determined at 25°C using an American Optical Abbe refractometer. Different amounts of solid potassium chloride were added for ionic strength adjustment. The polymer concentrations were determined by subtracting the salt contribution to the refractive index and dividing by the polymer refractive index increment which was determined to be 0.181mL/g at 25°C and constant up to 15% w/w polymer concentration.

Light-Scattering. Static and dynamic light-scattering were performed on a Brookhaven Instrument Corp. instrument with an argon laser light source at 488nm. A 2030 autocorrelator was used for the analysis of the dynamic scattering data. Prior to measurements, samples were filtered five times through 0.2 or 0.5μm Millipore filters to remove dust. Preliminary dynamic light-scattering experiments were performed using a Microscope Laser Light Scattering apparatus equipped with a light source at 633nm.

Fluorescence. A 10mg/L suspension of pyrene in water was formed by a 100-fold dilution in water of a 1g/kg solution of pyrene in ethanol. A small amount of the freshly prepared suspension was transferred to the polymer solutions which were buffered at pH 4.5 with 0.01M sodium acetate. The volume ratio of the polymer solution to the pyrene suspension was 100, so that the polymer concentration was practically unchanged, the final pyrene concentration in the polymer solution was 0.1mg/L, which is close to the solubility of pyrene in water and the ethanol concentration was 100ppm. A Spex Fluoromax fluorimeter was used for the measurement of the steady-state fluorescence spectra of the pyrene-containing polyampholyte solutions at an excitation wavelength of 333nm.

2.3 Results and Discussion

2.3.1 Polymer Synthesis

Table 2.1 lists the acrylic polyampholytes synthesized along with their molecular weight, sequence, composition and pH range of precipitation during titration of 1% w/w in 0.1M KCl. Ten ABC triblocks, one diblock, and two random terpolymers were prepared. The polymers are of relatively low molecular weight, the highest molecular weight examples being the two triblock polymers, 3 and 4, which are 15,000 Da. Our efforts to make random polymers with molecular weights 15,000 and 30,000 Da were unsuccessful, probably due to the presence of TMSMA in the monomer mixture. The slowing down effect of TMSMA in the above polymerization reactions may have been most dramatic because of the small amount of initiator required for synthesis of the higher molecular weight polymers. The acid-to-base molar ratio in the polymers is a very important quantity because it determines the isoelectric point of the polymers and, therefore, the charge and pH-dependence of solubility. Most of the block polyampholytes carry acidic and basic monomers in equimolar amounts and, therefore, they have the same pH range for insolubility, 5.5 to 8. The differences among these polymers lie in molecular weight, block sequence, percentage of MMA, and presence of 2-phenylethyl methacrylate (PEMA). The molar percentage of MMA in the triblocks, except in copolymer 5, was kept constant at 33%.

The PEMA labelling of polymers 7 and 8 results in an increase in the UV-absorbance (250-280nm) by 2-3 times and renders the polymers more easily detectable. The ability in GTP to introduce the label as a polymerizable monomer is more convenient than the alternative of chemical label attachment after polymerization. Polymer 6 which contains a block of PEMA residues and is expected to exhibit an even higher UV-absorbance is unfortunately insoluble, probably due to the high hydrophobicity of the PEMA block.

2.3.2 Molecular Weights

The weight average and number average molecular weights, the polydispersity index, and the theoretical molecular weight of some representative polymers and polymer blocks are listed in Table 2.2. The low polydispersities, lower than 1.4 for all of the polymers, are typical for GTP. The samples indexed A and B represent the first block and the first two blocks of the triblock polymers, respectively. The third block of these polymers was TMSMA, the presence of which prevented GPC analysis, as the polymer is retained on the column. GPC for triblock copolymers 3 and 4 was performed because they did not contain TMSMA but THPMA which is not retained on the column. The higher apparent polydispersity of the first block of polymers 6, 9 and 10, which was poly(DMAEMA), as compared to that of the first two blocks, as well as the difference between theoretical and experimental molecular weights of the first blocks are due to the interaction of poly(DMAEMA) with the column which results in broadening and shift of the peak to larger retention times (lower molecular weights). Poly(amine) adsorption on GPC columns has been observed by other researchers and has been attributed to the presence of residual carboxy functionalities on the column [34]. Figures 2.1a-d show the GPC traces of samples 3, 6A&B, 9A&B and 10A&B. After adding the second block, the distribution is still unimodal and narrow, which is indicative of the molecular weight-homogeneity of our polymers, which has already been manifested by the low polydispersity indices. The tails of the curves observed towards larger retention times are typical for polymers prepared by GTP as early termination of chain growth occurred.

2.3.3 Isoelectric Points

The isoelectric points of the polymers as approximated by the isoionic pHs as well as the midpoints of the pH range of precipitation are listed in Table 2.3. The values obtained from the two methods are in good agreement. The values of the isoelectric points from the isoionic pHs are considered more reliable because they were measured in the absence of salt which may interact with the polyampholyte. It has been reported that anions may bind to proteins [60] and that cations may interact with ampholytic latices [61] leading to a shift in the isoelectric point or the pH region of precipitation. The determination of the isoelectric pH from the isoionic pH is particularly useful for the random copolymers which are completely soluble and for which the precipitation method is not applicable. No acid, base or salt was added during the polymer preparation procedures with the exception of the catalytic amounts of dichloroacetic acid needed in the deprotection step. This implies that the polymers are essentially free of any ions other than H^+ or OH^- and, therefore, are in an isoionic state. Figure 2.2 illustrates the isoionic points of the polymers along with a theoretical prediction, based on the requirement that the net charge of the polymer is zero and that the dissociation constants are not composition dependent. According to this equation the isoelectric point depends on the acid to base molar ratio, R, and the dissociation constants of the negative and positive charges, pK_{ac} and pK_b:

$$pI = pK_b + \log\left\{\frac{1}{2}\left[\frac{1-R}{R} + \sqrt{\left(\frac{1-R}{R}\right)^2 + \frac{4}{R}10^{pK_{ac}-pK_b}}\right]\right\}$$

The values of the dissociation constants, taken from a previous study [62] on polyampholytes comprising the same monomers, are $pK_{ac} = pK_{MAA} = 5.35$ and $pK_b = pK_{DMAEMA} = 8.00$. It is worth mentioning that the equations that lead to this expression were first presented by Ehrlich and Doty [18] and Mazur et al. [20] but no analytical solution was derived. This equation can be very useful for estimating protein isoelectric points from the amino acid composition (the ratio of acidic to basic amino acids). For proteins with low contents of histidine (pK = 6.2) and arginine (pK = 12) the appropriate dissociation constants should be $pK_{ac} = pK_{\text{Aspartic Acid}} = 4.5$ and $pK_b = pK_{\text{Lysine}} = 10.04$ [63].

2.3.4 Hydrogen-Ion Titrations

The titration curves of 1% w/w solutions of polymer 2 at 0.02, 0.1 and 0.5M KCl are shown in Figure 2.3. The curves are generated by interpolation between the experimental points and are not based on any model. It should be pointed out that there are no experimental points around the isoelectric point in the titration curves at the two lower salt concentrations because the polymer precipitates. The portion of the curve at high pH corresponds to the titration of the basic groups and that at low pH to the titration of the acidic groups. The interpolated curves intersect at a pH near the isoelectric point. In the calculations for the construction of the curves, the pH of zero net charge was fixed at 6.6 for all three salt concentrations. The effect of increasing salt concentration at constant pH is to decrease the charge of the group being titrated in that pH region (decrease in the dissociation of the acidic residues or decrease in the protonation of the basic residues). This weakening of the acidic or basic character of the polymer groups can be attributed to the decrease in intrapolymer attractive electrostatic interactions by the salt and has been predicted theoretically [20,62,64,65] and observed experimentally in the titration of biological polyampholytes (proteins) [59] and synthetic polyampholytes [62].

2.3.5 Solubility Curves

Figure 2.4 shows the pH-dependence of the solubility of Polymer 2 at different salt concentrations, 0.1, 0.3, 0.5 and 0.7M KCl. The solubility around the isoelectric point, which is 6.6, is much lower than that 1 pH unit away. By increasing the salt concentration, the solubility around the isoelectric point increases. At 0.9M KCl the polymer is completely (at least 10% w/w) soluble, even at the isoelectric point. The polymer net charge is zero at the isoelectric point and, therefore, the electrostatic repulsion, which keeps the polymer in solution, is at a minimum. In contrast, the electrostatic attraction between the positive and negative charges, which are equal in number, is maximized. The increase in salt concentration leads to the screening of the attractions around the isoelectric point and results in increase in solubility. The above behavior was observed for the first time with proteins [59,66,67], in which a solubility minimum was observed at their isoelectric point and in which addition of salts led to an increase in protein solubility, called the salting-in effect. Tanford used the linearized Poisson-Boltzmann equation to develop expressions for the charge and salt concentration dependence of the solubility of globular proteins. In these expressions the protein solubility increases exponentially with the square of the net charge [59].

Comparison of triblock copolymer 2 with its random counterpart copolymer 12 indicates that factors other than the net charge can influence the solubility. Polymer 12 is soluble, at least 15% w/w, over the entire pH-range, even at the isoelectric point and in the absence of salt. This can be attributed either to the smaller effective size of the random copolymer (no micelles, see also Chapter 9) or to the random distribution of the positive and the negative charges on the polymer which leads to a dipole moment lower than that necessary for enhancing interpolymer association at the isoelectric point. Supporting the latter interpretation is the precipitation of diblock copolymer 11 at the isoelectric point despite the absence of micelles, the lower molecular weight (2,400 Da) and lower hydrophobicity (no MMA residues). However, it should be mentioned that diblock copolymer 11 salts-in very easily.

It was expected that the solubility of triblock polymer 2 should be essentially zero because, as it was evidenced by the turbidimetric titrations of Chapters 5 and 6, the same polymer could be precipitated from solutions of polymer concentration as low as 0.004%. The minimum solubility shown in Figure 2.4 is 1% and it is much higher than the expected value of 0.004%. This discrepancy is due to the presence of impurities which are taken as polyampholyte by the non-selective refractive index technique. We estimate that our triblock copolymers contain 5-10% impurities of homopolymer (terminated first block) and diblock. This is consistent with the long tails in the GPC plots (Figure 2.1) as well as with the findings of Möller and coworkers [46]. Since the total average polymer concentration of the samples was 10%, 10% of which was impurities, it can be calculated that the concentration of impurities was 1% (see also Chapters 4 and 7).

2.3.6 Light-Scattering

A light-scattering study was conducted to probe the micellization behavior of the block polymers. We compared triblock Polymer 2 and the corresponding random terpolymer, Polymer 12, which have the same molecular weight (4,000 Da) and composition, DMAEMA:MMA:MAA = 1:1:1. Solutions of the two polymers at pH 5 were studied by both static and dynamic light-scattering. The information obtained by these techniques is summarized in Table 2.4. The molecular weight of the random terpolymer, as determined by static light-scattering, is 5,500 $\pm$ 500 Da, in reasonable agreement with the expected value of 4,000 Da. The molecular weight of the triblock polymer, as determined by the same method, was found to be 125,000 $\pm$ 5,000 Da, which implies that aggregation occurs. To estimate the aggregation number, the effective molecular weight of the triblock polymer was divided by that of the random terpolymer, and the result is 23. Cubing the ratio of the corresponding hydrodynamic radii, as determined by dynamic light scattering gives a similar result, 21. Assuming the same segment density for the two poymers, this agreement implies that the aggregates are roughly spherical in shape. The second virial coefficient of the triblock polymer, as determined by static light-scattering is positive, indicating a repulsion between the positively charged micelles.

From these results we envision the block copolymer micelles to comprise 20-25 polymer chains with the middle hydrophobic block constituting the micellar core and the ionic blocks constituting the corona. The hydrodynamic diameter of 11nm of the micelles suggests that the chains are in an extended configuration in the micelles because the contour length of the chains (based on the theoretical molecular weight) is approximately 9nm (36 residues x 0.25nm/residue).

A subsequent QELS study on polymer 2 at pH 5 showed that the hydrodynamic size remains 11nm for all of the combinations of salt and polymer concentrations employed. The salt concentration was varied from 0.0 to 1.0M KCl, and the polymer concentration from 0.1 to 5%. Additional QELS studies showed that, while all the triblocks form micelles, the diblock copolymer does not.

The dependence of the hydrodynamic diameter of polymer 2 on pH appears in Figure 2.5. The qualitative trends in this Figure are in agreement with those of the solubility curves of Figure 2.4. Around the isoelectric point, big aggregates of size

100nm form because of the weak electrostatic repulsion. At intermediate pH, smaller micellar aggregates of size 11nm form. At extreme pH, the strong electrostatic repulsions destroy the micelles and the polymer molecules occur in solution as separate chains.

2.3.7 Fluorescence

The intensity ratio of peak 3 (382nm) to peak 1 (371nm) of pyrene emission appears in Figure 2.6 as a function of polymer concentration for block copolymer 2 and random copolymer 12. While the behavior of the two copolymers is identical at very low ($< 10^{-3}$%) and at very high (> 1%) polymer concentrations, it differs at intermediate concentrations. In the low concentration regime polymer-pyrene interactions are absent as the pyrene intensity ratio remains constant and equal to the control (pyrene solution without polymer) value of 0.52.

In the intermediate concentration region the pyrene intensity ratios for the two polymers increase with increasing polymer concentration reaching a value of 0.63 at 1% polymer concentration. This increase indicates that pyrene is transferred from an aqueous to a more hydrophobic environment as a result of the increasing polymer concentration. For block copolymer 2, the onset of the increase occurs at a concentration of 0.001%, while for random copolymer 12 the same change occurs at a concentration an order of magnitude higher. This can be attributed to the longer hydrophobic domains of the block copolymer which are offered for more efficient binding and, therefore, higher affinity for the hydrophobic fluorescent probe. For the same amount of pyrene to associate hydrophobically with the random copolymer, higher polymer concentrations are necessary. Another explanation for the different behavior of the two copolymers can be attributed to the micellization of the block copolymer. This can be supported by the observation that, in the case of the block polymer, the increase in the intensity ratio is sharp in the concentration range 10^{-3}-4.10^{-2}, potentially due to micellization, and becomes shallow in the concentration range 4.10^{-2}-1%, possibly due to completion of micellization at 4.10^{-2}%.

In the high concentration region, covering polymer concentrations higher than 1%, the intensity ratios of the two polymers become again the same and increase with increasing polymer concentration. The equality of their intensity ratios is in agreement with the fact that the two polymers have identical chemical compositions. The increase in intensity with polymer concentration may be due to a higher order of polymer-pyrene association or it may be simply due to the lower scattering of peak 3 at 382nm as compared to that of peak 1 at 371nm by the concentrated polymer solution. The scattering is inversely proportional to the fourth power of the wavelength (assuming independence of the refractive index on the wavelength) [68] and such a calculation can satisfactorily account for this increase. Supporting the latter interpretation is the trend in the absolute intensities of peaks 1 and 3 which increase monotonically up to 0.2% polymer concentration and then decrease at higher concentrations.

The onset of the increase in the intensity ratio of pyrene in solutions of block copolymers has been claimed to occur at the critical micellar concentration (CMC) [69,70] and was utilized for its determination. We may conclude that the CMC of the triblock copolymer is at 10^{-3}%. However, the increase in the intensity ratio of the random copolymer, which does not form micelles, suggests that such a behavior can also be explained by pyrene-unimer association as opposed to pyrene-micelle association.

2.4 Conclusions

Low-molecular weight random, diblock, and ABC triblock polyampholytes containing MAA, MMA, and DMAEMA were synthesized by GTP. Unlike the random terpolymers which are soluble over the entire pH range, the block polymers show a strong tendency to precipitate near the isoelectric point as a result of the high electric field intensity of the oppositely charged blocks. The presence of the hydrophobic block leads to the micellization of the triblocks. This micellization offers the opportunity for utilization of these polymers in solubilization applications which is further reinforced by the ability to vary polymer solubility as well as micellar stability by pH manipulations. A pyrene fluorescence study showed that the hydrophobic probe binds to the triblock polymer 2 more strongly than to its random counterpart, polymer 12, which may suggest a CMC value for the triblock of 10^{-3}%. Our results suggest that the structure of the polyampholytes affects significantly their properties. We expect to be able to use GTP to prepare novel polyampholytes of various other structures such as stars [71], ladders [72,73], grafts [74], combs [75] and gels.

2.5 Literature Cited

(1) McGrath, J. E. An Introductory Overview of Block Copolymers. *Block Copolymers: Science and Technology*; Meier, D. J., Ed.; MMI Symposium Series, Harwood: New York, 1983; Vol. 3, p 1-16.

(2) Morishima, Y. Photophysics in Amphiphilic Polyelectrolyte Systems. *Prog. Polym. Sci.* **1990,** *15,* 949-997.

(3) Balazs, A. C.; Gempe, M.; Lantman, C. W. Effect of Molecular Architecture on the Adsorption of Copolymers. *Macromolecules* **1991,** *24,* 168-176.

(4) Balazs, A. C.; Siemasko, C. P.; Lantman, C. W. Monte Carlo Simulations for the Behavior of Multiblock Copolymers at a Penetrable Interface. *J. Chem. Phys.* **1991,** *94,* 1653-1663.

(5) Patrickios, C. S.; Lansbury, P. T., Jr.; Hatton, T. A. Acrylic Polyampholytes as Protein Displacers. Paper presented at ACS 203rd meeting, San Francisco, 1992.

(6) Patrickios, C. S.; Gadam, S. D.; Cramer, S. M.; Hertler, W. R.; Hatton, T. A. Chromatographic Characterization of Acrylic Polyampholytes. *Polym. Prepr., Am. Chem. Soc. Div. Polym. Chem.* **1993,** *34(1),* 1073-1074.

(7) Patrickios, C. S.; Gadam, S. D.; Cramer, S. M.; Hertler, W. R.; Hatton, T. A. Chromatographic Characterization of Acrylic Polyampholytes. *Polyelectrolytes*; Schmitz, K. S., Ed.; ACS Symposium Series, in press.

(8) Patrickios, C. S.; Jang, C. J.; Hertler, W. R.; Hatton, T. A. Interaction of Proteins with Acrylic Polyampholytes. *Polym. Prepr., Am. Chem. Soc. Div. Polym. Chem.* **1993,** *34(1),* 954-955.

(9) Patrickios, C. S.;Jang, C. J.; Hertler, W. R.; Hatton, T. A. Interaction of Proteins with Acrylic Polyampholytes. *Polyelectrolytes*; Schmitz, K. S., Ed.; ACS Symposium Series, in press.

(10) Hughes, P.; Lowe, C. R. Purification of Proteins by Aqueous Two-Phase Partition in Novel Acrylic Co-Polymer Systems. *Enzyme Microb. Technol.* **1988,** *10,* 115-122.

(11) Patrickios, C. S.; Abbott, N. L.; Foss, R. P.; Hatton, T. A. Protein Partitioning in Two-Phase Aqueous Polymer Systems Containing Polyampholytes. *New Developments in Bioseparation*; Ataai, M. M., Sikdar, S. K., Eds.; AIChE Symposium Series: NY 1992; Vol. 88; pp 80-88.

(12) Righetti, P. G. *Isoelectric Focusing: Theory, Methodology and Applications*; Elsevier: Amsterdam, 1983; pp 50.

(13) Bekturov, E. A.; Kudaibergenov, S. E.; Rafikov, S. R. Synthetic Polymeric Ampholytes in Solution. *Macromol. Sci. Rev. Macromol. Chem. Phys.* **1990,** *C30(2),* 233-303.

(14) Alfrey, T.; Morawetz, H.; Fitzgerald, E. B.; Fuoss, R. M. Synthetic Electrical Analog of Proteins. *J. Am. Chem. Soc.* **1950,** *72,* 1864-1864.

(15) Alfrey, T.; Fuoss, R. M.; Morawetz, H.; Pinner, S. H. Amphoteric Polyelectrolytes. II. Copolymers of Methacrylic Acid and Diethylaminoethyl Methacrylate. *J. Am. Chem. Soc.* **1952,** *74,* 438-441.

(16) Alfrey, T.; Morawetz, H. Amphoteric Polyelectrolytes. I. 2-Vinylpyridine-Methacrylic Acid Copolymers. *J. Am. Chem. Soc.* **1952,** *74,* 436-438.

(17) Alfrey, T.; Pinner, S. H. Preparation and Titration of Amphoteric Polyelectrolytes. *J. Polym. Sci.* **1957,** *23,* 533-547.

(18) Ehrlich, G.; Doty, P. Macro-ions. III. The Solution Behavior of a Polymeric Ampholyte. *J. Am. Chem. Soc.* **1954,** *76,* 3764-3777.

(19) Katchalsky, A.; Miller, I. R. Polyampholytes. *J. Polym. Sci.* **1954,** *13,* 57-68.

(20) Mazur, J.; Silberberg, A.; Katchalsky, A. Potentiometric Behavior of Polyampholytes. *J. Polym. Sci.* **1959,** *35,* 43-70.

(21) McCormick, C. L.; Salazar, L. C. Water-Soluble Copolymers. 43. Ampholytic Copolymers of Sodium 2-(Acrylamido)-2-methylpropanesulfonate with [2-(Acrylamido)-2-methylpropyl]trimethylammoniun Chloride. *Macromolecules* **1992,** *25,* 1896-1900.

(22) Annaka, M.; Tanaka, T. Multiple Phases of Polymer Gels. *Nature* **1992,** *355,* 430-432.

(23) Baker, J. P.; Stephens, D. R.; Blanch, H. W.; Prausnitz, J. M. Swelling Equilibria for Acrylamide-Based Polyampholyte Hydrogels. *Macromolecules* **1992,** *25,* 1955-1958.

(24) Ebersole, R. C.; Foss, R. P.; Ward, M. D. Piezoelectric Cell Growth Censor.

Bio/Technology **1991,** *9,* 450-454.

(25) Higgs, P. G.; Joanny, J.-F. Theory of Polyampholyte Solutions. *J. Chem. Phys.* **1991,** *94,* 1543-1554.

(26) Higgs, P. G.; Orland, H. Scaling Behavior of Polyelectrolytes and Polyampholytes: Simulation by an Ensemble Growth Method. *J. Chem. Phys.* **1991,** *95,* 4506-4518.

(27) Kantor, Y.; Li, H.; Kardar, M. Conformations of Polyampholytes. *Phys. Rev. Lett.* **1992,** *69,* 61-64.

(28) Kamiyama, Y.; Israelachvili, J. Effect of pH and Salt on the Adsorption and Interactions of an Amphoteric Polyelectrolyte. *Macromolecules* **1992,** *25,* 5081-5088.

(29) Corpart, J.-M.; Candau, F. Aqueous Solution Properties of Ampholytic Copolymers Prepared i Microemulsions. *Macromolecules* **1993,** *26,* 1333-1343.

(30) Kamachi, M.; Kurihara, M.; Stille, J. K. Synthesis of Block Polymers for Desalination Membranes. Preparation of Block Copolymers of 2-Vinylpyridine and Methacrylic Acid or Acrylic Acid. *Macromolecules* **1972,** *5,* 161-167.

(31) Kurihara, M.; Kamachi, M.; Stille, J. K. Synthesis of Ionic Block Copolymers for Desalination Membranes. *J. Polym. Sci., Polym. Chem. Ed.* **1973,** *11,* 587-610.

(32) Varoqui, R.; Tran, Q.; Pefferkorn, E. Polycation-Polyanion Complexes in the Linear Diblock Copolymer of Poly(styrene sulfonate)/Poly(2-vinylpyridinium) Salt. *Macromolecules* **1979,** *12,* 831-835.

(33) Fujimoto, T.; Ohkoshi, K.; Miyaki, Y.; Nagasawa, M. Artificial Membranes from

Multiblock Copolymers. I. Fabrication of a Charge-Mosaic Membrane and Preliminary Tests of Dialysis and Piezodialysis. *J. Membr. Sci.* **1984,** *20,* 313-324.

(34) Miyaki, Y.; Iwata, M.; Fujita, Y.; Tanisugi, H.; Isono, Y.; Fujimoto, T. Artificial Membranes from Multiblock Copolymers. 2. Molecular Characterization and Morphological Behavior of Pentablock Copolymers of the ISIAI Type. *Macromolecules* **1984,** *17,* 1907-1912.

(35) Miyaki, Y.; Nagamatsu, H.; Iwata, M.; Ohkoshi, K.; Se, K.; Fujimoto, T. Artificial Membranes from Multiblock Copolymers. 3. Preparation and Characterization of Charge-Mosaic Membranes. *Macromolecules* **1984,** *17,* 2231-2236.

(36) Takahashi, S.; Matsumura, K.; Toda, M.; Fujimoto, T.; Hasekawa, H.; Miyaki, Y. Artificial Membranes from Multiblock Copolymers. IV. Four-Component Pentablock Copolymers of the DSD'AD Type Usable to Fabricate a Charge-Mosaic Membrane. *Polymer J.* **1986,** *18,* 41-49.

(37) Fujimoto, T.; Miyaki, Y.; Nagasawa, M. A New Charge-Mosaic Membrane from a Multiblock Copolymer. *Science* **1984,** *224,* 74-76.

(38) Itou, H.; Toda, M.; Ohkoshi, K.; Iwata, M.; Fujimoto, T., Miyaki, Y.; Kataoka, T. Artificial Membranes from Multiblock Copolymers. 6. Water and Salt Transports through a Charge-Mosaic Membrane. *Ind. Eng. Chem. Res.* **1988,** *27,* 983-987.

(39) Bekturov, E. A.; Frolova, V. A.; Kudaibergenov, S. E.; Schulz, R. C.; Zöller, J. Conformational Properties and Complex Formation Ability of Poly(Methacrylic acid)-*block*-Poly(1-methyl-4-vinylpyridinium chloride) in Aqueous Solution. *Makromol. Chem.* **1990,** *191,* 457-463.

(40) Bekturov, E. A.; Kudaibergenov, S. E.; Khamzamulina, R. E.; Frolova, V. A.; Nurgalieva, D. E.; Schulz, R. C.; Zöller, J. Phase Behavior of Block-Polyampholytes Based on Poly(Methacrylic acid)-*block*-Poly(1-methyl-4-vinylpyridinium chloride) in Aqueous Salt Solutions. *Makromol. Chem., Rapid Commun.* **1992,** *13,* 225-229.

(41) Spontak, R. J.; Zielinski, J. M. Confined Single-Chain Model of Microphase-Separated Multiblock Copolymers. 2. ABC Copolymers. *Macromolecules* **1992,** *25,* 663 and references cited therein.

(42) Sdranis, Y. S.; Kosmas, M. K. On the Conformational Behavior of an ABC Triblock Copolymer Molecule. *Macromolecules* **1991,** *24,* 1341-1351.

(43) Wu, S. Y.; Slater, G. W. Static Structure Factor and Shape of Reptating Telechelic Ionomers in Electric Fields. *Macromolecules* **1993,** *26,* 1905-1913.

(44) Sogah, D. Y.; Hertler, W. R.; Webster, O. W.; Cohen, G. M. Group Transfer Polymerization. Polymerization of Acrylic Monomers. *Macromolecules* **1987,** *20,* 1473-1488.

(45) Webster, O. W.; Hertler, W. R.; Sogah, D. Y.; Farnham, W. B.; RajanBabu, T. V. Group Transfer Polymerization. 1. A New Concept for Addition Polymerization with Organosilicon Initiators. *J. Am. Chem. Soc.* **1983,** *105,* 5706.

(46) Möller, M. A.; Augenstein, M.; Dumont, E.; Pennewiss, H. Controlled Synthesis and Characterization of Statistical and Block Copolymers by Group Transfer Polymerization. *New Polymeric Mater.* **1991,** *2,* 315-328.

(47) Ito, H.; Ueda, M. Thermolysis and Photochemical Acidolysis of Selected Polymethacrylates. *Macromolecules* **1988,** *21,* 1475 and references cited therein.

(48) Wang, J.; Varshney, S. K.; Jerome, R.; Teyssie, P. Synthesis of AB(BA), ABA and BAB Block Copolymers of *tert*-butyl Methacrylate (A) and Ethylene Oxide (B). *J. Polym. Sci., Polym. Chem. Ed.* **1992,** *30,* 2251-2261.

(49) Doherty, M. A.; Müller, A. H. E. Kinetics of Group Transfer Polymerization of *tert*-butyl Methacrylate in Tetrahydrofuran. *Makromol. Chem.* **1989,** *190,* 527-539.

(50) Choi, W.-J.; Kim, Y.-B.; Kwon, S.-K.; Lim, K.-T.; Choi, S.-K. Synthesis, Characterization and Modification of Poly(*tert*-butyl Methacrylate-b-alkyl Methacrylate-b-*tert*-butyl Methacrylate) by Group Transfer Polymerization. *J. Polym. Sci., Polym. Chem. Ed.* **1992,** *30,* 2243-2248.

(51) Wei, Y.; Wnek, G. N. Stereochemistry and Mechanistic Study of Group-Transfer Polymerization. *Polym. Prepr., Am. Chem. Soc. Div. Polym. Chem.* **1987,** *28(1),* 252-253.

(52) Taylor, G. N.; Stillwagon, L. E.; Houlihan, F. M.; Wolf, T. M.; Sogah, D. Y.; Hertler, W. R. Positive, Chemically-Amplified Aromatic Methacrylate Resist Employing the Tetrahydropyranyl Protecting Group. *Chem. Mater.* **1991,** *3,* 1031.

(53) Taylor, G. N.; Stillwagon, L. E.; Houlihan, F. M.; Wolf, T. M.; Sogah, D. Y.; Hertler, W. R. A Positive, Chemically Amplified, Aromatic Methacrylate Resist Employing the Tetrahydropyranyl Protecting Group. *J. Vac. Sci. Technol.* **1991,** *B9,* 3348-3356.

(54) Raymond, F. A.; Hertler, W. R. A Negative-Working Tonable Photoimaging Composition Based on Acid-Labile Acrylic Polymers. *J. Imag. Sci. Technol.* **1992,** *36,* 243.

(55) Hertler, W. R. Catalyzed Process for Reacting Carboxylic Acids with Vinyl Ethers. U.S. Patent 5,072,029, 1991.

(56) Kearns, J. E.; McLean, C. D.; Solomon, D. H. Polymers and Copolymers of Unsaturated Tetrahydropyranyl Esters. *J. Macromol. Sci.-Chem.* **1974,** *A8,* 673.

(57) Ainsworth, C.; Chen, F.; Kuo, Y.-N. J. Ketene Alkyltrialkylsilyl Acetals: Synthesis, Pyrolysis and NMR Studies. *Organomet. Chem.* **1972,** *46,* 59-71.

(58) Dicker, I. B.; Cohen, G. M.; Farnham, W. B.; Hertler, W. R.; Laganis, E. D.; Sogah, D. Y. Oxyanions Catalyze Group-Transfer Polymerization to Give Living Polymers. *Macromolecules* **1990,** *23,* 4034-4041.

(59) Tanford, C. *Physical Chemistry of Macromolecules*; Wiley: New York, 1961; pp 240, 461, 465, 466, 472, 555, 561.

(60) Velick, S. F. The Interaction of Enzymes with Small Ions. *J. Phys. Colloid Chem.* **1949,** *53,* 135.

(61) Healy, T. W.; Homola, A.; James, R. O.; Hunter, R. J. Coagulation of Amphoteric Latex Colloids: Reversibility and Specific Ion Effects. *Faraday Disc. Chem. Soc.* **1978,** *65,* 156-163.

(62) Merle, Y. Synthetic Polyampholytes. 5. Influence of Nearest-Neighbor Interactions on Potentiometric Curves. *J. Phys. Chem.* **1987,** *91,* 3092-3098.

(63) Creighton, T. E. *Proteins: Structures and Molecular Properties*; Freeman: New York, 1984; pp 7.

(64) Rice, S. A.; Harris, F. E. Chain Model for Polyelectrolytes. III. Equimolar Polyampholytes of Regularly Alternating Structure. *J. Chem. Phys.* **1956,** *24,* 326-335.

(65) Harris, F. E.; Rice, S. A. Chain Model for Polyelectrolytes. IV. Skeletal Distribution Effects in Equimolar Polyampholytes. *J. Chem. Phys.* **1956,** *24,* 336-344.

(66) Green, A. A. The Effect of Electrolytes on the Solubility of Hemoglobin in Solutions of Varying Hydrogen Ion Activity with a Note on the Comparable Behavior of Casein. *J. Biol. Chem.* **1931,** *93,* 517.

(67) Melander, W.; Horvath, C. Salt Effects on Hydrophobic Interactions in Precipitation and Chromatography of Proteins: An Interpretation of the Lyotropic Series. *Arch. Biochem. Biophys.* **1977,** *183,* 200-215.

(68) Hiemenz, P. C. *Principles of Colloid and Surface Chemistry*; Marcel Dekker: New York, 2nd ed., 1986; pp 238.

(69) Zhao, C.-L.; Winnik, M. A.; Riess, G.; Croucher, M. D. Fluorescence Probe Techniques Used to Study Micelle Formation in Water-Soluble Block Copolymers. *Langmuir* **1990,** *6,* 514-516.

(70) Wilhelm, M.; Zhao, C.-L.; Wang, Y.; Xu, R.; Winnik, M. A.; Mura, J.-L.; Riess, G.; Croucher, M. D. Poly(styrene-ethylene oxide) Block Copolymer Micelle Formation in Water: A Fluorescence Probe Study. *Macromolecules* **1991,** *24,* 1033-1040.

(71) Spinelli, H. J. Acrylic Stars Polymers. Int. Patent Appl. WO 8,600,626, 1986.

(72) Sogah, D. Y. Ladders, Stars and Combs by Group-Transfer Polymerization. *Polym. Prepr., Am. Chem. Soc. Div. Polym. Chem.* **1988,** *29(2),* 3.

(73) Sogah, D. Y. Acrylic Ladder Polymers. U.S. Patent 4,906,713, 1990.

(74) Hertler, W. R.; Sogah, D. Y.; Boettcher, F. P. Group-Transfer Polymerization on a Polymeric Support. *Macromolecules* **1990,** *23,* 1264-1268.

(75) Fleischmann, G.; Eck, H.; Schuster, J. Polyorganosiloxanes with Comb or Block Structure. Eur. Patent Appl. EP 355826, 1990.

Table 2.1 Architecture, block-sequence, composition and insolubility range of methacrylic polyampholytes (Molecular weight = 4,000).

Polymer	Formula[1]	pH insol. range
1	$M_{12}A_{12}B_{12}$	5.4-8.0
2	$B_{12}M_{12}A_{12}$	5.5-7.9
3[2]	$A_{36}M_{36}B_{36}$	
4[2]	$M_{36}A_{36}B_{36}$	
5	$B_{10}M_{20}A_{10}$	5.6-7.7
6	$B_{10}P_{10}A_{10}$	<9
7	$PB_{12}M_{12}A_{12}$	5.2-7.9
8	$B_{12}M_6PM_6A_{12}$	5.2-7.5
9	$B_{16}M_{12}A_8$	6.6-8.3
10	$B_8M_{12}A_{16}$	4.2-6.0
11[3]	$B_{10}A_{10}$	5.6-7.7
12[4]	$(BMA)_{12}$	none
13[4]	$(B_{1.33}MA_{0.67})_{12}$	none

[1]B = dimethylaminoethyl methacrylate; A = methacrylic acid; M = methyl methacrylate; P = phenylethyl methacrylate.

[2]MW = 15,000, prepared using THPMA.

[3]MW = 2,400.

[4]random.

Table 2.2 GPC and theoretical molecular weights of the block polyampholytes.

Polymer	M_w	M_n	M_w/M_n	M_n(theory)
3	22,200	17,500	1.27	15,000
4	19,300	14,500	1.33	15,000
6A[1]	1,000	800	1.25	1,550
6B[2]	3,600	3,200	1.14	3,440
9A[1]	1,600	1,200	1.37	2,520
9B[2]	4,900	4,000	1.22	3,730
10A[1]	730	580	1.28	1,260
10B[2]	2,500	2,100	1.17	2,460

[1]First block.

[2]First two blocks.

Table 2.3 Isoelectric points of the polyampholytes.

Polymer	$pI_{isoionic\ pH}$	$pI_{precipitation}$
2	6.6	6.7
5	6.5	6.6
7	6.3	6.5
8	6.8	6.4
9	8.0	7.5
10	5.4	5.1
11	6.9	6.7
12	6.6	
13	8.2	

Table 2.4 Results of static and dynamic light-scattering characterization of Polymers 2 and 12 at pH 5.

Polymer	QELS		Static Light-Scattering			
	d_h (Å)	Aggr#	M_w	A_2[1]	d_g (Å)	Aggr#
12 (random)	40		5,500			
2 (triblock)	110	21[2]	125,000	20.4	188	23[2]

[1]In mL.mole/kg^2.

[2]See text for details of calculation.

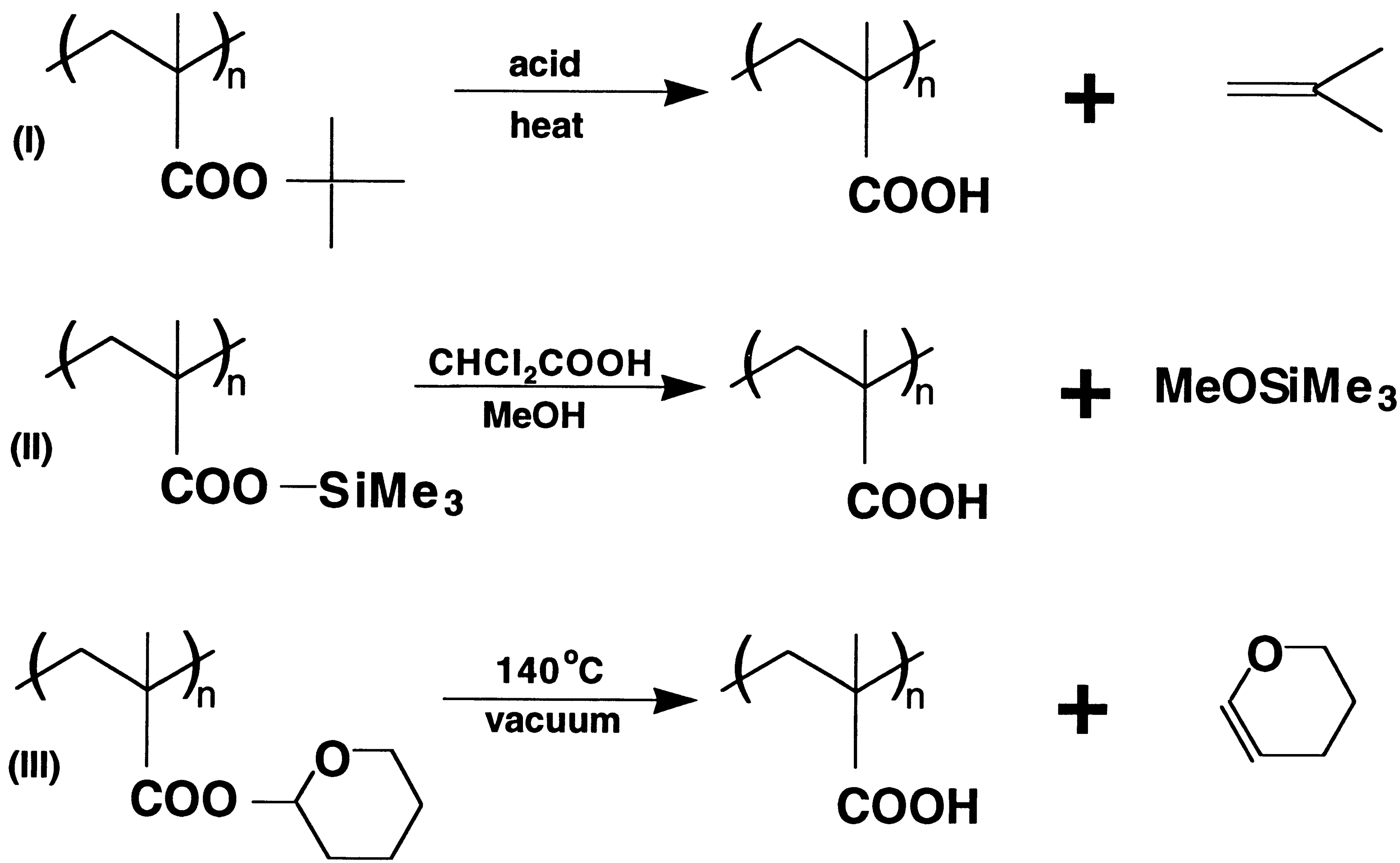

Deprotection Schemes of pre-methacrylic acid residues.

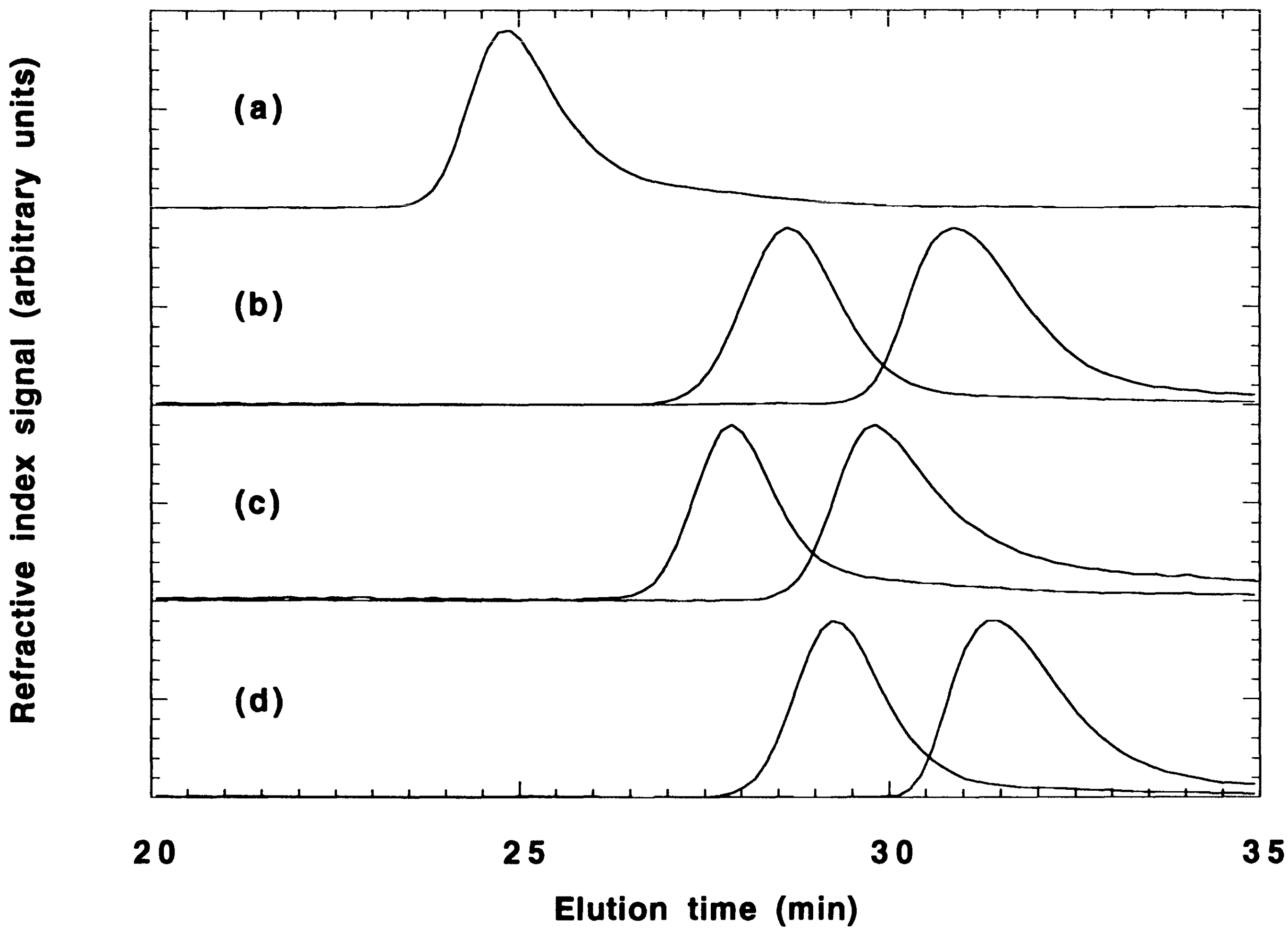

Figure 2.1 Molecular weight distributions of the block copolymers by GPC. Polymer 3 before thermolysis (a); first and first two blocks of Polymer 6 (b), Polymer 9 (c) and Polymer 10 (d).

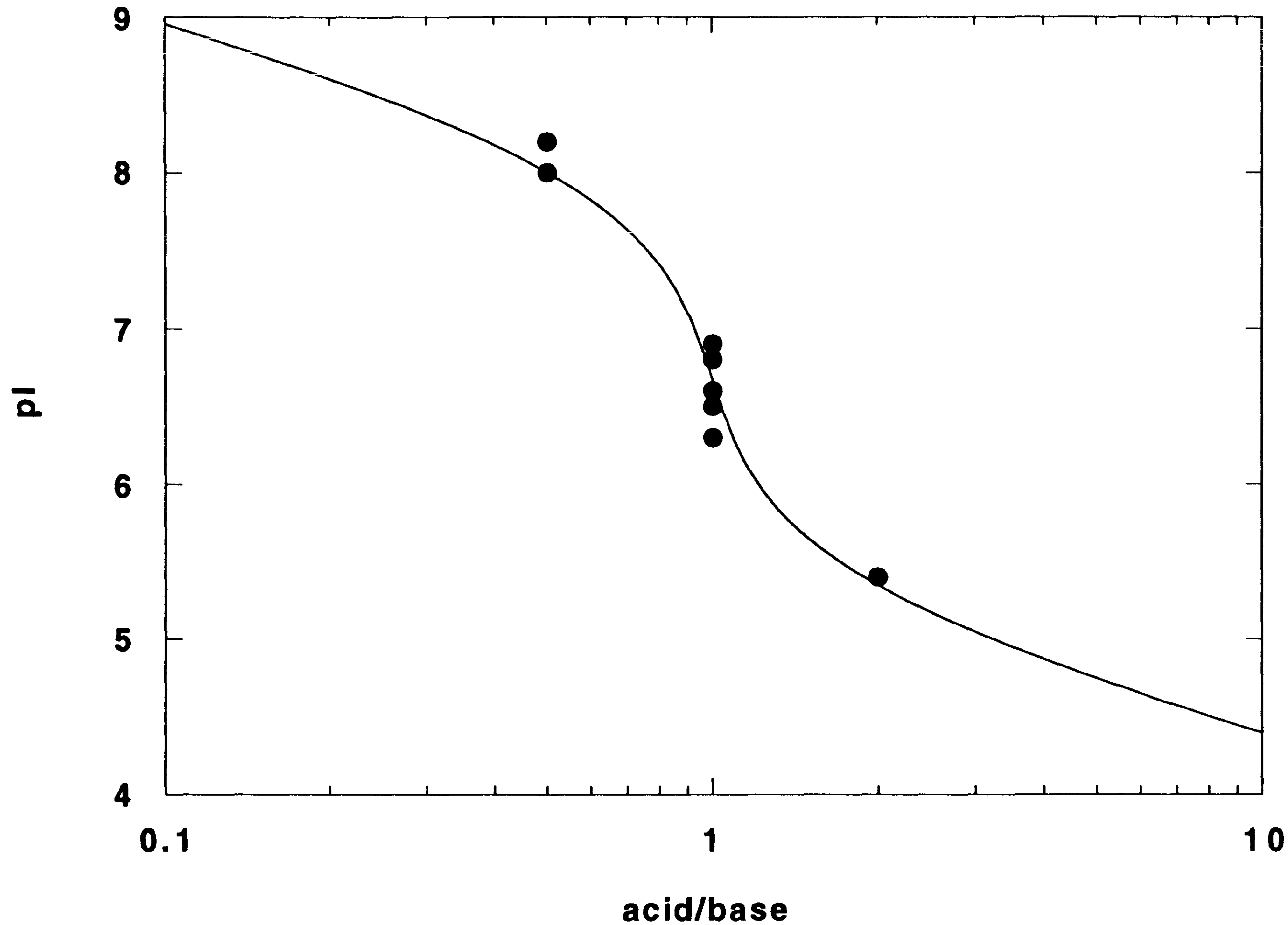

Figure 2.2 Experimental isoelectric points of the polyampholytes. The solid line represents a theoretical prediction.

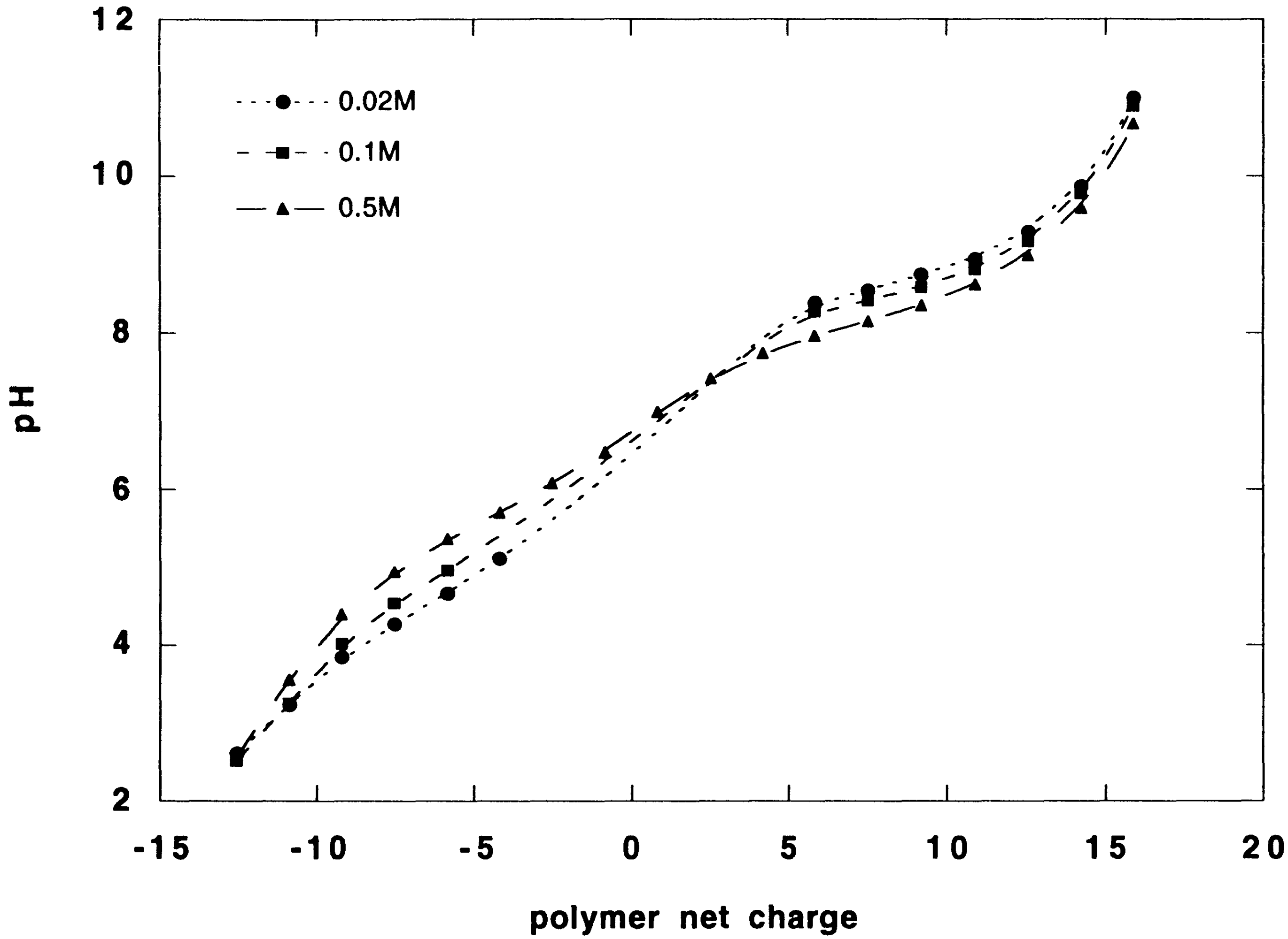

Figure 2.3 Titration of triblock copolymer 2 at different KCl concentrations.

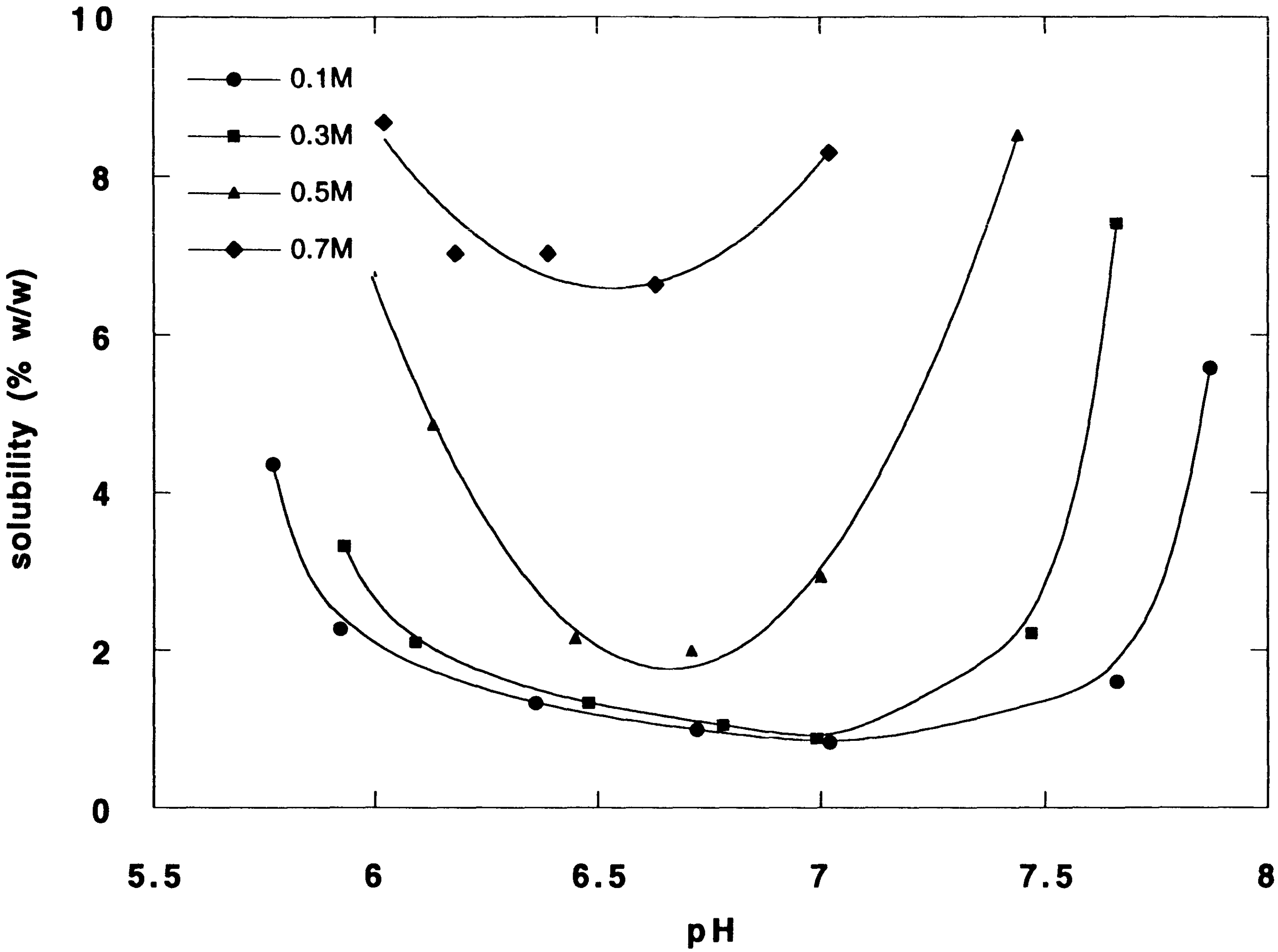

Figure 2.4 Solubility of triblock copolymer 2 as a function of pH at different KCl concentrations.

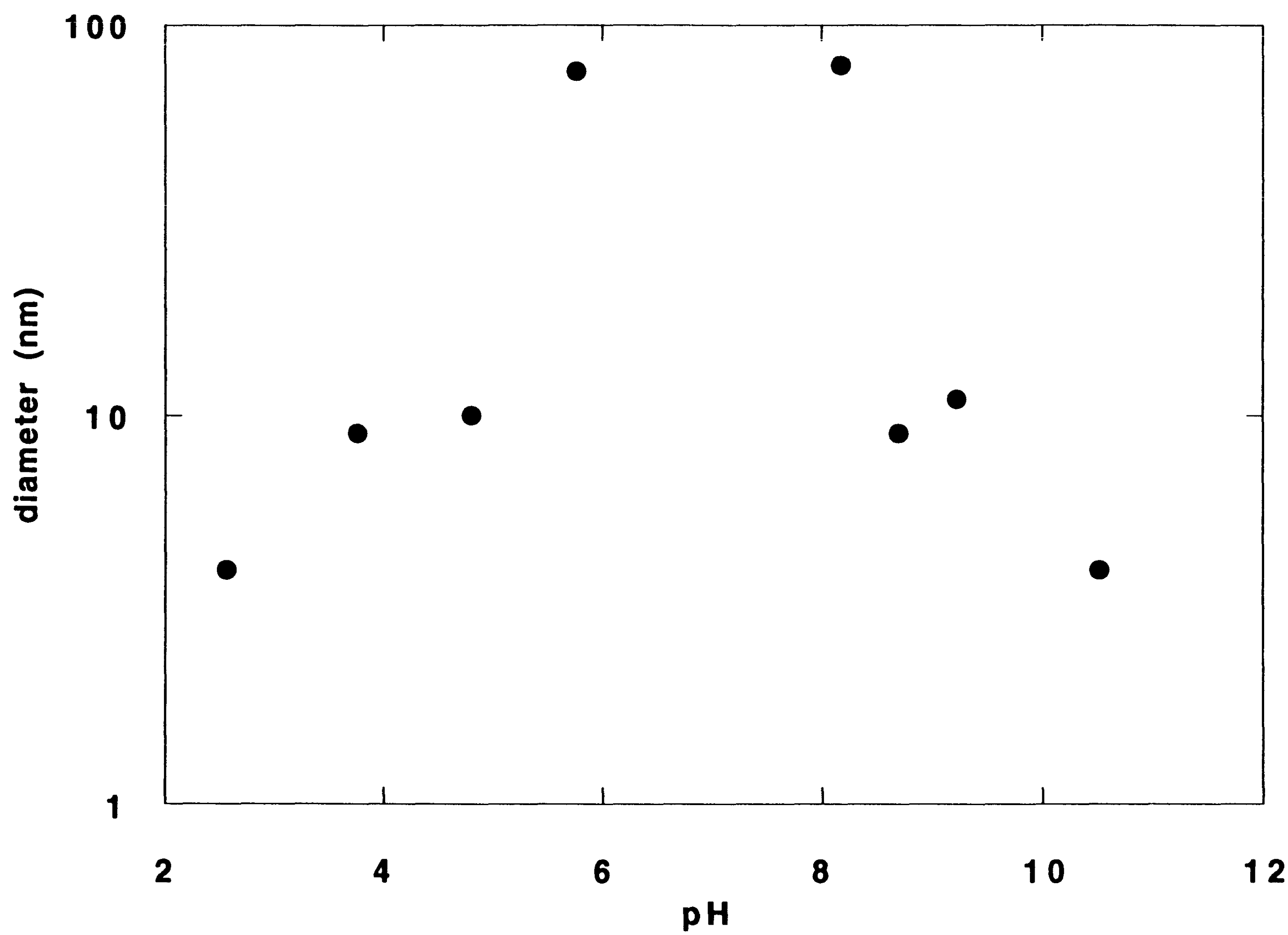

Figure 2.5 Hydrodynamic diameter of triblock copolymer 2 at different pH with no added salt.

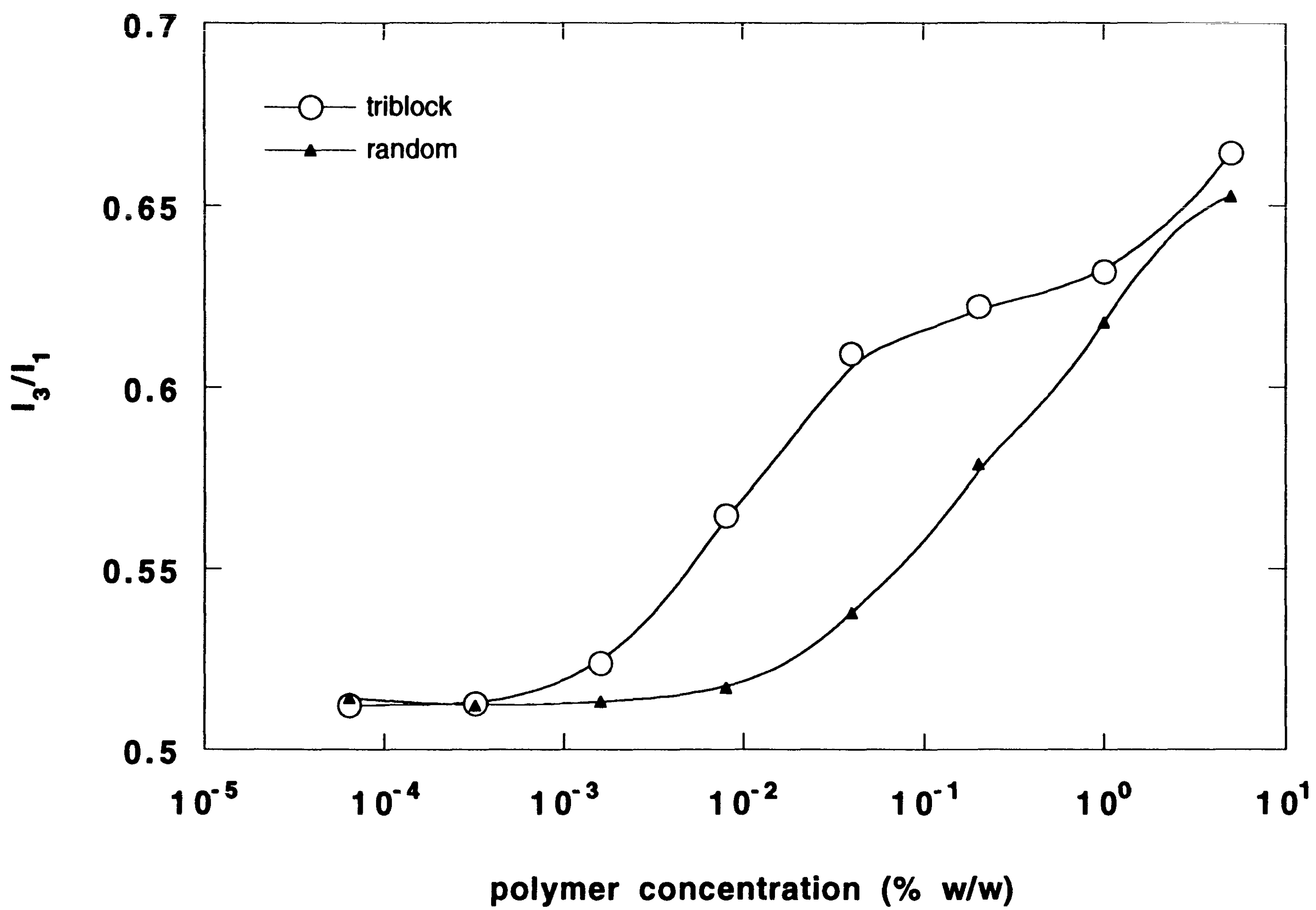

Figure 2.6 Comparison of the intensity ratio of pyrene fluorescence of triblock polymer 2 and random polymer 12.

Chapter 3.

Aqueous Size Exclusion Chromatography of the Methacrylic Polyampholytes.

3.1 Introduction

In addition to the static and dynamic light-scattering, and steady-state pyrene fluorescence techniques employed in Chapter 2 [1] to probe the micellization of the methacrylic polyampholytes, it was considered necessary to perform Size Exclusion Chromatography (SEC) in water. The SEC confirmation of the results obtained by the other characterization methods will be of great significance because the size determination by SEC is direct and, in contrast to the scattering techniques, not the product of mathematical calculations. More importantly, SEC provides the whole molecular weight distribution profile.

The first attempts of aqueous SEC characterization of the copolymers did not give results due to adsorption of the polymers on the columns. The conditions used then must have favored adsorption. The value of the pH was at 5 which rendered the polyampholyte net charge positive. The SEC columns bear some undesired acidic functionalities that charge them negatively. Furthermore, although the ionic strength employed was moderately high, at 0.2M KCl, it must still have been relatively low for our polymers, which are rather highly charged. It is known that, depending on the nature of the packing and the charge density and molecular weight of the polymer, an ionic strength between 0.05 and 0.6M may be required to prevent polyelectrolyte adsorption on to SEC columns [2].

In this study, the conditions were chosen so that adsorption was disfavored. The value of the pH was 8.5 so that the polymers were net negatively charged. The ionic strength was very high, at 1M KCl, in order to effectively suppress the electrostatic interactions. Although the most detrimental type of ionic interaction would be adsorption of the positively charged block to the matrix, other types of such interactions would be ion exclusion (also referred to as electrostatic depletion) of the net negatively charged polyampholyte from the pores of the matrix [2-4], ion inclusion of the cationic counterions of the polyampholyte [2] and intramolecular electrostatic expansion of the polyampholyte [2]. We recognize that the structure of the micelles might be influenced by the salt concentration, and, therefore, the conclusions of this study should only be considered pertinent to the high ionic strength conditions.

It should be noted that we have already characterized the polyampholytes (prior to pre-acid deprotection) by SEC using tetrahydrofuran as the mobile phase [1]. Tetrahydrofuran is not a selective solvent for any of the blocks which means that the block copolymers can not form micelles in this solvent. Therefore, the present SEC study is the first one that probes the micellar structures of the polyampholytes.

3.2 Experimental Section

3.2.1 Materials

Tris(hydroxymethyl) aminomethane (Tris) and tris(hydroxymethyl) aminomethane hydrochloride (Tris hydrochloride) were purchased from Sigma Chemical. Potassium Chloride was purchased from Mallinckrodt. Milli-Q water was obtained from a Millipore five-cartridge assembly. Narrow molecular weight distribution poly(ethylene oxide) molecular weight standards were purchased from Polysciences and Toyo Soda. Bovine serum albumin, chicken egg albumin, horse radish peroxidase, ribonuclease A and cytochrome c were purchased from Sigma Chemical Co.

3.2.2 Methods

The mobile phase, Tris buffer containing 50mM of Tris hydrochloride and 1M KCl at pH 8.5, was freshly prepared and filtered through 0.2μm Millipore filters prior to use. Volumes of 2mL of 1% w/w polyampholyte solutions were prepared by diluting 10% stock solutions of polyampholytes at pH 8.5 into the mobile phase. The polymer samples were filtered once through 0.2μm Millipore filters into vials which were sealed. A Hewlett-Packard 1090 HPLC system connected to a 1037A Hewlett-Packard differential refractometer was used. A TSK Model PWH guard column, a TSK Model G5000PW (1000 Å average pore size) column and a TSK Model G3000PW (200 Å average pore size) column were connected in series. Volumes of 25μL of samples were injected by a Model 7010 Rheodyne autoinjector. The refractive index traces of the samples were recorded on a Model 3396B Hewlett-Packard integrating recorder.

3.3 Results and Discussion

Figure 3.1 presents the molecular weight calibration curves with PEO standards and globular proteins. Both calibration curves lie in the linear region of the resolving range of the columns as the semilogarithmic plots result in straight lines. The slopes of the two lines are similar probably because of similar Mark-Houwink exponents of proteins and PEO [5]. Because of the compact spherical structure of the proteins as compared to the loose random coil structure of PEO, for a given retention time, the protein molecular weight is approximately four times higher than that of the corresponding PEO species.

We do not expect the random polyampholytes to exhibit the compact structure of the proteins because they are linear macromolecules without any folding patterns. Additionally, because of their similar viscosities (Chapter 10), we expect the block polyampholytes to have the same loose structure as their random counterparts. Furthermore, at the conditions of intermediate pH and high salt concentration employed in this study, the polymers will behave as uncharged random coils rather than charged rigid rods. However, we do not expect the polyampholytes to follow quantitatively the PEO calibration curve because of the different stiffness and Q-factors for the two types of polymers. A Q-factor is defined as the molecular weight per unit length of the fully extended chain [5]. Using an average molecular weight of 114 for the methacrylate residues, it can be calculated that the polyampholyte to PEO ratio of Q-factors is 3.9 =(114/2)/(44/3). Ignoring differences in chain stiffness, the latter may imply that the polyampholytes are described well by the protein calibration curve. On the other hand, taking into account the greater stiffness of the polymethacrylate chain (characteristic ratio = 7 for non-isotactic polymethacrylates, [6]) as compared to that of the PEO chain (characteristic ratio = 4, [6]) impies that the polyampholytes are not as compact as the Q-factors alone suggest, and therefore, their behavior should be intermediate between those of PEO and the proteins.

The most accurate method to deduce molecular weights from SEC is by universal calibration based on the polymer hydrodynamic volume [7]. It is experimentally established that polymers with the same hydrodynamic volume have the same retention in SEC columns. The hydrodynamic volume is the product of the molecular weight and the intrinsic viscosity. This method requires that the intrinsic viscosities of the molecular weight standards and of the sample under investigation be known. As this was not the case, the universal calibration was not pursued.

Table 3.1 lists the results of this study. The polymer structure and the theoretical molecular weight based on the monomer to initiator ratio during synthesis are also given. The peak retention times are converted to molecular weights using the PEO and the protein calibration curves. It can be observed that the calculated molecular weights of the triblocks are much higher than the theoretical values which are around 4,000. On the other hand, the calculated molecular weights for the diblock and the two random polyampholytes, are close to the expected values. More specifically, the theoretical molecular weight is higher than the molecular weight based on the PEO calibration and lower than that based on the protein calibration, as expected. For random Polymer 12, the value of the molecular weight determined by static light-scattering is quoted [1] and compares well with the theoretical value. These observations suggest that the triblock polyampholytes aggregate into micellar structures and the diblock and the random copolymers do not. Therefore, the micellization can be attributed to the presence of the hydrophobic poly(methyl methacrylate) block in the triblocks.

Polydispersity indices of synthetic polymers calculated from SEC may be overestimated if appropriate dispersion corrections are not made. The latter, however, can be very tedious and require highly specialized software [5]. A convenient means to estimate the size inhomogeneity of a polymer sample qualitatively is to compare the peak width at half height of its SEC trace to that of monodisperse standards. The peak width in a monodisperse standard is due to dispersion, while in the case of a non-monodisperse sample, it is due to dispersion and size inhomogeneity.

In Figure 3.2, the peak width at half height of the narrow PEO standards and the protein standards is plotted as a function of the retention time. Although there is peak width dependence on retention time, there is no dependence on the chemical nature of the sample, as expected [5]. Table 3.2 lists the peak widths for the polyampholytes. It can be observed that for the triblock polyampholytes, with the exception of Polymer 9, the peak widths correspond to monodisperse distributions, as they are very close to those of the monodisperse standards. This suggests that the micelles are of spherical as opposed to cylindrical shape. It is known that, while cylindrical micelles are highly inhomogeneous in size, spherical micelles are fairly monodisperse [8].

To estimate the aggregation number of the triblock copolymers within the micelles, the calculated molecular weight is divided by the calculated molecular weight of random Polymer 12. The results are shown in the last columns of Table 3.2. It is interesting to see that the aggregation numbers calculated from the two different calibration curves agree well and range between 10 and 40. The aggregation numbers calculated from replicate experiments are shown in parentheses. It should be pointed out that the aggregation number of Polymer 2 calculated here to be 10 differs from the value of 23 determined in Chapter 2 from static light-scattering data. The largest micelles are formed by Polymer 1 that bears the hydrophobic block at the edge of the molecule. We can anticipate that aggregates formed by triblocks bearing the hydrophobic block in the middle (Polymers 2, 9, 5, 10) of the molecule will have a size approximately one-half of that of the aggregates of Polymer 2. Polymers 7 and 8 contain one hydrophobic and bulky residue (phenylethyl methacrylate) per chain which makes them have similar aggregation behavior as Polymer 1.

Figure 3.3 is a semilogarithmic plot that compares the SEC retention times of the polyampholytes with the hydrodynamic size of the same polymers as determined by QELS. It has to be noted that although their pH was around 8.5, the samples studied by QELS contained no salt. The two families of data correlate very well and they fall on an almost straight line.

3.4 Conclusions

The SEC experiments of this study unambiguously confirm the aggregation behavior of the methacrylic polyampholytes which was observed independently by QELS. The present observations suggest that the triblock copolymers form micelles with aggregation numbers ranging from 10 to 40. The diblock and random copolymers, lacking a hydrophobic block, do not aggregate and the calculated molecular weights are in reasonable agreement with those expected from the polymerization stoichiometry.

3.5 Literature Cited

(1) Patrickios, C. S.; Hertler, W. R.; Abbott, N. L.; Hatton, T. A. Synthesis and Solution Properties of Random and Block Methacrylic Polyampholytes. Accepted for publication in *Macromolecules*.

(2) Barth, H. G. Characterization of Water-soluble Polymers Using Size-Exclusion Chromatography. *Water-Soluble Polymers: Beauty with Performance*; Glass, J. E., Ed.; ACS Symposium Series 213, American Chemical Society: Washington DC 1986, 31-55.

(3) Dubin, P. L.; Larter, R. M.; Wu, C. J.; Kaplan, J. I. Size-Exclusion Chromatography of Polyelectrolytes: Comparison with Theory. *J. Phys. Chem.* **1990,**

94, 7243-7250.

(4) Hoagland, D. A. Electrostatic Interactions of Rodlike Polyelectrolytes with Repulsive, Charged Surfaces. *Macromolecules*, **1990**, *23*, 2781-2789.

(5) Tung, L. H.; Moore, J. C. Gel Permeation Chromatography. *Fractionation of Synthetic Polymers: Principles and Practices;* Tung, L. H., Ed.; Marcel Dekker: New York 1977, 545-648.

(6) Flory, P. J. *Statistical Mechanics of Chain Molecules*; Oxford Univ. Press: New York, 1988; pp 41-42.

(7) Grubisic, Z.; Rempp, P.; Benoit, H. A Universal Calibration for Gel Permeation Chromatography. *J. Polym. Sci., Polym. Let.* **1967**, *5*, 753-759.

(8) Israelachvili, J. *Intermolecular and Surface Forces*; Academic Press: London, 1992; pp 354-362.

Table 3.1 Peak molecular weights of the polyampholytes.

Pol	Formula[1]	MW(theory)[2]	t_R (min)	MW(PEO)	MW(prot)
11	$B_{10}A_{10}$	2430	19.368	2330	8900
12	$(BMA)_{12}$	4116[3]	19.165	2730	10500
13	$(B_{1.33}MA_{0.67})_{12}$	4400	19.000	3100	12100
2	$B_{12}M_{12}A_{12}$	4116	16.185	28000	121000
9	$B_{16}M_{12}A_{8}$	4400	15.740	39600	174000
5	$B_{10}M_{20}A_{10}$	4430	15.361	53200	238000
10	$B_{8}M_{12}A_{16}$	3812	15.145	63000	284000
7	$PB_{12}M_{12}A_{12}$	4306	15.070	66800	301000
8	$B_{12}M_{6}PM_{6}A_{12}$	4306	14.789	83000	380000
1	$M_{12}A_{12}B_{12}$	4116	14.520	103000	473000

[1]B = dimethylaminoethyl methacrylate; A = methacrylic acid; M = methyl methacrylate; P = phenylethyl methacrylate.

[2]End-group contribution not included.

[3]Weight-average molecular weight was determined to be 5500 by static light-scattering.

Table 3.2 Peak widths and aggregation numbers of the polyampholytes.

Polymer	Width (min)	n(PEO)	n(protein)
11	2.448	------	-------
12	2.186	1	1
13	3.161	------	-------
2	1.241	10 (11)	11 (13)
9	2.621	15 (18)	17 (21)
5	1.592	20 (20)	23 (23)
10	1.307	23	27
7	1.469	24 (24)	29 (29)
8	1.202	30	36
1	1.225	38 (38)	45 (45)

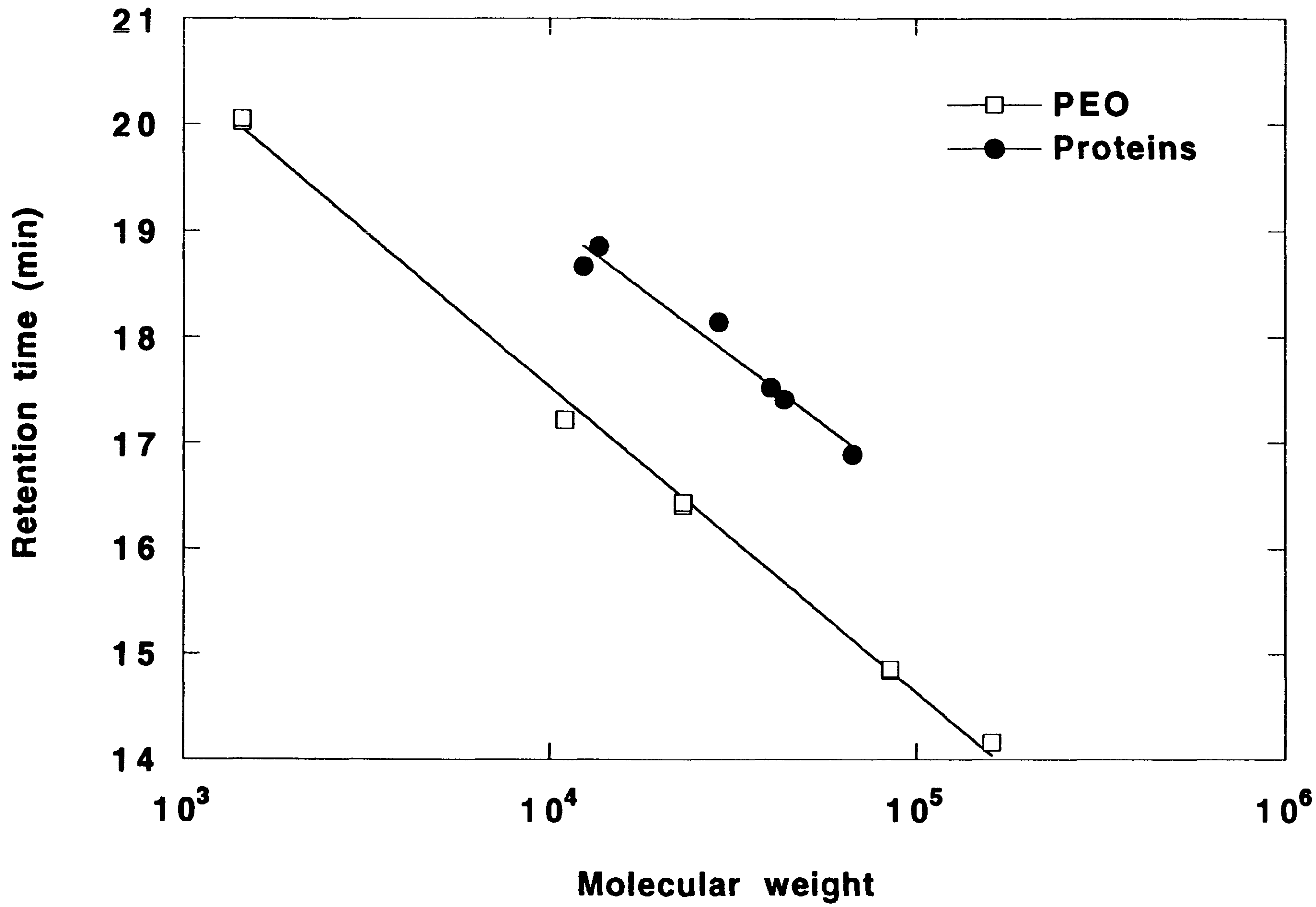

Figure 3.1 Molecular weight calibration curves with poly(ethylene oxide) standards and globular proteins.

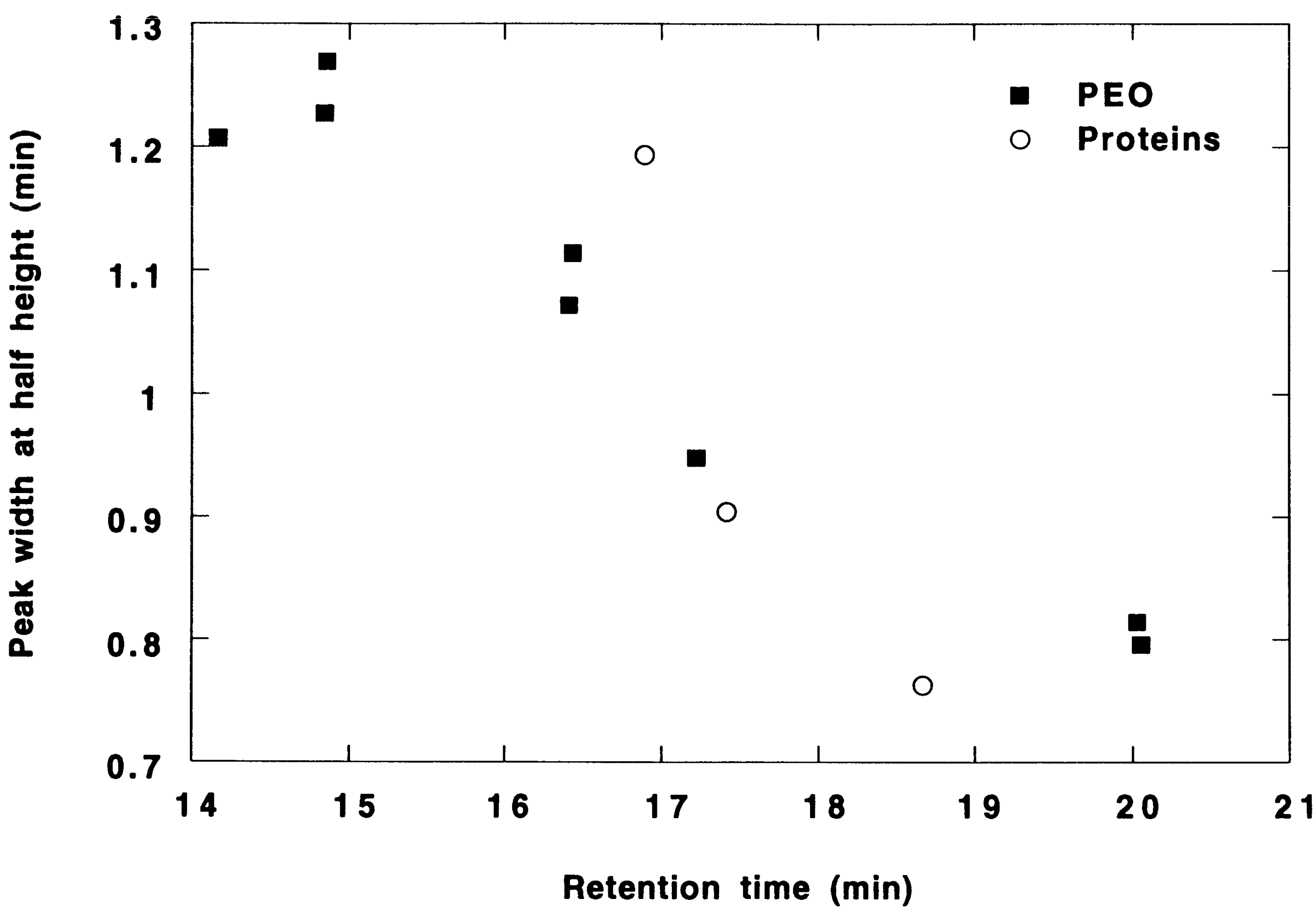

Figure 3.2 Dependence of band broadening on retention time.

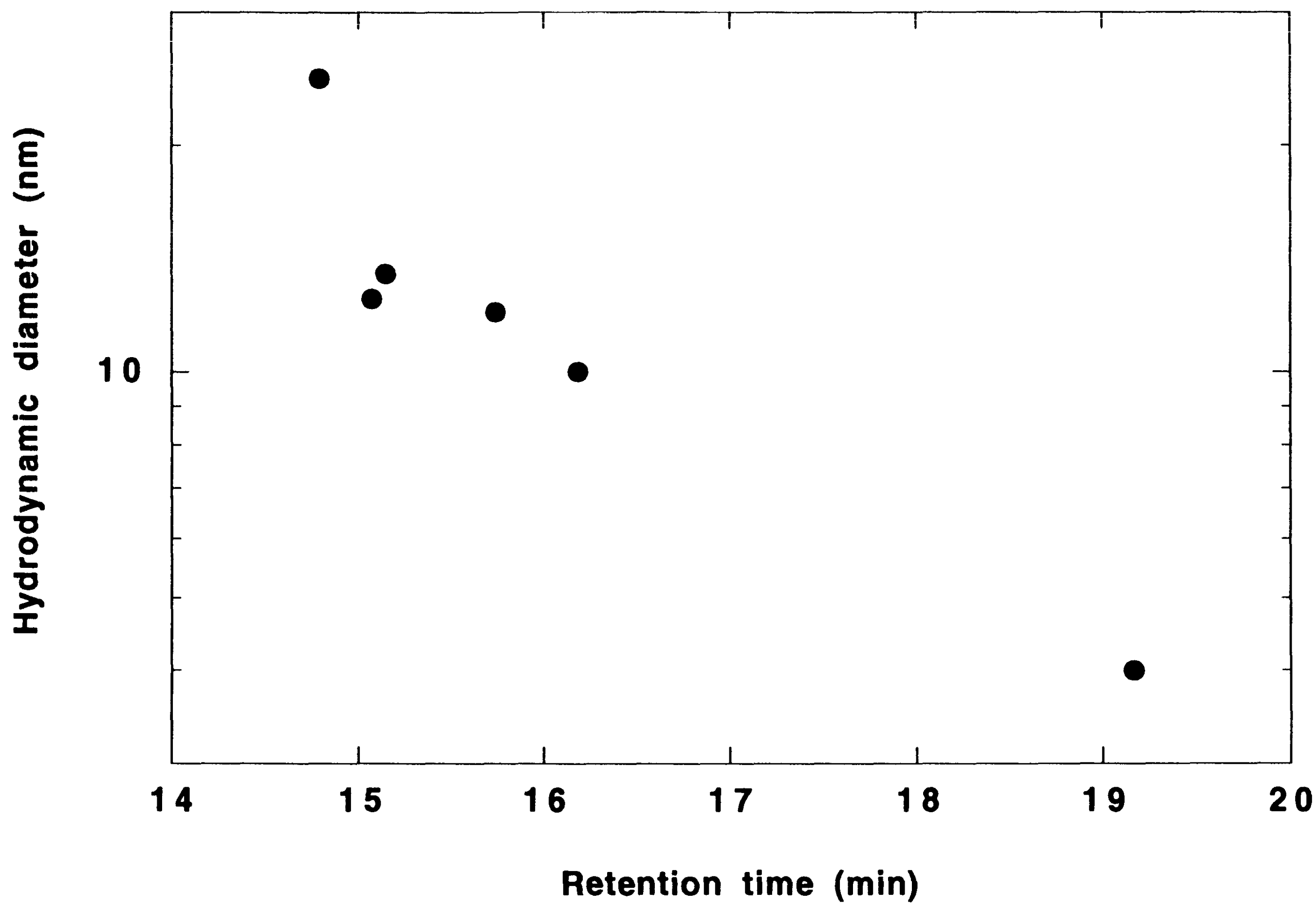

Figure 3.3 Comparison of hydrodynamic size determined by QELS with retention time in SEC columns.

Chapter 4.

Anion-Exchange Characterization of the Methacrylic Polyampholytes.

Following the SEC characterization of the polymers presented in Chapter 3, we proceed in this Chapter to their characterization in ion-exchange columns. Unlike the thrust of the previous Chapter which was to distinguish which polymers form micelles and which do not, the objective here is to determine the polymer affinity for the column. The information obtained from the ion-exchange characterization will be useful in Chapter 7 where the polymers will be used as ion-exchange displacers for protein separation. More specifically, from the salt gradient elution experiments in this chapter, it will be concluded that, while the random copolymers have a low ion-exchange affinity, the block copolymers, including the diblock, have an affinity higher than that exhibited by proteins. This suggests that the block copolymers can efficiently displace proteins from ion-exchange columns, and the random copolymers can not.

4.1 Introduction

Ion-exchange displacement chromatography of proteins is a separation technique in which a mixture of proteins is adsorbed on the column and subsequently displaced by a polyelectrolyte of higher column affinity, the displacer. This technique results in concentrated protein fractions and is therefore particularly suitable for separations of mixtures in which the desired proteins occur in very low concentrations. As displacement chromatography is gaining popularity, the quest for more efficient displacers is becoming necessary [1].

Block polyampholytes would be attractive displacers for ion-exchange displacement chromatography, because the various blocks could perform various distinct tasks. The adsorbing block should be made such that, at the displacement conditions, it acquires a high charge density (of polarity opposite to that of the matrix) so that the polymer as a whole has a high affinity for the stationary phase. The repelling block should be able to acquire a high charge density (of the same polarity as that of the matrix) at conditions different from those of the displacement so that column regeneration is facilitated. Other blocks might be added to offer other advantages. For example, a hydrophobic block would be added to make possible polymer precipitation (at different conditions from those of displacement and regeneration) which would facilitate polymer reuse. With these thoughts we proceeded to the synthesis of the block polyampholytes described in Chapter 2 [2].

These polyampholytes contain up to four different methacrylic residues: methacrylic acid (Ac) which can be negatively charged and has a pK of 5.4 [3], dimethylaminoethyl methacrylate (B) which can be positively charged and has a pK of 8.0 [3], methyl methacrylate (M) which is neutral and hydrophobic, and phenylethyl methacrylate (P) which is neutral and more hydrophobic than methyl methacrylate. The Group Transfer Polymerization (GTP) technique used for the synthesis resulted in polymers with polydispersities as low as 1.3 and high composition homogeneity. The molecular weight of the polyampholytes is approximately 4,000 Da, with the exception of one polymer which is 15,000 Da. One neutral and one base-rich random polyampholytes were also synthesized. One polyampholyte is a neutral diblock (MW = 2,400 Da) and the rest are ABC triblocks with different acid/base ratio, hydrophobicity, and block sequence. Table 4.1, in the Results and Discussion section, gives the composition and sequence of most of our copolymers. The polymer numbering in this Table is consistent with the numbering in Table 2.1. Both the diblock and the triblock copolymers precipitate around the isoelectric point. Light scattering studies revealed that at intermediate pH (=3-10) the triblocks, not the diblock, form micelles with a hydrodynamic size larger than 10 nm. A steady-state pyrene fluorescence study on Polymer 2 (Table 4.1) at pH 4.5 indicated a very low critical micellar concentration (around 0.01mg/mL) suggesting that, at the polymer concentrations employed in this study, typically 10 mg/mL, the triblock polyampholytes occur as micellar aggregates rather than free chains.

The aim of this study is to investigate the chromatographic behavior of these novel polyampholytic displacers in the absence of proteins. Most of the experiments were performed at pH 8.5 at which all of the polymers are soluble. The polymer parameters determined are the adsorptive capacity, the characteristic charge, and the steric factor [4-7]. The characteristic charge is determined as the number of ionic bonds that a polymer forms with the stationary phase. The steric factor is the number of inaccessible column sites per polymer molecule at maximum (lowest salt concentration) column saturation.

4.2 Experimental Section

4.2.1 Materials

An analytical Waters Ion Exchange column of internal diameter 5mm was packed to a length of 39mm with 8μm strong anion exchange (quaternary methylamine) beads of 100 nm average pore size. The same column was used for both the gradient elution and the frontal experiments. The equilibration buffer was Tris, typically at pH 8.5 and containing 50 mM Cl^-. A Waters Maxima 820 workstation was used for data acquisition.

4.2.2 Methods

Gradient Elution. A linear 10 min-gradient from 0.2 to 1.0M NaCl was applied at a flow rate of 0.5 mL/min using a Waters 600 Multisolvent Delivery System. The gradient delay was 9 min (due to the volume of the mixing chamber) and the dead volume of the column was 0.6 mL. A Waters 481 Lamda-Max LC Spectrophotometer was used to monitor the column effluent at 240 nm. It was not convenient to employ the wavelength of 310 nm used in the frontal experiments because the signal-to-noise ratio was very low. 20μL of 10 mg/mL polymer samples prepared in Tris of pH 8.5 and 50 mM Cl^- were injected using a Rheodyne manual injector.

Frontal Experiments. Five frontal experiments (five steps) were performed for the characterization of each polymer at column saturation [6]. An LKB 2150 HPLC pump was used for solvent delivery and a Spectroflow 757 detector was used to measure the absorbance of the effluent at 310 nm. A ten-port Valco manual injector with a 10 mL loop was used to inject the polymer, the nitrate, and the regenerant solutions. In the first frontal experiment (step 1), the column capacity in small anions was calculated by passing a front of 100 mM sodium nitrate at 0.5 mL/min through the equilibrated column and determining the nitrate breakthrough time. Second, after reequilibrating the column with buffer, a front of 10 mg/mL polyampholyte solution was passed at 0.2 mL/min, the polymer breakthrough time was determined and the amount of adsorbed polymer was calculated (step 2). The lower flow rate in step 2 secures low levels of pressure drop and adequate time for polymer adsorption. The non-adsorbed polymer in the dead volume was washed with buffer for 10 column volumes. Third, with the polymer adsorbed, a 30 mM sodium nitrate front was introduced at 0.2 mL/min, the nitrate breakthrough time was determined and the number of column sites not occupied by the polymer was calculated (step 3). The low sodium nitrate concentration was chosen so that the nitrate not displace any polymer. In the case of the one experiment at which the buffer used was only 5 mM Cl^-, a 5 mM sodium nitrate concentration was used. Fourth, a 1M NaCl in 100 mM phosphate solution at pH 7.5 or 3.0 was introduced at 0.2 mL/min to desorb the displacer and regenerate the column (step 4). Fifth, after regeneration, the column was equilibrated with the buffer and a 100 mM sodium nitrate front was passed at 0.5 mL/min to test the regeneration efficiency by determining the nitrate breakthrough time and calculating the column capacity in nitrate (step 5).

In steps 2 and 3, the effluent between the column dead volume and the breakthrough volume was collected and analyzed for polyampholyte by gradient elution, and for chloride ions according to the ASTM assay [8]. For calibration, 1 mL chloride standards in Tris buffers of different pH as well as in deionized water were transferred to 50 mL deionized water and titrated against 0.01M silver nitrate using potassium chromate indicator solution. It was found that while standards in 50 mM Cl^- Tris buffers at pH 7.2 and 7.5 gave the same slope (μmoles of Cl^-/mL of titrant) as standards in deionized water, standards in 50 mM Cl^- Tris buffers at pH 8.5 gave approximately twice the slope probably due to the increased concentration of Tris Amine at this pH which competes with silver ions for chloride. We also observed that the presence of the polycationic impurities in the polyampholytes sometimes caused different color changes in the assay.

4.3 Results and Discussion

Both the gradient elution and the frontal experiments were performed at concentrations of 10 mg/mL that belong to the non-linear part of the polymer isotherm (with the exception perhaps of the random copolymers). The non-linearity at 10 mg/mL was established in preliminary frontal experiments with triblock copolymers and showed that an increase in the feed polymer concentration from 10 to 50 mg/mL had no effect on the amount of polymer adsorbed. Polyelectrolytes of high charge density, such as DEAE-dextran or dextran sulphate, typically exhibit square isotherms with the linear part lying at concentrations below 1 mg/mL [6].

4.3.1 Gradient Elution

Figure 4.1 is the gradient elution chromatogram of the acid-rich triblock polyampholyte (Polymer 10 in Table 4.1). Similar chromatograms were obtained for the other polymers listed in Table 4.1. Polymer 10 comes out of the column after 14 min which corresponds to a salt concentration of 470 mM. The sharpness of this peak suggests that the polymer is homogeneous in composition. Besides the major peak, three small unretained peaks appear that add up to less than 5% of the area of the major peak. This means that the polymer is very pure. The peak at 1 min corresponds to the dead volume of the column and is probably a polycationic impurity (terminated first block and diblock). The other two peaks are probably polymer with a small number of negative charges (early terminated triblock).

The estimation of 95% purity of Polymer 10 is based on the assumption that the impurities and the pure polymer have similar extinction coefficients. If the extinction coefficients of the impurities are smaller than that of the polymer, the purity is lower than 95%. For this reason it was necessary to estimate the purity by a second method. Polymer was dissolved in acid solution and precipitated at the isoelectric point by addition of the appropriate volume of potassium hydroxide solution. This procedure resulted in the purification of the polymer because the impurities do not precipitate. The dissolution-precipitation cycle was repeated five times and, finally, the polymer was dried. A solution of the purified polymer was subjected to gradient elution analysis and the obtained chromatogram was compared to that of the unpurified polymer. The major peak of the unpurified polymer was 15% smaller than that of the purified polymer both in terms of area and height. This suggests that the original sample contained 15% impurities, which can still be considered a small contamination. These results are in agreement with the findings of Möller and coworkers [9] who determined impurity levels around 10% for their copolymers synthesized by GTP.

Table 4.1 summarizes the results of the gradient elution experiments. The retention time at the peak maximum was determined and converted to the corresponding salt concentration. The number of negative charges per polymer molecule (taken from the experimental titration curves) at the pH of the experiment also appears in Table 4.1. By examining the Table, we can make four important observations.

First, the random copolymers (Polymers 13 and 12) are not retained, despite the fact that they have the same composition and molecular weight as block copolymers that are retained (Polymers 9 and 1 and 2). This can be attributed to the random distribution of the adsorbing residues of the random copolymers which results in a lower local charge density. By comparing, for example, Polymers 12 and 2, we can estimate that the linear density in negative charges of the former is the one third of that of the latter. Like the random polyampholytes, most proteins are not retained above 200mM NaCl (in the presence of 50mM Cl^- from the buffer) again due to the random distribution of charges on the protein surface. This suggests a similar ion-exchange affinity of random polyampholytes and proteins which implies that it is unlikely that the former can act as a displacer of the latter.

Second, although the diblock copolymer (Polymer 11) and the random copolymers do not form micelles [2], the diblock is retained. More specifically, it can be observed that it is retained more strongly than triblock Polymer 1 that does form micelles. These imply that, unlike the random copolymers, the diblock copolymer can be used as a displacer successfully.

Third, although all the block polyampholytes are retained, there is no correlation between the retention and the length of the negative block. There is also no correlation between the retention and the net charge (not shown in the Table). There is, however, a strong effect of the hydrophobic block on retention. Focusing on Polymers 11, 2, and 5, which have similar lengths of negative and positive blocks but different lengths of the methyl methacrylate block in the middle, we can see that retention increases with the length of the methyl methacrylate block. This can be attributed to two effects: first, the middle block spaces away from the adsorbing surface the repelling amine block and, second, lateral middle block interpolymer hydrophobic interactions enhance retention. The comparison of the retentions of Polymers 5 and 6 points towards the greater importance of the hydrophobic interactions as the retention of Polymer 6, which bears the very hydrophobic phenylethyl methacrylate residues, is stronger, despite the shorter spacer length. Since the hydrophobic interactions are of short range and since the hydrophobic blocks of the adsorbed molecules are probably not in direct contact, one could dispute the two-dimensional hydrophobic interaction scheme. A different explanation can be given by considering the hydrophobic interactions in three dimensions, i.e. the micellization of the triblocks in solution. The polymer migrates down the column probably not as single chains but as micelles with a charge several times that of the chain monomer. It is likely that a more hydrophobic block will result in micelles with larger aggregation numbers and, therefore, higher micellar charge. It might be expected that retention would correlate well with the micellar charge.

Fourth, by examining Polymers 1 and 4, the significance of the position of the adsorbing block can be inferred. These polymers show decreased retention when the adsorbing block is in the middle of the molecule, which leads to steric hindrance and decreased flexibility of the adsorbing block. Another negative factor is the close proximity of the repelling block to the adsorbing surface. Polymer 4 is retained more than Polymer 1 because it is three times larger.

The above interpretations on the order of elution are qualitative and are not based on any model. A more complete analysis should be performed in the future based on isocratic elution of polymer samples at different salt concentrations which will result in the determination of the characteristic charge and the equilibrium constant [7]. These two quantities define the affinity of the solute for the stationary phase according to the model of Brooks and Cramer [7]. It is therefore likely that the block copolymers with similar adsorbing blocks (and probably similar characteristic charge) exhibited different elution times because of different equilibrium constants. The equilibrium constant is expected to incorporate the effects of the length of the neutral block (hydrophobic interactions and spacing out of oppositely charged blocks) and of the block sequence, in addition to those of the lengths of the adsorbing and repelling blocks (electrostatic interactions). It is worth pointing out that the saturation capacities determined by the frontal analysis in the following section, performed mainly at a single set of conditions, are not expected to be influenced by the equilibrium constant, but should be dictated only by the characteristic charge and the steric factor [7]. Consequently, it should not be surprising if hydrophobic interactions appear to play no role in these results.

4.3.2 Frontal Experiments

Figure 4.2 shows two typical polymer fronts at pH 8.5 and 50 mM Cl^- as monitored at 310 nm. The midpoint of the polymer breakthrough is very clear and can be used to calculate the amount of polymer adsorbed. The shallow breakthrough from 2.5 min (dead volume of the column) to the polymer breakthrough is due to displaced salt and unretained impurities. Samples collected from this volume and analyzed by gradient elution showed the absence of polymer and the presence of unretained impurities. Also chloride analysis demonstrated the presence of chlorides at concentrations higher than that of the buffer. The exact amount of chlorides displaced by the polymer was determined from the chloride analysis. For stoichiometric polymer adsorption, this amount of chloride corresponds to the number of bonds between the polymer and the column.

As already mentioned, after polymer adsorption and washing with buffer, the number of sites inaccessible to the polymer are calculated by passing sodium nitrate and determining the breakthrough volume of the front. Sodium nitrate was chosen as the nitrate ion has a high absorbance at 310nm. Samples collected from this step and analyzed by gradient elution showed an absence of polymer. This analysis confirmed that the nitrate does not displace any polymer, which was expected because the nitrate concentration was lower than that of the chloride in the buffer. As the nitrate front moved through the column, it displaced the chloride ions bound to the column sites which were inaccessible to the polymer. Samples collected from this step and analyzed for chloride resulted in the determination of a number of inaccessible column sites very similar to that determined by the nitrate breakthrough volume. The number of sites occupied by the polymer can be calculated by subtracting the number of inaccessible sites from the total small-ion column capacity of approximately 132 μmoles.

One can argue that the nitrate front will also displace the chloride counterions of the positively charged residues of the adsorbed polyampholyte as well. This will result in an overestimation of the number of inaccessible sites and an underestimation of the number of occupied sites. We checked the extent of this error by comparing the number of occupied sites calculated in step 3 from the nitrate front with the number of occupied sites determined in step 2 from the chloride analysis. The difference was less than 5% which is within experimental error. This should have been expected because at the pH of most of the experiments (=8.5), 40% of the amine residues are uncharged.

Regeneration in step 4 was always successful and it took place in less than two column volumes. At the beginning of regeneration the pressure drop rose up to 20 atm for 2-3 min due to the high concentration of the polymer that was released. The nitrate frontal experiment in step 5 showed that the ion capacity of the column was fully recovered.

Effect of Polymer Type. Table 4.2 summarizes the results obtained for different polymers at pH 8.5 and 50 mM Cl^- and includes the adsorptive capacity, the number of occupied sites as determined from the nitrate front of step 2, and the characteristic charge calculated as the number of occupied sites per adsorbed polymer molecule. By examining the fourth column of the Table it can be observed that, with the exception of random Polymer 12, the number of polymer molecules adsorbed increases as the number of negative charges per molecule decreases. By examining now the sixth column we can see that, again with the exception of the random polymer, the number of occupied sites is always the same, independent of polymer composition. This can be understood because all the polymers have the same adsorbing block, poly(methacrylic acid), located at the end of the molecule. The number of occupied column sites does not appear to be affected by the different lengths of the positive block or the absence of hydrophobic block in Polymer 11. A frontal experiment with poly(methacrylic acid) (an oligomer of 12 units) showed that the homopolymer occupied the same number of column sites as the block copolymers. This confirmed that, at this pH, the non-adsorbing blocks do not affect the adsorption and probably extend vertically from the adsorbing surface as shown in Figure 4.3. The calculated characteristic charge of the block copolymers follows the same trend as the number of negative charges obtained from the experimental titration curves. The random copolymer has the negative charges randomly distributed and "mixed" with the positive ones. This results in a weak driving force for adsorption and in a flat adsorption conformation. These lead finally to the small amount of polymer adsorbed and the smaller number of column sites occupied per molecule.

Effect of pH. Table 4.3 shows the results for the adsorption of the acid-rich polymer at pH from 7.2 to 8.5. It was not possible to go to lower pH because the polymer precipitated. We can see that more polymer molecules were adsorbed as the pH was lowered. For the pH range studied the number of occupied sites did not appreciably change and the experimental hydrogen-ion titration curve suggested that the number of negative charges on the polymer is almost constant. On the other hand, by decreasing the pH from 8.5 to 7.2, the hydrogen-ion titration curve suggested that the number of positive charges per molecule increased from 5 to 8. It seems, therefore, that the stronger repulsion between the matrix and the amine block at lower pH allowed only for a smaller number of negative residues per molecule to interact with the adsorbing surface. Since the number of occupied sites was constant, more polymer molecules per column area adsorbed. It seems that the effect of the increase in the repulsion between the positively charged blocks at lower pH was not as important. It is possible that this increased repulsion was counteracted by the increased attraction between the positive block and the negative block.

Effect of Salt Concentration. We performed one experiment with Polymer 2 at the very low chloride concentration of 5 mM at pH 8.5 to test whether the 50 mM chloride concentration, used in all the previous experiments, was low enough to lead to maximum column occupancy. The results, listed in Table 4.4, indicate that, at the lower ionic strength, more polymer is adsorbed and more column sites are covered. This can be attributed to the weaker screening of the electrostatic interactions between the matrix and the polymer at the lower salt concentration. The constant value of the characteristic charge at the two chloride concentrations suggests that the adsorption conformation remains the same. Assuming now that the column occupancy will not increase further by going to even lower chloride concentrations, we calculate the steric factor for the polymer as the number of inaccessible sites per adsorbed polymer molecule at 5 mM chloride. The steric factor equals 7.3 and the ratio of the steric factor to the characteristic charge equals 7.3/7.2=1.01 which is very similar to that of dextran sulphate [6]. A similar result was obtained in the frontal experiment with the oligo(methacrylic acid) giving again a steric factor to characteristic charge ratio close to one. This is in agreement with the very low (5%) isotacticity of polymethacrylates synthesized by GTP at room temperature [10] which implies that only 50% of the carboxylates can be oriented towards the adsorbing surface.

4.4 Conclusion

The chromatographic techniques of this investigation are powerful tools for providing an understanding of the complicated behavior of our block polyampholytes in two dimensions. At low loading, the polymer affinity to the column is enhanced by the hydrophobic interactions. At column saturation and pH 8.5, the adsorptive capacity is dictated by the size of the adsorbing methacrylic acid block and not by the amine block which is only partially charged (Figure 4.3). At column saturation and at lower pH, the adsorptive capacity is also influenced by the amine (repelling) block which gets fully charged.

4.5 Literature Cited

(1) Cramer, S. M. Displacement Chromatography. *Nature* **1991,** *351,* 251-252.

(2) Patrickios, C. S.; Hertler, W. R.; Abbott, N. L.; Hatton, T. A. Synthesis and Solution Properties of Random and Block Methacrylic Polyampholytes. Accepted for publication in *Macromolecules.*

(3) Merle, Y. Synthetic Polyampholytes. 5. Influence of Nearest-Neighbor Interactions on Potentiometric Curves. *J. Phys. Chem.* **1987,** *91,* 3092-3098.

(4) Kopaciewicz, W.; Rounds, M. A.; Fausnaugh, J.; Regnier, F. E. Retention Model for High-Performance Ion-Exchange Chromatography. *J. Chromatogr.* **1983,** *266,* 3-21.

(5) Jen, S. C. D.; Pinto, N. G. Dextran Sulfate as a Displacer for the Displacement Chromatography of Pharmaceutical Proteins. *J. Chromatogr. Sci.* **1991,** *29,* 478-484.

(6) Gadam, S. D.; Jayaraman, G.; Cramer S. M. Characterization of Non-Linear

Adsorption Properties of Dextran-Based Polyelectrolyte Displacers in Ion-Exchange. *J. Chromatogr.* **1993,** *630,* 37-52.

(7) Brooks, C. A.; Cramer, S. M. Steric Mass-Action Ion Exchange: Displacement Profiles and Induced Salt Gradients. *AIChE J.* **1992,** *38,* 1969-1978.

(8) ASTM *Standard Test Methods for Chloride Ion in Water, Annual Book of ASTM Standards*; Vol. 11.01, ASTM, Philadelphia, PA.

(9) Möller, M. A.; Augenstein, M.; Dumont, E.; Pennewiss, H. Controlled Synthesis and Characterization of Statistical and Block Copolymers by Group Transfer Polymerization. *New Polymeric Mater.* **1991,** *2,* 315-328.

(10) Sogah, D. Y.; Hertler, W. R.; Webster, O. W.; Cohen, G. M. Group Transfer Polymerization. Polymerization of Acrylic Monomers. *Macromolecules* **1987,** *20,* 1473-1488.

Table 4.1 Salt concentration required for polyampholyte elution at pH 8.5.

Polymer	Formula[1]	$[NaCl]^2$ (mM)	# negative charges
13[3]	$(B_{1.33}MA_{0.67})_{12}$	<200	8
12[3]	$(BMA)_{12}$	<200	12
1	$M_{12}A_{12}B_{12}$	247	12
11[4]	$B_{10}A_{10}$	298	10
4[5]	$M_{36}A_{36}B_{36}$	376	36
2	$B_{12}M_{12}A_{12}$	432	12
10	$B_8M_{12}A_{16}$	470	16
8	$B_{12}M_6PM_6A_{12}$	490	12
7	$PB_{12}M_{12}A_{12}$	498	12
9	$B_{16}M_{12}A_8$	500	8
5	$B_{10}M_{20}A_{10}$	525	10
6	$B_{10}P_{10}A_{10}$	550	10

[1]B = dimethylaminoethyl methacrylate; A = methacrylic acid; M = methyl methacrylate; P = phenylethyl methacrylate.

[2]Salt concentration at peak maximum.

[3]Random copolymers.

[4]MW = 2,400.

[5]MW = 15,000.

Table 4.2 Adsorptive capacity and characteristic charge of synthetic polyampholytes at pH 8.5.

Pol	adsorbed (μmoles)	unoc. sites (μmoles)	occ. sites (μmoles)	char. charge	# neg. charges	fraction bound
10	6.39	78.2	53.8	8.4	16	0.53
2	7.52	78.9	53.1	7.1	12	0.59
11	6.63	81.9	50.1	7.6	10	0.76
12	2.91	104.9	27.1	9.3	12	0.78
9	11.3	82.1	49.9	4.4	8	0.55

Table 4.3 Effect of pH on the adsorptive capacity and characteristic charge of the acid-rich triblock polyampholyte (Polymer 10).

pH	adsorbed (μmoles)	unoc. sites (μmoles)	occ. sites (μmoles)	char. charge	# neg. charges	fraction bound
7.2	10.8	75.0	57.0	5.3	15	0.35
7.5	10.0	68.1	63.9	6.4	16	0.40
8.5	6.4	78.2	53.8	8.4	16	0.53

Table 4.4 Effect of salt concentration on the adsorptive capacity and characteristic charge of the neutral triblock polyampholyte (Polymer 2) at pH 8.5.

$[Cl^-]$ (mM)	adsorbed (μmoles)	unoc. sites (μmoles)	occ. sites (μmoles)	char. charge	steric factor
5	9.1	66.2	65.8	7.2	7.3
50	7.5	78.9	53.1	7.1	---

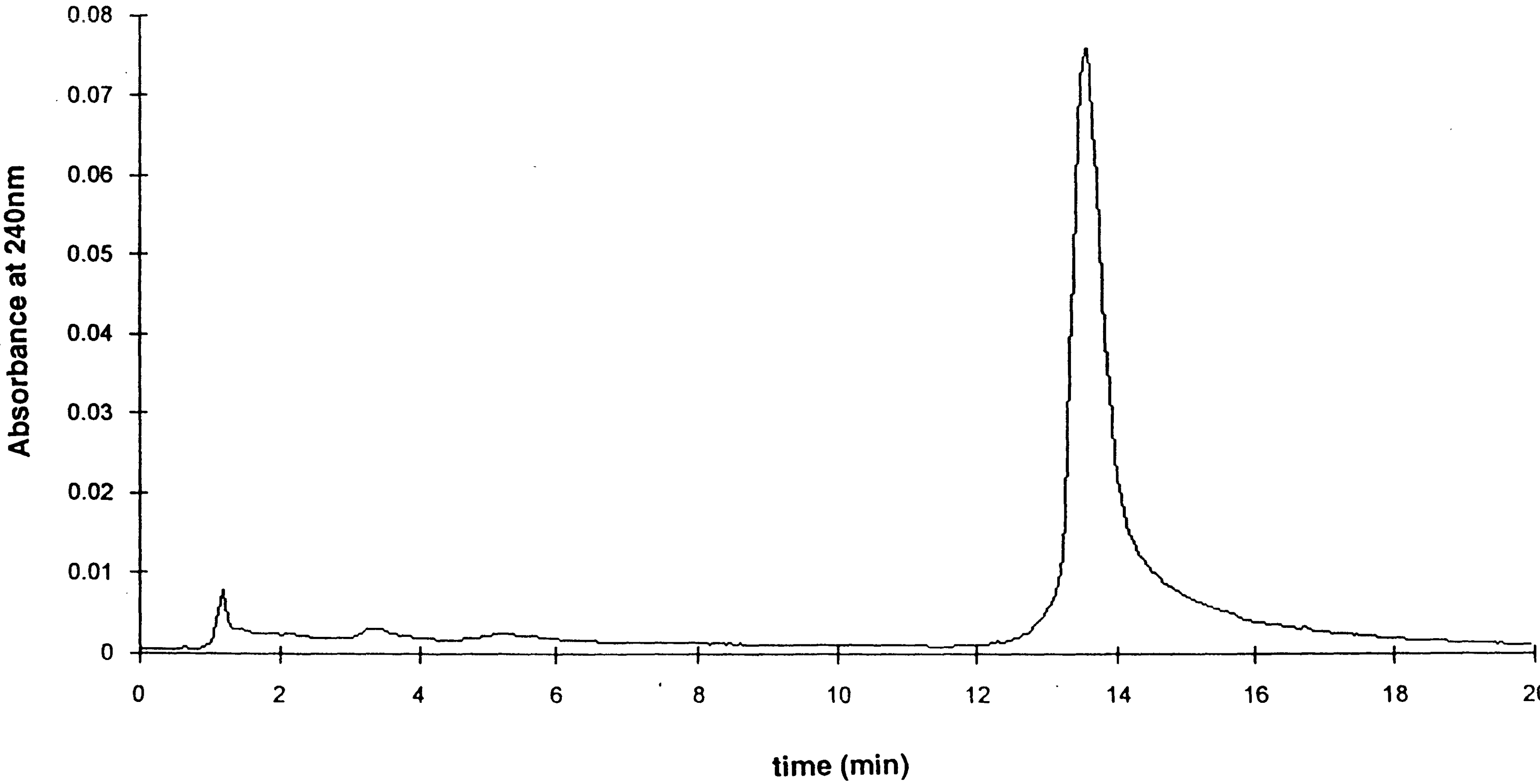

Figure 4.1 Elution of the acid-rich triblock polyampholyte by a linear 0.2-1.0M NaCl gradient at pH 8.5 and flow rate of 0.5mL/min.

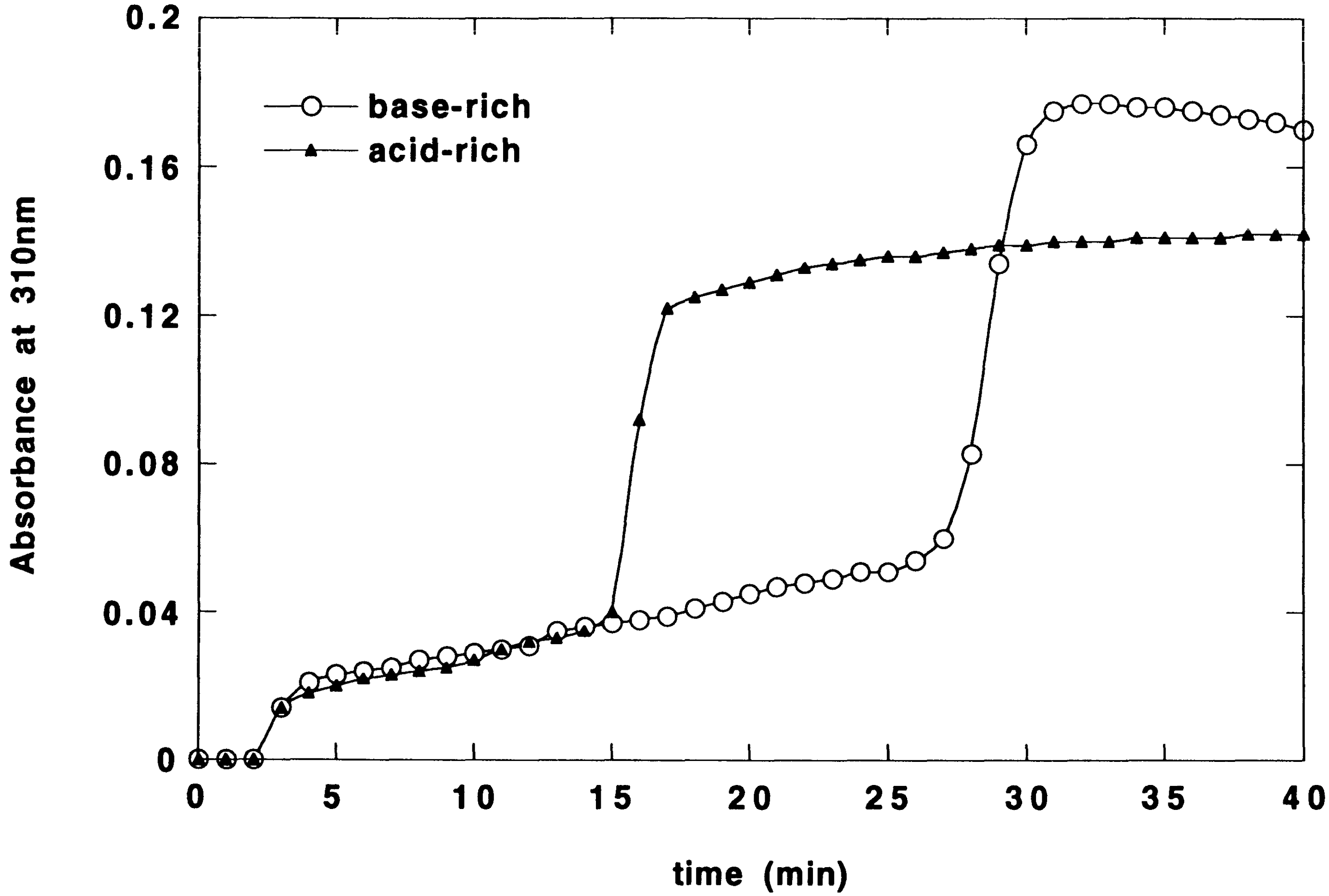

Figure 4.2 Fronts of the acid-rich and base-rich polyampholytes at polymer concentration of 10mg/mL, pH 8.5 and flow rate of 0.2mL/min.

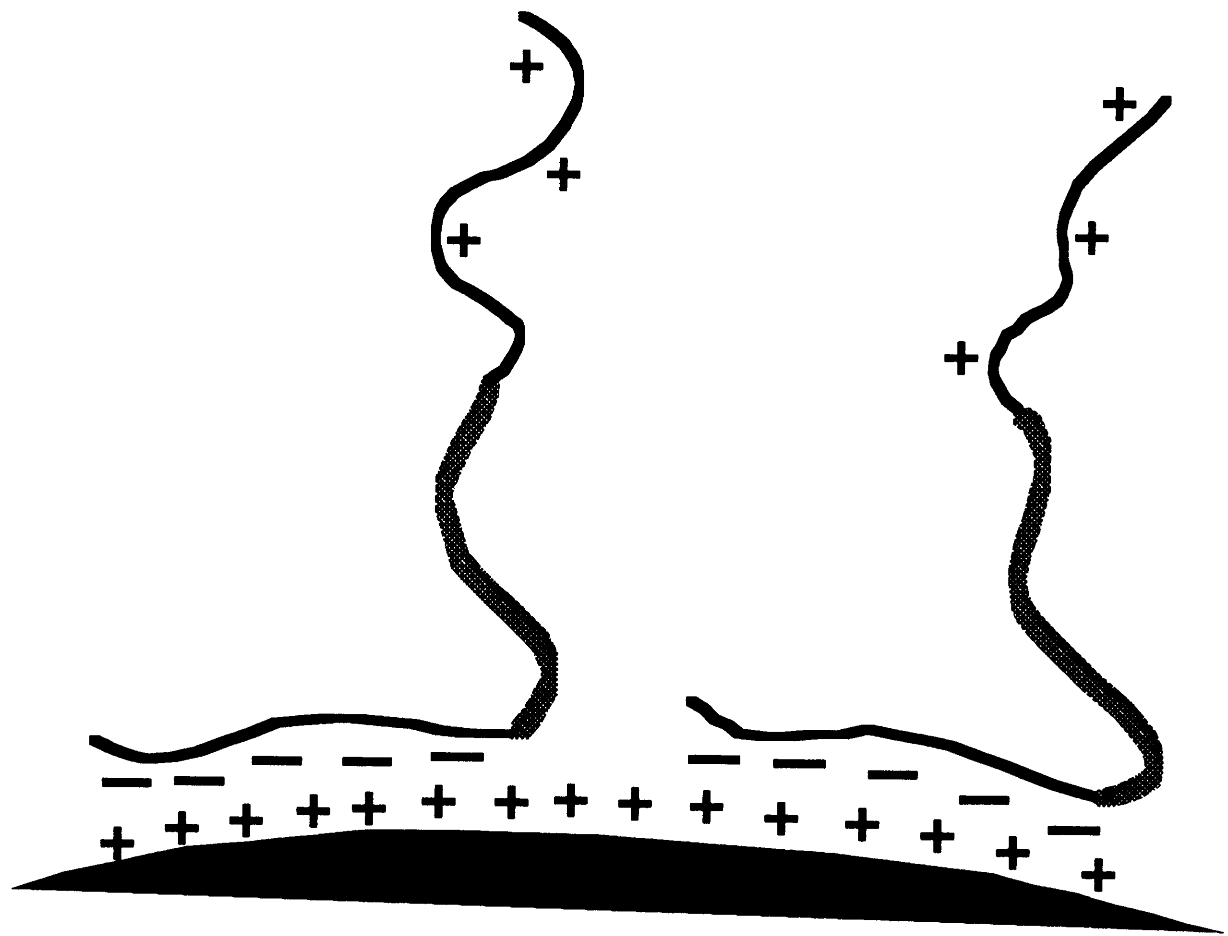

Figure 4.3 Adsorption conformation of a triblock polyampholyte at pH 8.5.

Chapter 5.

Identification of Electrostatic Interactions Between Triblock Methacrylic Polyampholytes and Proteins.

In this chapter we present a preliminary turbidimetric titration study that, besides polyampholyte precipitation, investigates coprecipitation of protein-polyampholyte binary mixtures. The pH at which precipitation or coprecipitation initiates, the critical pH, is determined for different systems and the effect of salt concentration and protein concentration is explored. Protein-polyampholyte interaction is identified by the shift of the critical pH from the value that corresponds to pure polymer to a different value for the binary mixture, generally closer to the isoelectric point of the protein. Owing to the large dilutions at the later stages of titration, the turbidity values are accurate only in the beginning of titration until the critical pH. In Chapter 6, more careful experimental procedures are employed so that dilution is completely avoided and the whole turbidity profile is proper for interpretation.

5.1 Introduction

Synthetic polyelectrolytes are known to interact strongly with proteins of opposite charge and form soluble or insoluble complexes [1]. When the complexation products are insoluble, this interaction may be employed for protein separation [2-6]. The important contribution of the electrostatic forces in these interactions is manifested by the strong dependence of the complexation on pH, salt concentration and the polymer-protein ratio [2-6]. Other determining factors can be the existence of charge patches [1,7] or charged blocks [8] on the protein as well as polymer-protein hydrophobic interactions [9].

While a wide variety of polyelectrolytes has been tested, very few reports involve the utilization of polyampholytes, polymers with both positive and negative charges [10]. In this study we utilize low-molecular-weight block polyampholytes based on methacrylic acid (Ac), dimethylaminoethyl methacrylate (B) and methyl methacrylate (M) and prove that these polymers interact strongly with proteins of opposite net charge. The block acrylic polyampholytes were synthesized by a living polymerization technique and are of a well-defined composition and size, with polydispersity indices less than 1.3. Contrary to previous studies in which the polyelectrolyte polydispersity indices varied from 2 to 10 [2,6] the data interpretation with our polymers is free of size inhomogeneity effects. Another advantage of these polyampholytes related to the protein separation process is their property to precipitate around their isoelectric point, which could facilitate polymer recycling after protein separation. In the previous polyampholyte-protein study [10], a random copolymer was used that did not precipitate at the isoelectric point.

5.2 Experimental Section

5.2.1 Materials

Table 5.1 lists the synthetic polyampholytes utilized in this study along with the number of residues per molecule and the isoelectric point. All the polymers have a molecular weight of approximately 4,000 Da. The first three are triblock copolymers with block sequence B/M/Ac and the fourth is a random terpolymer. All four polymers were introduced in Chapter 2 in Table 2.1. The proteins used are soybean trypsin inhibitor (STI, pI = 4.5), ovalbumin (pI = 4.7), ribonuclease (pI = 8.8) and lysozyme (pI = 11.0).

5.2.2 Methods

Most of the experiments were turbidimetric titrations of pure polymer, pure protein or polymer-protein binary mixtures. Fresh stock solutions of 0.01% w/w polymer and 0.05% w/w protein in 0.01M McIlvane's buffer (citrate and phosphate) were prepared before the titrations. 1 mL of polymer solution or 1 mL of protein solution was taken for the titration of the pure species. Binary solutions of protein and polymer were prepared by mixing 0.5 mL of a 0.05% w/w protein solution with 0.5 mL of a 0.01% w/w polymer solution. The salt concentration was adjusted by adding the appropriate volume of 3M KCl solution. The pH was gradually changed by adding one or two drops of KOH (in most of the experiments) or HCl (in one experiment) of the appropriate concentration. The pH was varied between 4 and 10, and at each pH, the optical density at 420 nm was measured. The experiments were designed so that the pH at which the optical density increases abruptly, the critical pH, was reached within the addition of a small number of drops of reagent in order to keep the extent of protein and polymer dilution as well as the decrease in ionic strength at negligible levels. All the experiments were completed by extensive addition of reagent in order to show the redissolution of the complex after crossing the isoelectric point of the polymer or the protein. The resulting dilution of the mixture allows only qualitative interpretation of the optical density signal, particularly after the critical pH. Another limitation for the interpretation of the data after the critical pH arises from the time-dependence of the optical density. However, it was observed in the kinetic study that the optical density increases very quickly within the first two minutes and subsequently it increases very slowly. Therefore, since the pH change and measurement of the optical density took place less frequently than every two minutes, it can be considered that we were in the regime of a quasi-steady state.

The time-dependence of aggregation was followed using solutions of Polymer N at concentrations 0.004, 0.01, 0.02, and 0.04% w/w prepared at the non-aggregating pH of 4.4. Each sample was transferred to the cuvette and a precalculated amount of KOH solution was added to change the pH to the aggregating value of 6.1. The cuvette compartment of the spectrophotometer was immediately closed and the optical density was measured as a function of time on a chart recorder.

To study the extent of polymer-protein complexation quantitatively, mixtures of Polymer B and STI were prepared at different pH and protein concentrations. Equal volumes of 0.01% polymer and 0.02, 0.05, 0.10, and 0.2% protein were mixed and adjusted to two pH levels, 4.8 and 5.1. After centrifugation for 30 min at 4,000 rpm a two-phase system, composed of an optically clear supernatant and a solid precipitate, resulted. The supernatant was analyzed for protein by measuring the absorbance at 280 nm and the amount of precipitated protein was calculated by mass balance.

5.3 Results and Discussion

Figure 5.1 depicts the time-dependence of aggregation of Polymer N at different polymer concentrations. With increasing polymer concentration the turbidity increases. For the most concentrated solution the optical density exceeds the value of one very quickly. The curves, however, have similar shape and can be divided into two time regimes borderlined at two minutes from the beginning of the experiment. In the early regime the curves are very steep indicating a high rate of aggregation. After two minutes, however, the rate of increase in the optical density is noticeably slower, approaching a constant value.

All but one of the turbidimetric titrations that will be presented below were performed by changing the pH from low to high values and will be referred to as forward titrations. The only backward titration (pH changed from high to low values) is the one presented in Figure 5.4(b). The direction of titration is indicated in the Figures by an arrow.

Figures 5.2(a) and (b) are the turbidimetric titrations of Polymer N and illustrate the effect of polymer concentration and salt concentration, respectively. Figure 5.2(a) shows that the polymer precipitates at pH 5.5 and goes back into solution at pH 8.0. This is a direct result of the pH-dependence of the solubility of the polyampholyte which is very low around the isoelectric point and increases sharply 1-2 pH units away from the isoelectric point. Although the curves of higher polymer concentration display a higher optical density, the critical pH is the same for all polymer concentrations, with a value of 5.5. The independence of the critical pH on polymer concentration is a consequence of the fact that the critical pH is determined by a critical net charge which does not depend on polymer concentration. It is well known that polymer concentration does not influence the titration curve of a polymer. Figure 5.2(b) shows that increasing salt concentration suppresses polyampholyte precipitation. As the concentration of KCl was increased from 0.0 to 0.1, 0.35 and 0.75M, the values of the optical density decreased, and at the same time the critical pH increased approaching the value of the isoelectric pH at the highest salt concentration. The salt weakens the attractive Coulombic interactions and a better balance between positive and negative charges is required for phase separation. This drives the critical pH closer to the isoelectric point of the polymer.

Figure 5.3(a) presents the optical densities of pure Polymer N, pure STI and a mixture of the two. While pure protein solution does not precipitate, pure polymer solution does at pH 5.3 and redissolves close to pH 8. The polymer-protein mixture exhibits a critical pH of 4.6 which is lower than that of pure polymer and close to the isoelectric point of the protein; the mixture also exhibits an optical density higher than that of the pure polymer. Both of the above indicate a strong polymer-protein interaction. Figure 5.3(b) illustrates the effect of salt concentration on Polymer N-STI interaction. The trends are similar to those of Figure 5.2(b). Salt suppresses the interaction as manifested by the decrease in optical density. The critical pH is shifted towards the isoelectric point of the polymer rather than that of the protein because the former has a higher charge density than the latter and, therefore, controls the interaction.

Figure 5.4(a) illustrates the interaction between Polymer B and STI. The trends are identical to those of Figure 5.3(a). The critical pH of the more basic Polymer B is 5.6, slightly higher than that of Polymer N. The critical pH of the mixture, on the other hand, is almost the same for the two polymers and has a value of 4.6. Similar results were obtained for the Polymer B-ovalbumin system. The difference, however, between the critical pHs of pure polymer and the protein-polymer mixture, as well as the difference between the maximum optical densities of pure polymer and the mixture were less pronounced in the ovalbumin case as compared to the STI case, despite the higher molecular weight of ovalbumin. This can be attributed either to extensive charge patches on STI or to the greater hydrophobicity of STI. Figure 5.4(b) is the back titration of Figure 5.4(a) in which the pH was changed from high to low values. Pure polymer solution aggregated at pH 8.0. In the protein-polymer mixture, a first increase in optical density was observed at pH 8.0, due to polymer aggregation, and a second more pronounced increase was observed at pH 5-6 due to polymer-protein aggregation.

In another experiment (not presented here) which involved Polymer R and STI, neither polymer nor polymer-protein interaction was observed because of the lack of charge localization of the random copolymer (low charge density).

Figure 5.5 shows quantitatively the extent of complexation between Polymer B and STI at pH 4.8 and 5.1. These pHs are near the pH of maximum optical density of Figure 5.4(a). The units of the axes are inverse absorbance at 280 nm. The straight-line correlation between the experimental points suggests that the complexation follows the Langmuir model [11]. This can be understood by considering the protein as the adsorbate and the polyampholyte as the adsorbent with a fixed number of binding sites which become saturated as the protein concentration increases. This also seems to imply that the number of polymer molecules available for binding is independent of protein concentration. The latter can be realized only if all or most of the polyampholyte appears in the precipitate. Unfortunately, we were not able to justify this hypothesis because it was not possible to analyze for the very low concentrations of the polymer in the supernatant or the very small amounts of precipitate. However, since in this set of experiments the protein/polymer mass ratio ranged from 2 to 20, we feel that most of the polyampholyte was associated with protein and precipitated. The y-intercepts of the lines correspond to the maximum amount of protein that can complex with the given amount of polymer.

Unlike Figures 5.3-5.5, Figures 5.6 and 5.7 illustrate protein/polymer pairs in which the polymer is more acidic than the protein and, therefore, the polymer-protein critical pH is reached after the polymer critical pH (for forward titrations).

Figure 5.6 presents the optical densities of pure Polymer A and of mixtures of Polymer A with two different concentrations of ribonuclease, 0.025 and 0.25%, with no added salt. The optical density of pure protein solution (not shown) was lower than 0.01. As seen by the sharp changes in optical density, pure polymer aggregates at pH 4.6 and goes back into solution at pH 6.6. The curves of the mixtures preserve the increase in optical density due to pure polymer aggregation and additionally exhibit a peak due to polymer-protein interaction which is 4 to 6 times more intense than that of pure polymer. The critical pH for polymer-protein interaction is 6.2 and drops to 6.1 when the protein concentration is increased by 10 times. By increasing the pH, approaching the isoelectric point of the protein, the polymer-protein complex falls apart as indicated by the decrease in the optical density. The occurrence of the polymer-protein interaction within the pH interval defined by the polymer and protein isoelectric points, where they bear opposite net charges, implies that the interaction is mainly electrostatic. The insensitivity of the critical pH to protein concentration suggests that, for the given polymer, the onset of polymer-protein interaction is defined by a critical protein net charge rather than a combination of protein quantity and charge.

Figure 5.7 demonstrates the interaction between Polymer A and lysozyme. Lysozyme is more basic than ribonuclease A and has an isoelectric point of 11.0. The bottom curve (open triangles) was obtained for pure protein and shows that lysozyme, in the absence of polymer, does not precipitate. The middle curve (open circles) corresponds to pure polymer which precipitates over a pH range of 4.6 to 6.6 which spans the isoelectric point of 5.4. The upper curve (filled squares), which corresponds to the mixture of protein and polymer, implies that there is an interaction between the protein and the polymer because the optical density of the mixture is much greater than that of the average of the protein and the polymer and also because the critical pH of the mixture of 6.4 is very different from that of polymer alone, 4.6.

5.4 Conclusions

We have demonstrated that low-molecular-weight block methacrylic polyampholytes, a new class of charged copolymers, at certain conditions of pH and salt concentration, interact strongly both with themselves and with proteins to form precipitates. The pH-range for interaction is determined by the polymer and protein net charge. Pure polymer self-aggregates around the isoelectric pH, even at the very low polymer concentrations used in this investigation, typically 0.01% w/w. Pure protein does not show any aggregation behavior around its isoelectric pH for the protein concentrations employed in this study, typically 0.05% w/w. Polymer-protein mixtures interact in a pH-range between the isoelectric point of the protein and the self-aggregation pH of the polymer. Increasing salt concentration suppresses the polymer-polymer and protein-polymer interaction, confirming that the main driving force for self-aggregation and polymer-protein complexation is electrostatic. Like the homopolyelectrolyte-protein interaction, the polyampholyte-protein interaction can be used for protein separation processes, exploiting the selective complexation of the polymer with proteins of opposite charge. However, the self-aggregation of the polymer will provide the ability for polymer removal and recycling at the end of the process. One disadvantage of these polymers for the proposed separation process is the low molecular weight. It is expected that block polyampholytes with molecular weight of typically 50,000 will be more efficient both in terms of self-aggregation and polymer-protein interaction.

5.5 Literature Cited

(1) Park, M. P.; Muhoberac, B. B.; Dubin, P. L.; Xia, J. Effects of Protein Charge Heterogeneity in Protein-Polyelectrolyte Complexation. *Macromolecules* **1992**, *25*, 290-295.

(2) Strege, M. A.; Dubin, P. L.; West, J. S.; Flinta, C. D. Protein Separation via Polyelectrolyte Complexation. *Protein Purification*; Ladisch, M. R., Willson, R. C., Painton, C. C., Builder, S. E., Eds., ACS Symposium Series, Washington, DC 1990; Vol. 427, 66-79.

(3) Strege, M. A.; Dubin, P. L.; West, J. S.; Flinta, C. D. Complexation of Poly(dimethyldiallylammonium chloride) and Globular Proteins. *Downstream Processing and Bioseparation*; Hammel, J.-F., Hunter, J. B., Sikdar, S. K., Eds., ACS Symposium Series, Washington, DC 1990; Vol. 419, 158-169.

(4) Dubin, P. L.; Ross, T. D.; Sharma, I.; Yegerlehner, B. E. Coacervation of Protein-

Polyelectrolyte Complexes. *Ordered Media in Chemical Separations*; Hinze, W. L., Armstrong, D. W., Eds., ACS Symposium Series, Washington, DC 1987; Vol. 342, 162-169.

(5) Clark, K. C.; Glatz, C. E. Protein Fractionation by Precipitation with Carboxymethyl Cellulose. *Downstream Processing and Bioseparation*; Hammel, J.-F., Hunter, J. B., Sikdar, S. K., Eds., ACS Symposium Series, Washington, DC, 1990; Vol. 419, 170-187.

(6) Shieh, J.; Glatz, C. E. *Polym. Prepr.* **1991,** *32,* 606.

(7) Xia, J.; Dubin, P. L.; Kim, Y.; Muhoberac, B. B.; Klimkowski, V. J. Electrophoretic and Quasi-Elastic Light Scattering of Soluble Protein-Polyelectrolyte Complexes. *J. Phys. Chem.* **1993,** *97,* 4528-4534.

(8) Parker, D. E.; Glatz, C. E.; Ford, C. F.; Gendel, S. M.; Suominen, I.; Rougvie, M. A. Recovery of a Charged-Fusion Protein from Cell Extracts by Polyelectrolyte Precipitation. *Biotech. Bioeng.* **1990,** *36,* 467-475.

(9) Sternberg, M.; Hershberger, D. Separation of Proteins with Polyacrylic Acids. *Biochim. Biophys. Acta* **1974,** *342,* 195-206.

(10) Morawetz, H.; Hughes, W. L., Jr. The Interaction of Proteins with Synthetic Polyelectrolytes. I. Complexing of Bovine Serum Albumin. *J. Phys. Chem.* **1952,** *56,* 64-69.

(11) Scopes, R. K. *Protein Purification: Principles and Practice*; Springer-Verlag: New York, 2nd ed., 1988; pp 81-84.

Table 5.1 Properties of the polyampholytes.

Polymer	# in Table 2.1	B/M/Ac	pI
A (acidic)	10	8/12/16	5.4
N (neutral)	2	12/12/12	6.6
B (basic)	9	16/12/8	8.0
R (random)	12	12-12-12	6.6

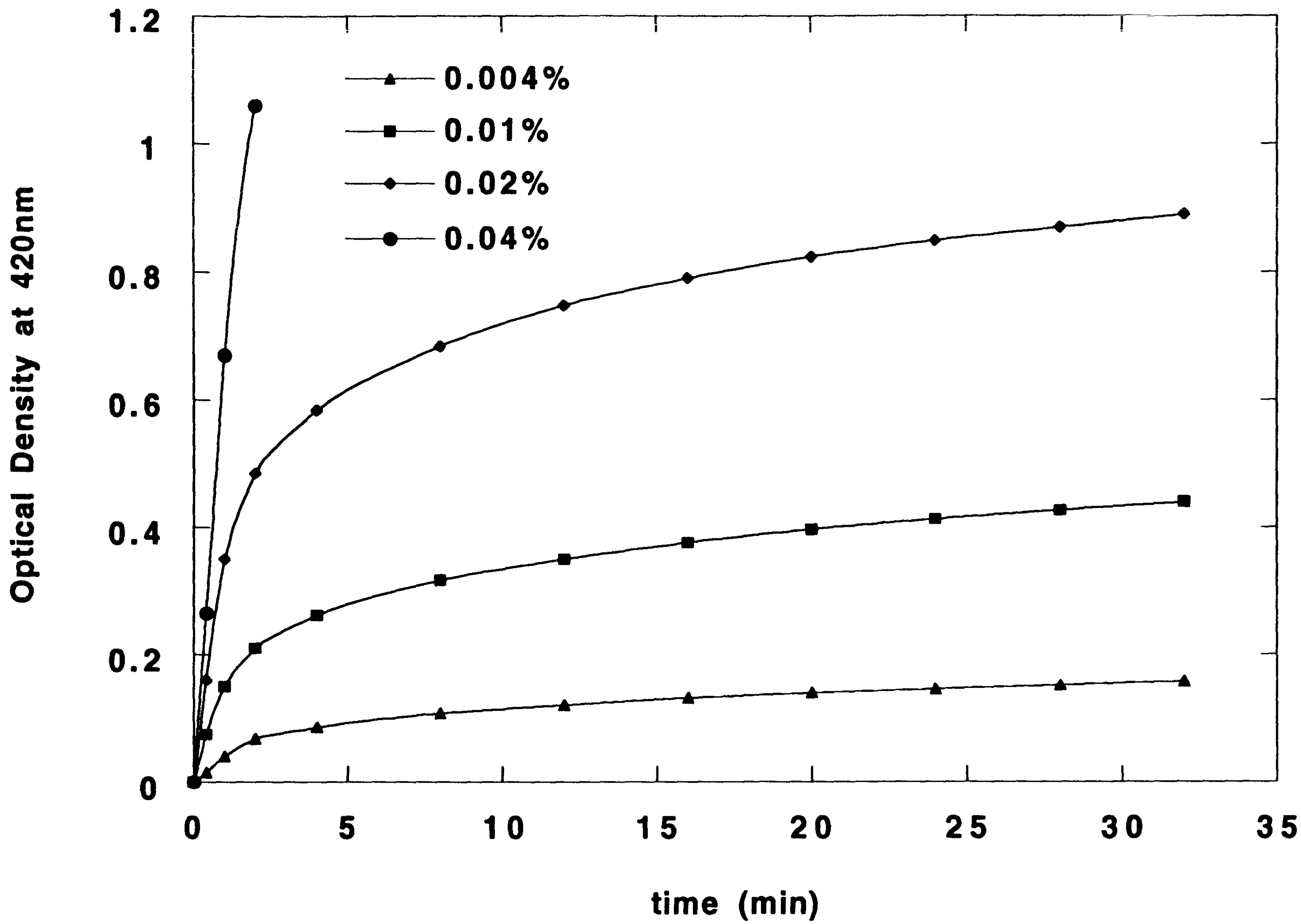

Figure 5.1 Time-dependence in self-aggregation of Polymer N at different polymer concentrations at pH 6.1.

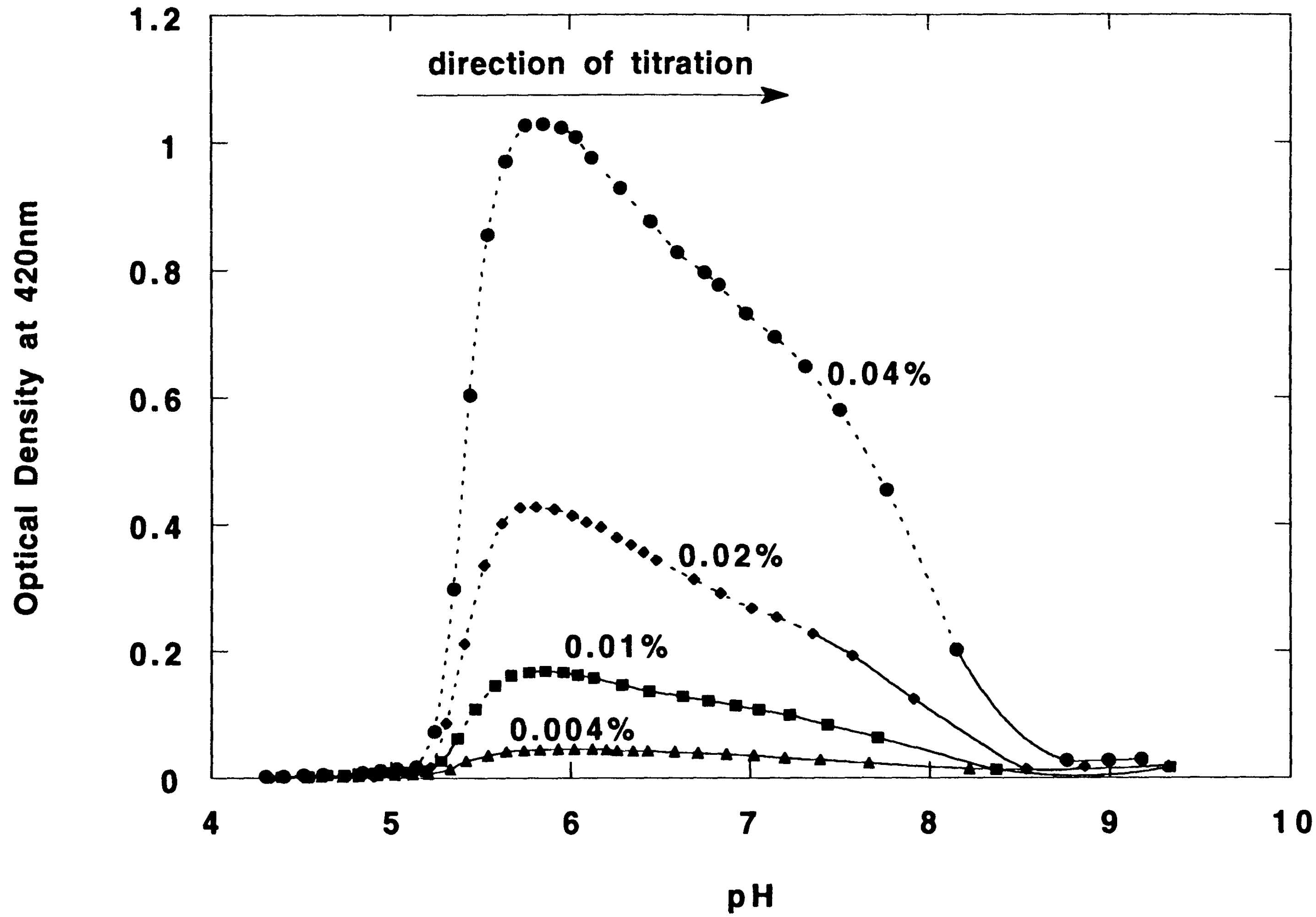

Figure 5.2(a) Self-aggregation of Polymer N at different polymer concentrations. Dotted lines denote unstable optical density readings.

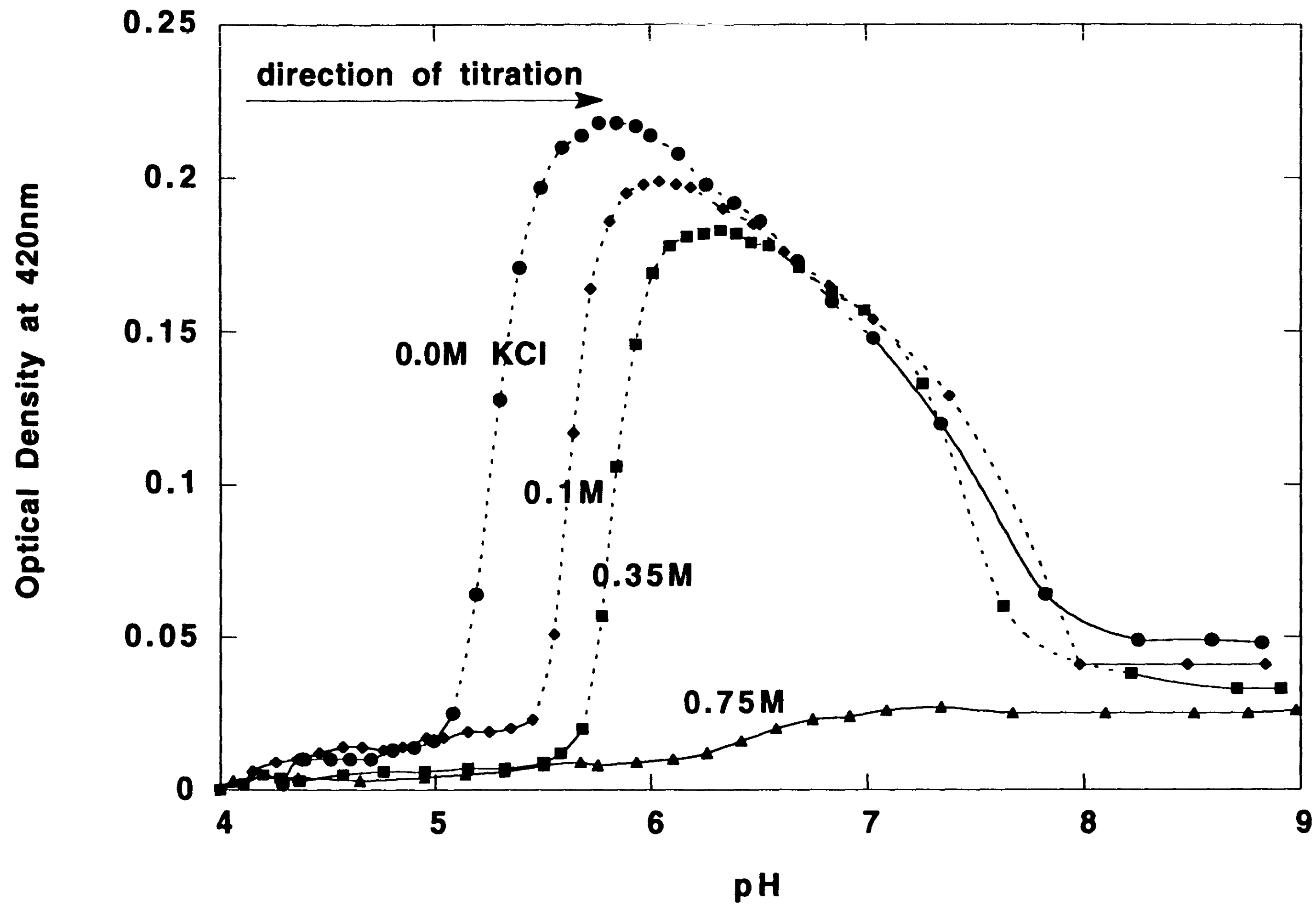

Figure 5.2(b) Self-aggregation of 0.01% Polymer N at different salt concentrations. Dotted lines denote unstable optical density readings.

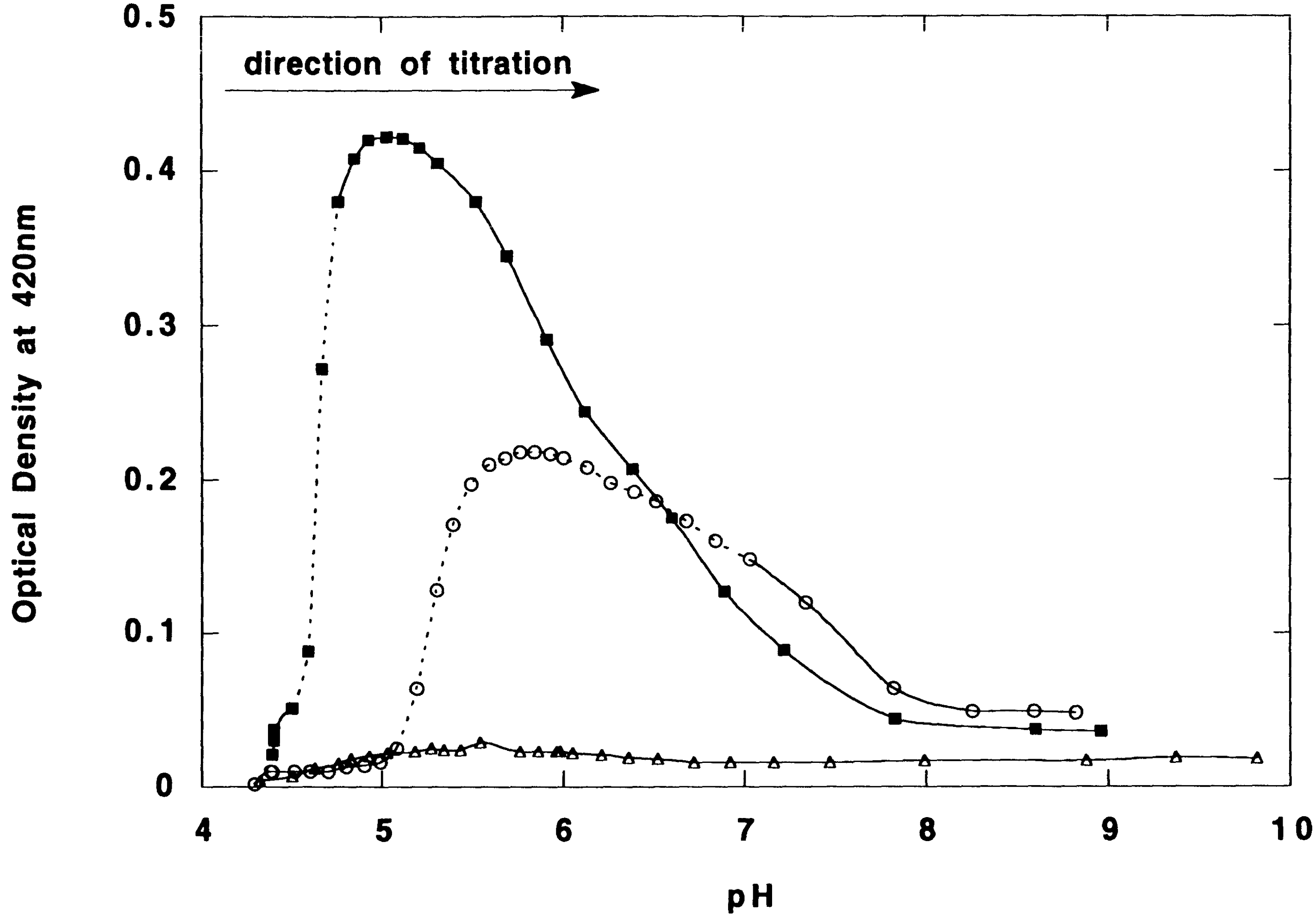

Figure 5.3(a) Optical densities of 0.01% Polymer N (open circles), 0.05% STI (open triangles) and mixture containing 0.025% STI and 0.005% Polymer N (filled squares).

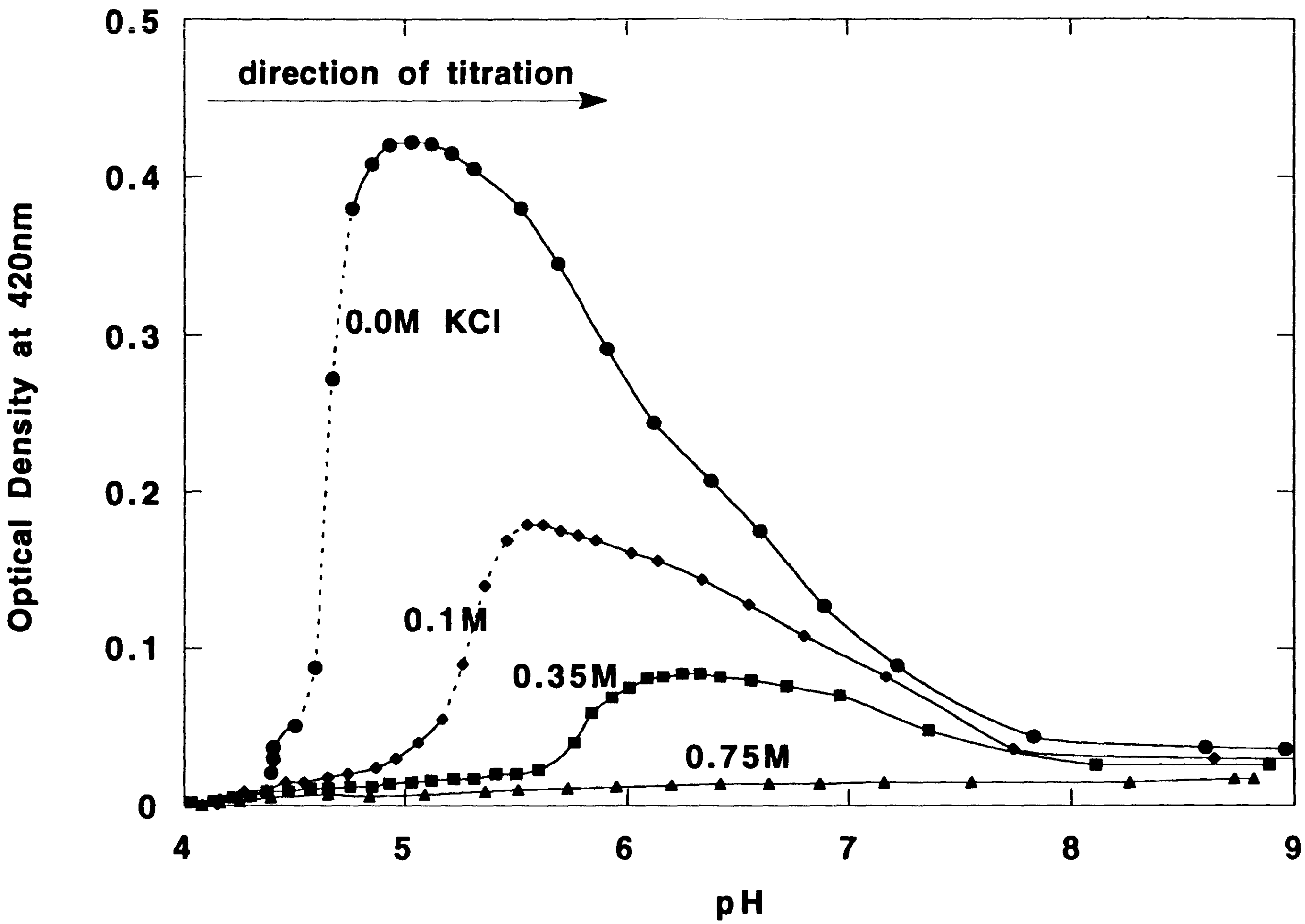

Figure 5.3(b) Complexation of 0.025% STI with 0.005% Polymer N at different salt concentrations.

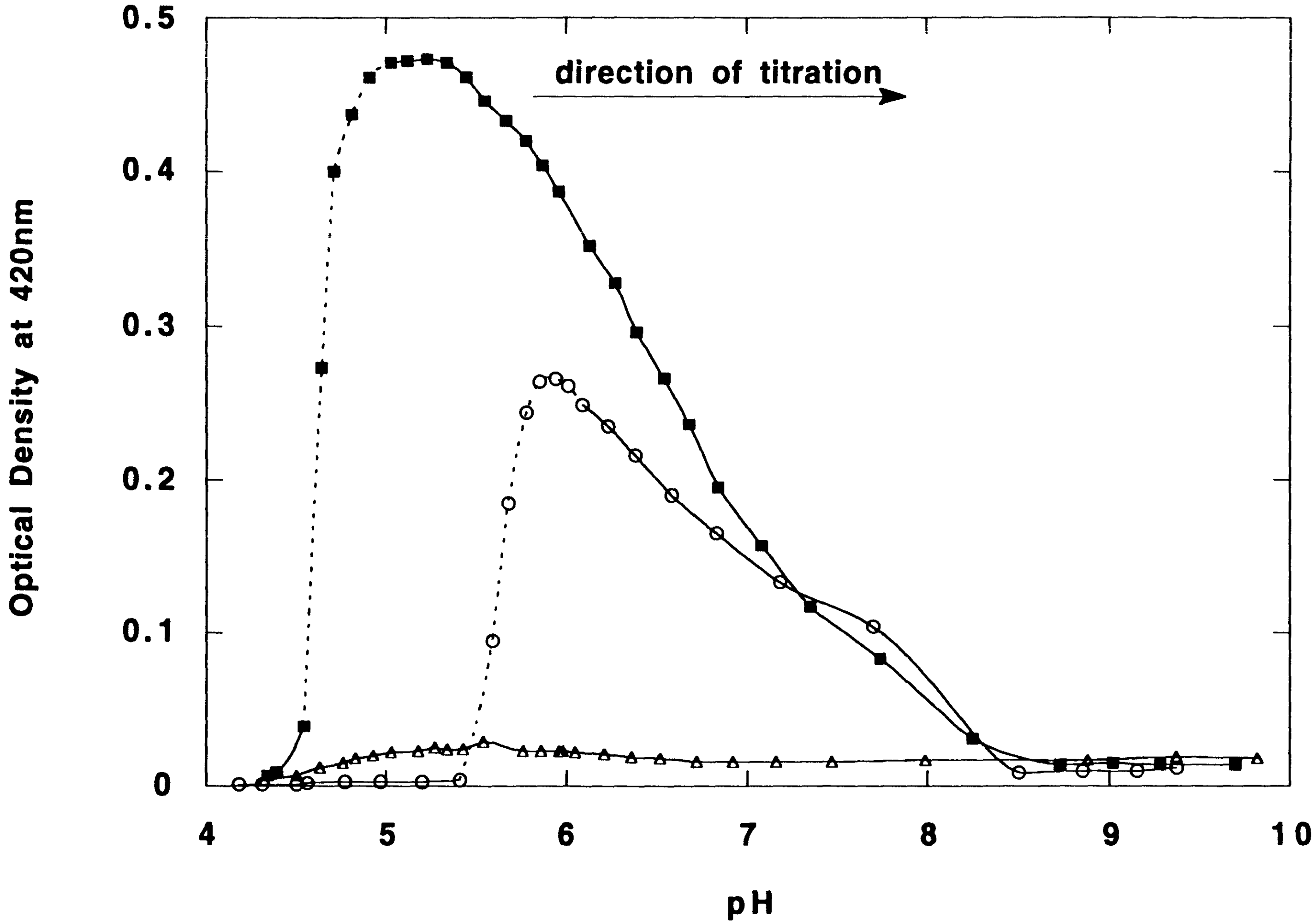

Figure 5.4(a) Optical densities of 0.01% Polymer B (open circles), 0.05% STI (open triangles) and mixture containing 0.005% Polymer B and 0.025% STI (filled squares).

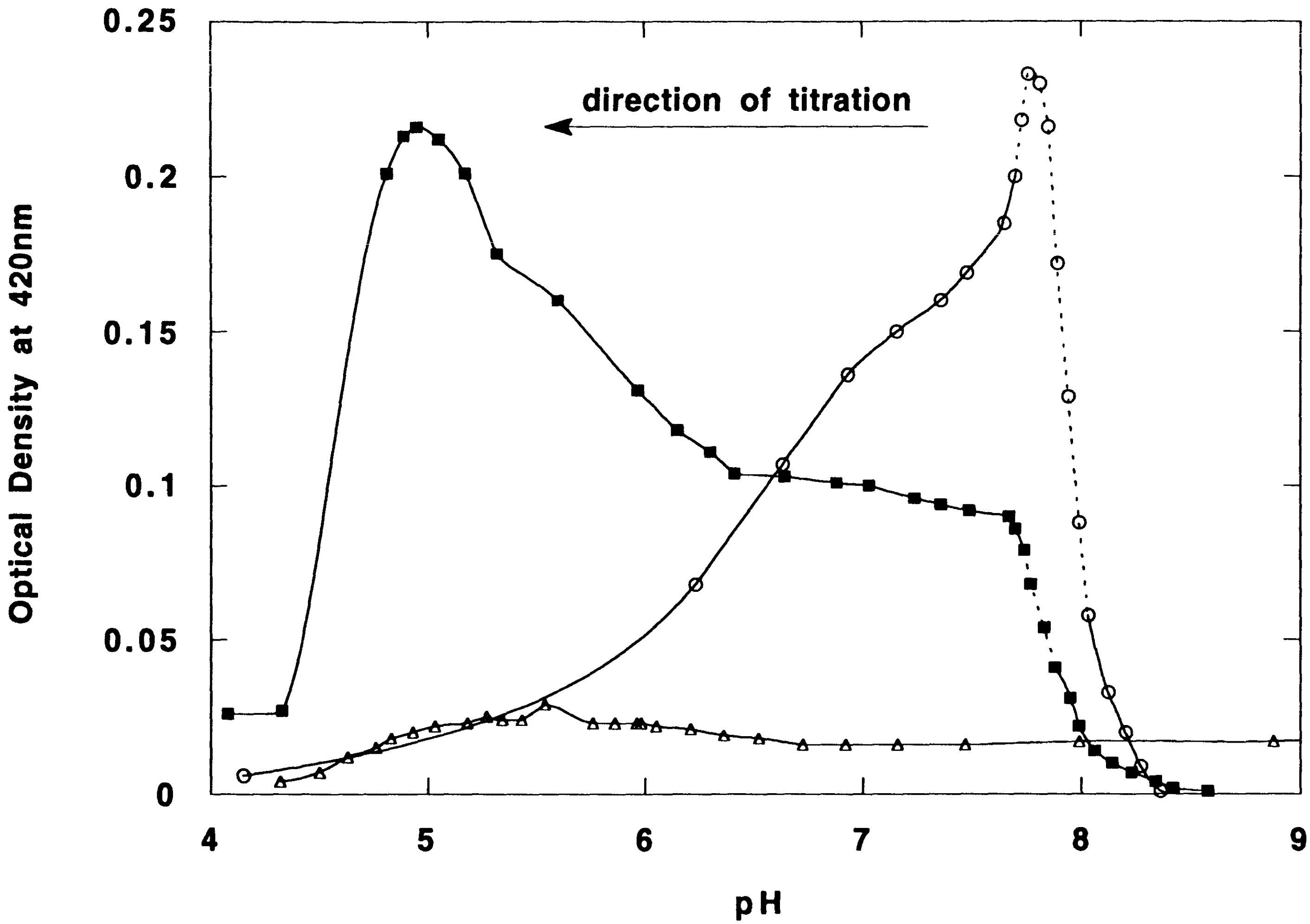

Figure 5.4(b) Back titrations of Figure 5.4(a). Optical densities of 0.01% Polymer B (open circles), 0.05% STI (open triangles) and mixture containing 0.005% Polymer B and 0.025% STI (filled squares).

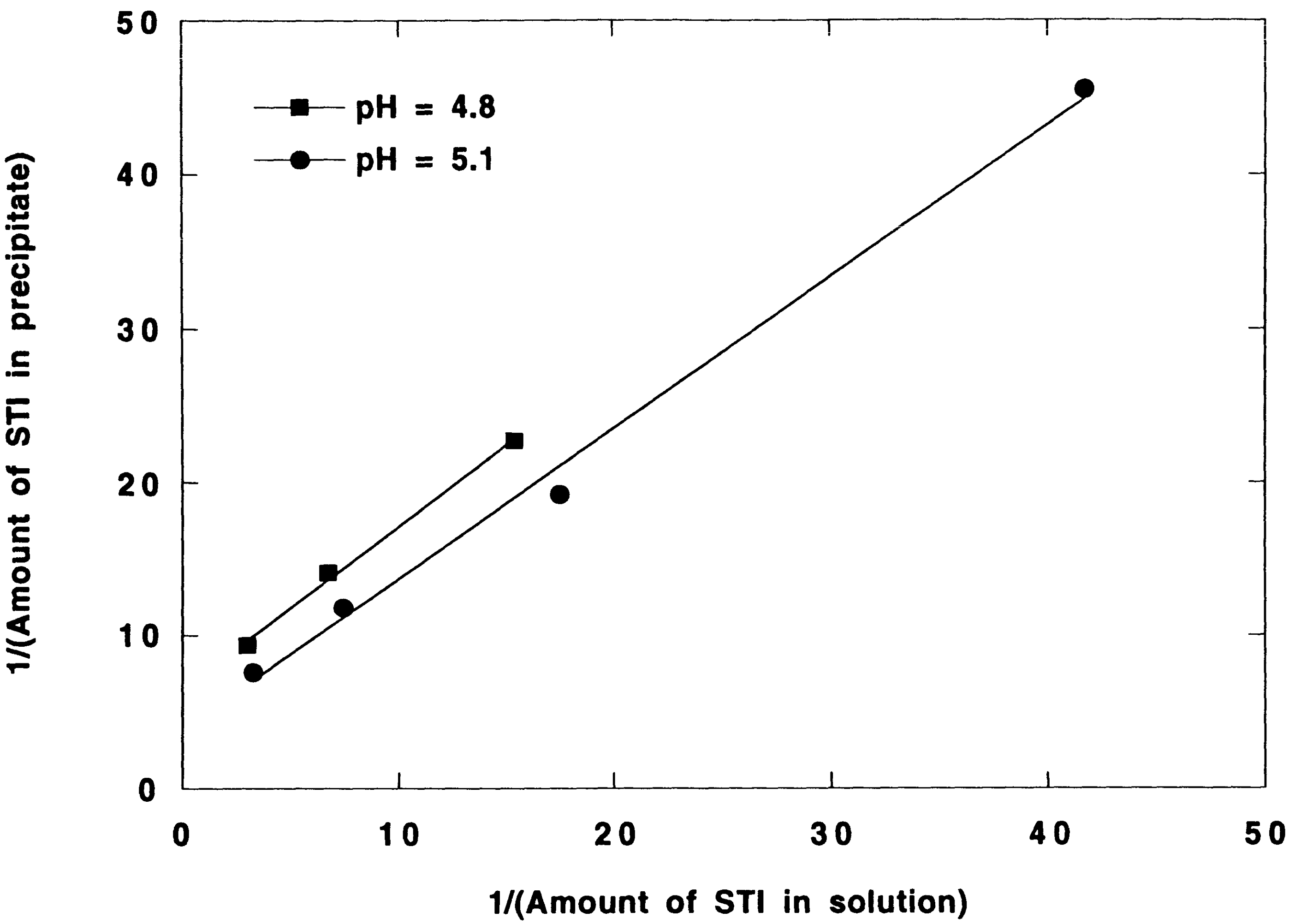

Figure 5.5 Langmuir plot of the complexation of 0.005% Polymer B with different concentrations of STI at pH 4.8 and 5.1.

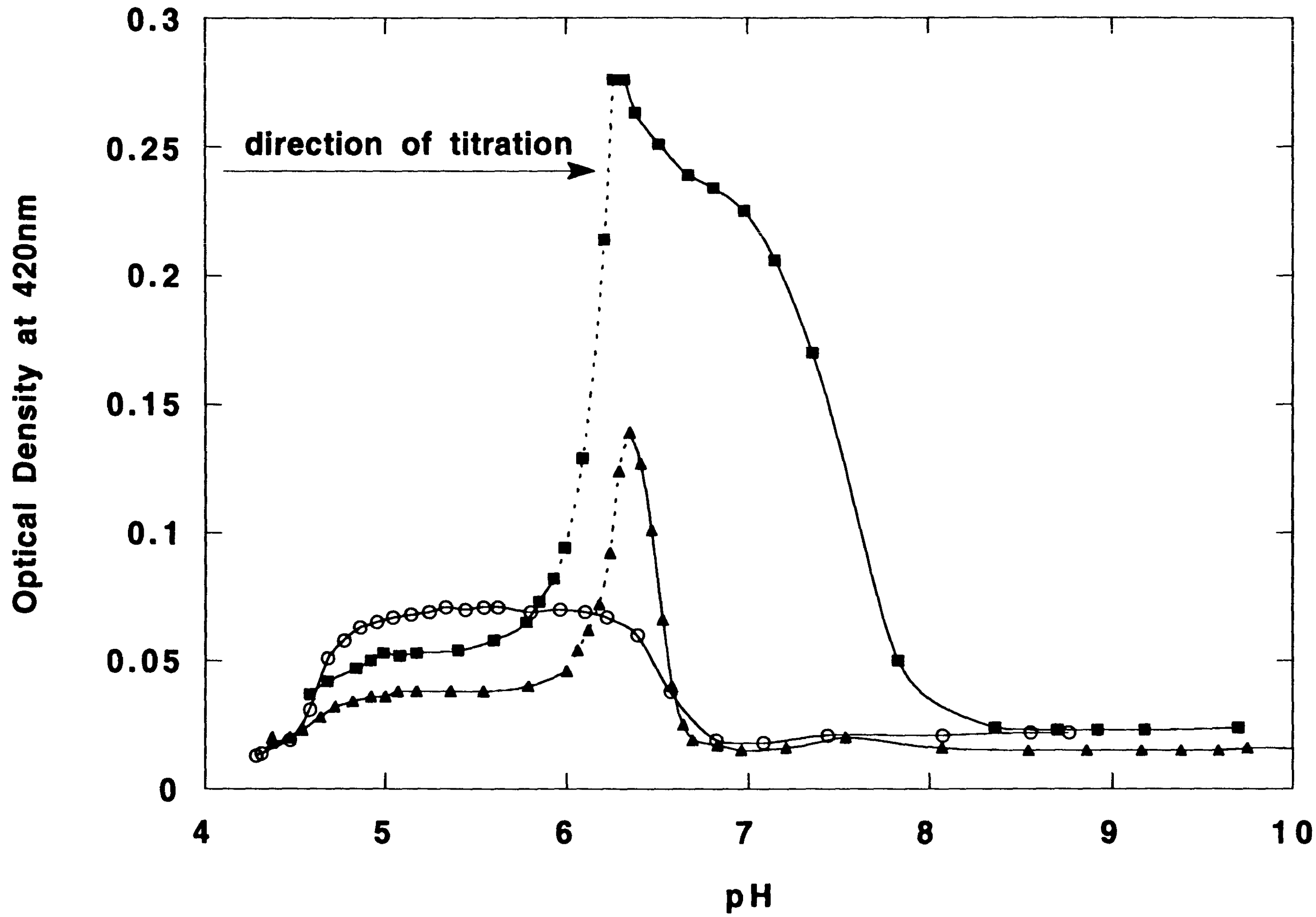

Figure 5.6 Optical densities of 0.01% Polymer A (open circles) and mixtures of 0.005% Polymer A with 0.025% (filled triangles) and 0.25% ribonuclease (filled squares).

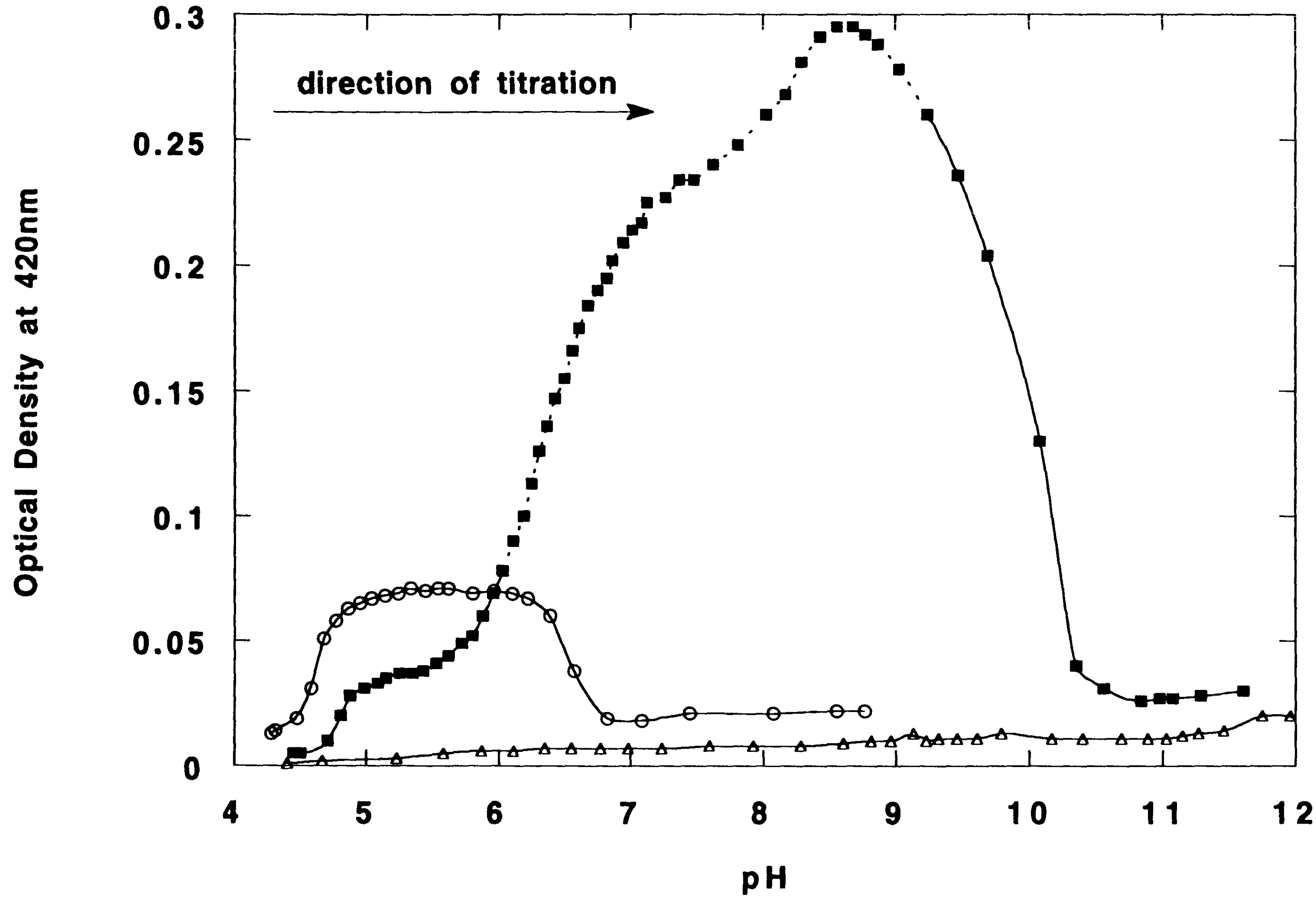

Figure 5.7 Optical densities of 0.01% Polymer A (open circles), 0.05% lysozyme (open triangles) and mixture containing 0.025% lysozyme and 0.005% Polymer A (filled squares).

Chapter 6.

Protein Complexation with Methacrylic Polyampholytes: Establishing the Potential for Protein Separation.

In this chapter the interaction between proteins and synthetic polyampholytes is further explored. The kinetics of polyampholyte and protein-polyampholyte precipitation are carefully studied. The pH-variation experiments are performed in such a way that, unlike Chapter 5, no dilution effects take place. Besides the protein-polyampholyte binary mixtures, a tertiary mixture composed of two proteins and one polyampholyte is studied. The observation of two distinct turbidity peaks in the latter experiment, each due to the binary protein-polyampholyte interactions, points towards the opportunity for utilization of the protein-polyampholyte coprecipitation for protein separation.

6.1 Introduction

Protein separation is one of the challenging issues in biotechnology today. Among the several different methods used for protein separation, the most widely used is chromatography. The high cost of equipment and difficulty of scale-up, however, provide some incentive to develop or improve alternative methods for protein separation. Precipitation with inorganic salts, such as ammonium sulfate, one of the oldest methods for protein separation, is based on the fact that different proteins start to precipitate at different salt concentration [1]. Other methods include two-phase protein partitioning which relies on the uneven distribution of proteins between two aqueous polymer phases [2]. The method we study here is protein separation by complexation and precipitation with a synthetic polyampholyte and is based on the attraction of a protein to an oppositely charged polyelectrolyte. The separation mechanism is, therefore, the same as that of ion-exchange chromatography. A difference between the two methods is that, in chromatography, the medium that interacts with the proteins is a solid, the porous beads, while in the polyampholyte-complexation technique, the medium is a fluid, the polyampholyte solution. From this comparison, one might conclude the superiority of chromatography as there is no need for subsequent separation of the proteins from the separation medium, because the latter is kept in the column with filters. However, the properties of synthetic polyampholytes provide a convenient means for freeing the proteins from the separation medium, namely by isoelectric precipitation of the polyampholyte.

Figure 6.1 presents several examples of complexation of polyelectrolytes of opposite charge. The simplest case, shown in Figure 6.1(a), is the complexation between a positively and a negatively charged homopolyelectrolyte and has been reviewed by Tsuchida and coworkers [3]. When stoichiometric, this complexation can be used for polyelectrolyte determination. Terayama et al. [4] reported on poly(acrylic acid) determination by titration with poly(dimethylallylamine chloride) and using toluidine-blue indicator. Blaakmeer and coworkers [5] reported successful use of this assay for poly(acrylic acid) determinations within 2% accuracy at ionic strengths lower than 0.01M KNO_3. The same authors reported ineffectiveness of the assay at higher ionic strengths, probably due to weak binding of the oppositely charged polyelectrolytes [6]. Figure 6.1(b) presents the complexation of a polycation with a protein of net negative charge. This interaction has been studied [7-10] and applied to protein separations [11-14]. Figure 6.1(c) illustrates the complexation between a protein (a biological polyampholyte) and a synthetic diblock polyampholyte. In this example, the synthetic polyampholyte bears a net positive charge, and the protein bears a net negative charge. Very few studies have dealt with the polyampholyte-protein system [15,16], and only one utilized block polyampholytes [17].

In general, the resulting complex can be either soluble or insoluble [12], but for the purpose of protein separation, it must be insoluble so that the precipitate can be separated from the rest of the solution. In the proposed method for protein separation by precipitation, a polyampholyte is added to a mixture of two proteins to be separated, one with a net negative charge and the other with a net positive charge, as shown in Figure 6.2. Depending on the net charge of the polyampholyte added, one of the proteins forms a complex with the polyampholyte and precipitates, while the other remains in the supernatant phase. The resulting protein-polyampholyte precipitate can be removed from the system and redissolved at a different pH. Finally, protein and polyampholyte can be separated from each other by precipitating the polyampholyte at its isoelectric point. A prerequisite in the process is that the two oppositely charged proteins do not interact strongly with each other.

Protein separation by precipitation has several advantages. The scale-up can be easily accomplished, the resulting products are concentrated, and the method is relatively inexpensive in terms of materials and equipment [7-10]. In addition, high recoveries of enzymatic activities have been reported, indicating that there is very little denaturation during the separation [8,11]. The use of synthetic polyampholytes in protein separation by precipitation may be advantageous because of the ease of polyampholyte removal from the protein and the subsequent polymer recyclability, the polyampholyte non-toxicity and low price [18,19].

Although this investigation aims to identify the conditions at which a protein and a polymer interact and utilize them for protein separation, it also provides automatically the conditions at which a protein and a polymer do not interact. This type of information is valuable in another application of these polyampholytes, displacement chromatography [20]. This method for protein separation is the topic of Chapter 7 and requires that the proteins and polymer interact only with the chromatographic column and not with each other.

The work presented here is an experimental study that establishes the presence of interactions between proteins and methacrylic block polyampholytes and reveals the potential for utilization of these interactions for protein separation. It was observed that, around the pH of zero net charge, pure synthetic polyampholyte precipitated, even at the extreme dilutions employed. It was also found that, although dilute solutions of pure protein did not precipitate at any pH, protein-polyampholyte mixtures underwent extensive precipitation within the pH range over which the components were oppositely charged.

6.2 Experimental Section

6.2.1 Materials

Table 6.1 lists the synthetic polyampholytes and proteins used in this study, their isoelectric points and molecular weights. The synthetic polyampholytes are copolymers of methacrylic acid (Ac), dimethylaminoethyl methacrylate (B) and methyl methacrylate (M). The synthesis and characterization of these polymers have been described elsewhere [21]. One acidic protein, soybean trypsin inhibitor (STI), and a basic protein, ribonuclease A, both purchased from Sigma Chemical Co., with isoelectric points at pH 4.5 and 8.8 [22,23], respectively, were chosen for this study.

6.2.2 Methods

Fresh dilute solutions of polymer, typically 0.01% w/w, and protein, typically, 0.05% w/w, in citrate/phosphate buffer of total molarity of 0.01M, were prepared. Volumes of 1mL of polymer solution were used for the study of the pure species. Binary solutions of protein and polymer were prepared by mixing 0.5mL aliquots of protein and polymer solutions at concentrations twice as high the desired concentrations in the mixture. The ternary mixture was prepared by mixing 0.33mL aliquots of the solutions of the polymer and the two proteins of initial concentrations three times the concentration desired in the final mixture. All the solutions were prepared at a pH value lower than the aggregating pH, typically 4.

In the kinetic experiments, the time dependence of precipitation of pure Polymer N and STI-Polymer N mixtures was followed by recording the optical density at 420nm. Each sample was transferred to a quartz cuvette and a precalculated amount of KOH was added to change the pH to the desired aggregating value. Immediately after the addition of KOH, the cuvette was covered with parafilm and inverted twice for mixing. A chronometer was started after the second inversion to follow the time of the reaction. The cuvette compartment of the spectrophotometer was immediately closed and the optical density was read out every 15 seconds, in the beginning, and every one and five minutes, at the later stages of the experiment. Before each measurement of the optical density, the cuvette was taken out of the spectrophotometer and inverted once to ensure absence of sedimentation effects. It was observed that during the first five minutes of the reaction, the optical density before inversion was always lower than that after. This is probably due to the high initial aggregation rate which leads to a measurable increase in optical density during the 15 seconds that the inversion procedure takes. Between 10-60 minutes the optical density decreased by 1-2% per inversion, due to the shear-induced aggregate breaking [24]. After 60 minutes inversion caused increase in the optical density because of sediment resuspension. We also observed that after 12 hours complete sedimentation took place and cuvette inversion did not result in resuspension of the precipitate.

In the pseudosteady-state experiments, 1mL-samples were pipetted into polystyrene microcuvettes of 1.5mL capacity. It was established in initial experiments that the optical density measured in the plastic cuvettes was identical to that in quartz cuvettes. Unlike Chapter 5 [25], the pH was adjusted by adding 33 microliters of a KOH solution of the appropriate strength, in order to maintain small and uniform dilution for all of the samples. A pH range from 4 to 9 was covered. Ten to twelve samples were prepared in each series of experiments. The optical density at 420nm was recorded 30 minutes after the pH adjustment. The cuvettes were inverted twice in the beginning of the experiment for mixing of the components and twice towards the end of the experiment before the optical density reading to resuspend any sediments. It was observed in the kinetic experiments that, in 30 minutes, more than 95% of the optical density increase took place in the case of pure polymer and more than 80% in the protein-polymer mixture case.

6.3 Results and Discussion

Two families of data are presented below. The first, depicted in Figures 6.3-6.4, shows the kinetics of precipitation of pure polymer and protein-polymer mixtures as followed by turbidity. The second family, shown in Figures 6.5-6.9, presents the effect of pH on the pseudosteady-state turbidity. It is pointed out that, in order to maximize the intensity of the electrostatic interactions, no salt was added to the solutions.

Figure 6.3(a) shows the kinetics of precipitation of Polymer N at pH 5.6 and at polymer concentrations of 0.002, 0.005, 0.010, 0.015, and 0.020% w/w. The replications at 0.010 and 0.020% polymer concentration indicate the good reproducibility of the experiments. The optical density increased very quickly in the first 5 minutes of the experiments and leveled-off in approximately 20 minutes. All the curves have similar shapes and when fitted to the exponential expression

$$T = A\,[1 - \exp(-t/t_o)] \tag{6.1}$$

characteristic times of 2 to 3 minutes were calculated. In this equation T is the optical density (turbidity), A is the level-off value of the optical density, t is the time and t_o is the characteristic time. As it will become clear in the following paragraph, the exponential expression does not have any theoretical basis. Nevertheless, it was utilized for the convenient calculation of characteristic times.

The optical density is proportional to the particle size raised to some power n, and for non-optically-absorbing particles with size smaller than the wavelength of the scattered light (in our case 420nm) n equals 6 [26]. Exploiting the power-law correlation of the particle size and the optical density we can test whether the aggregation mechanism is diffusion-limited or reaction-limited. While for diffusion-limited aggregation (DLA) the logarithm of the particle size scales linearly with the logarithm of time, for reaction-limited aggregation (RLA) the logarithm of the particle size scales linearly with time [27]. In the inset of Figure 6.3 the data are replotted using double-logarithmic and semi-logarithmic axes. The satisfactory linearity at the early times in the double-logarithmic plot suggests that the aggregation was diffusion-limited rather than reaction-limited. This implies that for the range of concentrations employed, most of the collisions between the particles were effective, leading to combination of the colliding particles [28] as in the Smolukowski theory [29].

In Figure 6.3(b), the optical density at 30min (quasi-steady-state), is plotted as a function of polymer concentration. The data fall on a straight line with some small negative deviation observed in the lower concentration data points. The critical micelle concentration (CMC) of Polymer N can be estimated from fluorescence data of Chapter 2 to be around 0.001% w/w [21] which implies that at concentrations lower than 0.001% the polymer occurs as single chains, while at higher concentrations the polymer chains form micellar aggregates. The precipitation should be expected to be faster above the CMC as the polymer exists in larger entities for which the driving forces for precipitation, electrostatic, hydrophobic and dispersive, are stronger. The break-point of Figure 6.3(b) at 0.005% is reasonably consistent with the CMC.

The approximately linear dependence of the long-time turbidity on concentration implies that the precipitating aggregates of the polymer reach the same size at steady-state at all the polymer concentrations investigated. This conclusion is based on the equation [26]:

$$T = c\ S\ Q_{ext} \tag{6.2}$$

under the assumption that the extinction efficiency, Q_{ext}, is constant and independent of polymer concentration, c; S is the scattering cross-sectional area of the particles.

Figure 6.4(a) shows the kinetics of precipitation of binary mixtures of STI and Polymer N at pH 4.8 and at the constant protein-to-polymer mass concentration ratio of 5 to 1. The combinations of protein and polymer concentrations presented are 0.0125 and 0.0025%, 0.025 and 0.005% (replicated), and 0.050 and 0.010%. As in Figure 6.3(a), the optical density increased very rapidly in the first 5 minutes, and characteristic times between 2 to 3 minutes were determined (equation (6.1)). Unlike Figure 6.3(a), however, the optical density does not level-off but it continues to increase slightly, but constantly, even after 70 minutes. This implies that the kinetics of protein-polymer precipitation is slower than the kinetics of precipitation of pure polymer. This can be attributed to the weaker charge density and hydrophobicity of the protein as compared to that of the polymer. The same factors are responsible for the observed complete solubility of dilute pure protein solutions even at the isoelectric point. In the inset the data are replotted in double-logarithmic and semi-logarithmic axes. Again, a diffusion-limited aggregation mechanism can be concluded.

Figure 6.4(b) displays the optical densities of the mixtures at 30min as a function of the polymer concentration. For comparison, the optical density of pure polymer at 30min, taken from Figure 6.3(b), is also shown. As with the pure polymer, the turbidity of the protein-polymer mixture varies approximately linearly with polymer concentration. By comparing the two curves, it appears that the addition of protein to the polymer at the mass concentration ratio of 5/1 results in a doubling of the optical density.

Figure 6.5 illustrates the turbidity-pH profiles of the three triblock copolymers measured 30 minutes after the pH adjustment. The turbidity profiles of the three polymers have both similarities and differences. We discuss first the similarities. Two abrupt changes in turbidity occur, one on each side of the isoelectric point. The pH at the midpoint of each transition will be referred to as the acidic and basic critical pHs. These abrupt changes in the turbidity of pure polymer solution are due to the solubility of the polyampholytes which exhibits a pronounced minimum around the isoelectric point. This has been observed both for biological polyampholytes, e.g. proteins [30] and for synthetic polyampholytes [19,21,31]. In this pH region the net charge is close to zero and the interpolymer electrostatic repulsion which keeps the polymer in solution is almost absent. At the same time, the hydrophobic and dispersive attractive forces dominate and cause particle aggregation. Another similarity is that the width at half-height of the turbidity profiles of the three polyampholytes is 2-3 pH units. This is a measure of the non-electrostatic attractive forces (hydrophobic and van der Waals) which are responsible for the polymer precipitation even when the polyampholyte bears a non-zero net charge. A third similarity is that the pH value that corresponds to the arithmetic average of the two critical pH's is in fair agreement with the isoelectric points of the polymers with some deviation for the base-rich polyampholyte. Now, we discuss the differences. Although the polymer concentrations are the same, at 0.01% w/w, the turbidity maxima are different, and increase with increasing amine content in the polymer. One possible explanation for this discrepancy is that the increased hydrophobicity of the amine residue, as compared to that of the methacrylic acid residue, leads to the formation of larger precipitating particles in the case of the base-rich polyampholyte as compared to the neutral and acid-rich copolymers. This means a larger S in equation (6.2). Another possibility is that the extinction efficiency of the amine residue is simply greater than that of the methacrylic acid residue (equation (6.2)). Another difference is that, while the profile of Polymer A is almost flat, that of Polymer N exhibits two peaks and that of Polymer B one peak at the lower pH. The behavior of Polymer N may be due to the presence of two polymeric species with slightly different isoelectric points. The behavior of Polymer B may be due to the presence of a polyamine impurity which interacts with the polyampholyte electrostatically.

The turbidity profile of Polymer N is compared with that of the mixture of Polymer N and STI in Figure 6. Two differences in the profiles are evident. First, the acidic critical pH of the mixture is lower than that of the pure polymer, and close to the isoelectric point of the protein. Second, the maximum turbidity of the mixture is higher than that of pure polymer, with the former occurring at a lower pH than the latter. It is of interest to note that the presence of the protein gives rise to a peak in the turbidity profile of the mixture. This peak is defined by the isoelectric points of both the polymer and the protein. Additionally, it is only within the pH range of this peak (4.5-6) that the kinetics of precipitation are slowed down (data not shown). For pH values higher than 6 the turbidity levels-off quickly and the profiles of pure polymer and the mixture are very similar, suggesting the absence of protein-polymer interaction.

Figure 6.7 shows the interaction of STI with the three polyampholytes. All three mixtures have the same acidic critical pH, coinciding with the isoelectric point of STI, and they have different basic critical pHs, according to the polymer isoelectric point. For Polymers A and N the polymer-protein interaction peaks can be well distinguished, while for the case of Polymer B the interaction peak is not very clear and the optical density is the highest.

Figure 6.8 shows the interaction of Polymer B with the acidic and basic proteins, STI and ribonuclease A. The data for the STI-Polymer B system were taken from Figure 6.7. While STI and Polymer B interact strongly, Polymer B and ribonuclease appear not to interact as the turbidity profiles of pure polymer and the protein-polymer mixture coincide. This can be attributed to the proximity of the isoelectric points of the polymer (8.0) and the protein (8.8).

In Figure 6.9, the interactions in a ternary mixture composed of Polymer A, STI and ribonuclease are studied. The two proteins were chosen such that the one (STI) is more acidic than the polymer and the other (ribonuclease) more basic. Polymer A was chosen for the study of the mixture containing the two proteins because the turbidity profile of the pure polymer is almost flat and of lower intensity as compared to that of the other two polymers. This rendered the comparison of the turbidity profile of pure polymer with those of the polymer-protein binary and ternary mixtures easier.

The turbidity profile of the ternary mixture (filled squares) exhibits two peaks which coincide with those of the binary protein-polymer mixtures (open circles and open diamonds). This suggests that, at pH 4.5, ribonuclease does not participate or affect the complexation of the polymer with STI, and that, at pH 6.5, STI does not affect the interaction of the polymer with ribonuclease. These observations are important as they imply that, by the appropriate selection of pH, the polymer can selectively coprecipitate with one of the two proteins, pointing to the potential for protein separation.

Of special interest is the absence of an interaction peak in the turbidity profile of the STI-ribonuclease mixture. This indicates that the polymer and not the protein is primarily responsible for the polymer-protein binary interactions. This was expected as it is the polymers that have relatively long sequences of residues carrying charge of the same sign, and not the proteins. Additionally, the polymers, bearing the methyl methacrylate block, are more hydrophobic than the proteins.

We have not been able to analyze for protein in the ternary mixture because, on the one hand, the spectrophotometric determination at 280nm is not protein-selective and, on the other hand, chromatographic elution will not be successful due to the very low protein concentrations.

6.4 Conclusion

Low-molecular-weight block acrylic polyampholytes interact strongly both with themselves and with proteins and precipitate within a pH-range determined by the polymer and protein net charges. Pure polymer self-aggregates around the isoelectric pH, even at the very low polymer concentrations used in this investigation, typically 0.01% w/w. Polymer-protein mixtures interact in a pH-range between the isoelectric point of the polymer and the protein. The observation of two distinct turbidity peaks in the tertiary mixture, each due to the binary protein-polyampholyte interactions, indicates the potential of the protein-polyampholyte coprecipitation for protein separation. An advantage of polyampholytes is that their self-aggregation will provide the ability for polymer removal and recycling at the end of the process. This constitutes a potentially important economical advantage for industrial-scale separations. The kinetics of precipitation both of the pure polymer and the protein-polymer systems are fast and of the order of 5 minutes.

6.5 Literature Cited

(1) Scopes, R. P. *Protein Purification: Principles and Practice*; Springer-Verlag: New York, 2nd ed., 1988; p 45.

(2) Albertsson, P.-A. *Partition of Cell Particles and Macromolecules*; Wiley and Sons: New York, 3rd ed., 1986; p 1.

(3) Tsuchida, E; Osada, Y.; Ohno, H. Formation of Interpolymer Complexes. *J. Macromol. Sci.-Phys.* **1980,** *B17,* 683-714.

(4) Terayama, H. Method of Colloid Titration. (A New Titration between Polymer

Ions). *J. Polym. Sci.* **1952,** *8,* 243-253.

(5) Blaakmeer, J.; Böhmer, M. R.; Cohen Stuart, M. A.; Fleer, G. J. Adsorption of Weak Polyelectrolytes on Highly Charged Surfaces. Poly(acrylic acid) on Polystyrene Latex with Strong Cationic Groups. *Macromolecules* **1990,** *23,* 2301-2309.

(6) Wassmer, K.-H.; Schroeder, U.; Horn, D. Characterization and Detection of Polyanions by Direct Polyelectrolyte Titration. *Makromol. Chem.* **1991,** *192,* 553-565.

(7) Dubin, P. L.; Ross, T. D.; Sharma, I.; Yegerlehner, B. E. Coacervation of Polyelectrolyte-Protein Complexes. *Ordered Media in Chemical Separations*; Hinze, W. L., Armstrong, D. W., Eds., ACS Symposium Series, Washington, DC 1987; Vol. 342, 162-169.

(8) Strege, M. A.; Dubin, P. L.; West, J. S.; Flinta, C. D. Complexation of Poly(dimethyldiallylammonium chloride) and Globular Proteins. *Downstream Processing and Bioseparation*; Hammel, J.-F., Hunter, J. B., Sikdar, S. K., Eds., ACS Symposium Series, Washington, DC 1990; Vol. 419, 158-169.

(9) Park, M. P.; Muhoberac, B. B.; Dubin, P. L.; Xia, J. Effects of Protein Charge Heterogeneity in Protein-Polyelectrolyte Complexation. *Macromolecules* **1992,** *25,* 290-295.

(10) Xia, J.; Dubin, P. L.; Kim, Y.; Muhoberac, B. B.; Klimkowski, V. J. Electrophoretic and Quasi-Elastic Light Scattering of Soluble Protein-Polyelectrolyte Complexes. *J. Phys. Chem.* **1993,** *97,* 4528.

(11) Sternberg, M.; Hershberger, D. Separation of Proteins with Polyacrylic Acids. *Biochim. Biophys. Acta* **1974,** *342,* 195-206.

(12) Strege, M. A.; Dubin, P. L.; West, J. S.; Flinta, C. D. Protein Separation via Polyelectrolyte Complexation. *Protein Purification*; Ladisch, M. R., Willson, R. C., Painton, C. C., Builder, S. E., Eds., ACS Symposium Series, Washington, DC 1990; Vol. 427, 66-79.

(13) Clark, K. C.; Glatz, C. E. Protein Fractionation by Precipitation with Carboxymethyl Cellulose. *Downstream Processing and Bioseparation*; Hammel, J.-F., Hunter, J. B., Sikdar, S. K., Eds., ACS Symposium Series, Washington, DC, 1990; Vol 419, pp 170-187.

(14) Parker, D. E.; Glatz, C. E.; Ford, C. F.; Gendel, S. M.; Suominen, I.; Rougvie, M. A. Recovery of a Charged-Fusion Protein from Cell Extracts by Polyelectrolyte Precipitation. *Biotech. Bioeng.* **1990,** *36,* 467-475.

(15) Morawetz, H.; Hughes, W. L., Jr. The Interaction of Proteins with Synthetic Polyelectrolytes. I. Complexing of Bovine Serum Albumin. *J. Phys. Chem.* **1952,** *56,* 64-69.

(16) Rodkey, L. S.; Hirata, A. Studies of Ampholyte-Protein Interactions. *Prot. Biol. Fluids* **1986,** *34,* 745-748.

(17) Kudaibergenov, S. Y.; Bekturov, Y. A. Influence of the Coil-Globule Conformational Transition in Polyampholytes Affecting the Sorption and Desorption of Polyelectrolytes in Human Serum Albumin. *Polym. Sci. USSR* **1989,** *31,* 2870-2874.

(18) Hughes, P.; Low, C. R. Purification of Proteins by Aqueous Two-Phase Partition in Novel Acrylic Co-Polymer Systems. *Enzyme Microb. Technol.* **1988,** *10,* 115-122.

(19) Patrickios, C. S.; Abbott, N. L.; Foss, R. P.; Hatton, T. A. Protein Partitioning

in Two-Phase Aqueous Polymer Systems Containing Polyampholytes. *New Developments in Bioseparation*; Ataai, M. M., Sikdar, S. K., Eds.; AIChE Symposium Series: New York, 1992, Vol. 88, pp 80-88.

(20) Patrickios, C. S.; Gadam, S. D.; Cramer, S. M.; Hertler, W. R.; Hatton, T. A. Chromatographic Characterization of Acrylic Polyampholytes. *Polyelectrolytes*; Schmitz, K. S., Ed.; ACS Symposium Series, in press.

(21) Patrickios, C. S.; Hertler, W. R.; Abbott, N. L.; Hatton, T. A. Synthesis and Solution Behavior of Random and Block Methacrylic Polyampholytes. Accepted for publication in *Macromolecules*.

(22) Kopaciewicz, W.; Rounds, M. A.; Fausnaugh, J.; Regnier, F. E. Retention Model for High-Performance Ion-Exchange Chromatography. *J. Chromatogr.* **1983,** *266,* 3-21.

(23) Righetti, P. G.; Caravaggio, T. Isoelectric Points and Molecular Weights of Proteins. A Table. *J. Chromatogr.* **1976,** *127,* 1-28.

(24) Brown, D. L.; Glatz, C. E. Aggregate Breakage in Protein Precipitation. *Chem. Eng. Sci.* **1987,** *42,* 1831-1839.

(25) Patrickios, C. S.; Jang, C. J.; Hertler, W. R.; Hatton, T. A. Interaction of Proteins with Acrylic Polyampholytes. *Polyelectrolytes*; Schmitz, K. S., Ed.; ACS Symposium Series, in press.

(26) Hiemenz, P. C. *Principles of Colloid and Surface Chemistry*; Marcel Dekker: New York, 2nd ed., 1986; pp 271, 273.

(27) Lin, M. Y.; Lindsay, H. M.; Weitz, D. A.; Ball, R. C.; Klein, R.; Meakin, P.

Universality in Colloid Aggregation. *Nature* **1989,** *339,* 360-362.

(28) Ju, R. T. C.; Frank, C. W.; Gast, A. P. CONTIN Analysis of Colloidal Aggregates. *Langmuir* **1992,** *8,* 2165-2171.

(29) Probstein, R. F. *Physicochemical Hydrodynamics*; Butterworths: Boston, 1989; p 236.

(30) Tanford, C. *Physical Chemistry of Macromolecules*; Wiley: New York, 1961; p 242.

(31) Righetti, P. G. *Isoelectric Focusing: Theory, Methodology and Applications*; Elsevier: Amsterdam, 1983; p 50.

Table 6.1 Properties of the synthetic polyampholytes and the proteins.

Macromolecule	Polymer	B/M/Ac	MW	pI
Polymer A (acidic)	10	8/12/16	3800	5.4
Polymer N (neutral)	2	12/12/12	4100	6.6
Polymer B (basic)	9	16/12/8	4400	8.0
STI			20100	4.5
Ribonuclease A			13500	8.8

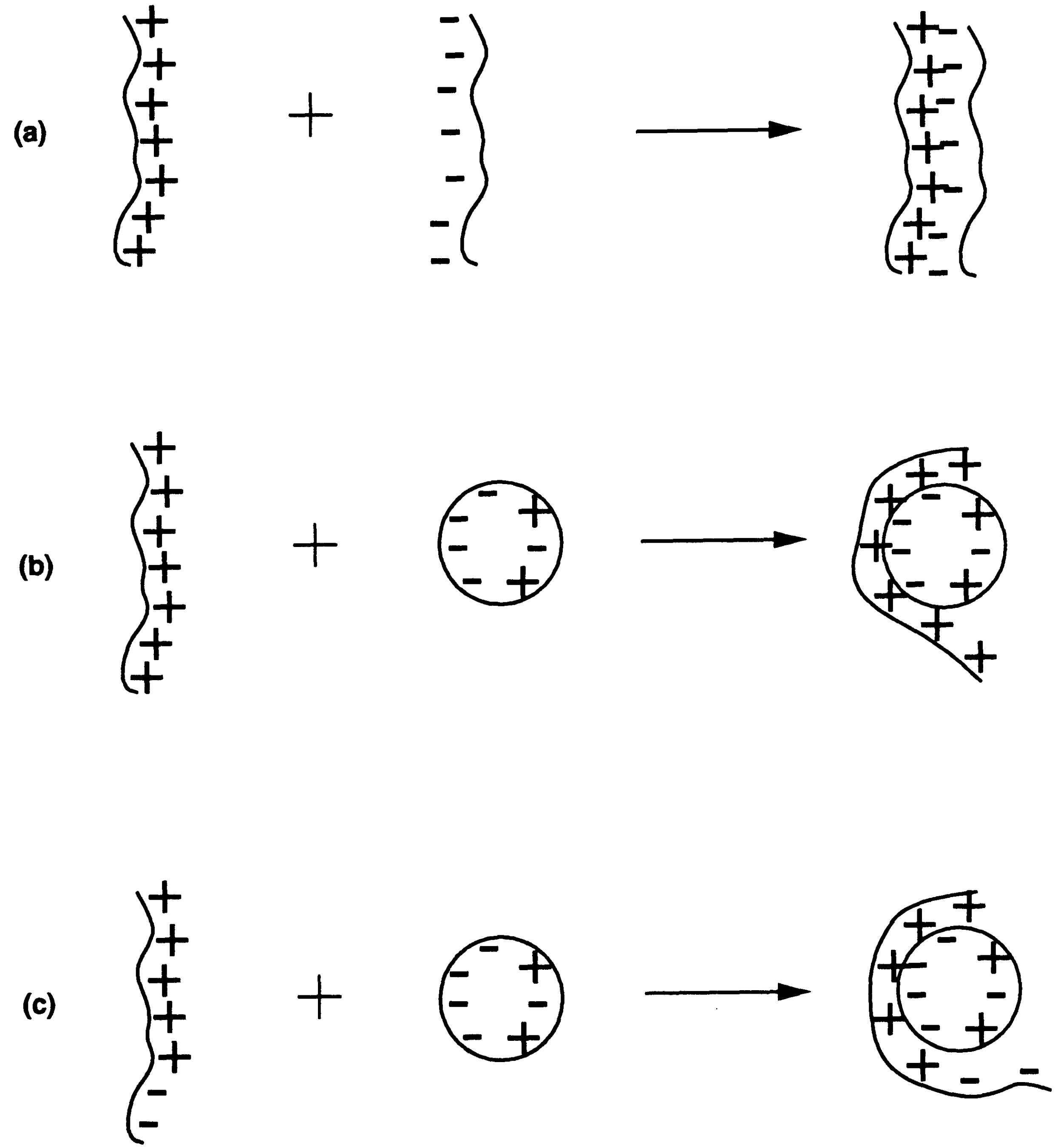

Figure 6.1 Examples of polyelectrolyte complexation: (a) polycation and polyanion, (b) polycation and protein, and (c) polyampholyte and protein.

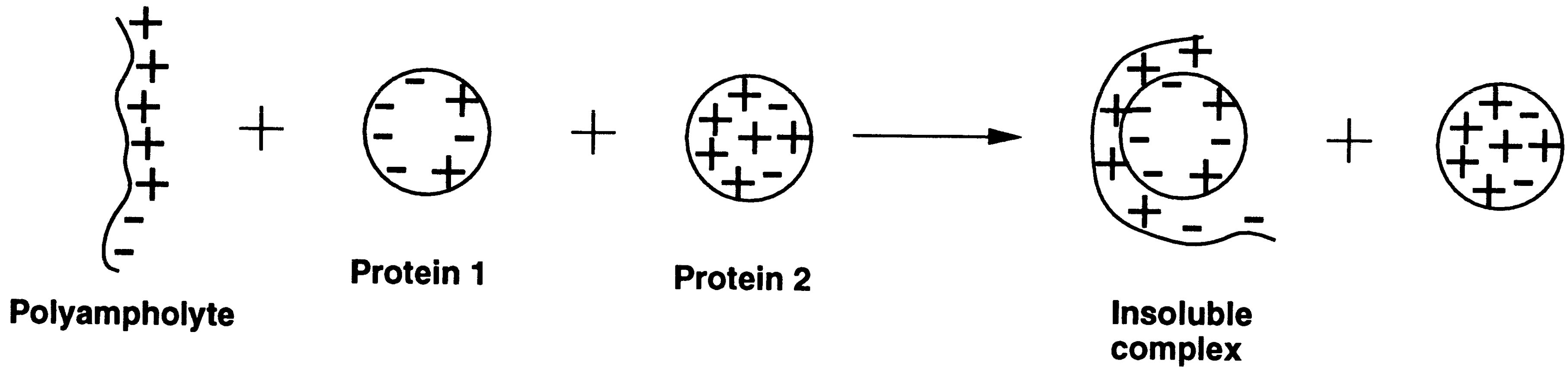

Figure 6.2 Polyampholyte-protein complexation for protein separation. The (net) positively charged polyampholyte will form a complex only with the (net) negatively charged protein.

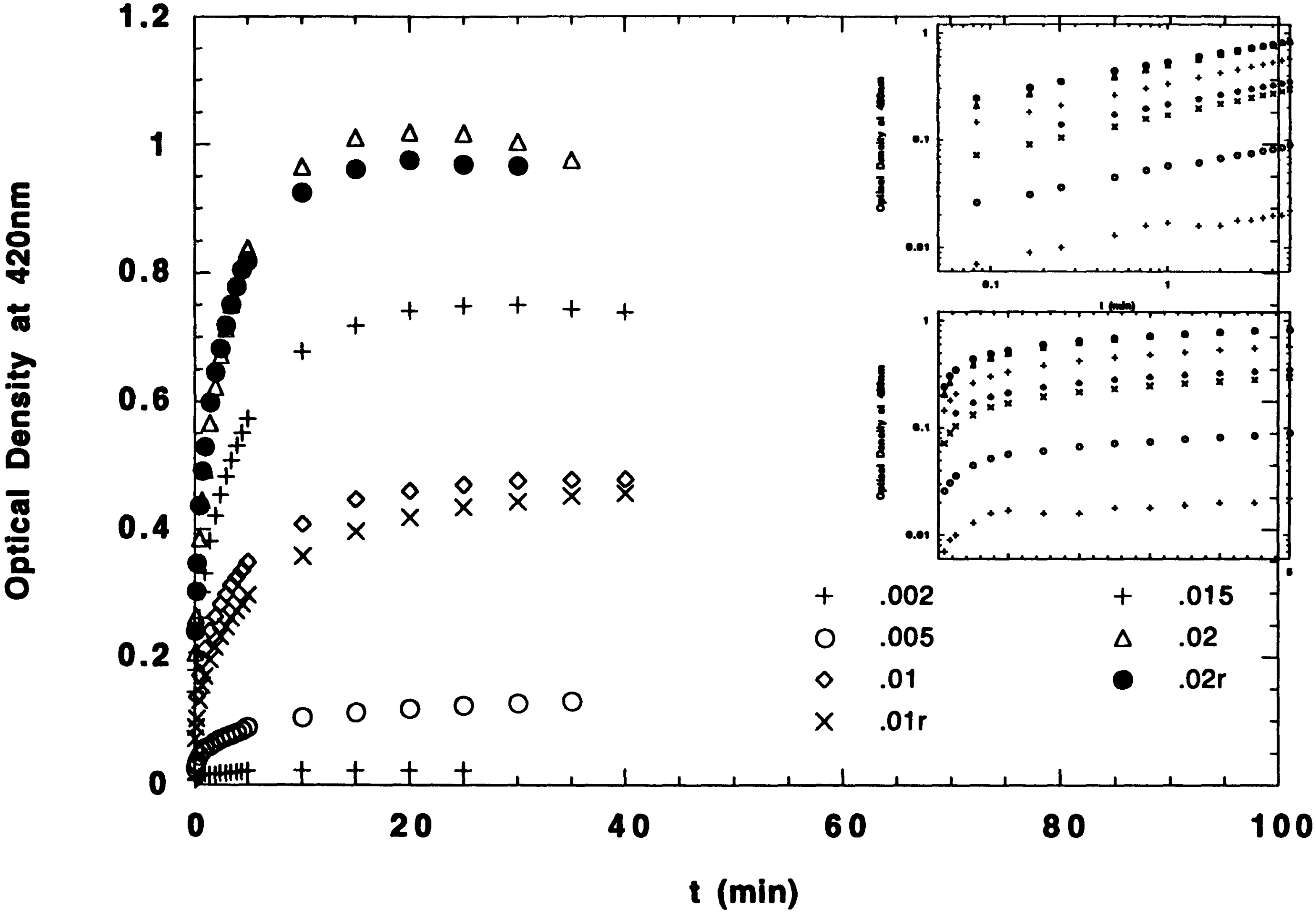

Figure 6.3(a) Kinetics of aggregation of Polymer N at pH 5.6 and different polymer concentrations. The letter "r" in the Figure indicates replication of the experiment. Inset : doubelog and semilogarithmic plot of same data.

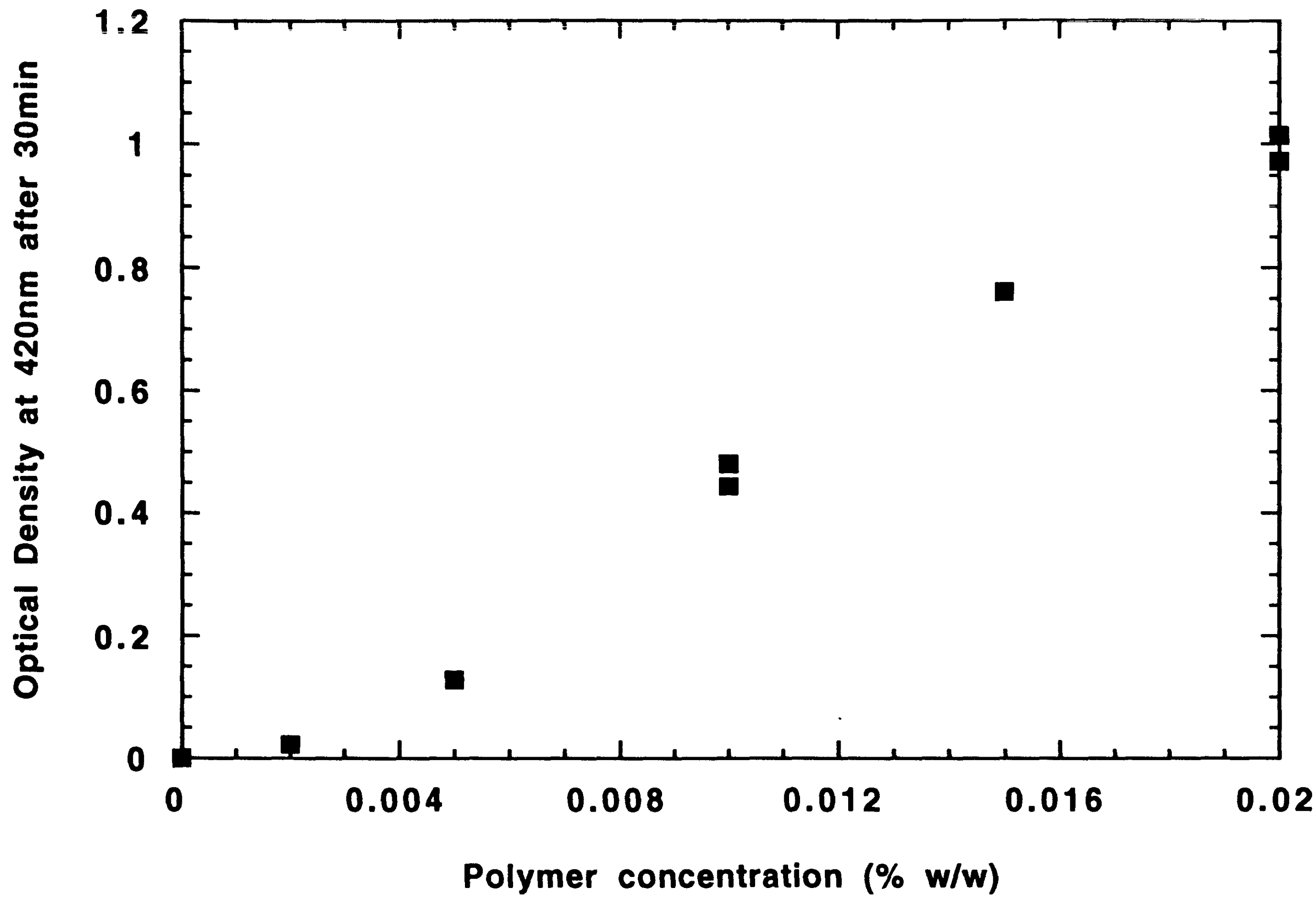

Figure 6.3(b) Pseudosteady-state optical density of aggregated Polymer N at pH 5.6 and at different polymer concentrations.

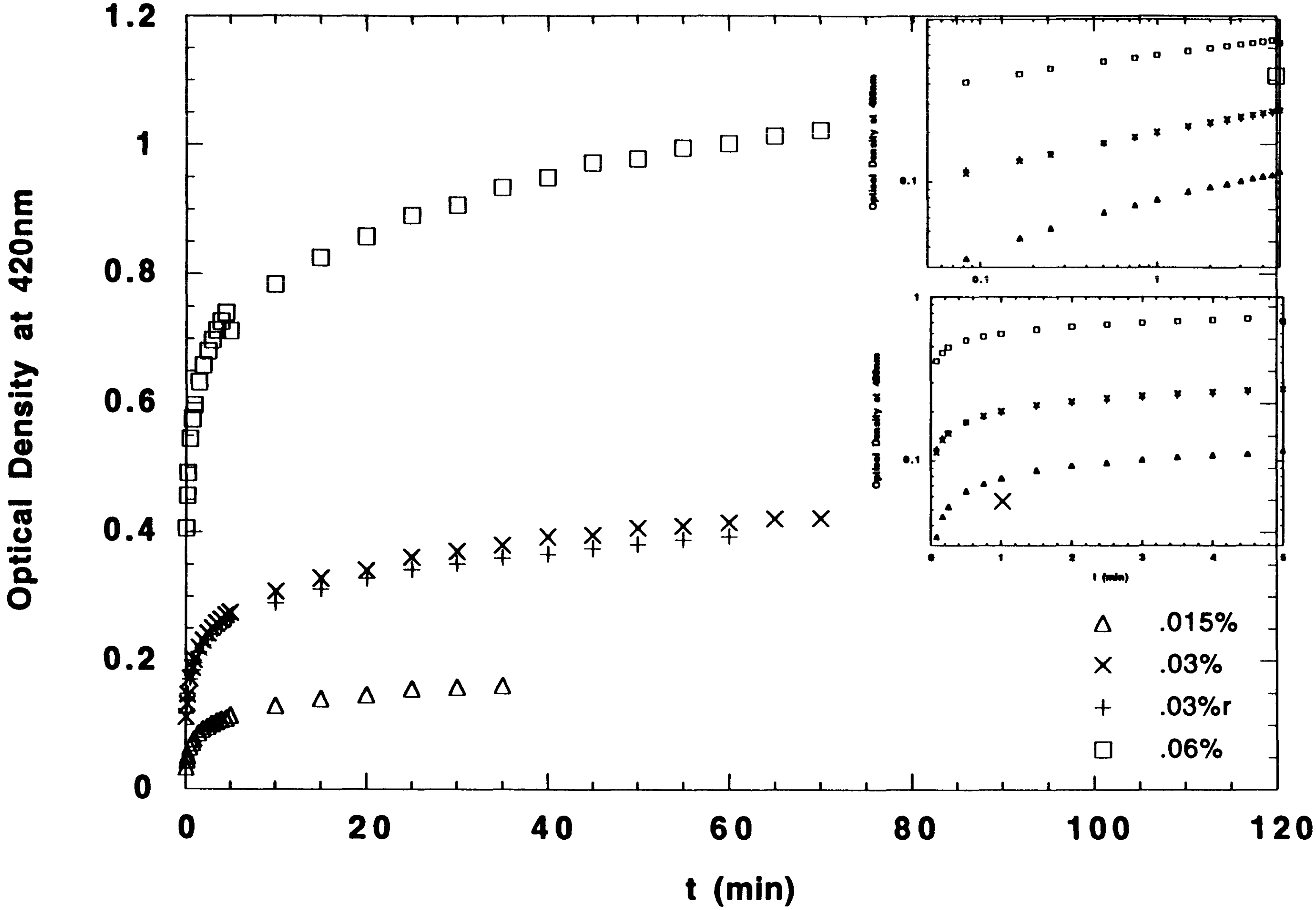

Figure 6.4(a) Kinetics of aggregation of Polymer N with STI at pH 4.8, at an 1/5 polymer/protein mass concentration ratio and different total (polymer plus protein) concentrations. Replication is indicated by letter "r".

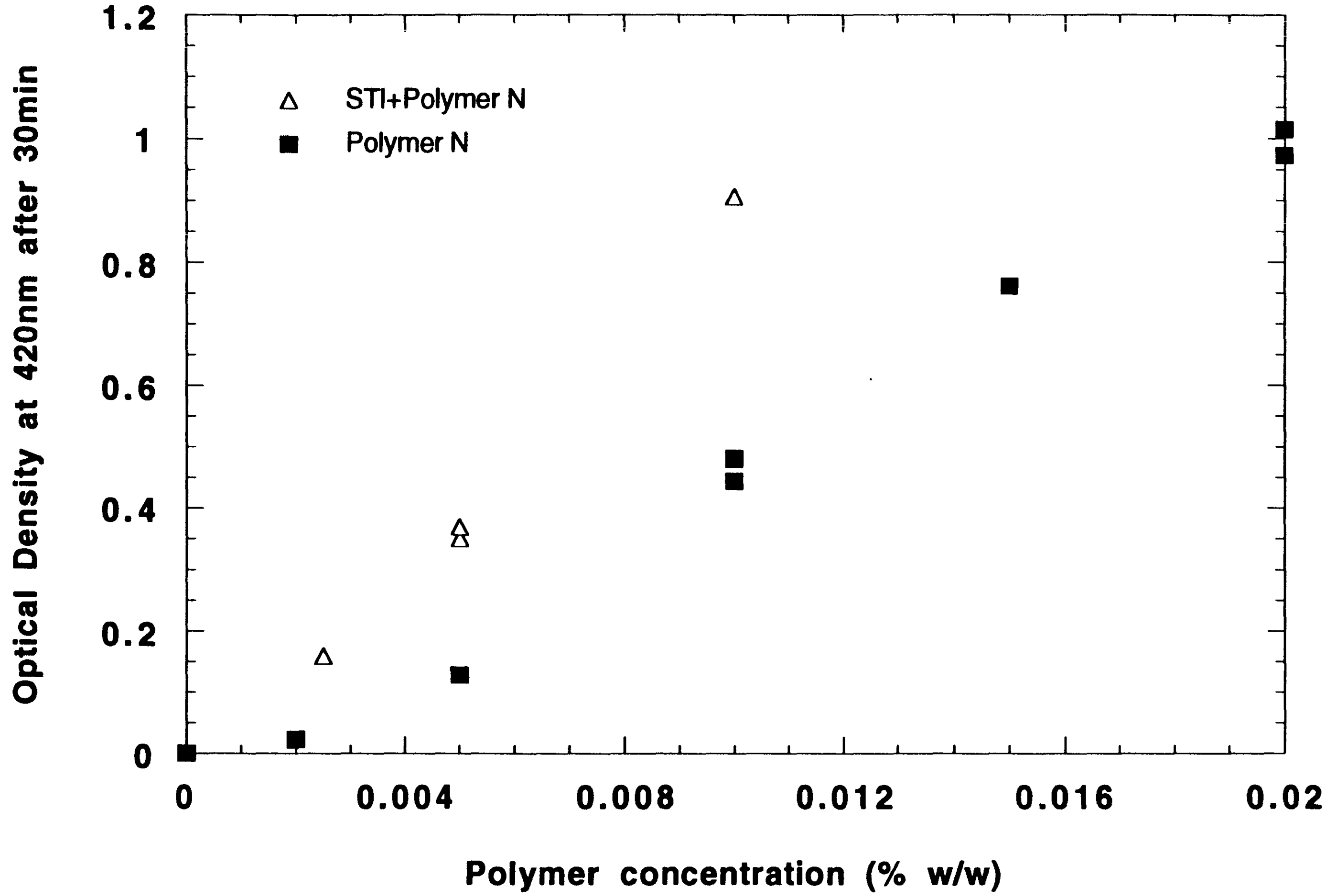

Figure 6.4(b) Pseudosteady-state optical density of aggregated mixture of STI with Polymer N at constant protein/polymer concentration ratio. For comparison, the aggregation of pure polymer is replotted from Figure 6.3(b).

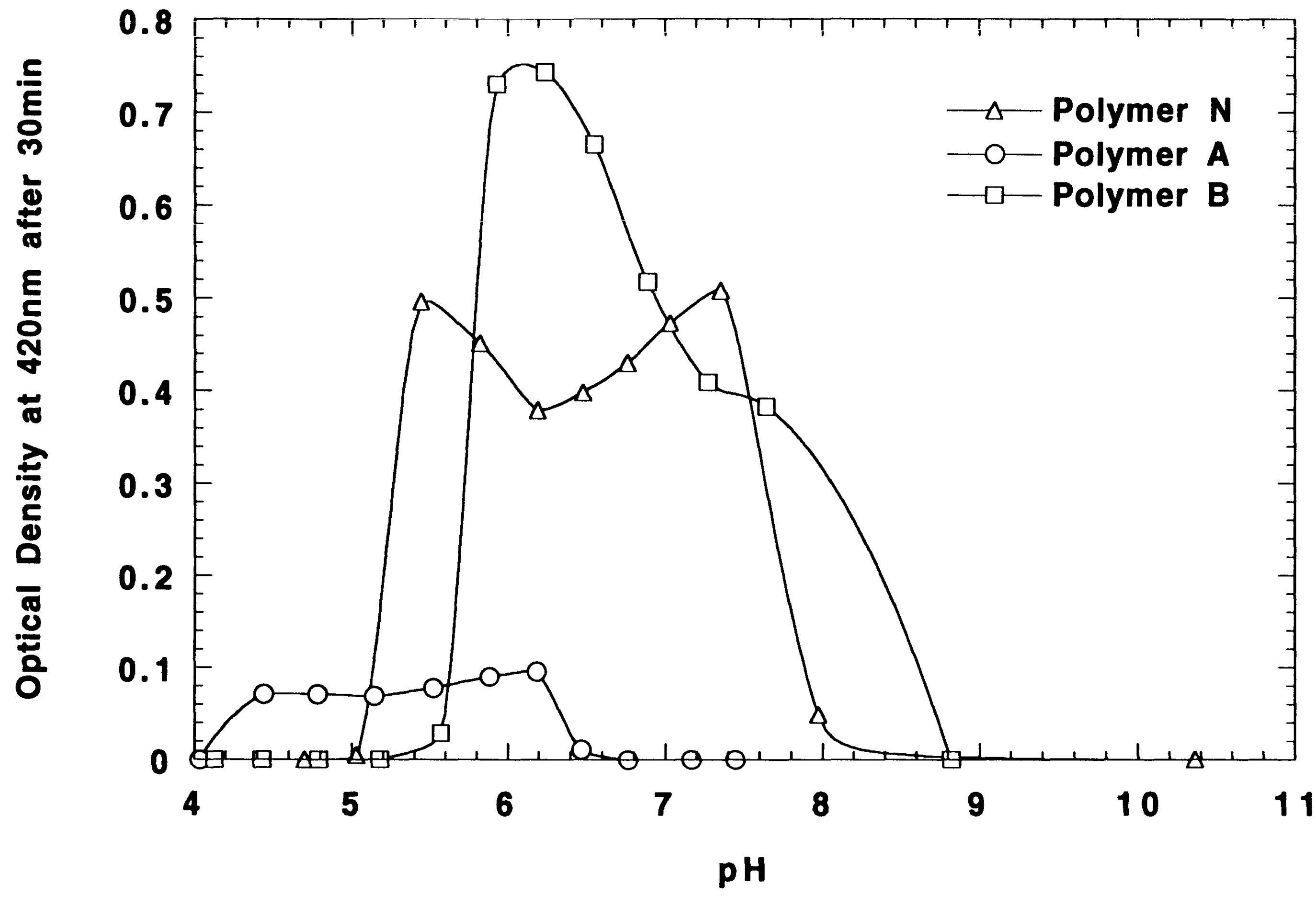

Figure 6.5 Pseudosteady-state optical density profiles of 0.01% w/w solutions of polyampholytes with no added salt.

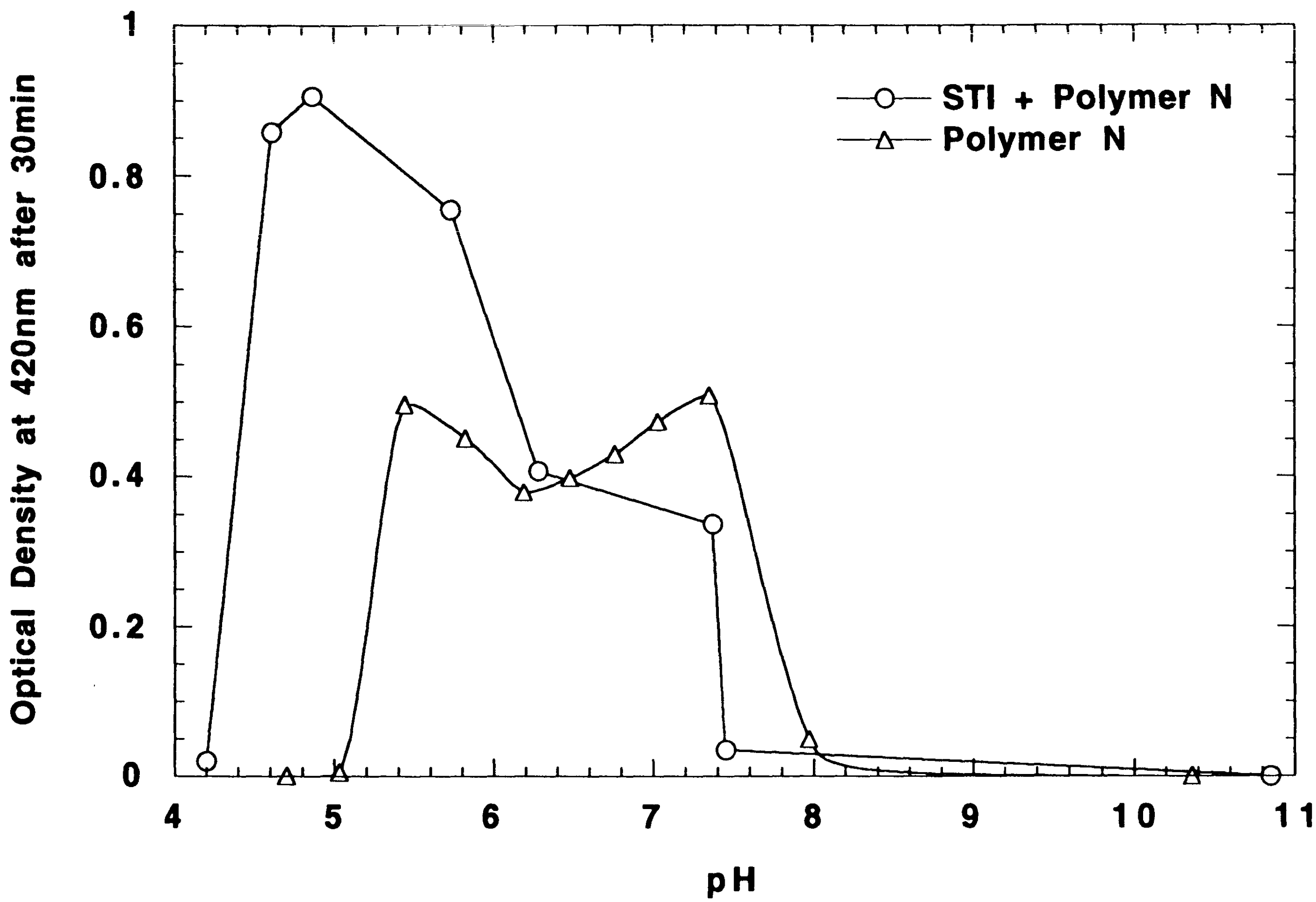

Figure 6.6 Pseudosteady-state optical density profile of a mixture containing 0.05% w/w STI and 0.01% w/w Polymer N. For comparison, the optical density profile of pure polymer (0.01%) is replotted from Figure 6.5.

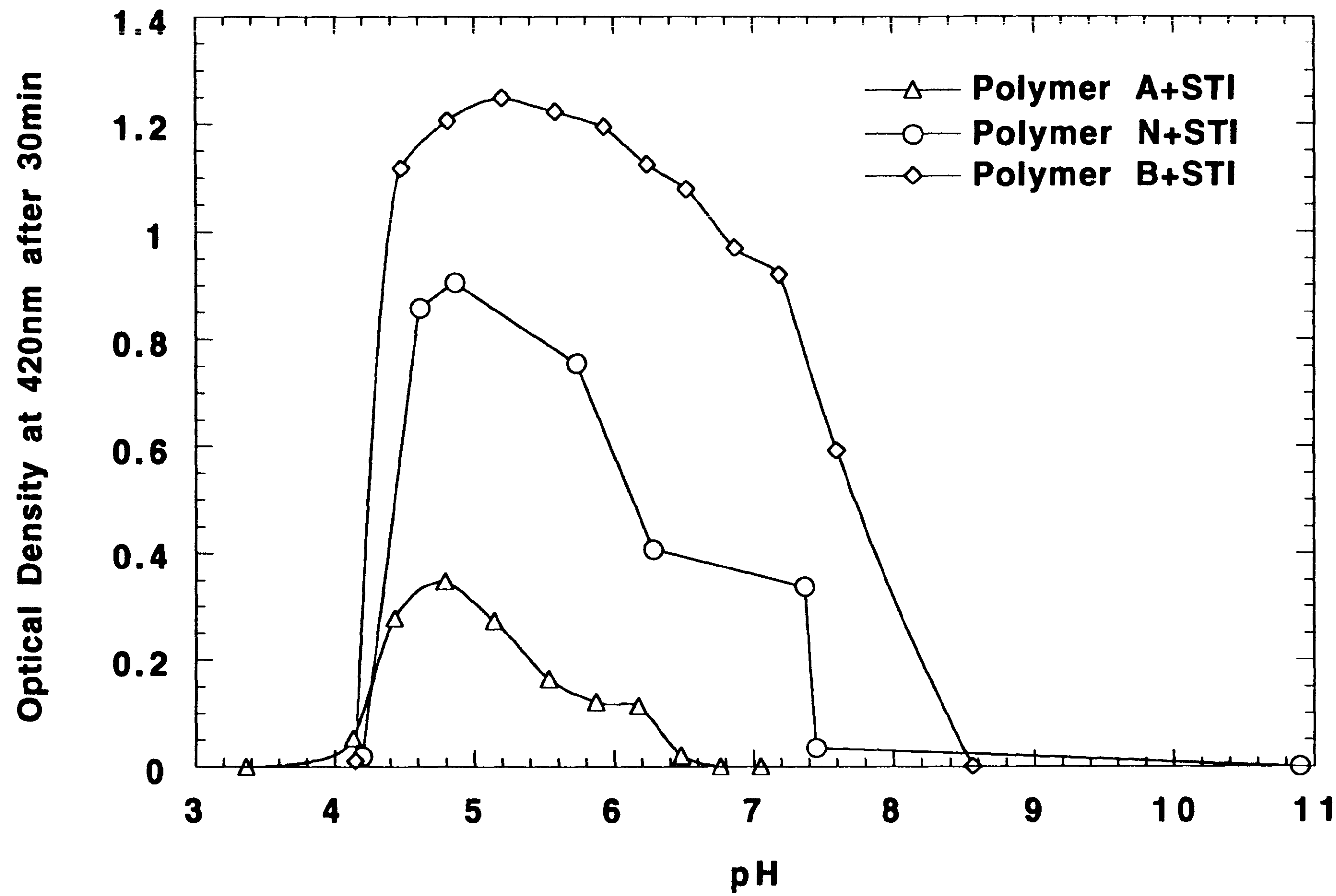

Figure 6.7 Pseudosteady-state optical densities of binary mixtures of STI (0.05%) with Polymer A (0.01%), Polymer N (0.01%), and Polymer B (0.01%).

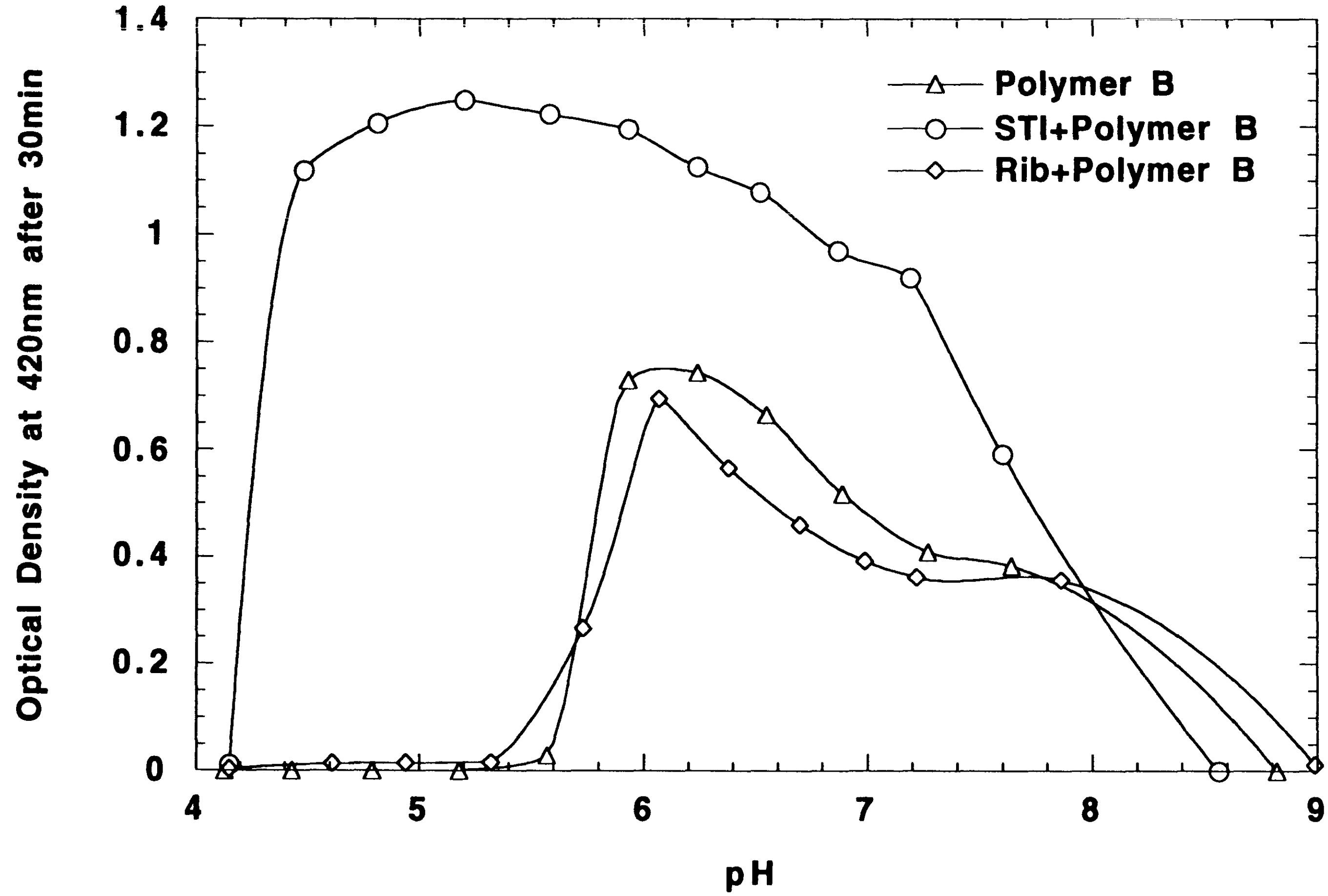

Figure 6.8 Pseudosteady-state optical density of binary mixtures of Polymer B (0.01%) with STI (0.05%) and with ribonuclease (0.05%). For comparison, the optical density of pure polymer solution (0.01%) is also shown.

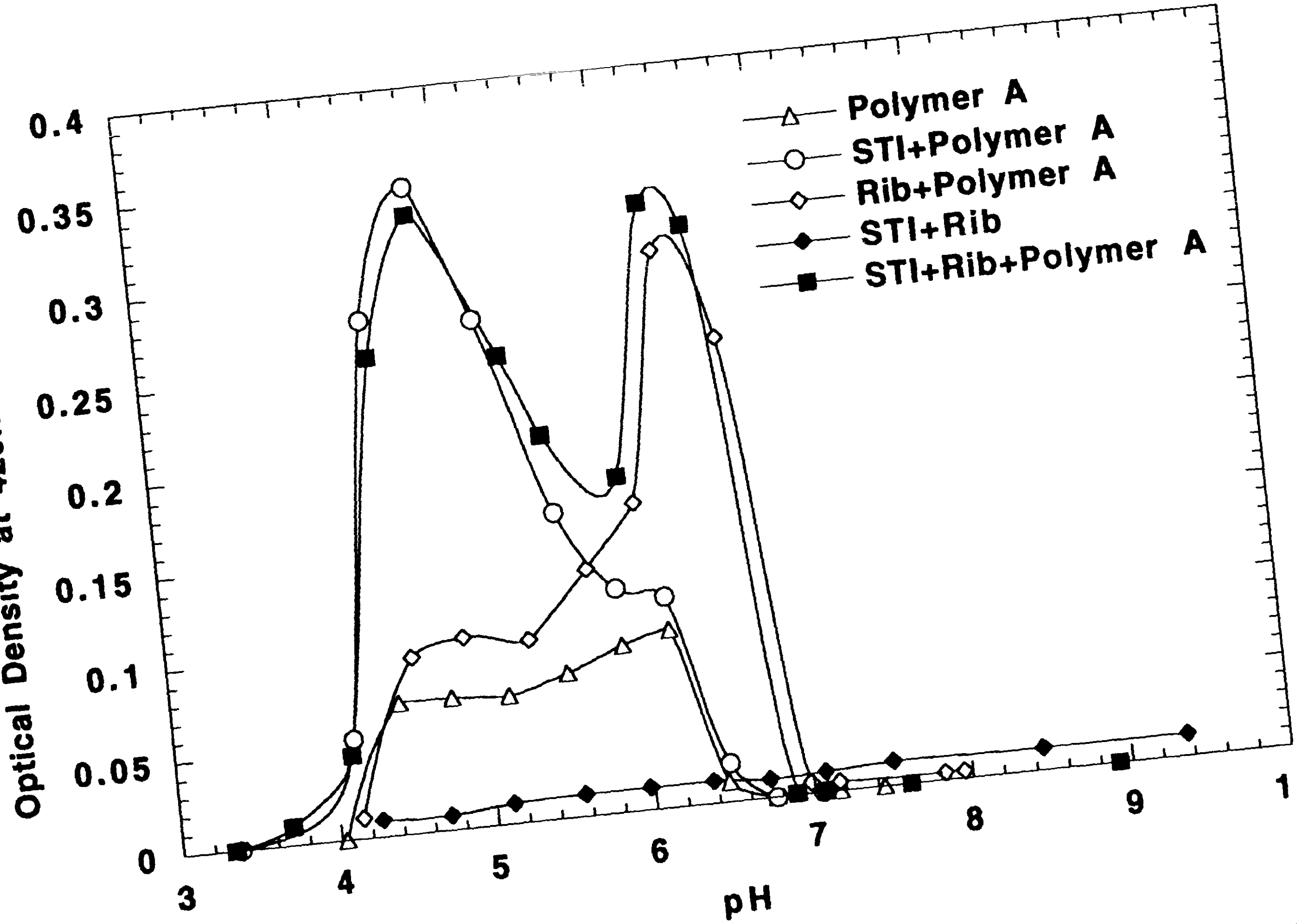

Figure 6.9 Pseudosteady-state optical density of a tertiary mixture composed of STI (0.05%), ribonuclease (0.05%) and Polymer A (0.01%). The optical densities of the binary mixtures and the polymer are also shown.

Chapter 7.

Triblock Methacrylic Polyampholytes as Protein Displacers in Ion-Exchange Chromatography.

In this chapter the utilization of the polyampholytes for protein separation by anion-exchange displacement chromatography is explored. It is already known from Chapter 4 that only block polyampholytes have high column affinity and, therefore, in this Chapter no random polymers are tested for protein separation. A homopolymer of methacrylic acid is used as a control in one displacement. The model protein feed that is used in the displacements is a crude mixture of β-lactoglobulins containing the A and B isoforms. The methacrylic block polyampholytes have two attractive process-scale features: (i) they can be desorbed for column regeneration at the mild conditions of elevated salt concentration as opposed to the traditionally employed extreme conditions of low pH and high salt concentration, and (ii) they can be precipitated at the appropriate pH and salt conditions and recycled. An aspect of fundamental interest resulting from their ampholytic nature is that these copolymers can be used for both anion and cation exchange displacements.

7.1 Introduction

Displacement chromatography is a promising preparative separation technique that, in contrast to traditional elution chromatography, allows for high throughput and results in the concentration of the components in addition to their resolution [1-3]. Furthermore, the tailing observed in preparative elution is greatly reduced in displacement chromatography due to the self-sharpening boundaries developed during the process. The distinguishing feature of the process is the utilization of the displacer, a high affinity species that displaces the adsorbed solutes from the stationary phase; nevertheless, the interaction of the components of the mixture with the stationary phase along the column length is still necessary for the development of the displacement train. This means that if the column is saturated with the mixture, the column length will not be sufficient for complete resolution of the components. Typically, 30% saturation allows for good separation.

Ion-exchange displacement chromatography is suitable for the preparative separation of charged biomolecules such as proteins. It can be particularly useful for the purification of pharmaceutical proteins because the desired species will be simultaneously separated and concentrated. Although recently there have been numerous studies on ion-exchange displacement chromatography of proteins, there has not been any effort towards the rational design of displacers. One reason for this is that displacers of biological origin, such as dextran derivatives [4-6], protamine [7], heparin [8] and pentosan polysulfate [9] have been used with some success and have attracted much attention as they are believed to be non-toxic and biocompatible. The absence of "optimal" displacers is one of the reasons for the slow acceptance of displacement chromatography at the process-scale.

A very recent example of designed displacers is starburst polymers [10] which are similar to proteins because they are compact monodispersed spherical molecules. Additionally, they have a high surface charge density, resulting in a high affinity for the stationary phase which ensures their ability to act as displacers.

Another example of designed displacers is block polyampholytes, which is the subject of the present report. These molecules are low-molecular-weight triblock copolymers of methacrylic acid (Ac), dimethylaminoethyl methacrylate (B) and methyl methacrylate (M). Table 7.1 lists the polymers used in this study along with their properties including the isoelectric point (pI). Polymer 14 is not a polyampholyte but a homopolymer and, therefore, it does not have a pI. The synthesis and characterization of the polyampholytes have been reported elsewhere [11]. We report here on their successful utilization as anion-exchange displacers for the separation of β-lactoglobulins A and B. It is interesting to point out that, as a result of their ampholytic nature, these copolymers can be used also for cation exchange displacements.

These novel displacers possess two attractive process-scale features. First, they can be desorbed for column regeneration in one column volume at the displacement operating pH by raising the salt concentration above 0.5M. These mild regeneration conditions are in contrast to the traditional extreme conditions of low pH and high salt concentration used with other displacers. Second, the displacer can be easily isolated from the concentrated column regenerant solution by precipitation at the isoelectric point.

7.2 Experimental Section

7.2.1 Materials

Tris(hydroxymethyl) aminomethane, tris(hydroxymethyl) aminomethane hydrochloride, sodium chloride, monosodium phosphate, sodium nitrate and β-lactoglobulins were purchased from Sigma (St. Louis, MO). The displacers, listed in Table 7.1, were synthesized by Group Transfer Polymerization [11] and characterized in terms of their non-linear adsorption properties [12] as described in Chapters 2 and 4, respectively. A Protein-Pak Q-8HR (100 X 5 mm i.d.) column was purchased from Waters Chromatography, Division of Millipore (Milford, MA). The packing material of this column is a strong anion-exchanger based on quaternary methylamine. A mini-column cartridge (50 X 5 mm i.d.) purchased from Waters was packed with perfusion strong anion-exchange material of quarternized polyethyleneimine purchased from Perseptive Biosystems (Cambridge, MA). A Protein-Pak DEAE-8HR (100 X 5 mm i.d.) weak anion-exchange column was a gift of Waters and was repacked with the same material to a length of 75mm (75% of full column length).

7.2.2 Apparatus

A Waters 600 Multisolvent Delivery System (Waters Chromatography, Division of Millipore, Milford, MA) was used for solvent delivery both in displacement and analysis. A Valco Model C10W ten-port manual injector (Valco Instruments, Houston, TX) fitted with 2-mL and 7-mL loops was used for the injection of proteins, displacer and regenerant. An LKB Model 2212 Helirac (Pharmacia-LKB Biotechnology) was used for fraction collection. A Rheodyne 7125 manual injector (Rheodyne, Cotati, CA) fitted with a 20-μL sample loop was used for sample injection. A Waters UV-Vis Detector was used for monitoring at 240nm the column effluent during sample analysis, and a Waters Integrator was used for recording and processing the results of the analysis.

7.2.3 Methods

Displacements. A 30mg/mL solution of the crude mixture of β-lactoglobulins A and B was prepared by dissolving protein powder in the mobile phase, which was Tris buffer containing 50mM Cl^- at pH 7.5 or 8.5. No pH adjustment was necessary after the dissolution because the resulting pH was the same as the original pH of the mobile phase. The solutions of the displacers were prepared by dissolving polymer powder into the mobile phase at a concentration slightly higher than that desired, adjusting the pH with concentrated (50% w/v) tris(hydroxymethyl) aminomethane solution and diluting with mobile phase to the desired polymer concentration. The Protein-Pak Q-8HR column was equilibrated for 10 column volumes with the mobile phase at a flowrate of 0.5mL/min. The flowrate during the introduction of the protein mixture and the displacer was 0.1mL/min. The solution of the protein mixture was loaded to the 2-mL loop on the Valco injector and 75% of it was injected into the column. During the injection of the protein mixture, the 7-mL loop of the Valco injector was loaded with the displacer solution. After the injection of 1.5mL of the solution of the protein mixture, the valve of the injector was switched to the other position to initiate the injection of the displacer solution. Only 75% of the volume of the 2-mL loop was injected to avoid the introduction of the tail of the loop in which the solution was diluted by dispersion. To avoid mixing in the flow cell, no detector was used, the fraction collector being connected directly to the outlet of the column. The first two fractions collected were 1.5mL each and corresponded to the dead volume of the column (1.4mL) and to the volume of the effluent during the loading of the protein solution (1.5mL). No proteins or displacer were expected in these fractions. All the subsequent fractions, covering elution volumes from the third to the eighth mL of column effluent, were of 0.1mL. The fractions were immediately diluted 20 times with mobile phase, refrigerated and analyzed within 24 hours.

Analyses. The weak anion-exchange column was used for the protein analysis. The flowrate was 0.75mL/min and the mobile phase was Tris buffer containing 20mM Tris hydrochloride at pH 8.0. For the non-overlapping protein fractions, the mobile phase contained 175mM NaCl that resulted in retention times of 2.5 and 3.0 minutes for the B and A isoforms, respectively. For the overlapping protein fractions, the resolution was increased by decreasing the salt concentration in the mobile phase to 145mM NaCl, shifting the retention times to 5 and 8 minutes, respectively.

For the polymer analysis, a salt gradient from 0.2 to 1.0M NaCl was employed at pH 8.5, with a flowrate of 1mL/min. The mini-column packed with the perfusion strong anion-exchange material was used. The polymer emerged at 7 minutes and every analysis cycle, including column reequilibration, lasted 20 minutes.

Displacer Characterization. After protein displacement, the fraction collector was removed and the displacer remaining in the dead volume was washed for five column volumes. The UV detector was connected at the outlet of the column and a front of 30mM sodium nitrate was introduced at 0.5mL/min to assess the column sites not occupied by the adsorbed displacer [5,12]. The column effluent was monitored at 310nm and the nitrate breakthrough time was determined.

Regenerations. After the displacement and the nitrate front experiment, the column was reequilibrated with the Tris buffer at pH 7.5 or 8.5, and the regenerant solution was introduced through the 7-mL loop of the Valco Injector. The regenerant was Tris buffer at pH 7.5 or 8.5 containing 1M NaCl and the flowrate was 0.2mL/min. The column effluent during regeneration was monitored at 310nm. The efficiency of the regeneration was tested by determining the capacity of the column in nitrate anions.

In the experiments for evaluating different regenerant solutions, the displacer solution was introduced directly to the column, with no prior protein displacement. Polymer 10 at 30mg/mL and pH 7.5 was chosen as the model displacer for these experiments. The regenerant solutions evaluated were: (1) 100mM phosphate at pH 2.3 without NaCl, (2) 100mM phosphate at pH 2.3 and 1M NaCl, and (3) Tris 50mM Cl- buffer at pH 7.5 containing 1M NaCl.

Polymer Recycling. A 100mg/mL solution of Polymer 10 was precipitated by adjusting the pH to the isoelectric point. After centrifugation and decanting, the precipitate was washed with distilled water to remove any entrapped salt and redissolved in acid solution. The dissolution-precipitation cycle was repeated five times and, finally, the polymer was dried and weighed. A 30mg/mL solution of the recycled polymer was prepared in Tris 50mM Cl^- and at pH 7.5. This solution was subjected to frontal adsorption on the Protein-Pak Q-8HR column and to salt gradient elution analysis on the perfusion column; the results were compared with those obtained using an identical solution of the virgin (not recycled) polymer.

7.3 Results and Discussion

Six issues are addressed and discussed in this section: displacements, characterization of displacers at column saturation, regeneration, displacer recycling, optimization of displacer and displacer toxicity.

7.3.1 Displacements

Figures 7.1 to 7.5 show the displacement chromatograms of a crude mixture of β-lactoglobulins A and B. Table 7.2 lists the displacer and displacer concentration employed in each Figure. All of the displacements were performed at pH 8.5 except that of Figure 7.1 which was performed at pH 7.5.

Figure 7.1 presents the complete resolution of β-lactoglobulins A and B by displacement using 40mg/ml of the acid-rich triblock polyampholyte at pH 7.5. This displacer concentration is equivalent to 167mM of methacrylic acid, which is the negatively charged displacing residue. The two proteins emerged as square zones, characteristic for fully developed displacements. The overlap between the two proteins as well as between the displacer and the more strongly retained protein, β-lactoglobulin A, was minimal.

Figure 7.2 shows the displacement of the same mixture by the same displacer at the same concentration at pH 8.5. In contrast to the results shown in Figure 7.1, the displacement train was not fully developed and the separation was not complete. The more weakly retained protein, β-lactoglobulin B, emerged as a skewed triangular band and the zones of the two proteins overlapped. This is a situation typical of insufficient column length [13]. The deterioration of the separation at pH 8.5 in Figure 7.2 as compared to that at pH 7.5 in Figure 7.1 can be attributed to the difference in the characteristic charge of the displacer. By increasing the pH from 7.5 to 8.5 the characteristic charge is increased from 5.7 to 9.5 (see below). Since the displacer concentration in the two runs is the same, the salt concentration in the induced salt front (salt displaced by the proteins and the displacer) at pH 8.5 is almost twice as high as that at pH 7.5. The environment of higher salt concentration at pH 8.5 results in a more pronounced screening of the electrostatic interactions between the stationary phase and the proteins. These interactions are responsible for the separation and their suppression will require a longer column for satisfactory resolution of the mixture. An additional effect of the increased pH is the enhancement of the affinity of both proteins for the stationary phase because they become more negative. However, the impact of this on the quality of the separation is not obvious. It would be positive only if the affinity of the more retained protein is increased and the affinity of the less retained protein is decreased.

To test whether the non-adsorbing blocks of Polymer 10 were responsible for the poor separation in Figure 7.2, the displacement was repeated by replacing the displacer by the homopolymer, poly(methacrylic acid), in Figure 7.3 . The concentration of the new displacer was only 14.4mg/mL to maintain the same methacrylic acid residue equivalence as that employed in Figure 7.2. The displacement chromatogram obtained was very similar to that in Figure 7.2, indicating that the copolymeric nature of the displacer did not deteriorate the displacement. On the contrary, the separation by the homopolymer was worse, as evidenced by the long tail of the more strongly retained protein within the displacer zone.

Figure 7.4 shows the displacement of Figure 7.2 repeated at half the displacer concentration. The polymer concentration was 20mg/mL, corresponding to 83mM of methacrylic acid residues. The complete separation can be attributed to the lower (than in Figure 7.2) salt concentration in the induced salt front which resulted from the lower displacer concentration. The less pronounced screening of the electrostatic interaction as compared to that in Figure 7.2 allowed for more extensive matrix-protein interaction leading to full development of the displacement train.

Figure 7.5 illustrates another successful displacement separation by a different triblock polyampholyte, containing a lower percentage of displacing residues. To ensure the same concentration as that used in Figure 7.4 (83mM) the concentation of the displacer was raised to 37mg/mL. The chromatogram obtained was very similar to that in Figure 7.4 and the separation was complete. However, a long tail of β-labtoglobulin A extended into the displacer zone indicating an interaction of the protein with the positive block of the polymer. There are three factors that could be responsible for such an interaction in the case of Polymer 5 and not in the case of Polymer 10. Polymer 5 has a smaller number of negatively charged residues, a larger number of positively charged residues and a longer sequence of neutral units separating the oppositely charged residues.

7.3.2 Characteristic Charge

Recently we reported on the characterization of the block polyampholytes based on the column adsorptive capacity for the polymer determined from the breakthrough of a displacer front and, subsequently, the column sites inaccessible to the polymer, from the breakthrough of a nitrate front [12]. Those experiments were performed in the absence of proteins. Here we report the same characterization, but in the presence of the displaced proteins. The breakthrough volume of the displacer was read off the displacement chromatograms (Figures 7.1-7.5) and appears in Table 7.2. The column capacity in the displacer is also shown in Table 7.2 and it was calculated by subtracting from the displacer breakthrough volume the dead volume of the column (1.4mL) and the volume of the effluent during the loading of the protein feed (1.5mL), and multiplying the result by the displacer concentration. The number of column sites occupied by the displacer was calculated by subtracting the number of column sites accessible to the nitrate in the presence of the adsorbed displacer from the total number of column sites (340μmoles). In agreement with the previous study [12] and with the exception of Polymer 5, the number of sites occupied by the displacer was constant. Shown in the last column of Table 7.2 is the characteristic charge, calculated as the number of column sites occupied by a displacer molecule. The characteristic charges determined previously using a different column and in the absence of proteins [12] are shown in parentheses and compare well with the values determined in this study. As discussed in the previous study, the increase in the characteristic charge of Polymer 10 with pH is not due to the increase in the degree of ionization of the negatively charged residues but to the decrease in the degree of ionization of the positively charged residues.

7.3.3 Column Regeneration

It was observed in a previous study [12] that the block polyampholytes elute at a salt concentration around 0.5M NaCl. This is due to the relatively short length of the adsorbing block and to the presence of a block of opposite charge. Since, the condition employed successfully for column regeneration has been 1M NaCl at the displacement pH.

In addition to successful regeneration, polymer recycling by precipitation is another important process-scale consideration. Since recycling will follow regeneration, there could be an opportunity to optimize the process by modifying the regeneration scheme such that the solution of the desorbed polymer be most appropriate for precipitation. Figure 7.6 shows the phase diagram of Polymer 10 at 10mg/mL in the salt-pH space. The two-phase (precipitation) region extends around the isoelectric point of 5.4 and narrows down with increasing salt concentration due to the salting-in effect.

The first attempt was to use a regenerant solution that does not utilize large amounts of salt. It was expected that if the pH of the regenerant was at a value lower than the isoelectric point of the polymer such that the latter had the same polarity as the stationary phase then the polymer could be successfully removed from the column. This was tested by injecting five column volumes of a regenerant solution composed of 100mM phosphate at pH 2.3 with no added salt. The regeneration was not successful. This was attributed to the large amounts of adsorbed polymer which, in concert with the large buffering capacity of the polymer, shifted the pH of the regenerant solution to a higher value. Using the experimental titration curve of the polymer, it was estimated that for successful polymer removal in one column volume the phosphate molarity should have been 300mM. This, however, was not pursued because the required phosphate concentration was considered relatively high and phosphate is expensive.

Next the regenerant traditionally utilized for the removal of polyanionic displacers was tested. This was 100mM phosphate at pH 2.3 containing 1M NaCl. The regeneration, although successful, required two column volumes of regenerant.

The third regenerant tested was the one that has been used for column regeneration after the protein displacements of this study. This was Tris 50mM Cl^- at pH 7.5 containing 1M NaCl. The regeneration with this solution was also successful and took place within one column volume. One would find counter-intuitive the fact that the second regenerant solution, despite its very low pH, was less efficient than the third solution. This can be attributed again to the buffering capacity of the adsorbed polymer which raised the pH of the second regenerant. We estimated that within the passage of one column volume of regenerant the pH approached the isoelectric point of the polymer that not only would disfavor desorption but it would create the risk for polymer aggregation within the column (Figure 7.6). Salt-regeneration is independent of the titration characteristics of the polyampholytes and this seems to be the best strategy for the removal of these polymers, especially because it can be accomplished at the operating pH, which is not at extreme values.

It should be pointed out that, unlike Polymer 10, some triblock polyampholytes become completely soluble at 1M salt. Such an example is Polymer 2, whose solubility curves at various salt concentrations were presented in Figure 2.4. It was observed that the isoelectric solubility of Polymer 2 at 0.3 and 0.5M KCl was fairly low, around 1%. Therefore, for the recycling of this polymer from column regenerant solutions whose salt and polymer concentration will be typically 1M and 10%, respectively, it is recommended that this solution be diluted two-fold or three-fold. This will make possible polymer precipitation at the isoelectric point and will result in substantial polymer recovery, around 70%.

7.3.4 Polymer Recycling

An 80% recovery was calculated for the polymer recycling by precipitation. The 20% loss was due to impurities which could not be precipitated and to particles of the precipitated polymer that were too small to be recovered. To test whether the recycled polymer retained its column affinity, the capacities of the Protein-Pak Q-8HR column for the recycled and for the virgin polymer were determined by frontal adsorption. The results showed that the amount of the recycled polymer adsorbed was 15% less than the amount of the virgin polymer. This can be attributed either to salt entrappment into the recycled polymer that would decrease the polymer affinity to the stationary phase or to the presence of 15% impurities in the virgin polymer. The salt gradient elution analyses showed that the second possibility is the case as a 15% higher polymer concentration was determined in the solution of the recycled polymer. This result is disappointing in the sense that more accurate results would have been obtained if the polymers had been purified by precipitation prior to the chromatography experiments. This was not done because of the anticipation that some salt would be retained within the precipitated polymer lowering its ion-exchange activity. However, the results are distorted only by 15% which can still be considered a small error. The same result is very encouraging for future practical applications of these polyampholytes because not only does the displacer retain its affinity after recycling, but it is also purified.

7.3.5 Displacer Optimization

Optimizing the polyampholytic displacers may seem to be a very complicated task because there are many polymer properties that might be varied independently from each other, including polymer size, composition, block architecture, structure in solution, chemical type of the residues. However, we are in position to make reasonable choices for the optimal values of some of these properties and we can predict the effects that result from the variation of the other properties.

The size of the displacers in this study was around 4,000Da and the number of the adsorbing residues per molecule was 10 and 20. Despite their relatively small size, the polymers were successful displacers at the appropriate conditions and efficiently separated the model protein mixture. Displacers with larger size (e.g. 40,000Da) would require extreme conditions for regeneration and displacers with much larger size (e.g. 400,000Da) would be excluded from the pores of the stationary phase. On the other hand, smaller polymer size would only create the risk for insufficient displacer affinity. Therefore, it is reasonable to assume that the polymers used here are about the optimal size.

The polyampholyte composition should be extreme so that there is a large excess of acidic over basic residues in anion-exchange displacement and an excess of basic residues in cation exchange. In this way the repelling (same polarity with the stationary phase) residues would have a minimal effect on the decrease in the affinity of the displacer and it would be less likely for the same residues to interact with the displaced proteins (Figure 7.5). However, this excess should not be too large because it will result in an extreme isoelectric point which should be achieved for polymer recycling. From a theoretical prediction [11] a 10/1 ratio (as compared to 2/1 for Polymer 10 of this study) would be satisfactory because it should result in an isoelectric point around 4.5, which is a non-extreme pH value.

It might be desirable to eliminate the micellar structures that the triblock polyampholytes form [11] because they were considered responsible for the high pressure drops observed in some displacements. This can be achieved by eliminating the hydrophobic block and staying at diblock polyampholyte architecture. Polymer 11 in Table 2.1 was such an example and it was shown in Chapter 4 that it had an ion-exchange affinity comparable to that of the triblocks [12]. Another advantage for the diblock polyampholyte is that the repelling block, being adjacent to the adsorbing block, would be less likely to interact with the proteins (note that Polymer 5 has 20 neutral residues spacing the two oppositely charged blocks). A disadvantage, however, of this polymer is that it is difficult to recycle because it salts-in very easily.

7.3.6 Toxicity

Unlike dextran-based displacers, the methacrylic polyampholytes are of synthetic rather than biological origin. Polymethacrylates are compatible with human tissue and, because of their transparency, they are the material from which hard and soft contact lenses are made [14]. A study on the toxicity of hydrophilic methacrylate gels on fibroblast cells showed that the methacrylic acid, the methyl methacrylate, the hydroxyethyl methacrylate and the trimethylaminoethyl methacrylate residues were non-toxic, while the dimethylaminoethyl methacrylate residue was mildly toxic [15]. This suggests that it would be better to use the quaternary amine residue for the polyampholytes than the tertiary amine. It also implies that while neutral dextran is non-toxic, the derivatized DEAE-dextran (diethylaminoethyl-dextran) that is used as a cation exchange displacer might be mildly toxic.

It should be stressed that, as with all synthetic monomers, methacrylate monomers are toxic. Methacrylic acid is corrosive and toxic and dimethylaminoethyl methacrylate is poisonous and is an irritant [16]. This implies that, after polymerization, it should be ensured that all traces of unreacted monomer are removed. The polyampholyte property of isoelectric precipitation offers a convenient means of such a purification in aqueous environment.

It appears, therefore, that these polyampholytes will prove not to be toxic. However, it is necessary that their intravenous toxicity also be tested before their utilization for the separation of pharmaceutical proteins is allowed.

7.4 Conclusion

A new class of efficient ion-exchange displacers has been introduced. These are synthetic block copolymers based on methacrylic acid. The small size of these molecules and their ampholytic nature facilitate column regeneration, which can be optimized by utilization of a 1M NaCl solution at the displacement operating pH. The property of these polyampholytes that they precipitate around the isoelectric point provides the opportunity for polymer recycling which constitutes a significant economic advantage for displacement chromatography at the process-scale. Before these polymers are used for the industrial displacement separation of pharmaceutical proteins, their intravenous toxicity must be determined.

7.5 Literature Cited

(1) Horvath, C. *The Science of Chromatography*; Brunner, F., Ed., Elsevier: Amsterdam, 1985; p 185.

(2) Frenz, J.; Horvath, C. *High Performance Liquid Chromatography: Advances and Perspectives*; Horvath, C., Ed., Academic Press: Orlando, FL, 1988; Vol. 8, p 211.

(3) Cramer, S. M.; Subramanian, G. Recent Advances in the Theory and Practice of Displacement Chromatography. *Sep. Purif. Methods* **1990,** *19*(1), 31-91.

(4) Jen, S. C. D.; Pinto, N. G. Dextran Sulfate as a Displacer for the Displacement Chromatography of Pharmaceutical Proteins. *J. Chromatogr. Sci.* **1991,** *29,* 478-484.

(5) Gadam, S. D.; Jayaraman, G.; Cramer, S. M. Characterization of Non-Linear Adsorption Properties of Dextran-Based Polyelectrolyte Displacers in Ion-Exchange. *J. Chromatogr.* **1993,** *630,* 37-52.

(6) Jayaraman, G.; Gadam, S. D.; Cramer, S. M. Ion-Exchange Displacement Chromatography of Proteins: Dextran-Based Polyelectrolytes as High Affinity Displacers. *J. Chromatogr.* **1993,** *630,* 53-68.

(7) Gerstner, J. A.; Cramer, S. M. Cation-Exchange Displacement Chromatography of Proteins with Protamine Displacers: Effect of Induced Salt Gradients. *Biotechnol. Prog.* **1992,** *8,* 540-545.

(8) Gerstner, J. A.; Cramer, S. M. Heparin as a Nontoxic Displacer for Anion-Exchange Protein Displacement Systems. *BioPharm* **1992,** *Nov.-Dec.,* 42-45.

(9) Gadam, S. D.; Cramer, S. M. Pentosan Polysulfate as Anion-Exchange Protein Displacer. Submitted to *J. Chromatogr.*

(10) Jayaraman, G. Ion-Exchange Displacement Chromatography of Proteins: Heuristic Approaches in Displacer Design. Rennselaer Polytechnic Institute, PhD Thesis, 1993.

(11) Patrickios, C. S.; Hertler, W. R.; Abbott, N. L.; Hatton, T. A. Synthesis and Solution Behavior of Methacrylic Polyampholytes. Accepted for publication in *Macromolecules*.

(12) Patrickios, C. S.; Gadam, S. D.; Cramer, S. M.; Hertler, W. R.; Hatton, T. A. Chromatographic Characterization of Acrylic Polyampholytes. *Polyelectrolytes*; Schmitz, K. S., Ed.; ACS Symposium Series, in press.

(13) Brooks, C. A., III On the Characterization of Equilibrium in Ion-Exchange Chromatography: Steric Mass-Action Ion-Exchange. Rennselaer Polytechnic Institute, PhD Thesis, 1993, p 102.

(14) King, R. N.; Andrade, J. D.; Ma, S. M.; Gregonis, D. E.; Brostrom, L. R. Interfacial Tensions at Acrylic Hydrogel-Water Interfaces. *J. Colloid Interface Sci.* **1985**, *103*, 62-75.

(15) Hattori, S.; Andrade, J. D.; Hibbs, J. B., Jr.; Gregonis, D. E.; King, R. N. Fibroblast Cell Proliferation on Charged Hydroxyethyl Methacrylate Copolymers. *J. Colloid Interface Sci.* **1985**, *104*, 72-78.

(16) Scientific Polymer Products, Product Catalogue. 1991/92, pp 25, 28.

Table 7.1 Properties of the displacers.

Polymer	Name	B/M/Ac	Molecular Weight	pI
10	acidic	8/12/16	3812	5.4
5	neutral	10/20/10	4430	6.6
14	homopolymer	0/0/12	1032	---

Table 7.2 Frontal characterization of the displacers.

Fig	Pol	c (mg/mL)	Vb (mL)	Ads. (μmoles)	occ. sites (μmoles)	char. charge
7.1	10	40	5.6	28.2	162	5.7 (6.4)
7.2	10	40	4.5	16.7	158	9.5 (8.4)
7.3	14	14.4	4.0	15.3	153	10.2 (10.1)
7.4	10	20	6.3	17.7	---	---
7.5	5	37	5.6	22.6	128	5.7

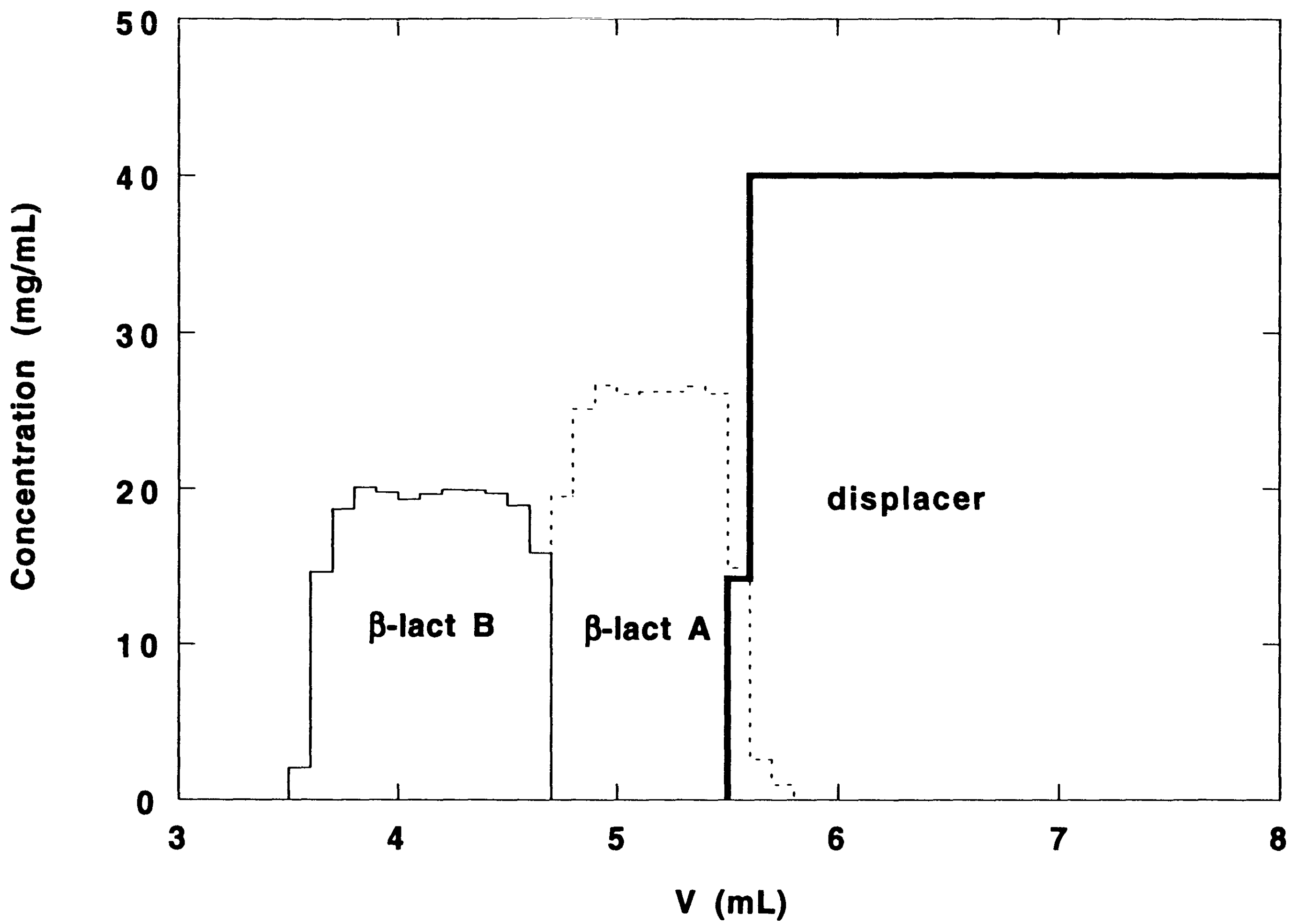

Figure 7.1 Displacement separation of β-lactoglobulins A and B by 40mg/mL of the acid-rich triblock polyampholyte at pH 7.5.

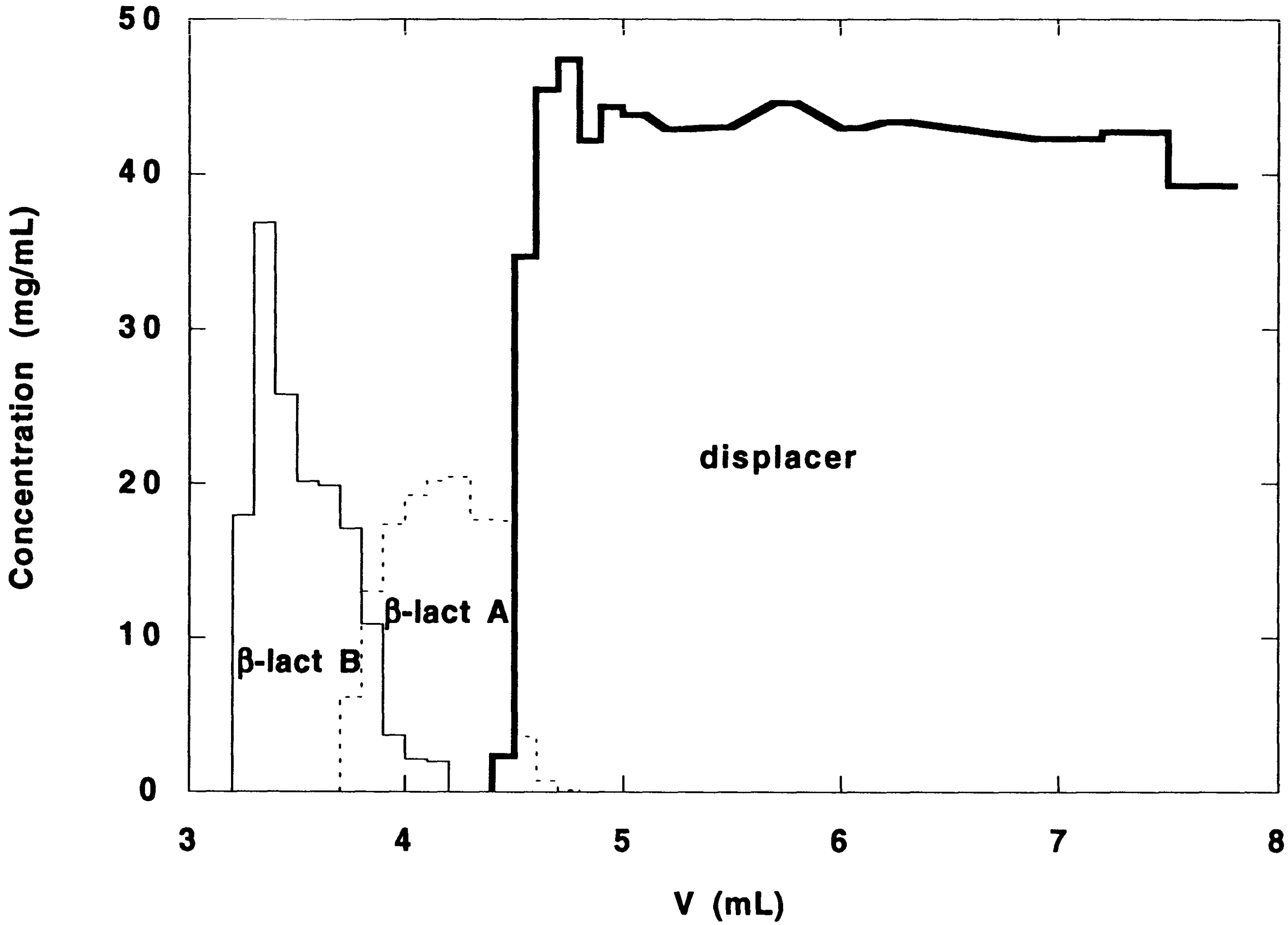

Figure 7.2 Displacement separation of β-lactoglobulins A and B by 40mg/mL of the acid-rich triblock polyampholyte at pH 8.5.

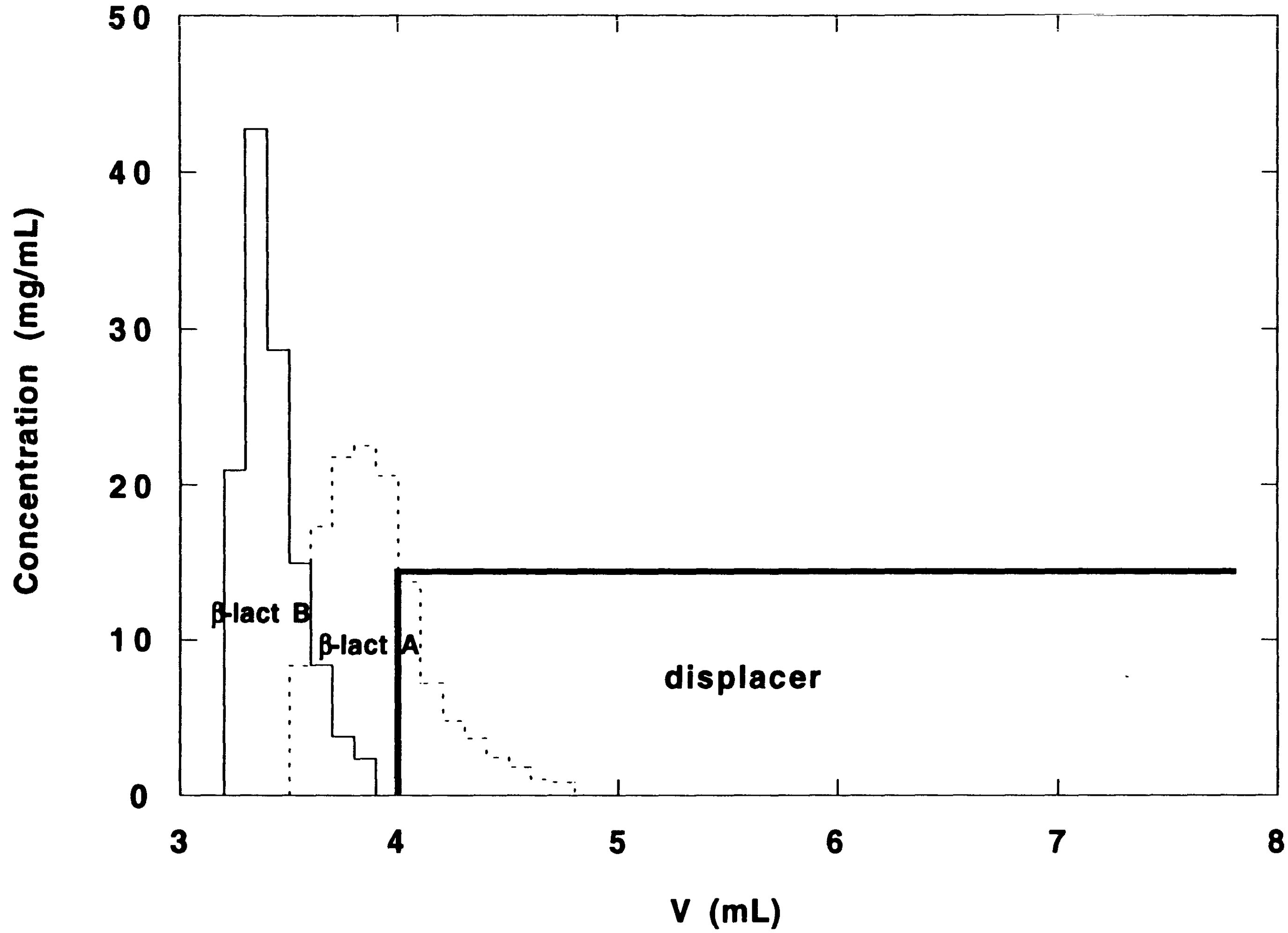

Figure 7.3 Displacement separation of β-lactoglobulins A and B by 14.4mg/mL of poly(methacrylic acid) at pH 8.5.

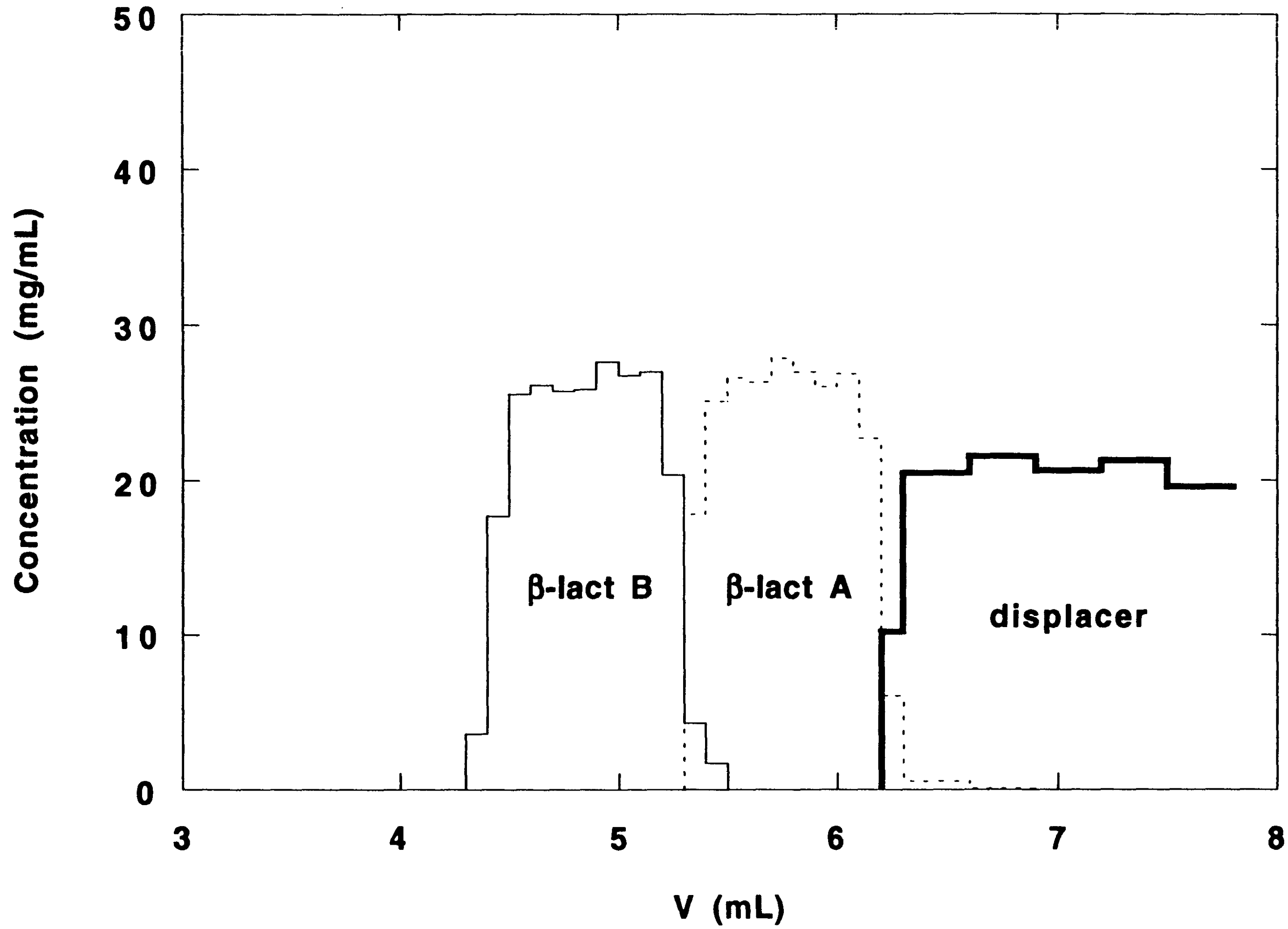

Figure 7.4 Displacement separation of β-lactoglobulins A and B by 20mg/mL of the acid-rich triblock polyampholyte at pH 8.5.

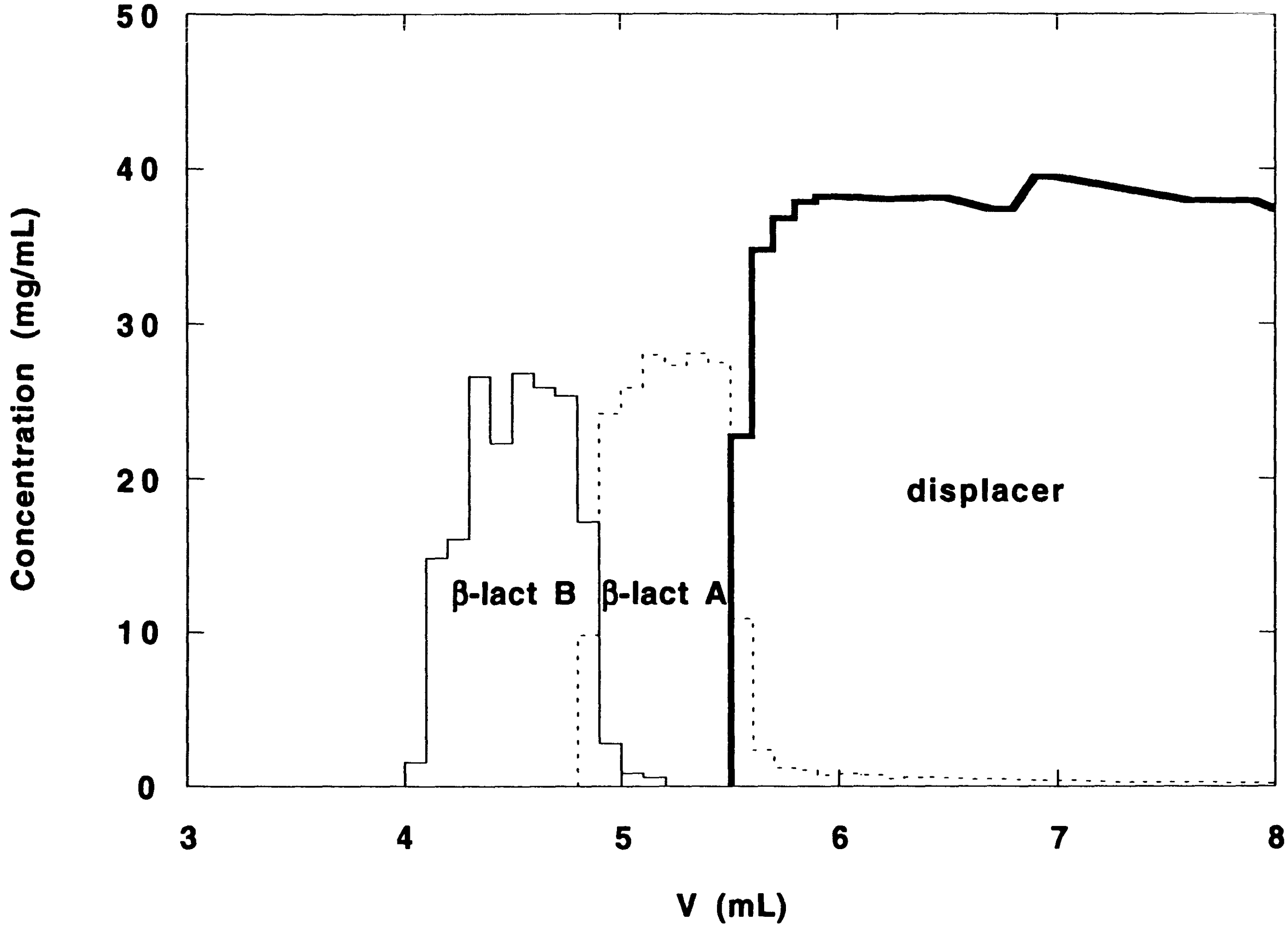

Figure 7.5 Displacement separation of β-lactoglobulins A and B by 37mg/mL of the neutral triblock polyampholyte at pH 8.5.

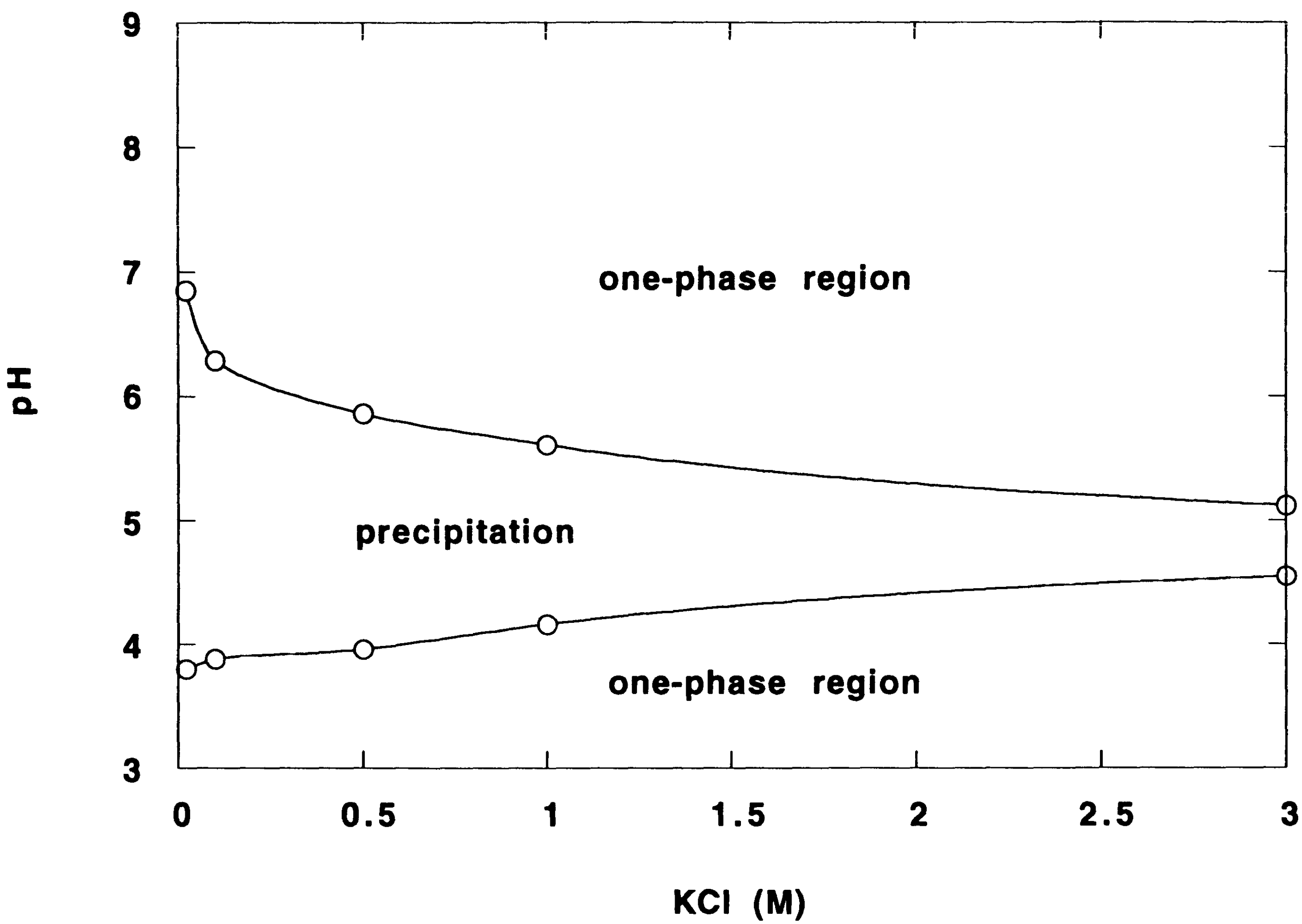

Figure 7.6 Phase diagram of the acid-rich triblock polyampholyte at a polymer concentration of 10mg /mL.

Chapter 8.

Random Acrylic Polyampholytes for Protein Extraction in Two-Phase Aqueous Polymer Systems.

Following the investigations of Chapters 5, 6 and 7 that dealt with the utilization of the polyampholytes for protein separation by coprecipitation and displacement chromatography, in this chapter we describe the application of the copolymers for protein extraction. A solution of poly(vinyl alcohol) and a polyampholyte solution are mixed and phase separate at the appropriate conditions of pH and salt concentration. In this aqueous two-phase polymer system proteins can be partitioned and fractionated. This study was performed chronologically first in the course of this thesis and the polyampholytes used were high molecular weight (30,000 and 80,000 Da) random copolymers synthesized by free radical polymerization. Another small difference between the polyampholytes of this Chapter and the polyampholytes described in the previous Chapters is that the acidic residue here was not methacrylic acid but acrylic acid. In Chapter 9, the phase-behavior of poly(vinyl alcohol) and the methacrylic polyampholytes synthesized by GTP is described. However, no protein partitioning was performed in these systems.

8.1 Introduction

Following twenty years of rapid progress in molecular biology, chemical engineering is now addressing many important and challenging issues in biotechnology at the process-scale. For example, bioproduct purification and protein refolding are two challenging areas where there is a strong need for the development of innovative and efficient large-scale processes. One approach to the purification of biomolecules which has received considerable attention is the extraction of proteins in two-phase aqueous polymer systems [1-5]. In particular, these systems appear attractive because of the large scale and continuous operability of the process. Other merits include the friendly aqueous environment which is provided for the labile protein products and the fast phase equilibration. On the other hand, a significant disadvantage of the process is the difficulty of protein recovery and polymer recycling. Furthermore, purified dextran used in the most common aqueous two-phase polymer system, the poly(ethylene glycol)-dextran system, is quite expensive and biodegradable [6,7].

To solve these problems, it is likely that the design and synthesis of new molecules to mediate and improve protein separation and purification will be necessary. Synthetic polymers and surfactants with varying chemical compositions and chain lengths and different affinity ligands are some examples of areas where much progress has been made. As increasing effort is devoted to the synthesis of highly functionalized molecules with very specific tasks, a major concern of the chemical engineer must be addressed, that of easy regeneration and recycling of the materials. Recycling is likely to be necessary in order to render these molecules attractive economically as well as to respond to an increasing environmental awareness.

In this work we have investigated the potential utility of random acrylic polyampholytes as novel phase-forming polymers in two-phase aqueous polymer systems for protein extraction. The polyampholytes form two-phase systems with poly(vinyl alcohol) under certain conditions. The effect of polymer concentration, salt concentration and cation type on phase composition and protein partitioning was studied experimentally.

A polyampholyte is a polyelectrolyte capable of acquiring both positive and negative charges. Examples of polyampholytes include biological molecules, such as proteins and nucleic acids and synthetic polyampholytes such as copolymers of acrylic acid (AA, potentially anionic residue), dimethylaminoethyl methacrylate (B, potentially cationic residue) and methyl methacrylate (M, neutral, hydrophobic residue). The prospect of using random acrylic polyampholytes for protein separations has been explored recently by Hughes and Lowe [6] who investigated their use with poly(vinyl alcohol) as phase-forming polymers for liquid-liquid extraction of proteins. Acrylic polyampholytes have several promising features in this regard. First, they can be easily recovered by isoelectric precipitation and recycled, leaving the proteins in solution. Second, their dual electrostatic nature as well as their hydrophobic character can be manipulated to achieve different interactions with proteins. Third, these polymers are biocompatible, non-biodegradable, inexpensive (block polyampholytes are more expensive than random polyampholytes) and buffers.

Both the acrylic polymers and proteins are polymeric ampholytes. Unlike proteins, acrylic polyampholytes exhibit no biological lability, are composed of only three kinds of residues (in this study) and do not form α-helices or β-sheets. The pKs of the charged groups of the polyampholytes are close to those of the corresponding groups of the amino acid residues. The pK of the AA residue is 4.2 and that of the B residue is 8.6. The pK of the side group of aspartic acid is 4.5, of glutamic acid is 4.6, of cysteine is 9.1 to 9.6, of tyrosine is 9.7 and of lysine is 10.4 [8]. For these reasons the synthetic polyampholytes have been considered to be an attractive non-biological model for the development of an understanding of the titration of proteins and nucleic acids [9,10].

The synthetic polyampholytes behave like proteins in terms of their isoelectric points, solubilities and titration curves. These similarities arise from the dual charge nature as well as the hydrophobic character of both the classes of polyampholytes. Unlike most proteins, however, these synthetic polyampholytes have no intramolecular covalent bridges, so that at extreme pH they can expand and acquire a rod-like conformation. One can consider that denatured proteins with reduced disulphide bridges behave like these synthetic polymers. Furthermore, our polyampholytes have a higher charge density than proteins. Five typical proteins (ovalbumin, chymotrypsinogen, lysozyme, bovine serum albumin, and human serum albumin) contain only 30% mole/mole ionizable residues [11], while our polyampholytes contain more than 60% mole/mole ionizable residues.

8.2 Experimental Section

8.2.1 Materials

Random polyampholytes were synthesized through the free-radical polymerization of methyl acrylate (MA), dimethylaminoethyl methacrylate (B), and methyl methacrylate (M). To avoid side reactions, such as acid-base reactions and Michael addition [12], which would decrease the yield of the polymerization, MA was used instead of acrylic acid (AA). After polymerization, the MA residues of the prepolymer were hydrolyzed selectively to AA residues with a stoichiometric amount of potassium hydroxide at 75°C. The methyl methacrylate residues are negligibly hydrolyzed, while the methyl acrylate residues are hydrolyzed in 30 minutes [12]. Table 8.1 lists the characteristics of the two polyampholytes studied systematically. The molar ratio of acidic, basic and neutral residues (AA:B:M) was determined from an elemental analysis, weight and number average molecular weights (MW_w, MW_n) were determined from gel permeation chromatography using poly(methyl methacrylate) standards in tetrahydrofuran, and the isoelectric points (pI) were determined from turbidity measurements.

Poly(vinyl alcohol) (PVA) of molecular weight 10,000 (with 10% mol acetylated residues), α-chymotrypsinogen A (cat.# C4879) and ovalbumin (cat.# A5503) were obtained from Sigma Chemical Company, St Louis, MO. Standard solutions of hydrochloric acid and potassium hydroxide as well as solid potassium hydroxide, potassium chloride, sodium chloride, lithium chloride, strontium chloride and magnesium chloride were purchased from Mallinckrodt Inc., Paris, KY. Cesium chloride was purchased from EM Science, Cherry Hill, NJ.

8.2.2 Methods

The two-phase systems were formed by mixing stock solutions of the polyampholyte (13% w/w), PVA (13% w/w) and protein (10g/l) with water and salt. The concentration of the proteins was determined by absorbance at 280nm using a

Perkin-Elmer Lambda 3B UV/VIS Spectrophotometer. The concentration of the polyampholyte was determined by titration. The concentration of PVA was determined from the refractive index of the solution after subtracting the contributions of the polyampholyte and the salt. For 10% w/w total polymer at 0.1M KCl, the salt contributed 5% of the total refractive index. The pH was measured with a miniature glass electrode (MI-405) and a microreference electrode with glass barrel (MI-409) from Microelectrodes, Inc., Londonderry, N. H.

8.3 Results and Discussion

8.3.1 Solubility

A low solubility at the isoelectric point is desirable if these polymers are to be used in industrial applications, because it will permit their effective removal from solution by precipitation. Figure 8.1 shows the solubility curve of polyampholyte 2 in pure water without added salts. The solubility at the pI is extremely low, 0.5%, while the solubilities 1.5 pH units on either side are 40 times higher. For comparison, the isoelectric solubilities without added salt of ovalbumin, lysozyme and carboxyhemoglobin are 9%, 4% [13] and 2.5% w/w [14], respectively. In the synthetic polyampholytes, the role of the hydrophobic methyl methacrylate residue in the acrylic copolymer is to reduce further the isoelectric solubility. If, however the content of MMA is too high, for example 50% mole/mole, the polymer solubility will be very low over the whole pH range.

8.3.2 Titration

The titration curve of polyampholyte 2 is also plotted in Figure 8.1. Since the acidic and the basic pKs are separated by more than 4 pH units ($pK_{ac}=4.2$ and $pK_b=8.6$), the basic residues are completely protonated during the titration of the acidic residues and the acidic residues are completely dissociated during the titration of the basic residues. The first sigmoidal portion at lower pH corresponds to the titration of the acidic residues, while the sigmoidal portion at higher pH corresponds to the titration of the basic residues. There are 150 acidic residues per polymer molecule titrated from pH 2 to pH 7 and 50 basic residues per polymer molecule titrated from pH 7 to pH 12. The ratio of acidic to basic residues determined from the titration curve (=3) agrees satisfactorily with the ratio obtained from elemental analysis (=3.7), the discrepancy probably being due to incomplete hydrolysis of the prepolymer. In the region around the isoelectric point there is only one point on the titration curve, as it is very difficult to obtain good titration data points near this region because the polymer precipitates and blocks the pH electrodes.

8.3.3 Isoelectric Point

A method for the determination of the pI from the titration curve is described below [15]. For the case of polymer 2, at pH<2 there are negligible negatively charged (dissociated acidic) residues and 50 positively charged (all of the basic) residues. At pH 3.8, 50 hydrogen ions per polymer molecule will dissociate, thus leaving 50 negatively charged and 50 positively charged residues on the molecule. This is by definition the pI of the polyampholyte and it agrees closely with the pI determined from the solubility curve (=3.8).

The experimental determination of the pI will be compared now with theoretical predictions. The pI of a polyampholyte can be determined mathematically from knowledge of the acid to base molar ratio, R, and the dissociation constants of the base and acid monomers, pK_b and pK_{ac}. Starting from the requirement that the total net charge is zero and assuming that the activity coefficients of the acid and base residues are equal to one (so that the pKs of the residues are equal to those of the monomers), we derived the following closed form expression for pI at low ionic strength:

$$pI=pK_b+\log\left\{\frac{1}{2}\left[\frac{1-R}{R}+\sqrt{\left(\frac{1-R}{R}\right)^2+\frac{4}{R}10^{pK_{ac}-pK_b}}\right]\right\}$$

In Figure 8.2, pI is plotted vs R according to this equation. The pKs of the monomers used in the plot were pK(AA) = pK_{ac} = 4.18 and pK(B) = pK_b = 8.58. In Chapter 2, the pK values used were not those of the monomers but those determined from the titration of the homopolymers. For R=1 the pI is equal to the arithmetic mean of pK_b and pK_{ac}. Near R=1 the pI is very sensitive to R, because the buffering capacity of an acrylic polyampholyte in this pH region is very low. For R=2 the pI is equal to pK_{ac}, because at pH=pK_{ac} half of the acidic and all of the basic residues are charged. For R=1/2 the pI is equal to pK_b, because at pH=pK_b half of the basic and all of the acidic residues are charged. For extreme values of R the pI approaches asymptotically the limiting forms:

$$pI\text{-}pK_{ac}\text{-}\log R \qquad for\ R>3$$

and

$$pI\text{-}pK_b\text{-}logR \qquad for\ R<1/3$$

For polyampholyte 2, R=3.7 and the predicted pI is 3.7, which compares well with the experimentally determined value of 3.8. For polyampholyte 1, R=0.9 and the theory predicts pI=7.4 which is significantly different from the experimentally determined value of 6.3. As mentioned above, the pI is extremely sensitive to R around the equimolar R region. Therefore, a small error in the value of R may lead to a large error in the calculated pI value. The compositions and the predicted isoelectric points of the two polyampholytes are indicated by arrows on Figure 8.2.

The pI of a polyampholyte is a function of ionic strength. Anions, especially at high ionic strengths, are known to bind to proteins resulting in an ionic strength-dependent shift of the pI to a lower pH [16]. For some proteins this shift can be dramatically large, reaching four pH units [17]. The experimental determination of the pI of our synthetic polymers was performed at very low ionic strength to avoid any pI-shift.

8.3.4 Phase-Behavior of the Two-Phase System

To understand protein partitioning in polyampholyte-rich two-phase aqueous polymer systems, we need to understand first the equilibrium phase behavior of the coexisting polymer solution phases. Figure 8.3 shows the phase behavior of a system composed of PVA and polyampholyte 1 as a function of pH and salinity. The qualitative nature of the phase separation is indicated by the pictures of the test tubes where the polyampholyte-rich phase is shaded. Although we have not yet determined the precise position of all the boundaries which divide the areas and denote different phase behaviors, the boundary between the one-phase and two-phase regions of behavior is indicated. At low pH (greater than one pH unit below the pI) and low salinity (1M or lower) the phase forming polymers were completely miscible. This miscibility was probably due to hydrogen bonding between the oxygens of PVA and the hydrogens of the (protonated) carboxylic groups of the polyampholyte. Enhanced miscibility of poly(acrylic acid)-PVA mixtures at low pH has also been attributed to hydrogen bonding [18]. At higher salt concentrations and low pH, the polyampholyte precipitated probably due to the salting-out effect. While a pure PVA solution did not precipitate at these salt and pH conditions, a pure polyampholyte solution did. Around the pI the polyampholyte precipitated again. At higher pH (typically one pH unit above the pI) and low salinity (lower than 0.7M but higher than 0.1M), we obtained a system with two phases of low viscosity, which is probably the optimum condition for the use of the system for protein partitioning. In the same region of pH and at higher salt concentrations (higher than 0.7M), phase inversion occurred with the polyampholyte-rich phase going to the top. At higher pH (typically three pH units above the pI), we again found the polyampholyte in the top phase, which coexisted with a very viscous bottom phase. Polyampholyte 2 exhibited similar behavior, where the "good" two-phase region for partitioning was again 1 pH unit above the pI.

Figures 8.4-8.8 show experimental results describing how the polymer concentration, the salt concentration and the cation type affect the phase composition of our system and the protein partitioning. While salt concentration, salt type and pH typically have only a small effect on the phase composition of non-ionic two-phase polymer systems (for salt concentrations less than 0.3M), in contrast they have a large effect on the phase composition of polyelectrolyte containing systems [1].

8.3.5 Effect of Polymer Concentration

Figure 8.4 shows the phase diagram for a system composed of PVA and polyampholyte 1 at 0.1M KCl and pH 7.2. The curve is fairly symmetrical and phase separation takes place at relatively low total polymer concentrations, typically below 10%. The symmetry of the binodal may be attributed to the molecular weights of the two polymers which are of the same order (10,000 and 80,000 for PVA and polyampholyte 1, respectively). The tie lines connect the phases in equilibrium. The tie line length increases with polymer concentration.

Figure 8.5 presents the partition coefficients of two proteins, ovalbumin and chymotrypsinogen, as a function of the tie line length. The conditions are identical to those of Figure 8.4. In the same graph, the partition coefficient of the polyampholyte is also plotted. The partition coefficient, K, of a substance is defined as the concentration in the upper phase divided by that in the lower phase. The pI of polyampholyte 1 is 6.3 and, therefore, at the solution pH of 7.2 the polyampholyte bears a net negative charge. The pIs of chymotrypsinogen and ovalbumin are 9.5 and 4.7 respectively and, therefore, the former is positively charged while the latter is negatively charged. It is interesting to observe in Figure 8.5 that the logarithms of the partition coefficients of the polyampholyte and chymotrypsinogen vs tie line length correspond to two parallel straight lines, that is, the positively charged chymotrypsinogen follows the oppositely charged polyampholyte in the lower phase. In contrast, the negatively charged ovalbumin partitions almost evenly for all the polymer concentrations. This suggests that other mechanisms influencing the partitioning of the proteins are operating in a direction opposite to that of the influence of the electrostatic interactions. Such mechanisms could be hydrophobic attractive interactions between the protein and the acrylic copolymer or steric interactions between the protein and the PVA-rich phase. We expect the acrylic polymer to be more hydrophobic than PVA because it is composed of 30% M hydrophobic residues. Although the same non-electrostatic forces may also be significant in the case of chymotrypsinogen partitioning, it appears, in this case, that electrostatic interactions dominate the observed partitioning behavior.

It is interesting to note that the average hydrophobicities of the two proteins investigated here are similar [11]. The molecular weights of the two proteins (ovalbumin: 45,000; chymotrypsinogen: 23,200) differ by a factor of two, so their radii differ only by a factor of 1.26. Therefore, the role of hydrophobic and size exclusion phenomena should be similar in both cases. If phase separation were possible at pH below the pI of the polyampholyte, for example at pH 5.4 (where the polyampholyte has about the same amount of charge but is of opposite sign than at pH 7.2), realizing that the two proteins will still have the same sign of charge as before, we would expect the behavior of the two solutes to be interchanged. Ovalbumin should follow the oppositely charged polyampholyte, while chymotrypsinogen should partition almost evenly between the two phases.

The selectivity of ovalbumin over chymotrypsinogen, defined as the ratio of the partition coefficients of the two proteins, increases with tie line length. This suggests that a mixture of the two proteins can be separated more effectively when higher polymer concentrations are used.

8.3.6 Effect of Salt Concentration

Figure 8.6 depicts the effect of ionic strength on the phase composition of a system composed of PVA and polyampholyte 1 at pH 7.2. By increasing the ionic strength, the upper PVA-rich phase becomes richer in PVA, while the lower polyampholyte-rich phase becomes poorer in polyampholyte. At the same time, the concentrations of the minor components in these phases remain essentially constant. At an ionic strength around 0.7M KCl we observed a phase inversion, with the PVA-rich phase resorting to the bottom. It is interesting to note that the observed decrease in the polyampholyte concentration in the polyampholyte-rich phase with increasing ionic strength is opposite to the behavior of the dextran sulfate-poly(ethylene glycol) system [1,19]. Intuitively, one might expect that a high salt concentration would result in a more concentrated in polyelectrolyte phase resulting from the screening of the intermolecular and intramolecular electrostatic repulsion. The deviation from the expected behavior may be attributed to the dual electrostatic nature of the polyampholyte. Besides the electrostatic repulsion, arising from the net charge of the polyampholyte, electrostatic attraction, arising from the opposite charges of the polymer, is also present. By increasing the ionic strength, we also screen the electrostatic attraction. The pH value of 7.2 is close to the experimentally determined isoelectric pH of 6.3 and, therefore, the polyampholyte net charge is very small. Furthermore, most of the AA residues and most of the B residues are charged. These imply that the net charge is only a small percentage of the absolute charge of the polyampholyte. Under these conditions, the electrostatic attraction (polyampholyte effect) should be expected to dominate the electrostatic repulsion (polyelectrolyte effect) [20]. Therefore, salt addition will result in reducing the electrostatic attraction rather than reducing the electrostatic repulsion, which implies that it will have an effect opposite to that observed with homopolyelectrolytes.

No phase separation was obtained for ionic strengths less than 0.1M KCl. Hughes and Lowe [6] reported that they did not observe phase separation of their polyampholytic system for ionic strength equal to 0.05M NaCl or lower. Humayun [19] observed phase separation in his sodium dextran sulphate-PEO system only for ionic strength equal to 0.3M NaCl or higher. Albertsson [1] reported that his sodium dextran sulphate-PEO system phase-separated for ionic strength equal to 0.15M NaCl or higher. These observations are in agreement with Van der Schee's [21] model on polyelectrolyte-solvent phase separation, which indicated that the phase separation is promoted by a low degree of dissociation of the polyelectrolyte and a high ionic strength.

Figure 8.7 shows the effect of salt on protein and polyampholyte partitioning under conditions identical to those of Figure 8.6. At low salinity, chymotrypsinogen partitioning follows that of the oppositely charged polyampholyte, while ovalbumin, having the same charge as the polyampholyte, resorts to the other phase. At higher salt concentration the two proteins follow the same trends. The discontinuities in the partition coefficient curves around 0.7M KCl arise from the phase inversion mentioned above. At low ionic strength, the partitioning of the two proteins appears to be governed by electrostatics. At higher ionic strength, the electrostatic interactions appear to be screened out and the partitioning is determined by other forces. For example, preference of both proteins for the polyampholyte-rich phase could be attributed to steric or hydrophobic interactions. The very similar values of their partition coefficients in the high ionic strength regime could be attributed to the similar hydrophobicities and sizes of the two proteins.

8.3.7 Effect of Cation Type

The effect of cation type on protein partitioning is shown in Figure 8.8. The system is composed of polyampholyte 2 and PVA at pH 4.6 and 0.1M ionic strength. The average polymer concentration of each two-phase system was held constant at 6.64% w/w polyampholyte and 3.53% w/w PVA. The partition coefficients of ovalbumin and chymotrypsinogen are insensitive to monovalent cation type (Li, Na, Cs, K). The partition coefficients significantly increase when a divalent cation (Mg, Sr) is substituted for a monovalent cation. This phenomenon can be attributed to the effect of the cation valence on phase composition. The tie line length is insensitive to monovalent cation type, but increases significantly when a divalent cation is introduced. This contrasts to the situation where monovalent cations increasingly favor the phase separation of the sodium dextran sulfate-poly(ethylene glycol) mixture in the order Li, Na, Cs, K [1,19]. As the flocculation efficiency of a divalent ion is much higher than that of a monovalent ion [22], the introduction of a divalent cation concentrates the polyampholyte in the lower phase. The high polymer concentration in the lower phase excludes the proteins, forcing them to partition into the upper phase. Since it bears a greater positive charge than ovalbumin, chymotrypsinogen partitions preferentially into the oppositely charged polyampholytic phase in comparison to ovalbumin. This observation suggests that the electrostatic interactions occurring between the proteins and the polyampholyte are important in determining the protein partitioning behavior.

It is interesting to contrast the influence of the divalent and monovalent cations on the phase behavior of the two-phase system to the influence of an increase in monovalent cation concentration (see Figure 8.6). That is, presence of a divalent cation enriches polyampholyte in the polyampholyte-rich phase, while the increase in 1:1 electrolyte concentration dilutes the polyampholyte in the polyampholyte-rich phase. The discrepancy is due to the localization of the charge of the divalent cation, whose main action is not to screen the electrostatic interactions but to form salt bridges between negatively charged polymeric sites. This non-covalent crosslinking has also been observed in other synthetic polyelectrolytes [23] as well as in proteins [16].

8.4 Conclusions and Future Directions

The polyampholyte-containing two-phase systems exhibit a number of properties that may be of advantage in developing novel protein separation strategies. They exhibit phase inversions, viscous and non-viscous phases and isoelectric precipitation. In particular, this latter property can be exploited for the recovery of proteins and the polyampholyte. As far as protein partitioning is concerned, experimental observations suggest that electrostatic interactions have an important influence on the partition of the protein. At low ionic strength, good selectivity can be achieved for proteins with net charge of opposite sign.

It is hoped that the experimental results presented in this paper will serve as a guide for the further development of novel polyampholytes for protein partitioning studies. Future possible directions include varying the types of monomers polymerized and utilizing block instead of random copolymers. In particular, the use of stronger acidic and basic residues may result in some advantages in the properties of the system. Stronger dissociation behavior of the polyampholyte implies that the polyelectrolyte-polyelectrolyte and polyelectrolyte-protein interaction will be stronger and also extend over a wider pH-range. The use of stronger acid and base residues also implies that the isoelectric collapse of the polyampholyte will be more pronounced and, therefore, the isoelectric solubility will be lower. Residues derivatized with sulfuric or sulfonic acid (pK=2) are much stronger acids than acrylic acid (pK=4.2). Residues carrying quaternary amine groups (pK=12) are much stronger bases than B which carries a tertiary amine group (pK=8.6).

The polyampholytes used in this investigation were random copolymers with the different residue types distributed statistically along the chain. When block copolymers are used instead, we expect that the polyelectrolyte-polyelectrolyte and polyelectrolyte-protein interactions will be stronger due to the localization of the charges of the same sign. The study of the phase-behavior of PVA with such block polyampholytes of low molecular weight is presented in the following Chapter.

8.5 Literature Cited

(1) Albertsson, P.-A., *Partition of Cell Particles and Macromolecules*, Wiley: New York, 3rd ed., 1986; p 35-36.

(2) Walter, H., D. E. Brooks and D. Fisher (eds), *Partitioning in Aqueous Two-Phase Systems*, Academic Press: New York, 1985.

(3) Baskir, J. N.; Hatton, T. A.; Suter, U. W. Protein Partitioning in Two-Phase Aqueous Polymer Systems. *Biotechnol. Bioeng.* **1989**, *34*, 541-558.

(4) Abbott, N. L.; Hatton, T. A. Liquid-Liquid Extraction for Protein Separations. *Chem. Eng. Prog.* **1988**, *Aug.*, 31-41.

(5) Abbott, N. L.; Blankschtein, D.; Hatton, T. A. On Protein Partitioning in Two-Phase Aqueous Polymer Systems. *Bioseparation* **1990**, *1*, 191-225.

(6) Hughes, P.; Lowe, C. R. Purification of Proteins by Aqueous Two-Phase Partition in Novel Acrylic Co-Polymer Systems. *Enzyme Microb. Technol.* **1988,** *10,* 115-122.

(7) Kokkoris, A.; Blair, J. B.; Shaeiwitz, J. A. Yeast Cell Debris and Protein Partitioning in the Poly(ethylene glycol)-Poly(vinyl alcohol) Biphasic System. *Biochim. Biophys. Acta* **1988,** *966,* 176-180.

(8) Creighton, T. E. *Proteins*; Freeman: New York 1984; p 7.

(9) Mazur, J.; Silberberg, A.; Katchalsky, A. Potentiometric Behavior of Polyampholytes. *J. Polymer Sci.* **1959,** *35,* 43-70.

(10) Bekturov, E. A.; Kudaibergenov, S. E.; Rafikov, S. R. Synthetic Polymeric Ampholytes in Solution. *J. Macromol. Sci.* **1990,** *C30,* 233-303.

(11) Baskir, J. N. Thermodynamics of the Separation of Biomaterials in Two-Phase Aqueous Polymer Systems. Massachusetts Institute of Technology, PhD Thesis, 1988.

(12) Foss, R. P. Acrylic Amphoteric Polymers. U.S. patent 4,749,762 (1988).

(13) Guo, M.; Narsimhan, G. Solubility of Globular Proteins in Polysaccharide Solutions. *Biotechnol. Prog.* **1991,** *7,* 54.

(14) Green, A. A. The effect of Electrolytes on the Solubility of Hemoglobin in Solutions of Varying Hydrogen Ion Activity with a Note on the Comparable Behavior of Casein. *J. Biol. Chem.* **1931,** *93,* 517.

(15) Merle, Y.; Merle-Aubry, L.; Selegny, E. Synthetic Polyampholytes. Preparation and Solution Properties. *Polymeric Amines and Ammonium Salts*; Goethals, E. J., Ed.;

Pergamon Press 1980.

(16) Bell, D. J.; Hoare, M.; Dunnill, P. The Formation of Protein Precipitates and Their Centrifugal Recovery. *Advances in Biochemical Engineering/Biotechnology*, No 26, Fiechter, A., Ed.; Springer-Verlag: Berlin, 1983.

(17) Velick, S. F. The Interaction of Enzymes with Small Ions. *J. Phys. Colloid Chem.* **1949,** *53,* 135.

(18) Minh, L. V.; Nose, T. Phase Equilibrium of Poly(acrylic acid) Partially Neutralized by NaOH-Poly(vinyl alcohol)-Water System. *Polym. J.* **1983,** *15,* 145.

(19) Humayun, M. S. Protein Partitioning in Aqueous Two-phase Poly(ethylene glycol)-Dextran Sulfate Systems. Massachusetts Institute of Technology, BSc Thesis, 1989.

(20) Higgs, P. G.; Joanny, J.-F. Theory of Polyampholyte Solutions. *J. Chem. Phys.* **1991,** *94,* 1543-1554.

(21) Van der Schee, H. A. An Experimental and Theoretical Study of Oligo- and Polyelectrolyte Adsorption. Wageningen, The Netherlands, PhD Thesis, 1984.

(22) Hiemenz, P. C. *Principles of Colloid and Surface Chemistry*; Marcel Dekker: New York, 2nd ed., 1986; p 717-722.

(23) Allcock, H. R.; Kwon, S. An Ionically Cross-Linkable Polyphosphazene: Poly[bis(carboxylatophenoxy)phosphazene] and its Hydrogels and Membranes. *Macromolecules* **1989,** *22,* 75.

Table 8.1 Characteristics of the acrylic polyampholytes.

Amph	AA:B:M	MW_w	MW_n	pI
1	0.9:1:1	88,500	69,000	6.3
2	3.7:1:1	43,000	31,000	3.8

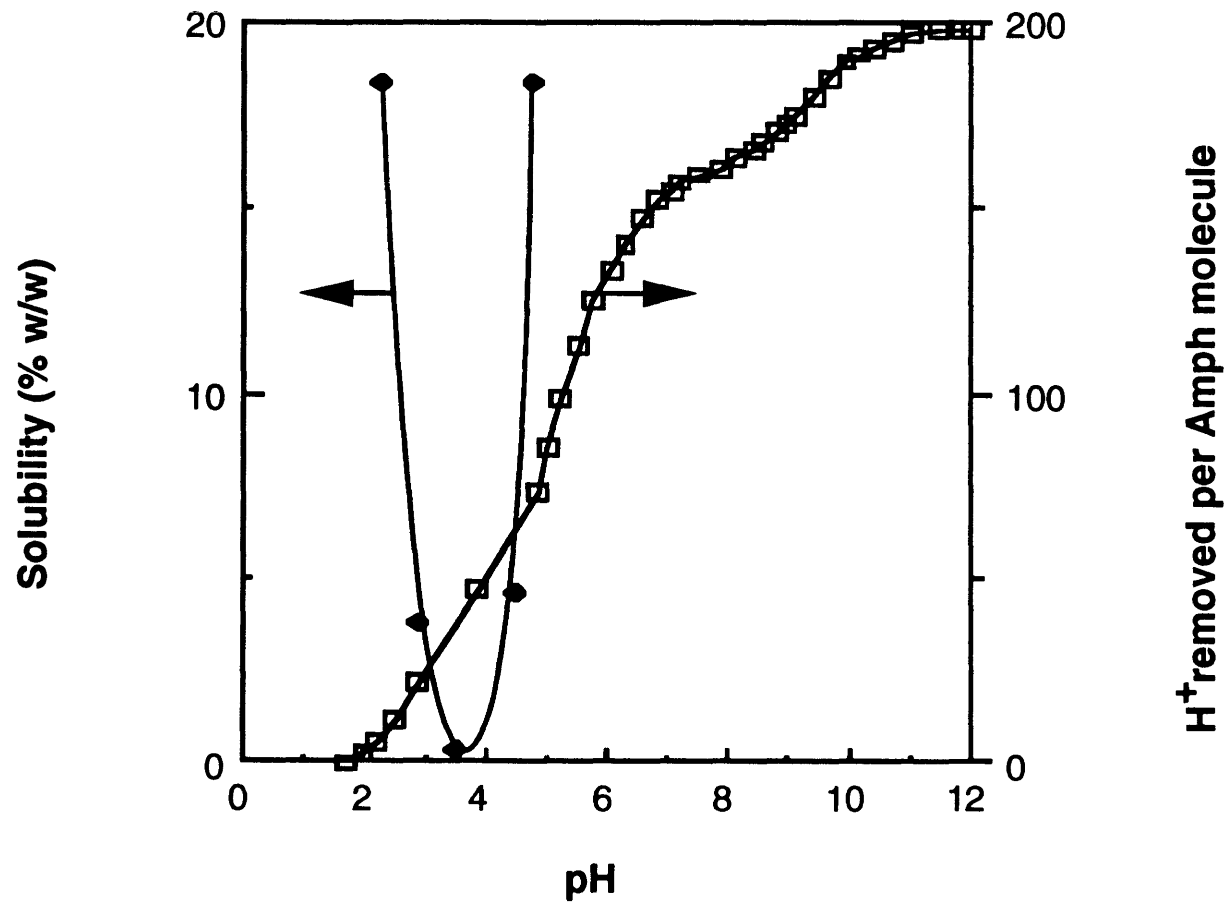

Figure 8.1 Solubility and titration curves of polyampholyte 2.

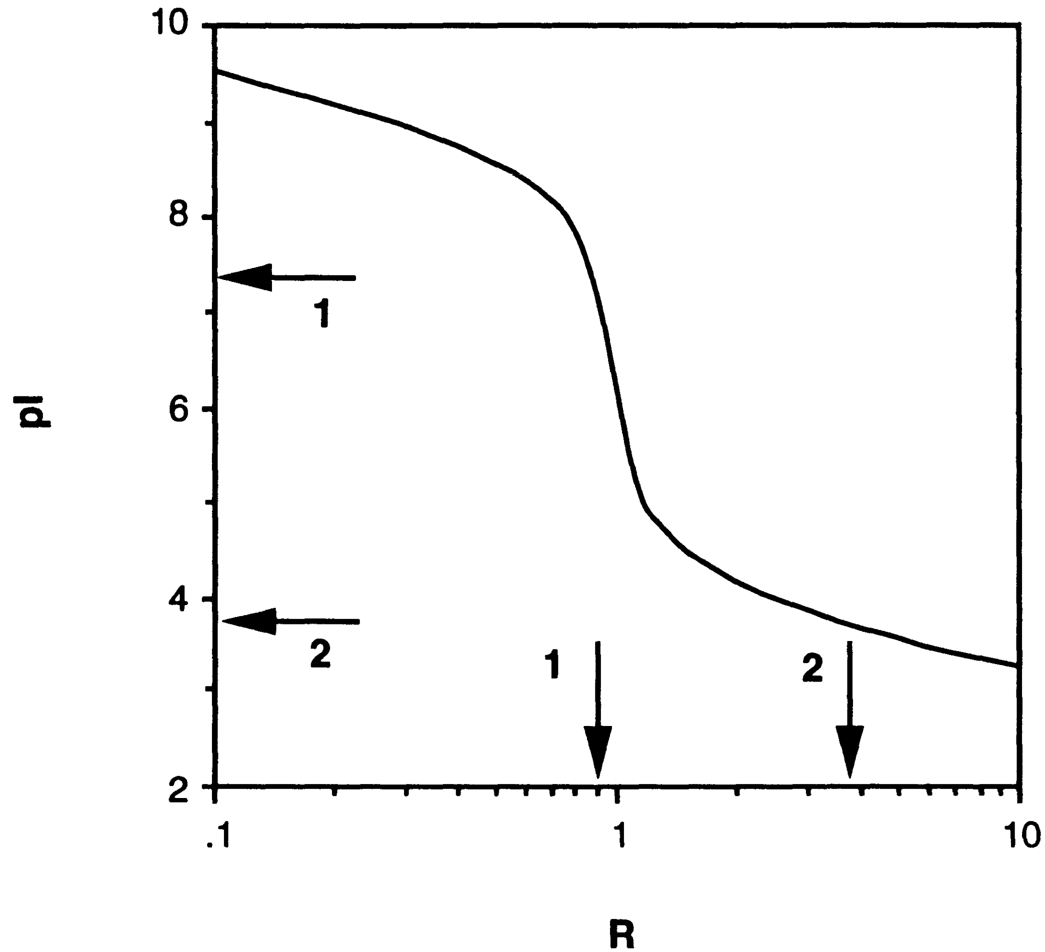

Figure 8.2 Calculated dependence of the isoelectric point on polyampholyte composition.

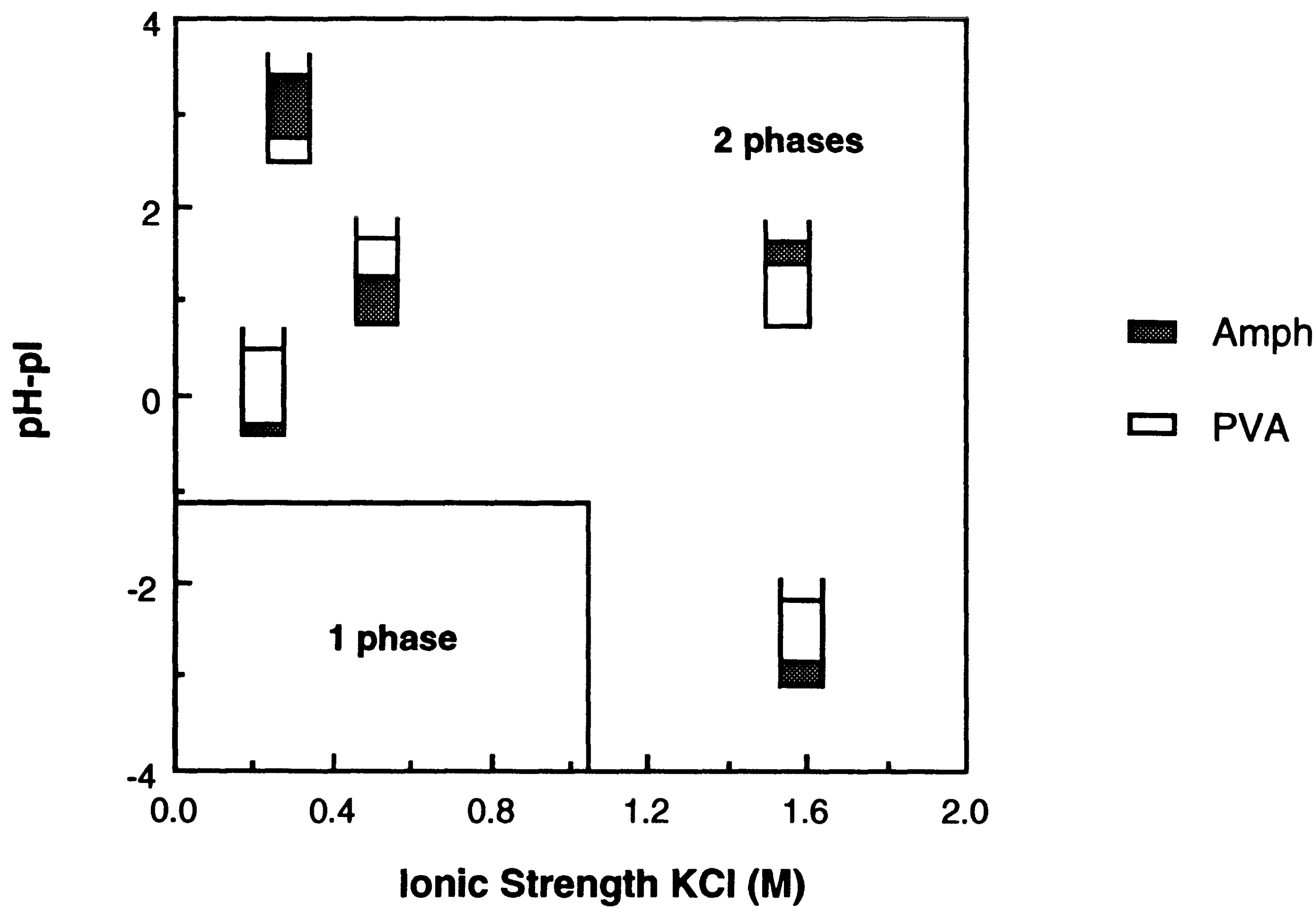

Figure 8.3 Phase diagram of polyampholyte 1 and PVA as a function of pH and salt concentration.

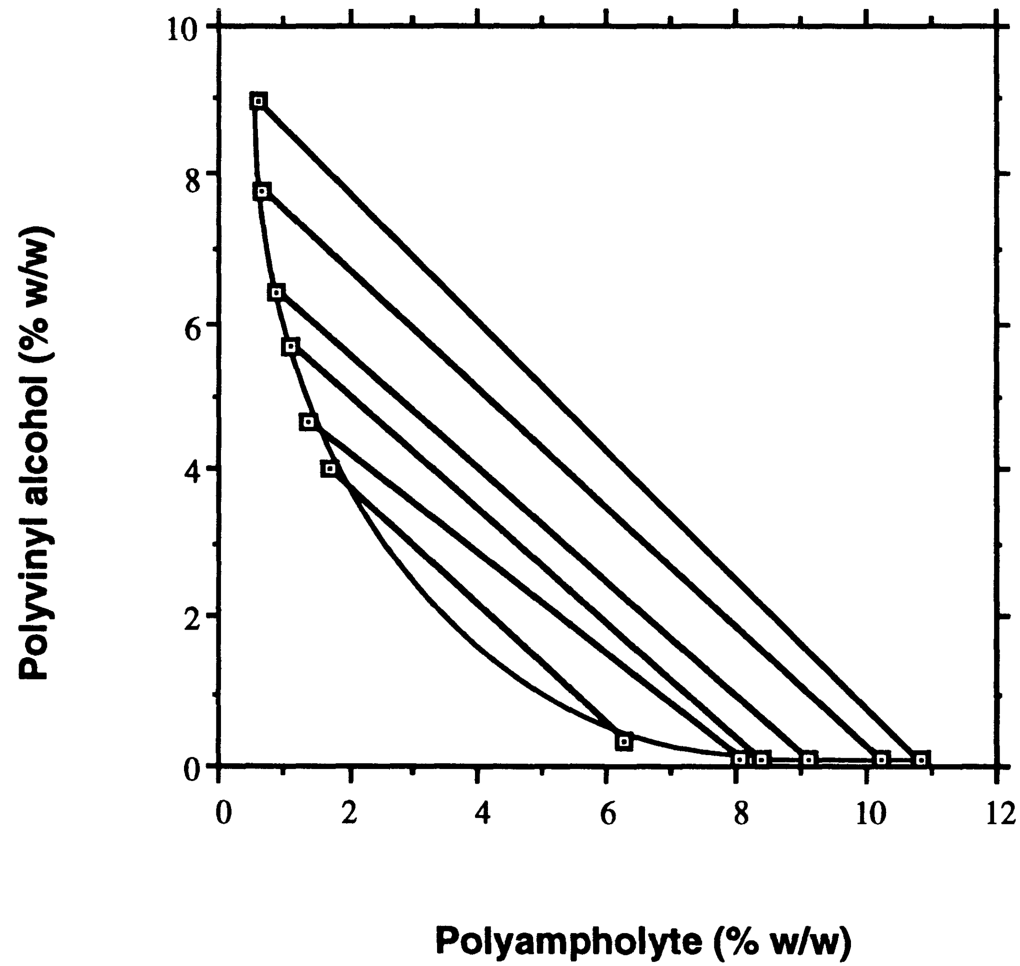

Figure 8.4 Phase diagram of the system containing polyampholyte 1 and PVA at pH 7.2 and 0.1M KCl.

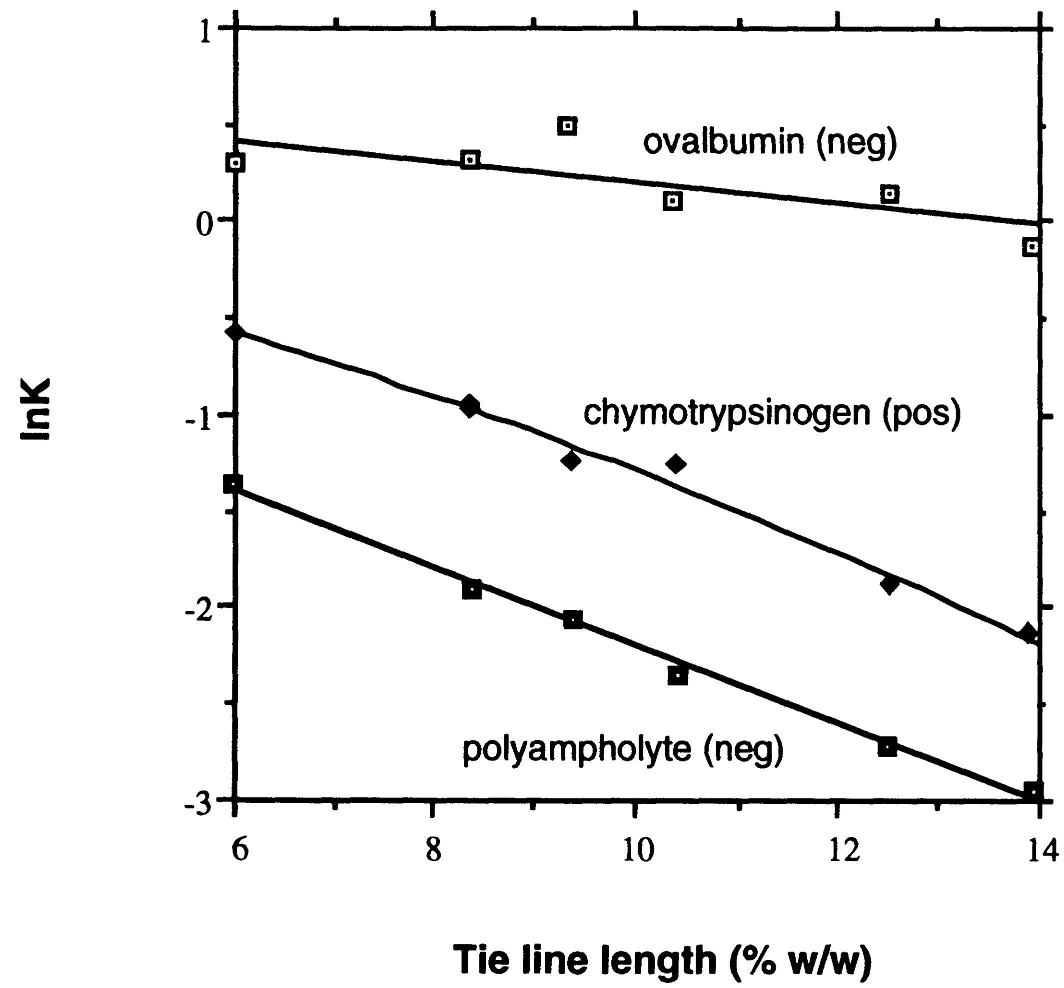

Figure 8.5 Effect of the tie line length on the partitioning of ovalbumin and chymotrypsinogen in the system polyampholyte 1 and PVA at pH 7.2 and 0.1M KCl.

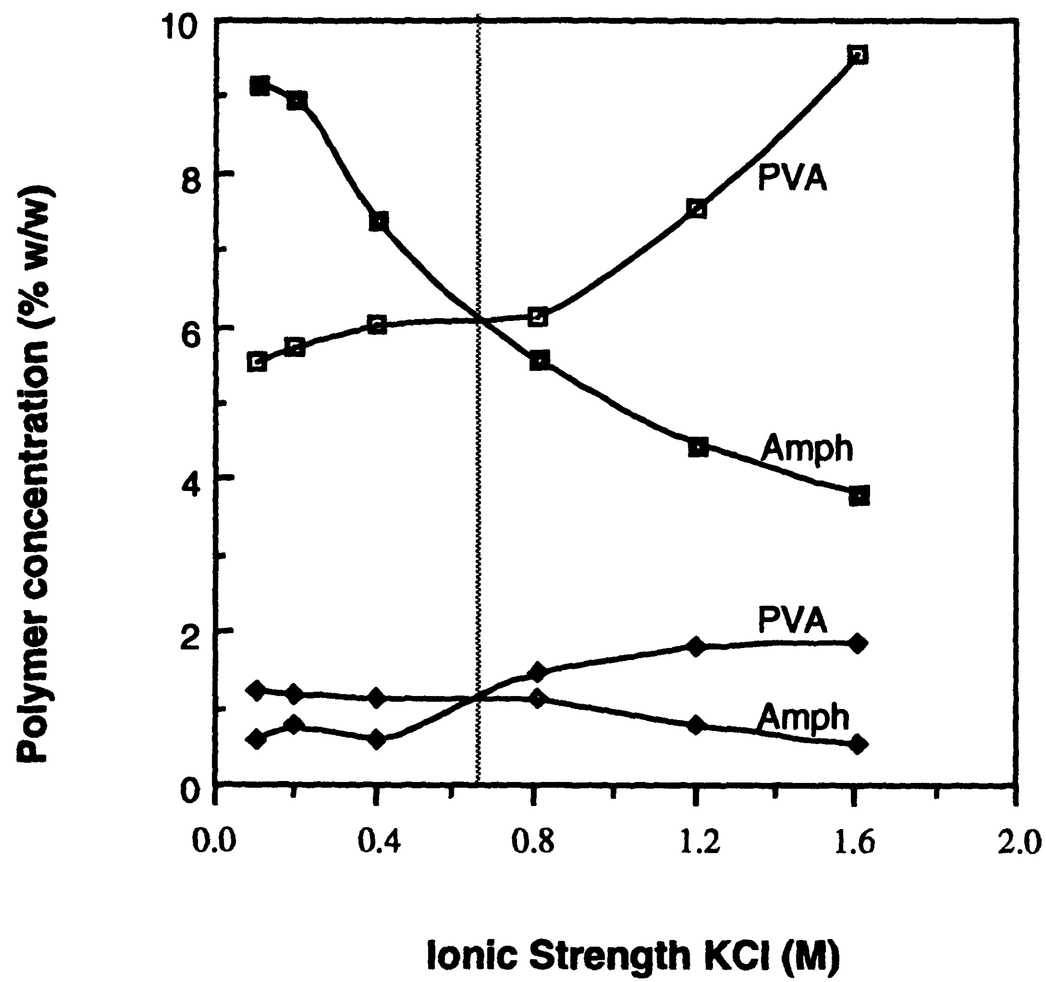

Figure 8.6 Effect of ionic strength on the phase composition of the system polyampholyte 1 and PVA at pH 7.2. The vertical dotted line denotes the phase inversion.

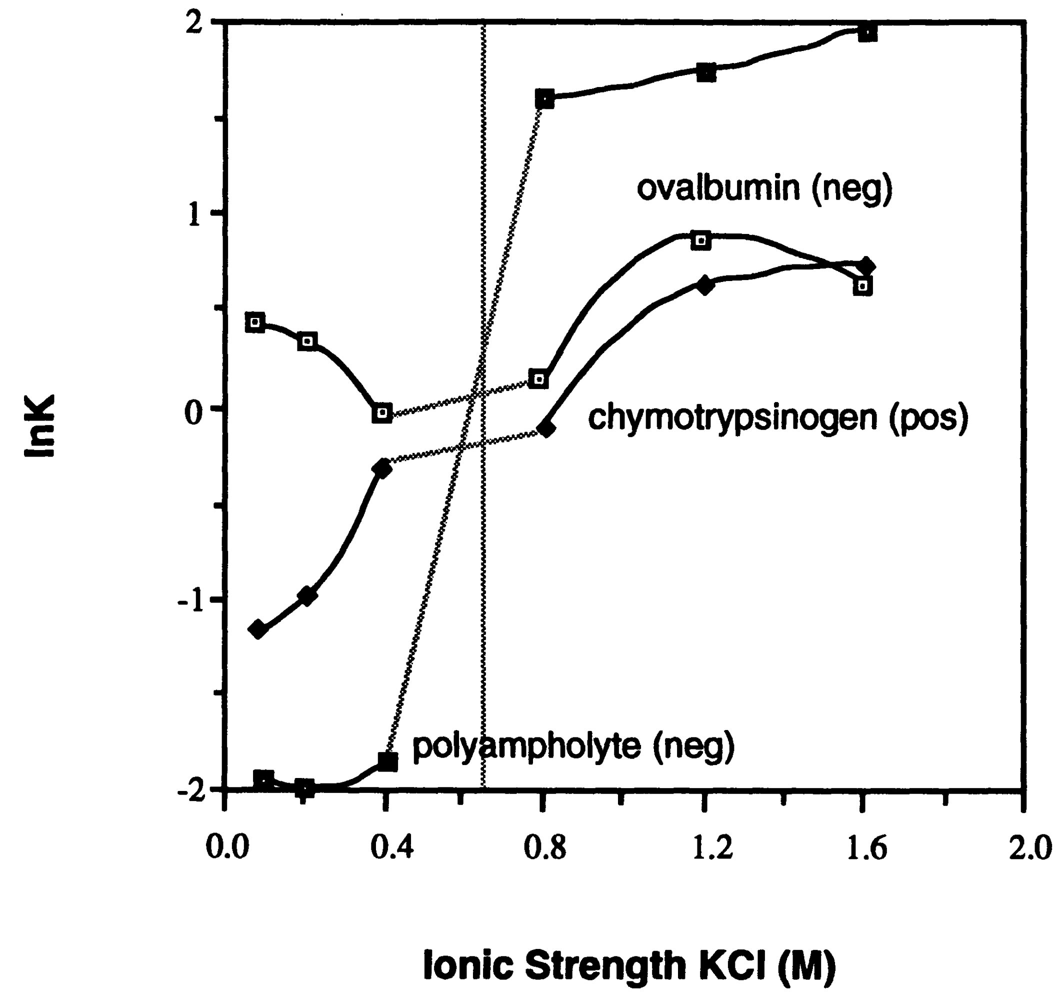

Figure 8.7 Effect of ionic strength on the partitioning of ovalbumin and chymotrypsinogen in the system containing polyampholyte 1 and PVA at pH 7.2. The vertical dotted line represents the phase inversion.

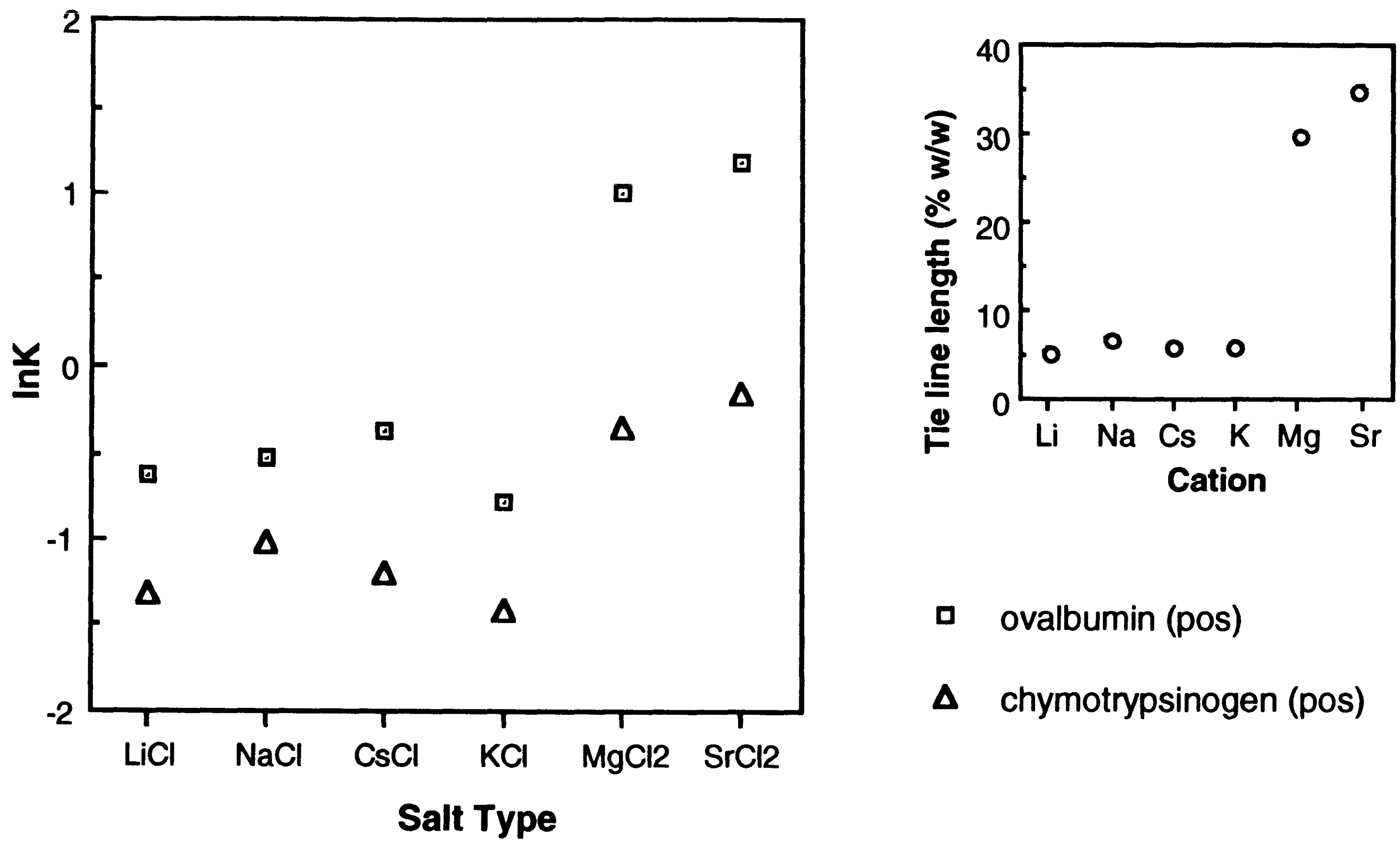

Figure 8.8 Effect of cation type on the partitioning of ovalbumin and chymotrypsinogen and phase composition of the system containing polyampholyte 2 and PVA at pH 4.6 and at salinity of 0.1M.

Chapter 9.

Phase-Behavior of Random and Triblock Methacrylic Polyampholytes with Poly(vinyl alcohol).

Following the protein partitioning studies in two-phase aqueous systems of PVA and random polyampholytes made by free radical polymerization, in this chapter we investigate the phase separation of solutions of PVA with the polyampholytes synthesized by Group Transfer Polymerization. A similarity will be observed in the qualitative features of phase separation of the low-molecular-weight triblock copolymers and the high molecular weight random copolymers. This is probably due to the similarity in the size of the random polyampholytes and the micellar size of the triblock polyampholytes. It is noted that no protein partitioning was pursued in the two-phase systems of this Chapter.

9.1 Introduction

Protein purification is one of the challenging issues in biotechnology today. One of the most promising protein purification methods is the partitioning in two-phase aqueous polymer systems [1]. Unlike most of the conventional phase systems containing organic solvents, two-phase aqueous polymer systems have neither the denaturing effects nor a strong interfacial tension which can destroy biological products, thus providing a friendly and mild aqueous environment for the labile protein products [1]. Also, the two-phase polymer systems are suitable for scale-up, they are fast in equilibration and they can be operated continuously [2].

In our experiments, methacrylic polyampholytes of molecular weight 4,000 and poly(vinyl alcohol) (PVA) of molecular weight 10,000 were used as the components of the two-phase systems. Polyampholytes were chosen for their low isoelectric solubilities, which facilitate the recovery of the protein from the polyampholyte-rich phase, as well as the recycling of the polyampholytes [3]. Moreover, the low cost and non-biodegradability of the polyampholytes make the process economically feasible [3].

The components of the polyampholytes in our study are methacrylic acid (Ac), dimethylaminoethyl methacrylate (B), methyl methacrylate (M) and 2-phenylethyl methacrylate (P). The hydrophobicity of the monomers increases as Ac<B<M<P. Ac and B are the least hydrophobic because they bear the negative and positive charges of the polyampholyte, respectively. B is more hydrophobic than Ac because it bears a side chain comprising four more carbon atoms than that of Ac. While Ac and B are water soluble, the more hydrophobic M and P are completely water-insoluble. Although B carries four carbon atoms in the side chain and M only one, B is still more hydrophilic than M because the former carries a nitrogen atom in the side chain. P is the most hydrophobic component comprising eight carbon atoms in the side chain, six of which form a benzene ring.

In our experiments, we studied the phase separation behavior of the methacrylic polyampholytes as a function of the solution pH, salt concentration, and salt type.

9.2 Experimental Section

9.2.1 Materials

PVA of 10,000 molecular weight and 10% mole acetylated residues was purchased from Sigma. The inorganic salts were purchased from Mallinckrodt. The synthetic polyampholytes were synthesized by Group Transfer Polymerization (GTP) as described in Chapter 2. The polyampholytes studied in this Chapter as well as their composition and isoelectric points are listed in Table 9.1. The polymer numbers are the same as those used in Chapter 2.

9.2.2 Methods

Solid polyampholytes were dissolved in acidified and alkaline water to prepare one acidic (pH below the isoelectric point, typically pH=4.5) and one basic (pH above the isoelectric point, typically pH=8.5) stock solution for each copolymer at a concentration of 10 or 15% w/w. A 13% w/w poly(vinyl alcohol) stock solution was also prepared by dissolving the appropriate amount of polymer powder in distilled water. Seven 0.5mL aliquots of polyampholyte solution were transferred into seven different test tubes and each one was adjusted at a different pH by adding the proper amount of concentrated acid or base solution, thus covering a pH range between 3 and 9. After that, 0.5mL of poly(vinyl alcohol) stock solution were added to each test tube. Following vortex mixing, each tube was centrifuged for approximately 10 minutes and examined for phase separation. Vortexing and centrifugation were repeated at three higher salt concentrations, 0.10, 0.35, and 0.75M KCl. The above salt concentrations were achieved by adding 0.03, 0.1, and 0.2mL of 3M KCl solution to the tubes. To investigate the effect of ion type on phase behavior, the following additional 3.0M salt solutions were prepared: KF, KBr, KI, LiCl, NaCl, RbCl, CsCl, and $(NH_4)_2SO_4$. A set of nine test tubes, each one for a different salt type, with the ninth type being KCl, containing poly(vinyl-alcohol) and Polymer 2 at pH 8.2 were studied in terms of their phase behavior at salt concentrations 0.10, 0.35, and 0.75M.

9.3 Results

Figures 9.1 through 9.8 present the phase behavior of the acrylic polyampholytes with poly(vinyl alcohol) as a function of pH and KCl concentration. Figures 9.1 through 9.6 correspond to block copolymers and Figures 9.7 and 9.8 correspond to random copolymers. The squares with the cross and the filled circles in the Figures indicate the regions where phase separation takes place. The squares with the cross show "good" phase separation, i.e., two phases of relatively low viscosity, while the filled circles correspond to two-phase systems where the bottom phase is a compact precipitate. The open circles indicate no phase separation.

As can be seen, there is a significant difference between block and random copolymers in terms of the size of the region where phase separation occurs. In Figure 9.7, the solution of random copolymer 13 precipitated at pH 8.45 and KCl concentration up to 0.1M. Random polyampholyte 1 resulted in two low viscosity phases at the pH range between 6.3 and 7.2 and KCl concentration again up to 0.1M. Consequently, most of the pH-[KCl] space of the random copolymers is a one-phase region. On the other hand, all the block copolymers showed phase separation at pH between 4.6 and 9.3 regardless of the salt concentration.

In most cases, increasing salt concentration broadened the "good" two-phase region of block polyampholytes. At low salt concentration (0-0.1M), the pH window for "good" phase separation was narrow, of the order of tenths of a pH unit for all of the polymers. An exception was polymer 10 (Figure 9.5) which showed a broad, 2-pH-unit, "good" two-phase region at low salt concentration and it was not affected by increasing salt concentration. Polymers 2, 8, and 5 (Figures 9.2, 9.3, and 9.6, respectively) showed identical "good" two-phase regions, covering the same pH-[KCl] area.

Polymer 9 (Figure 9.1) has the narrowest "good" two-phase region among the block copolymers while Polymer 1 (Figure 9.4) has the broadest. For all the block copolymers, except for Polymer 1, "good" two-phase regions do not start appearing until KCl concentration reaches 0.1M. Polymer 1 has the largest two-phase region compared to all other polymers.

Figures 9.9 and 9.10 show the phase behavior of the system Polymer 2/poly(vinyl alcohol) as a function of salt type and salt concentration. Figure 9.9 includes $(NH_4)_2SO_4$ and four potassium halides, KF, KCl, KBr, and KI. Figure 9.10 includes five alkaline chlorides, CsCl, RbCl, KCl, NaCl, and LiCl. Both Figures 9.9 and 9.10 show that no phase separation occurred without added salt. Figure 9.9 shows that at 0.1M salt concentration, all the solutions precipitated except the solutions with KBr and KI, which showed "good" two-phase separation. For the solutions containing $(NH_4)_2SO_4$ and KF, precipitation took place for the salt concentration of 0.1M up to 0.75M. The solution with KCl precipitated at 0.1M salt, but at higher salt concentration, the precipitate disappeared, resulting in "good" two-phase separation. At 0.35M salt concentration, KCl, KBr, and KI presented "good" two-phase separation, but at 0.75M salt, the solutions became one phase for KBr and KI while KCl still remained to show two-phase separation. In Figure 9.10, the metal chlorides caused precipitation at 0.1M salt concentration, but they showed "good" two-phase separation at salt concentrations 0.35M and 0.75M. LiCl at 0.75M was the exception resulting in a one-phase system. It is interesting to note that while Figure 9.10 shows no specific cation effects up to 0.35M of salt, Figure 9.9 manifests specific anion effects for the whole range of salt concentrations.

9.4 Discussion

A rather significant distinction was observed depending on the types of polymers used. Block copolymers showed much larger two-phase regions compared to that of random copolymers. This difference arises from the structural difference between the two copolymers. Random copolymers consist of different kinds of monomers randomly combined to each other, while block copolymers consist of blocks of the same kinds of monomers in an orderly manner. The charges and the hydrophobic groups of the block copolymers are localized, thus interacting more strongly with each other as well as with the PVA molecules. On the other hand, random copolymers have weaker interactions because the three types of residues are randomly distributed. As a result of the strong hydrophobic interactions between the neutral blocks, the block copolymers associate and form micelles, and they behave as larger entities than the original copolymer molecules. The light-scattering study in Chapter 2 revealed that the micelles of polymer 2 contain 20-25 copolymer molecules. A larger polymer molecule is less soluble in the solvent and its solutions are less miscible with solutions of other polymers [4]. It is worth mentioning that, with no added PVA, the random polyampholytes are soluble, typically above 10% w/w, over the entire pH range, while the block polyampholytes exhibit a pronounced decrease in their solubility around the isoelectric point.

The salt concentration has a strong effect on the phase behavior of the block copolymers. In most cases, precipitation occurred for the salt concentrations of 0.0 up to 0.1M KCl. Beyond this point, the added salt increases the solubility of the polyampholyte and, therefore, increasing salt concentration broadens the "good" two-phase region at the expense of the precipitation region. An exceptional case is polymer 10, whose phase separation pattern seemed hardly influenced by the increasing salt concentration. Polymer 10 presented the widest "good" two-phase region and the narrowest precipitation region. This is probably due to the increased hydrophilicity of the polymer which is the richest in the most hydrophilic residues, the acidic. On the other hand, polymer 9, having the largest basic fraction, is the most hydrophobic. Consequently, Polymer 9 has the broadest insoluble region. However, one might question why Polymers 8, 2, and 5 (Figure 9.2, 9.3, and 9.6 respectively) behave similarly, having different percentage of neutral residues (they all have acidic/basic ratio 1/1). To explain the similarity in phase behavior, micellization should be taken into account. The methyl or the phenyl groups of the polymer associate with each other and take their position in the middle of the micelles. Being in the middle, they do not actively participate in the interaction taking place in the solution side. Therefore, only the effect of the acid and the basic groups, which are placed in the solution side, remains important. Supporting the significance of the acidic/basic ratio, random copolymer 13, acidic/basic = 1/2, appeared as precipitate in the same region where Polymer 12, acidic/basic = 1/1, which is less hydrophobic than polymer 13, formed two separate phases.

Phase separation behavior is also dependent on the block sequence in the block copolymer. Polymer 1, unlike all the other block copolymers, has the acidic block in the middle of the molecules. The "good" phase separation below the isoelectric point at relatively low salt concentrations (0.1 and 0.35M KCl) may be due to the inability of the acidic block to form hydrogen-bonds with PVA because it is presumably located between the shell and the core of the polymer micelles.

Salt type is an another factor which influences the phase separation behavior of the polyampholyte-PVA system. Our results show that the phase separation effectiveness (considering precipitation more effective phase separation than "good" two-phase formation) increases in the order of $I^- = Br^- < Cl^- < F^- = SO_4^{2-}$ for the anions and $Li^+ = Na^+ < K^+ = Rb^+ = Cs^+$ for the cations. Figures 9.9 and 9.10 show that increasing the salt concentration from 0.35 to 0.75M converts the systems containing KI, KBr and LiCl from two-phase to one-phase systems. The above results agree with the Hofmeister series, which show that the salting-out ability for some common ions is in the increasing order of $SCN^- < ClO_4^- < NO_3^- < Br^- < Cl^- <$ acetate$^- < SO_4^{2-} < PO_4^{3-}$ for anions and $Na^+ < K^+ < NH_4^+$ for cations [5]. It is worth noting that while for cations the salting-out ability increases as the ion hydration number decreases, for anions the salting-out ability increases as the ion hydration number increases [6].

9.5 Conclusions

The phase separation behavior of both triblock and random polyampholytes in an aqueous mixture with poly(vinyl alcohol) was compared and it was found that, due to their structural differences, the two types of polymers behave differently. It was also found that the acidic/basic ratio of the polymer as well as the block sequence largely affect the phase separation behavior. In addition, the salt concentration and the solution pH are found to be the important governing factors. Typically, the phase separation of the block polyampholytes covers a rectangle in the pH-ionic strength space which extends from 0 to 0.75M KCl and from pI-2 to pI+2 in pH. "Good" phase separation appears at 0.1M KCl and it is located one pH unit above the isoelectric point, extending to a short pH range. Below that pH, precipitation prevails. With increasing ionic strength the "good" two-phase pH region expands to lower pH values until, at 0.75M KCl, it covers the whole two-phase region. The extend of phase separation of random copolymers appeared much smaller, covering the space defined by potassium chloride concentrations from 0.0 to 0.1M and, at most, one unit in pH, centered at the isoelectric point. The effect of salt type on the phase separation behavior can be explained by the Hofmeister series, which show that phase separation is facilitated in the presence of strong salting-out salts.

9.6 Literature Cited

(1) Albertsson, P.-A. *Partition of Cell Particles and Macromolecules*; Wiley and Sons: New York, 3rd ed., 1986.

(2) Patrickios, C. S.; Abbott, N. L.; Foss, R. P.; Hatton, T. A. Protein Partitioning in Two-Phase Aqueous Polymer Systems Containing Polyampholytes. *New Developments in Bioseparation*; Ataai, M. M., Sikdar, S. K., Eds.; AIChE Symposium Series: New York, 1992, Vol. 88, p 80-88.

(3) Hughes, P.; Low, C. R. Purification of Proteins by Aqueous Two-Phase Partition in Novel Acrylic Co-Polymer Systems. *Enzyme Microb. Technol.* **1988,** *10,* 115-122.

(4) Flory, P. J. *Principles of Polymer Chemistry*; Cornell University Press: Ithaca, 1953, p 546.

(5) Scopes, R. P. *Protein Purification: Principles and Practice*; Springer-Verlag: New York, 2nd ed., 1988; p 50.

(6) Israelachvili, J. *Intermolecular and Surface Forces*; Academic Press: London, 1991, 2nd ed., p 55.

Table 9.1 Characteristics of the polyampholytes studied.

Polymer	Figure	Formula[1]	pI
9	9.1	$B_{16}M_{12}A_8$	8.0
8	9.2	$B_{12}M_6PM_6A_{12}$	6.8
2	9.3	$B_{12}M_{12}A_{12}$	6.6
1	9.4	$M_{12}A_{12}B_{12}$	6.6
10	9.5	$B_8M_{12}A_{16}$	5.4
5	9.6	$B_{10}M_{20}A_{10}$	6.5
13	9.7	$(B_{1.33}MA_{0.67})_{12}$	8.2
12	9.8	$(BMA)_{12}$	6.6
2	9.9	$B_{12}M_{12}A_{12}$	6.6
2	9.10	$B_{12}M_{12}A_{12}$	6.6

[1]B = dimethylaminoethyl methacrylate; A = methacrylic acid; M = methyl methacrylate; P = phenylethyl methacrylate.

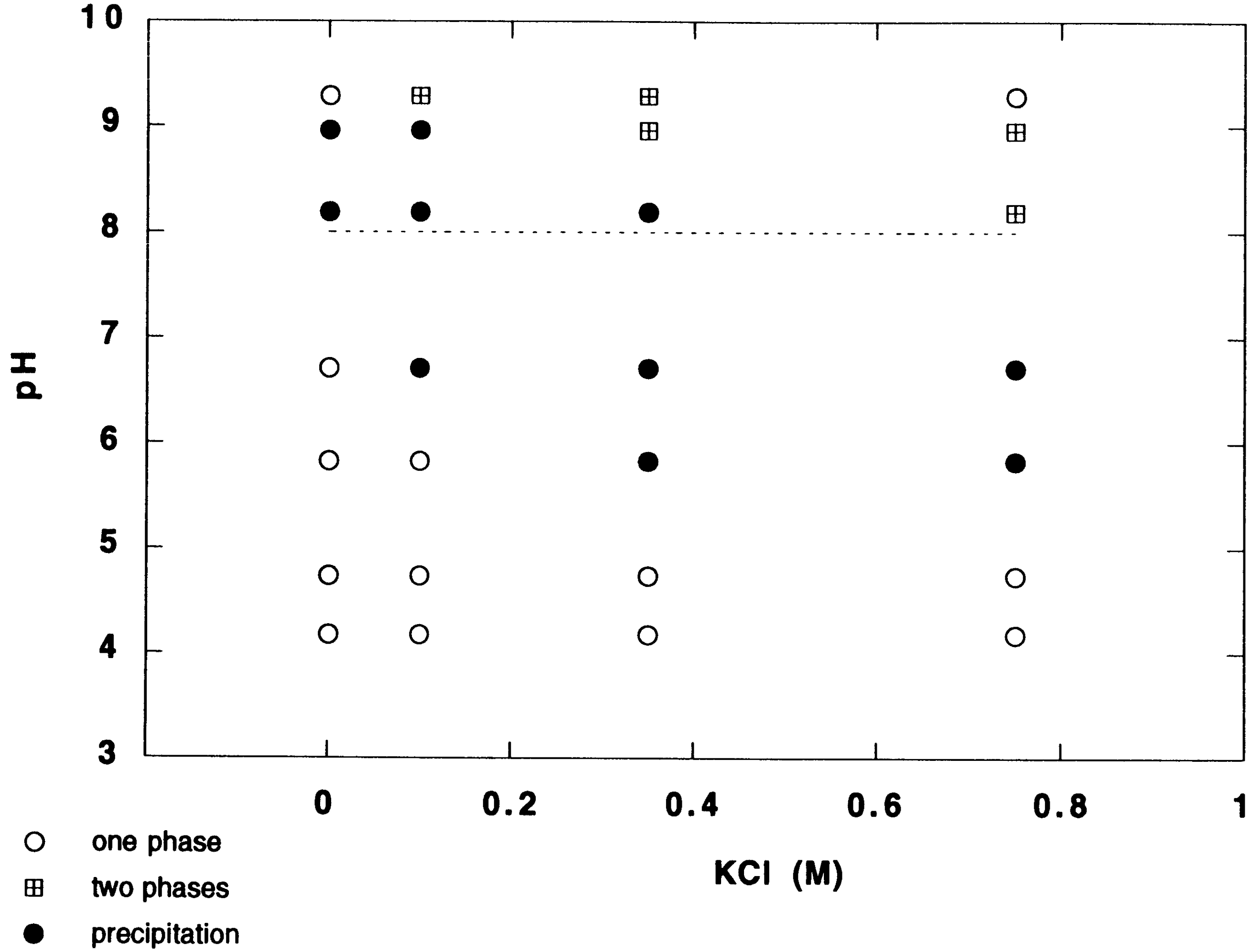

Figure 9.1 Phase-behavior of triblock Polymer 9 with poly(vinyl alcohol). The dotted line denotes the isoelectric point.

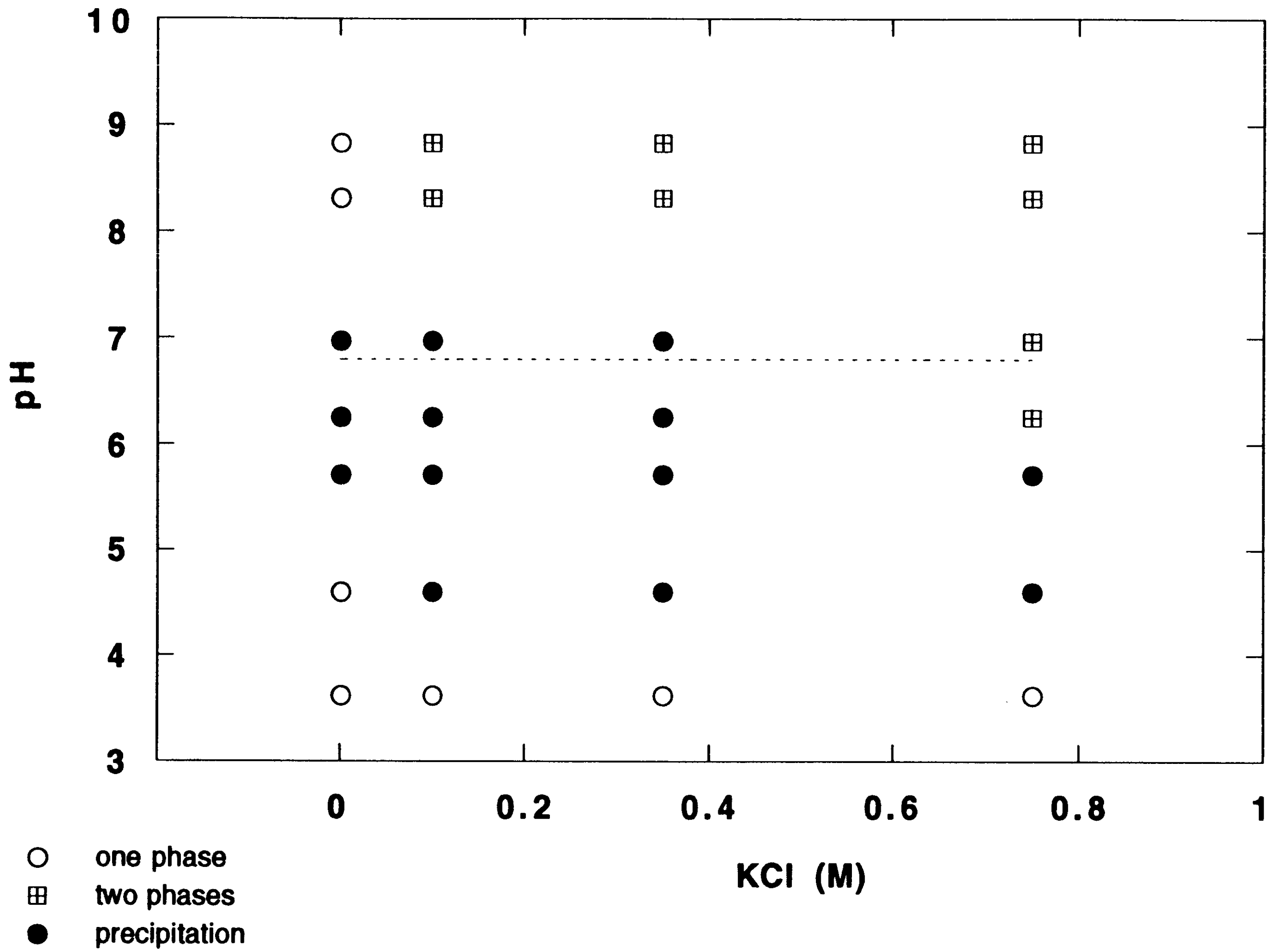

Figure 9.2 Phase-behavior of triblock Polymer 8 with poly(vinyl alcohol). The dotted line denotes the isoelectric point.

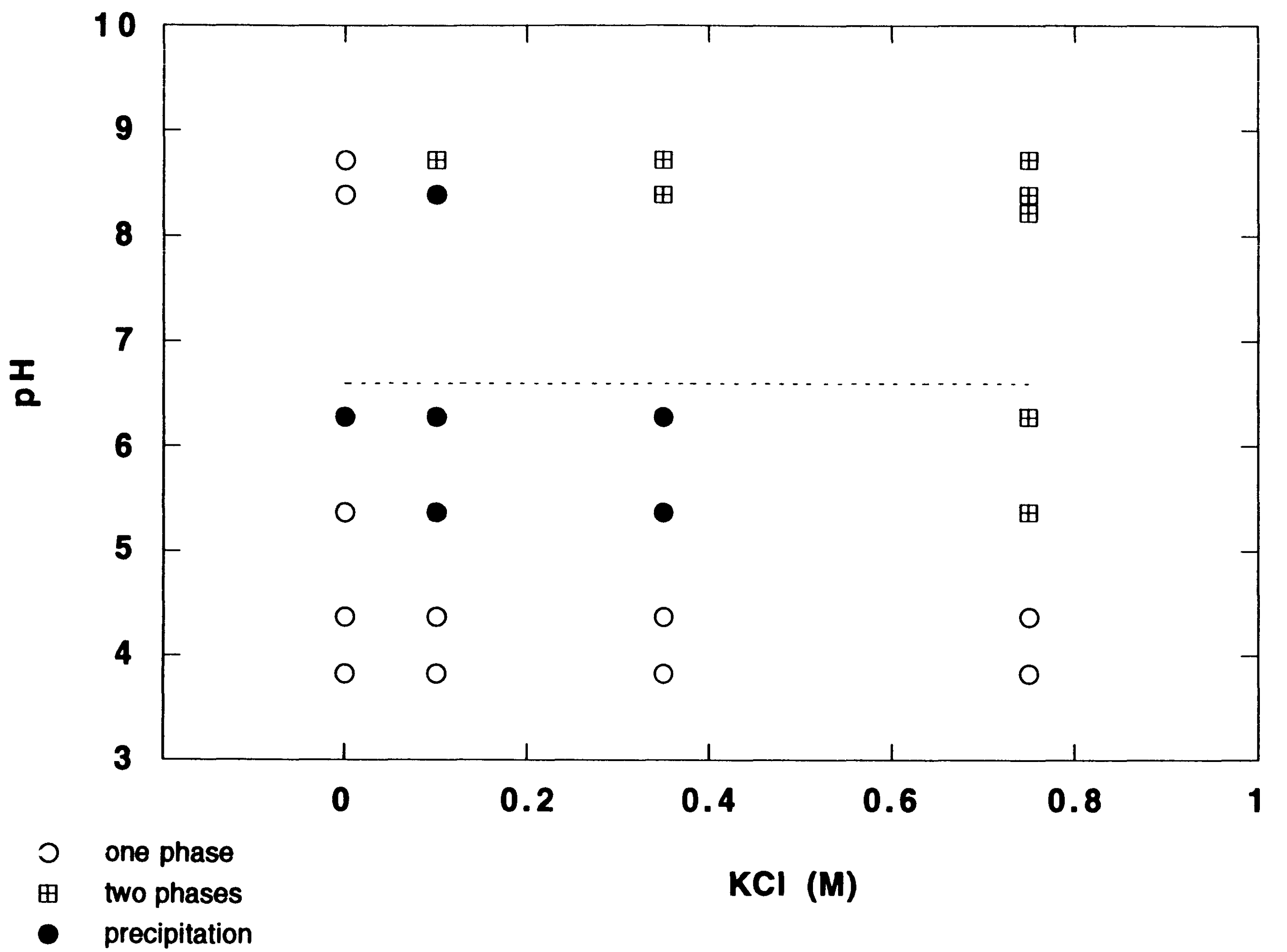

Figure 9.3 Phase-behavior of triblock Polymer 2 with poly(vinyl alcohol). The dotted line denotes the isoelectric point.

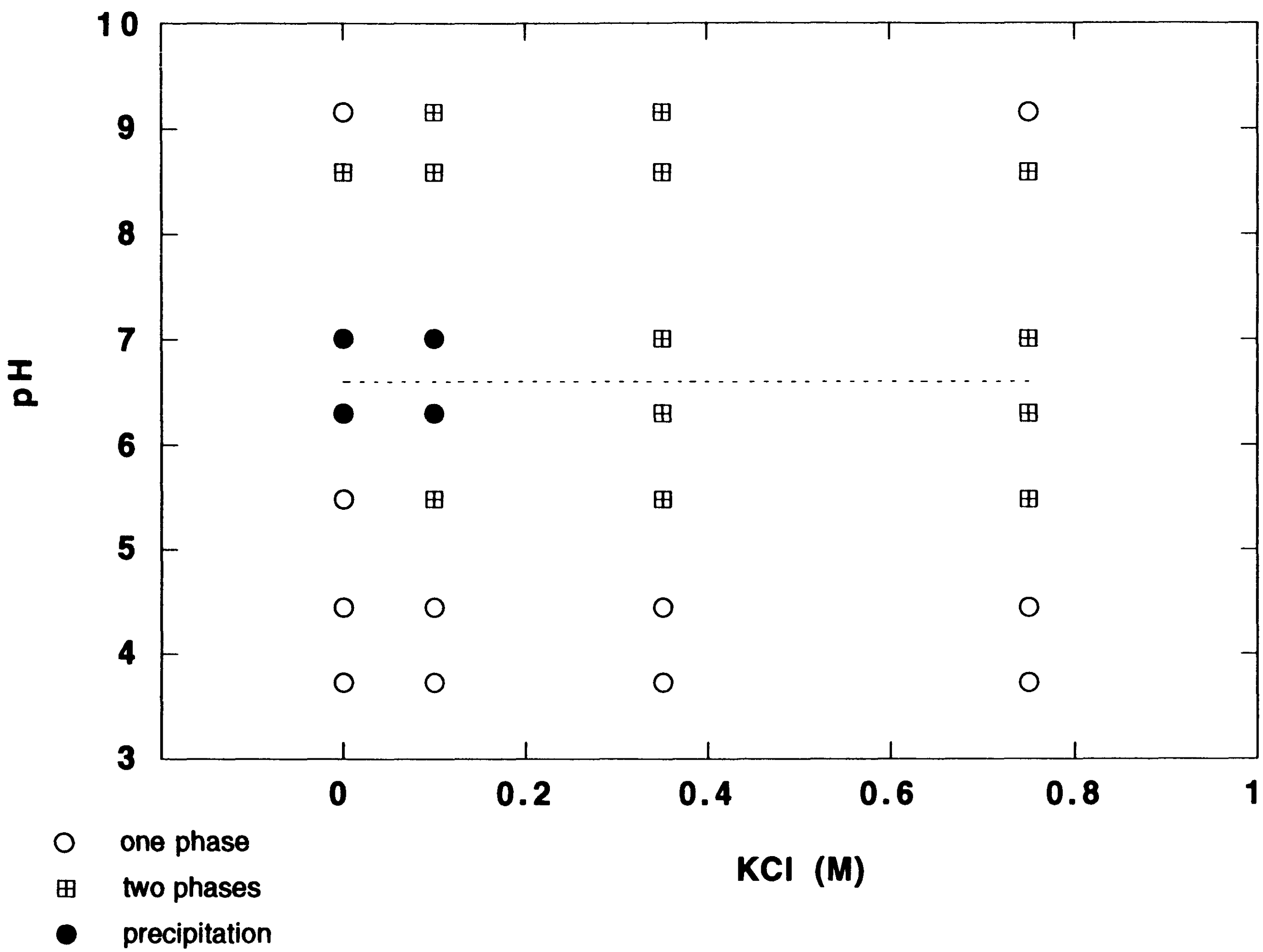

Figure 9.4 Phase-behavior of triblock Polymer 1 with poly(vinyl alcohol). The dotted line denotes the isoelectric point.

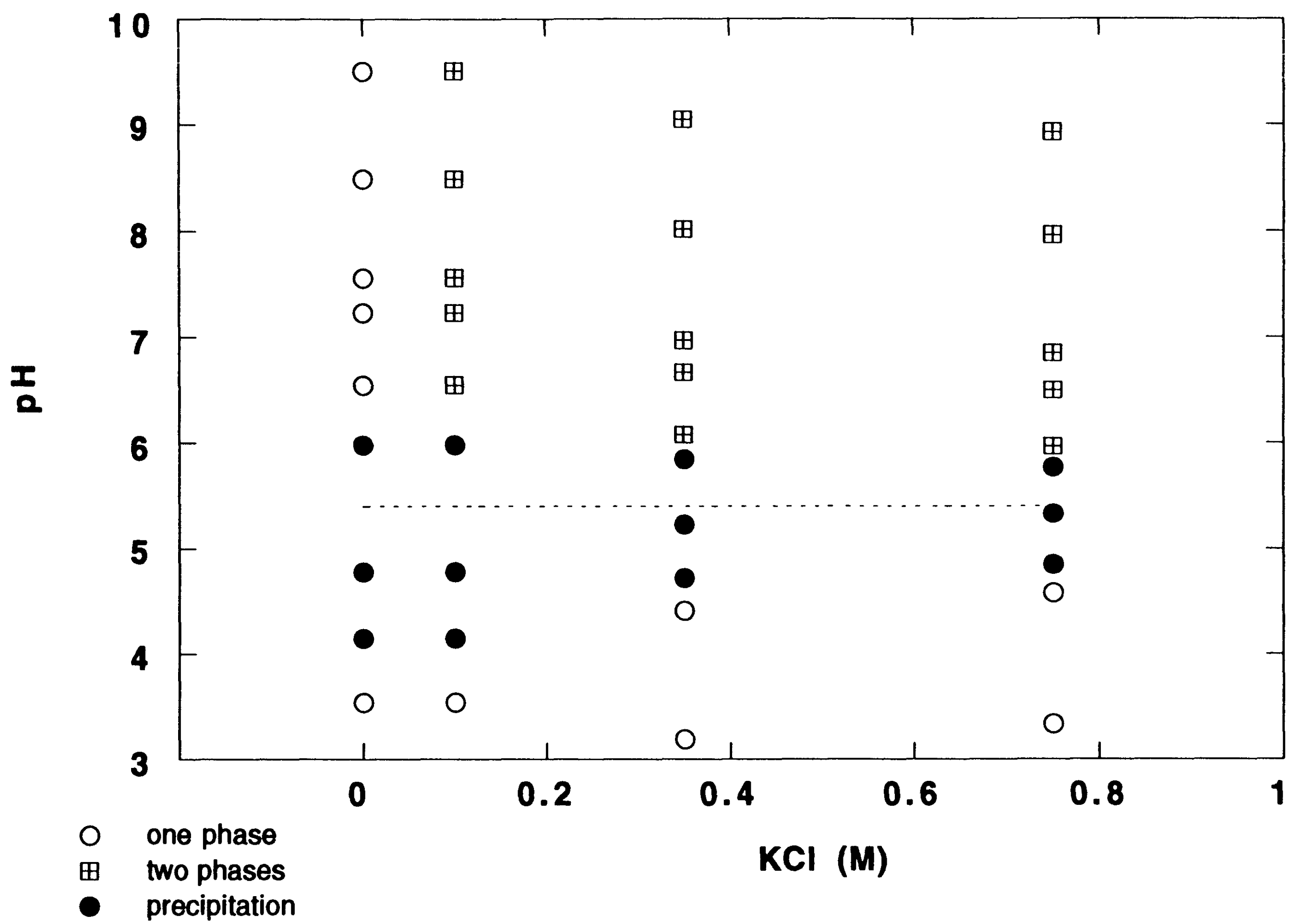

Figure 9.5 Phase-behavior of triblock Polymer 10 with poly(vinyl alcohol). The dotted line corresponds to the isoelectric point.

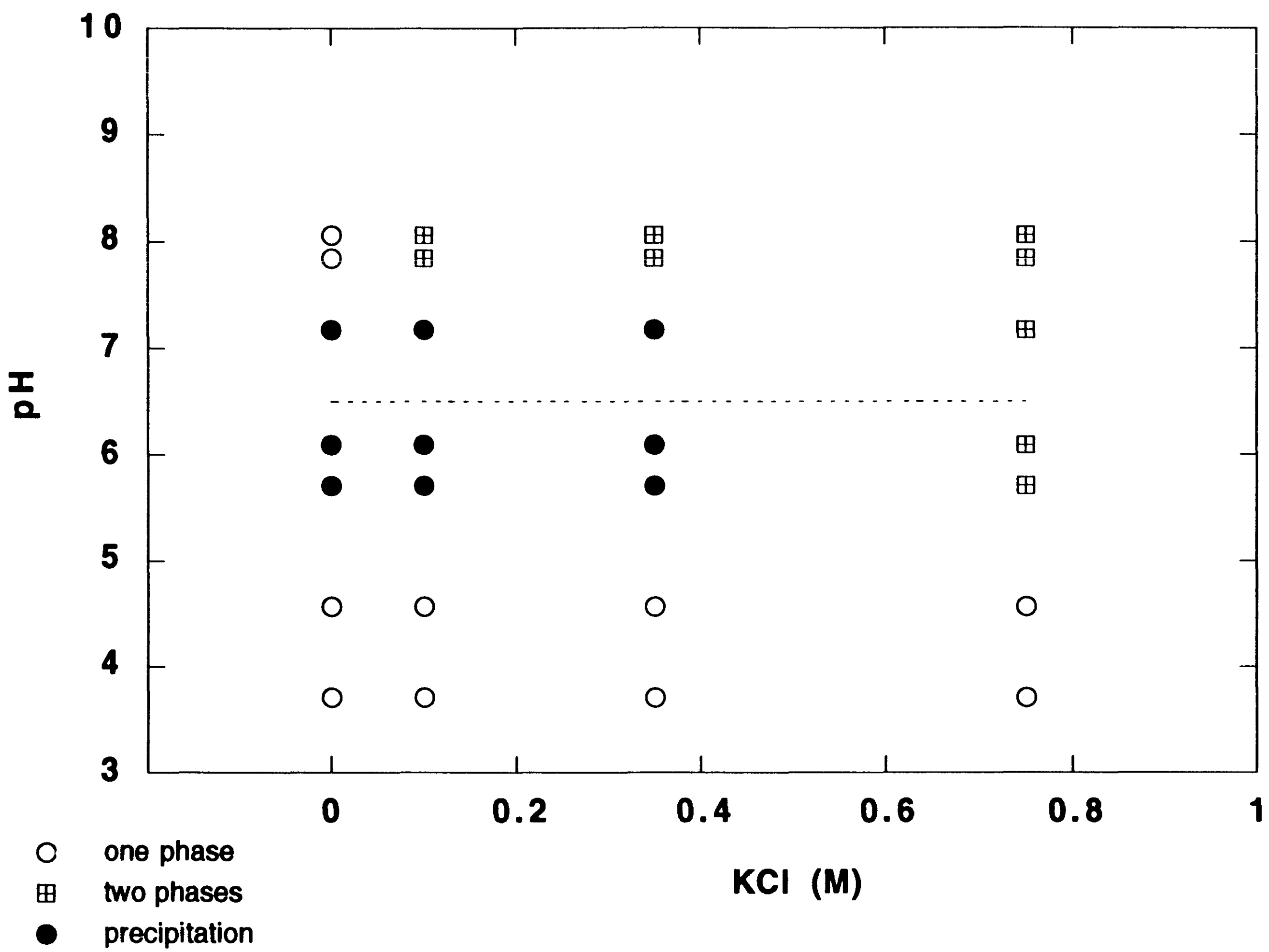

Figure 9.6 Phase-behavior of triblock Polymer 5 with poly(vinyl alcohol). The dotted line denotes the isoelectric point.

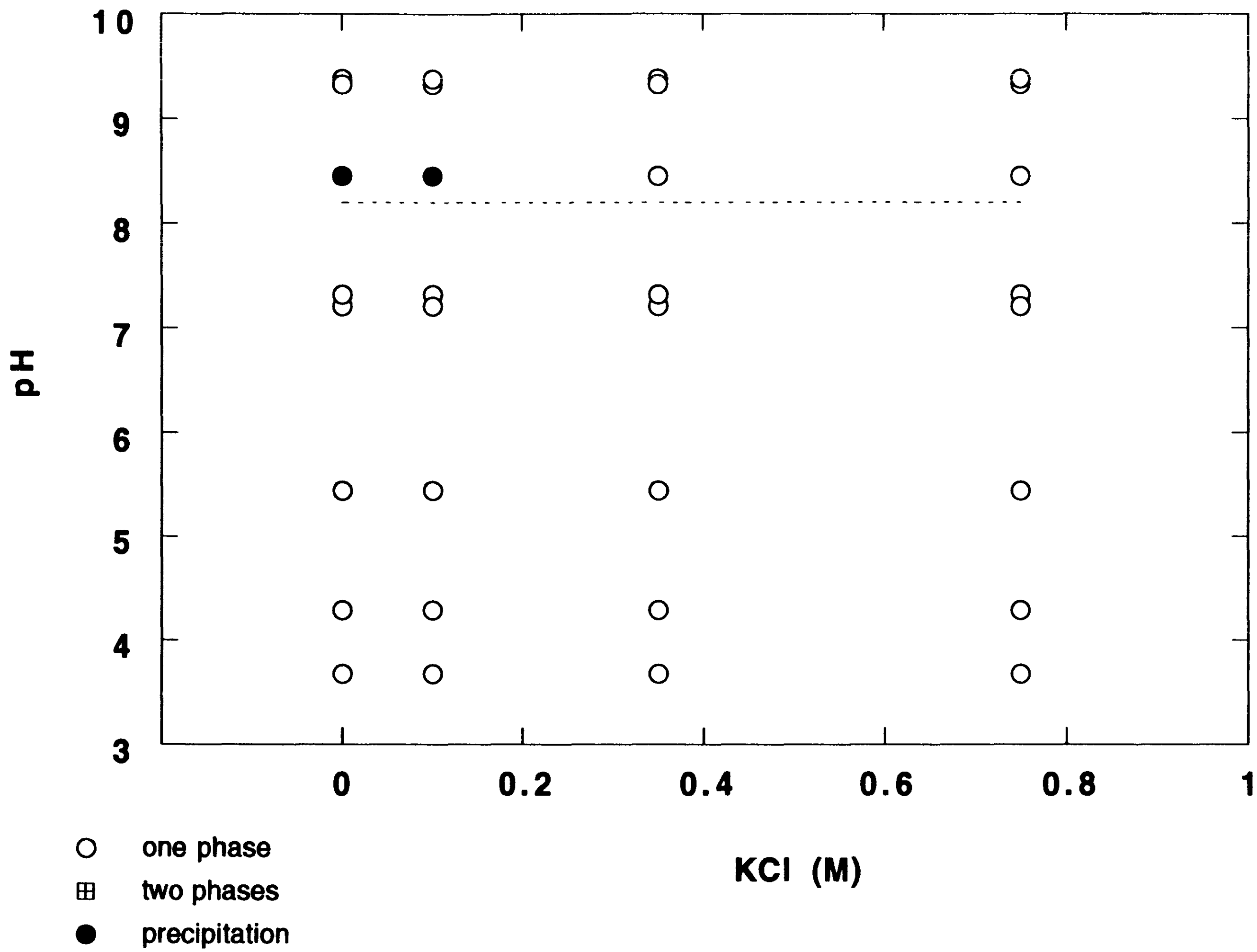

Figure 9.7 Phase-behavior of random Polymer 13 with poly(vinyl alcohol). The dotted line corresponds to the isoelectric point.

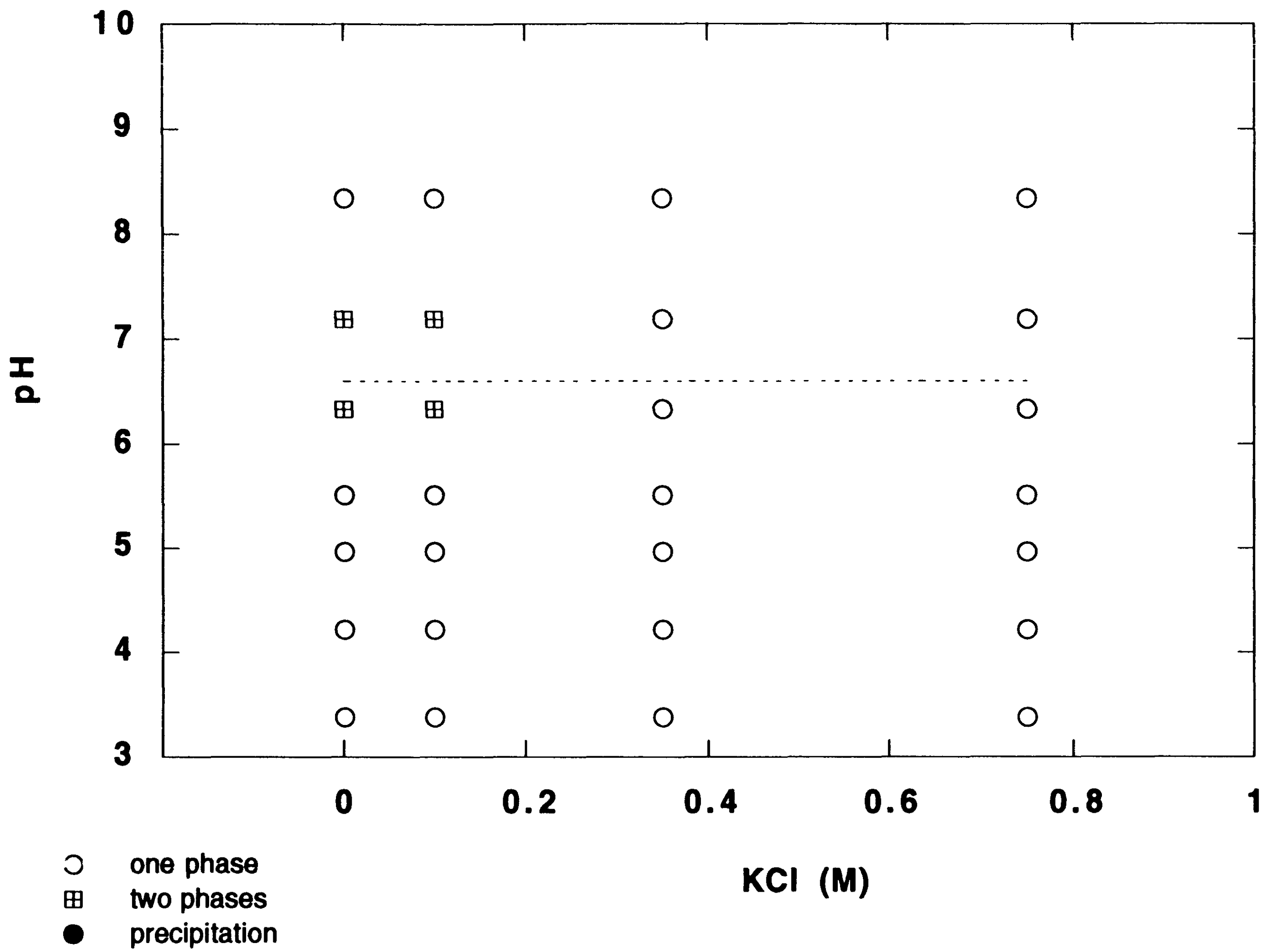

Figure 9.8 Phase-behavior of random Polymer 12 with poly(vinyl alcohol). The dotted line denotes the isoelectric point.

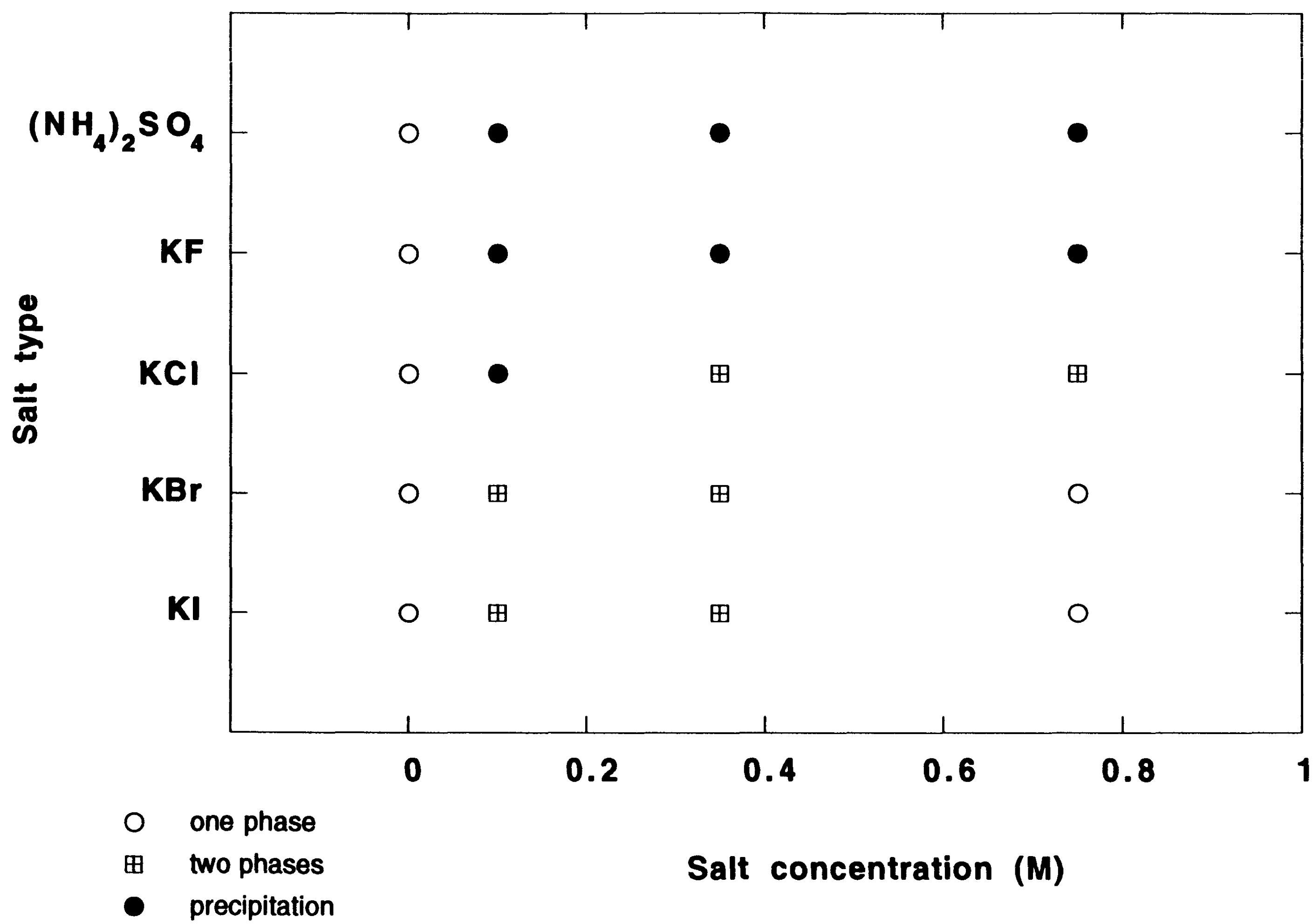

Figure 9.9 Effect of anion type on the phase-behavior of triblock Polymer 2 with poly(vinyl alcohol) at pH 8.2.

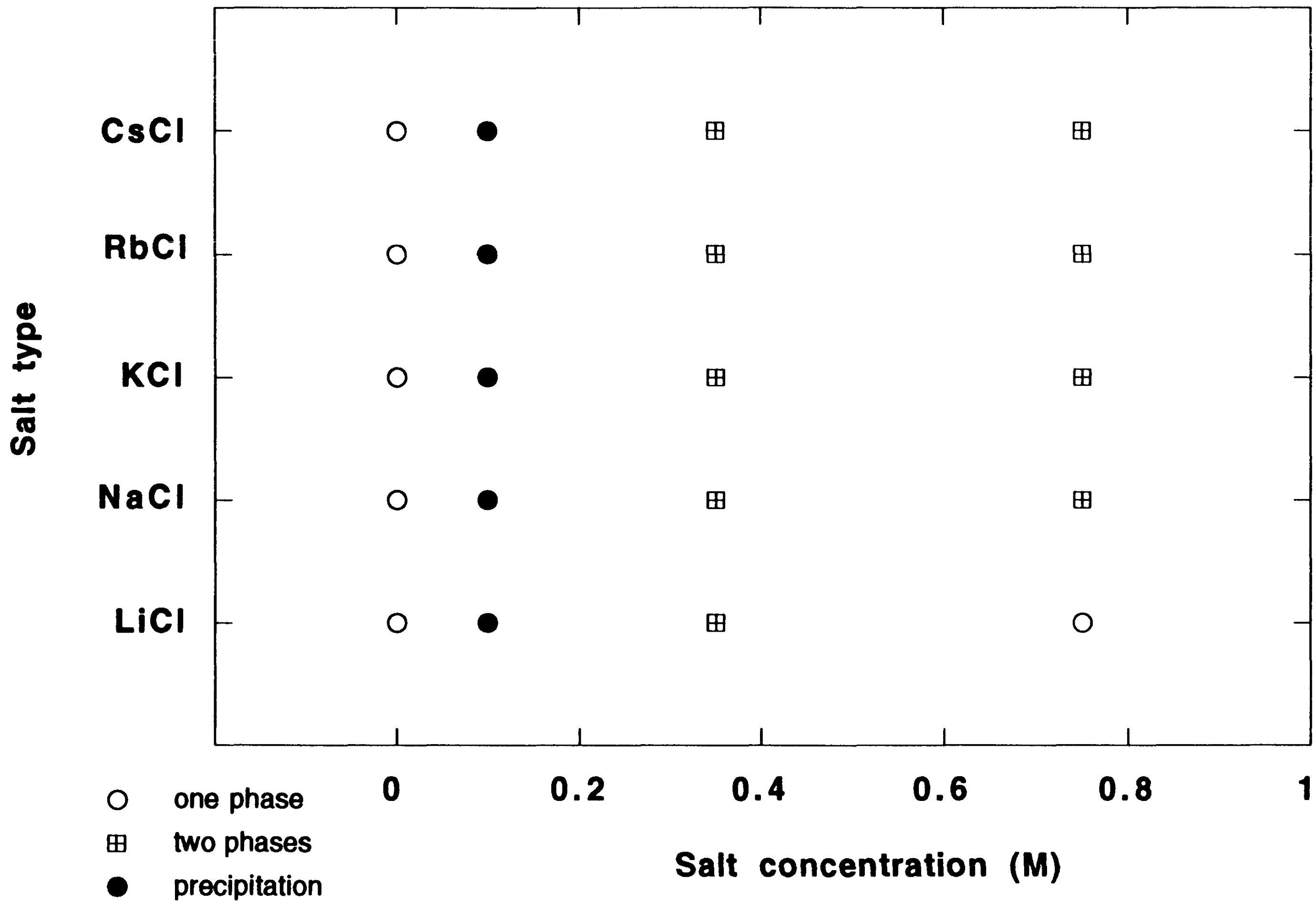

Figure 9.10 Effect of cation type on the phase-behavior of triblock Polymer 2 with poly(vinyl alcohol) at pH 8.2.

Chapter 10.

Conclusions and Recommendations.

10.1 Conclusions

We have developed a new class of water-soluble block copolymers with interesting properties and usefulness in protein separation processes. These methacrylic copolymers were synthesized by a new polymerization technique, Group Transfer Polymerization, which allowed for control in polymer size and architecture. The combination of ampholytic and hydrophobic character in the triblocks was responsible for the phase-behavior of the aqueous solutions of these polymers with respect to pH: (i) precipitation around the isoelectric pH, (ii) formation of micelles at intermediate pH and (iii) dispersion to single polymer chains at extreme pH. The performance of the polyampholytes as mediators in protein separation by anion-exchange displacement chromatography, coprecipitation and biphasic aqueous polymer extraction was comparable to that of homopolyelectrolytes. However, the property of these copolymers to precipitate around the isoelectric point offers the opportunity for polymer recycle and reuse which constitutes a significant process-scale advantage of polyampholytes over polyelectrolytes.

The relatively low molecular weights (4,000) of these polyampholytes were appropriate for displacement chromatography because they facilitated column regeneration without excessive compromise of displacer affinity. Higher (typically 40,000) polyampholyte molecular weights would be beneficial for protein coprecipitation and protein partitioning as they would strengthen the Coulombic interaction which is the main driving force for the separation.

As the power of displacement chromatography is being recognized, we foresee a great potential for the utilization of the triblock polyampholytes as ion-exchange displacers of proteins. The ability for polymer recycle and reuse will add to the already existing attractive features of simultaneous fractionation and concentration of the proteins.

The novelty of these polymers prevented us from focusing on a specific aspect of their behavior or potential application. Instead, we probed their properties by a variety of characterization techniques and evaluated them in a number of applications. It is our feeling that a new field has been created that calls for in-depth investigation.

10.2 Another Potential Application

The pH-dependence of the phase-behavior of the triblock polyampholytes may prove attractive for the extraction of environmental pollutants in three stages: (i) the pollutants are solubilized into the polyampholyte micelles at intermediate pH (ii) the pollutants are freed at low pH by the destruction of the micelles and delivered to a "waste-sink" and (iii) the polyampholyte is precipitated at the isoelectric point for concentration and recycle.

10.3 Degradability

It has been reported that the acrylic polyampholytes are non-degradable [1]. This may simply mean that no backbone scissions occur over time. It is possible, however, that chemical alterations of the side-groups take place. Righetti has reported a 20% per year hydrolysis of a tertiary amine (pK = 9.3) monomer used for the synthesis of gels which served as immobilized pH gradients for isoelectric focusing [2]. Similarly, it has been observed [3] that for tertiary ester amines, including dimethylaminoethyl methacrylate, ester hydrolysis may occur over a period of weeks leading to the formation of methacrylic acid and ethanolamine. It is possible that the mild toxicity observed in dimethylaminoethyl methacrylate gels [4] is due to the released ethanolamine. It is recommended to substitute the tertiary amine with a quaternary amine such as trimethylaminoethyl methacrylate. The increased steric hindrance caused by the additional methyl group will prevent hydrolysis by inhibiting the formation of the required intermediate. Supporting this scenario is the non-toxicity of the gel made of trimethylaminoethyl methacrylate [4].

10.4 Toxicity

As mentioned in the previous paragraph, the replacement of the tertiary amine residues by quaternary amine residues may prevent the hydrolytic degradation of the side-group, leading to the reduction or elimination of toxicity. Describing carrier ampholytes, which are acrylic buffers for isoelectric focusing, Righetti mentions that the basic (pH = 9-11) ampholytes were found mitogenic on quiescent human diploid lung fibroblasts [5]. We may attribute this to degradation too, because these ampholytes contained large percentage of tertiary amine residues. However, Righetti also says that all commercial ampholytes, when used at high concentration (usually above 2-3mg/mL) have an inhibitory effect and are cytotoxic [5].

The most toxic components of our polyampholytes are probably the low-molecular-weight impurities which can be separated from the polymer by repeated precipitation of the latter at the isoelectric point.

10.5 Purification

Repetitive polyampholyte precipitation at the isoelectric point will not only decrease toxicity but increase polymer homogeneity. It is recommended that the polymers be precipitated at least twice (and dried) before any further experiments. In this thesis, the impurities may have affected the frontal results in Chapter 4. However, since the impurity content was relatively small, around 10%, the observed trends should still be valid. Interestingly, Righetti notes that the recycled carrier ampholytes were more homogeneous than the unrecycled fresh material [5].

10.6 Viscosity

Viscosity measurements were conducted using a Cannon-Fenske viscometer. To probe the effect of micelle formation on viscosity, both micellar (triblock polymers at pH 5) and non-micellar (triblock polymers at pH 2.5 and random copolymers) solutions were studied at different polymer concentrtions. The results, appearing in Figures 10.1 and 10.2, did not allow for any rigid conclusions as the viscosity differences were small and no trend was obvious. It is interesting to speculate, however, that the comparable viscosities of the micellar and non-micallar solutions suggest that the micelles are of spherical shape.

10.7 Surface tension

Surface tensions of polyampholyte solutions were measured by the Wilhelmy plate technique at 25°C. Most of the polymer solutions tested were rather concentrated (1% or higher) and, therefore, no surface tension values were obtained within the dilute regime whithin which the CMCs lie. As can be seen in Figures 10.3 and 10.4, random copolymers were more surface active than the block polymers probably because of the smaller availability of block copolymer chains due to micellization. The effect of pH was minor. While long equilibration times were observed for the block copolymers, short equilibration times were required by the random copolymers. This can attributed to the slow transport of block polymer chains from the micelles to the plate, or to the slow displacement of block polymer chains by a small amount of highly surface active impurities [6-8]. The surface tensions of both dilute and concentrated solutions of triblock Polymer 2 are shown in Figure 10.5. The various values of surface tension at the same polymer concentration correspond to measurements at different times. No clear break in the surface tension curve can be distinguished and, therefore, no CMC can be assigned.

10.8 Solubilization of DPH

The absorbance of solutions containing diphenyl hexadiene (DPH) and different concentrations of triblock Polymer 2 at pH 4.5 and at different temperatures (15, 25, 35 and 45°C) was examined to determine the CMC [9]. The enhancement of the signal took place at a concentration of 0.04% w/w which was 20 times higher than that in Figure 2.6 (0.002% w/w) where pyrene was used as the probe. This discrepancy can be attributed to the more hydrophobic character of pyrene which could bind to the micelles or pre-micelles (or even unimers) at a lower polymer concentration than DPH. Most interestingly, no effect of temperature was observed (the signal enhancement occurred at the same polymer concentration for all temperatures).

10.9 Gels and Stars

Motivated by the work of Tanaka and coworkers on gels [10-13], we sought the synthesis of block polyampholyte gels. Although random polyampholyte gels have been prepared [13], no report has dealt with block polyampholyte gels. It was attempted to cross-link the block copolymers by shining γ-radiation to their concentrated (1-10%) solutions. Several polymer samples were irradiated at different doses (1-20 Mrad) but no gel formation resulted because poly(methacrylates) tend to undergo more scissions than cross-links under radiation [14,15].

It was therefore decided to follow a chemical route for the gel synthesis. This would require the preparation of end-functionalized polyanions and polycations and their subsequent linking by a multifunctional agent. Since our collaborators, Shefer and Grodzinsky, had already prepared the end-functionalized polyanion (polyacrylic acid) [16], we only needed to prepare the end-functionalized polycation. This was successfully done by free-radical polymerization of dimethylaminoethyl methacrylate in the presence of an iniferter [16]. As confirmed by end-group (sulfur) analysis, the telomer had the expected molecular weight of 2,000. We did not have the time to proceed to the last step for the gel preparation which was the linking of the polyanion and polycation by a chemical agent such as tri(4-isocyanatophenyl)methane [17]. This, however, is easy to do.

It is interesting to note that the use of a high ratio of telomers to cross-linker will result in the preparation of star polyampholytes.

10.10 Modelling

Necessary and hopefully easy to perform with existing software [18] is modelling polyampholyte adsorption on ion-exchange columns. The results from the frontals in Chapter 4 can provide an experimental data base for evaluating the results of the model. A successful model can reveal all the details on the adsorption conformation and predict the effects of polymer composition and pH. A Masters student from Steve Cramer's group at RPI has presumably undertaken this task and results should be expected soon.

10.11 Characteristic Charge by Isocratic Elution

It is recommended that the polyampholyte characteristic charges be evaluated by a second method that is based on the isocratic elution of polymer samples at different polymer concentrations [19]. Compared to the frontal experiments of Chapter 4, this method is rapid, economical in polymer and allows for the calculation of the free energy of binding as well.

10.12 Literature Cited

(1) Hughes, P.; Lowe, C. R. Purification of Proteins by Aqueous Two-Phase Partition in Novel Acrylic Co-Polymer Systems. *Enzyme Microb. Technol.* **1988,** *10,* 115-122.

(2) Righetti, P. G. *Immobilized pH Gradients: Theory and Methodology*; Elsevier: Amsterdam, 1990; pp 31.

(3) Horn, D., BASF AG, Polymer Research Division, personal communication.

(4) Hattori, S.; Andrade, J. D.; Hibbs, J. B., Jr.; Gregonis, D. E.; King, R. N. Fibroblast Cell Proliferation on Charged Hydroxyethyl Methacrylate Copolymers. *J. Colloid Interface Sci.* **1985,** *104,* 72-78.

(5) Righetti, P. G. *Isoelectric Focusing: Theory, Methodology and Applications*; Elsevier: Amsterdam, 1983; pp 73, 75.

(6) Mysels, K. J.; Florence, A. T. The Effect of Impurities on Dynamic Surface Tension-Basis for a Valid Surface Purity Criterion. *J. Colloid Interface Sci.* **1973,** *43,* 577-582.

(7) Mysels, K. J. Surface Tension of Solutions of Pure Sodium Dodecyl Sulfate. *Langmuir* **1986,** *2,* 423-428.

(8) Alexandridis, P.; Hatton, T. A. Surface Tensions of Pluronics. In preparation.

(9) Alexandridis, P.; Holzwarth, J. F.; Hatton, T. A. Micellization of Poly(ethylene oxide)-Poly(propylene oxide)-Poly(ethylene oxide) Triblock Copolymers in Aqueous Solutions: Thermodynamics of Copolymer Association. Submitted for publication.

(10) Tanaka, T. Gels. *Scientific American* **1981,** *244,* 124-138.

(11) Suzuki, A.; Tanaka, T. Phase Transition in Polymer Gels Induced by Visible Light. *Nature* **1990,** *346,* 345-347.

(12) Ilmain, F.; Tanaka, T.; Kokufuta, E. Volume Transition in a Gel Driven by Hydrogen Bonding. *Nature* **1991,** *349,* 400-401.

(13) Annaka, M.; Tanaka, T. Multiple Phases of Polymer Gels. *Nature* **1992,** *355,* 430-432.

(14) Stevens, M. P. *Polymer chemistry: An Introduction*; Oxford Univ. Press: New York, 1990, 2nd Ed.; p 305.

(15) Chapiro, A. Radiation Chemistry of Polymeric Systems; Wiley: New York, 1962; p 509.

(16) Shefer, A.; Grodzinsky, A. J.; Prime, K. L.; Busnel, J.-P. Free-Radical Telomerization of *tert*-Butyl Acrylate in the Presence of Bis(4-aminophenyl) Disulfide as a Useful Route to Amino-Terminated Telomers of Poly(acrylic acid). *Macromolecules* **1993,** *26,* 2240-2245

(17) Shefer, A.; Grodzinsky, A. J.; Prime, K. L.; Busnel, J.-P. Novel Model Networks of Poly(acrylic acid): Synthesis and Characterization. Submitted to *Macromolecules.*

(18) Blaakmeer, J.; Böhmer, M. R.; Cohen Stuart, M. A.; Fleer, G. J. Adsorption of Weak Polyelectrolytes on Highly Charged Surfaces. Poly(acrylic acid) on Polystyrene Latex with Strong Cationic Groups. *Macromolecules* **1990,** *23,* 2301-2309.

(19) Kopaciewicz, W.; Rounds, M. A.; Fausnaugh, J.; Regnier, F. E. Retention Model for High-Performance Ion-Exchange Chromatography. *J. Chromatogr.* **1983,** *266,* 3-21.

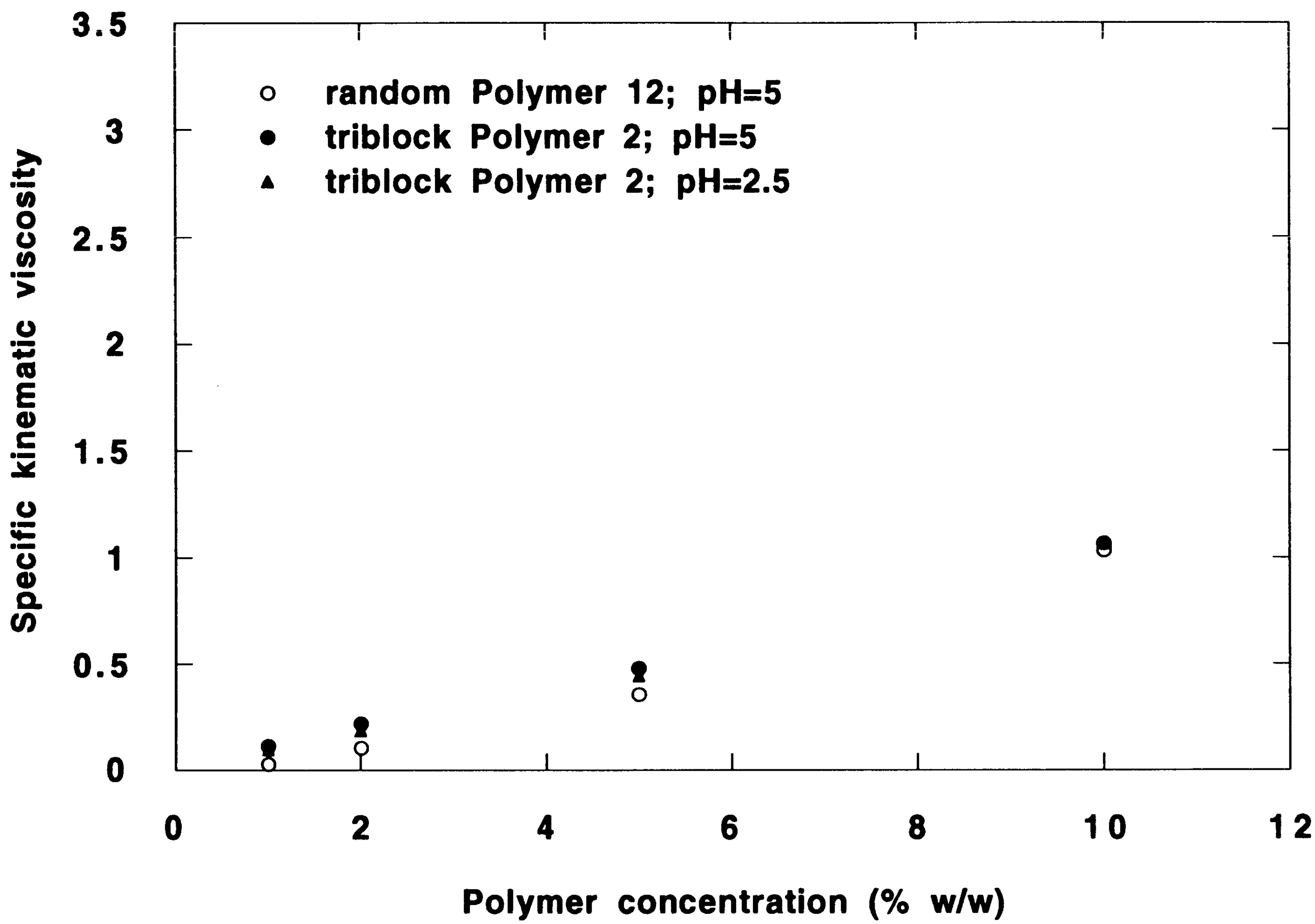

Figure 10.1 Concentration-dependence of the specific viscosity of the neutral polyampholytes. Effect of pH and polymer architecture.

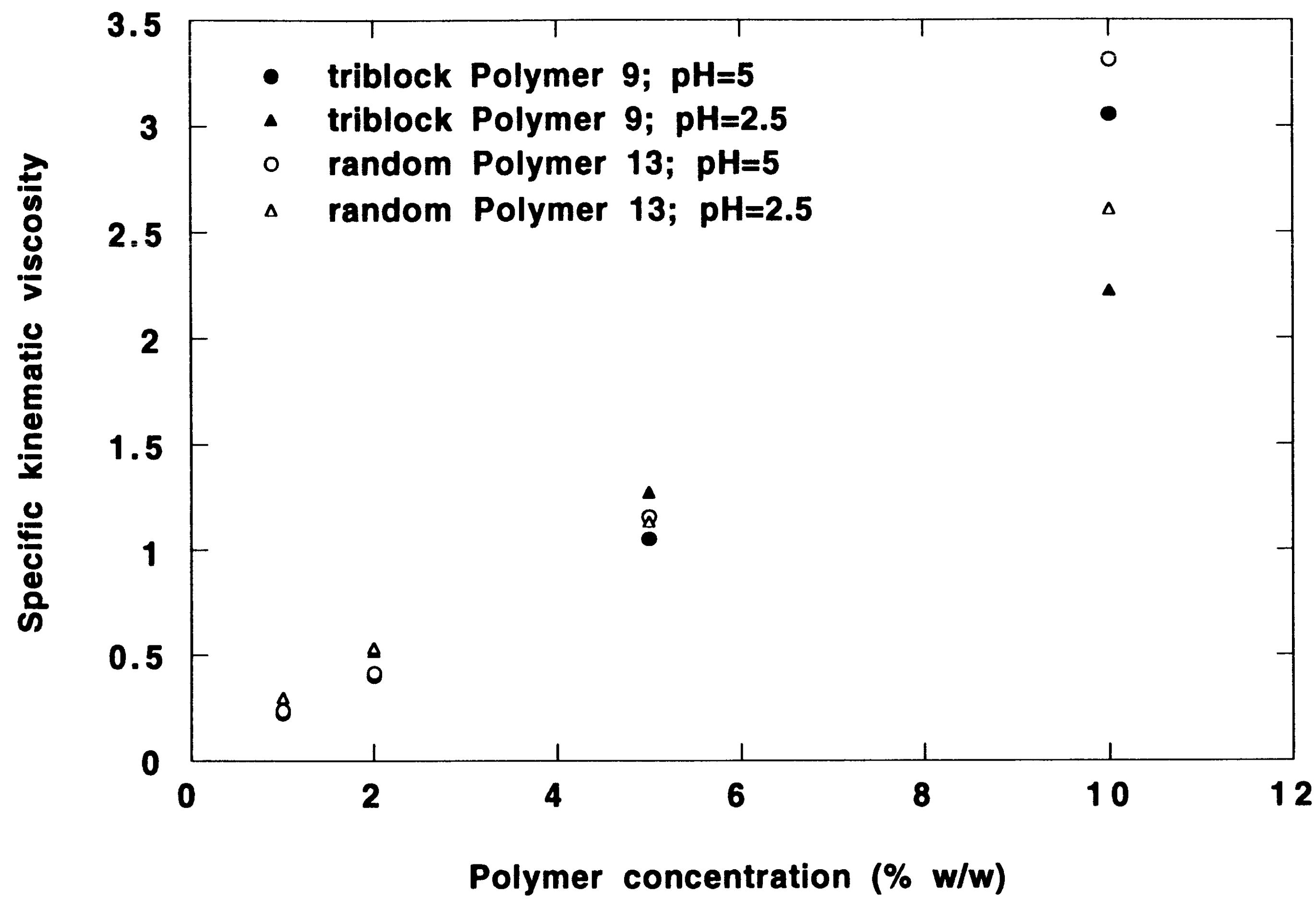

Figure 10.2 Concentration-dependence of the specific viscosity of the basic polyampholytes. Effect of pH and polymer architecture.

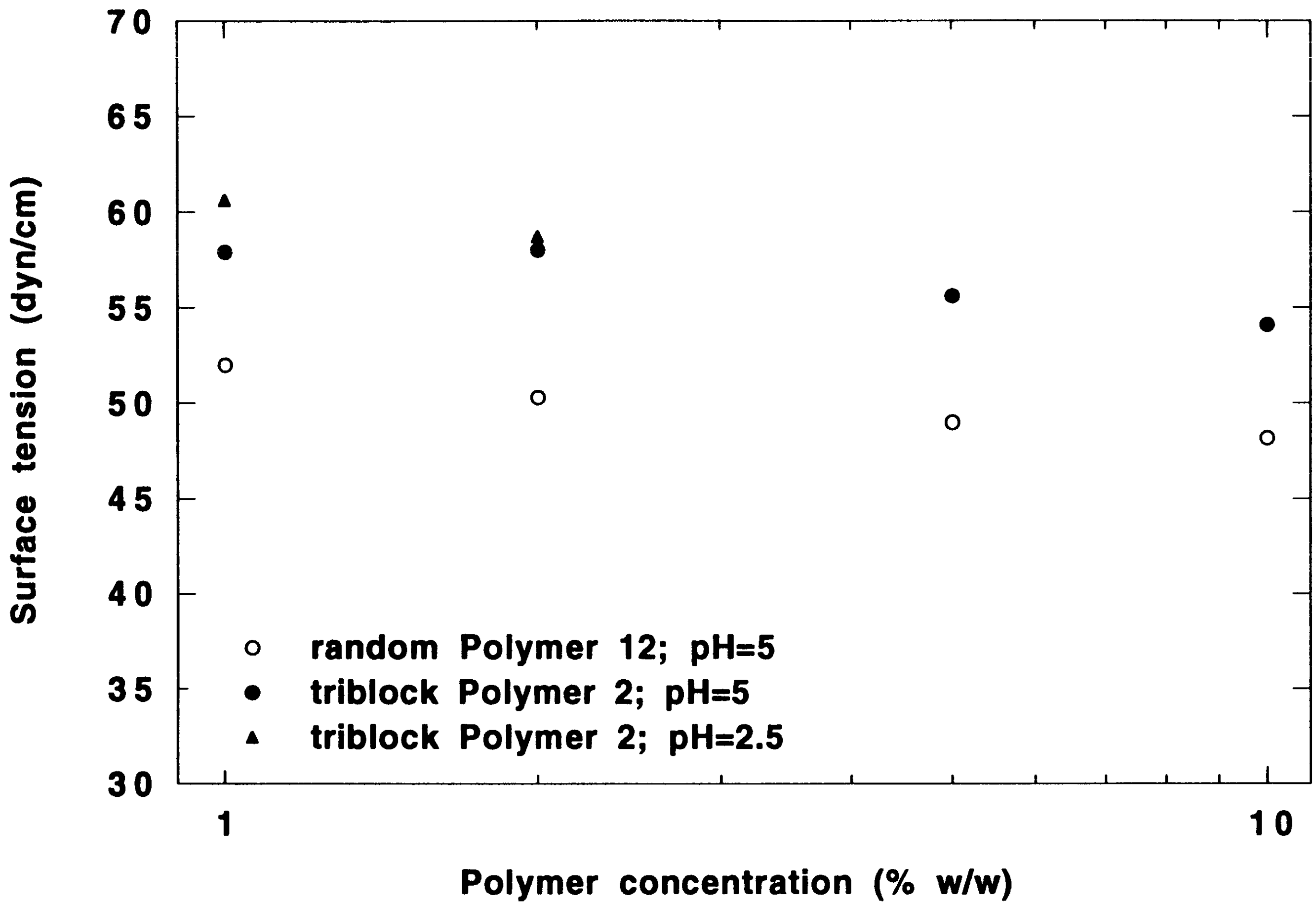

Figure 10.3 Concentration-dependence of the surface tension of the neutral polyampholytes. Effect of pH and polymer architecture.

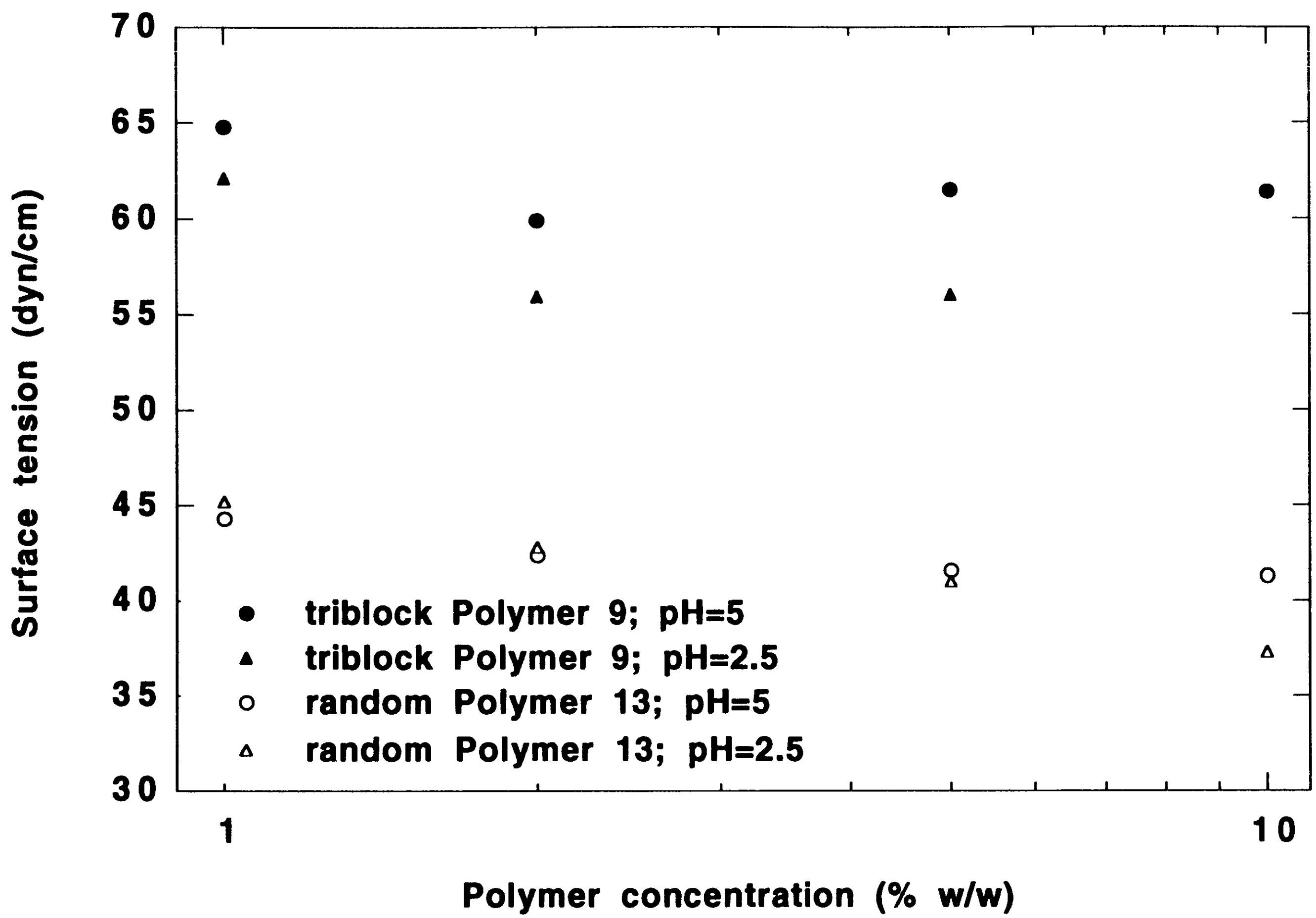

Figure 10.4 Concentration-dependence of the surface tension of the basic polyampholytes. Effect of pH and polymer architecture.

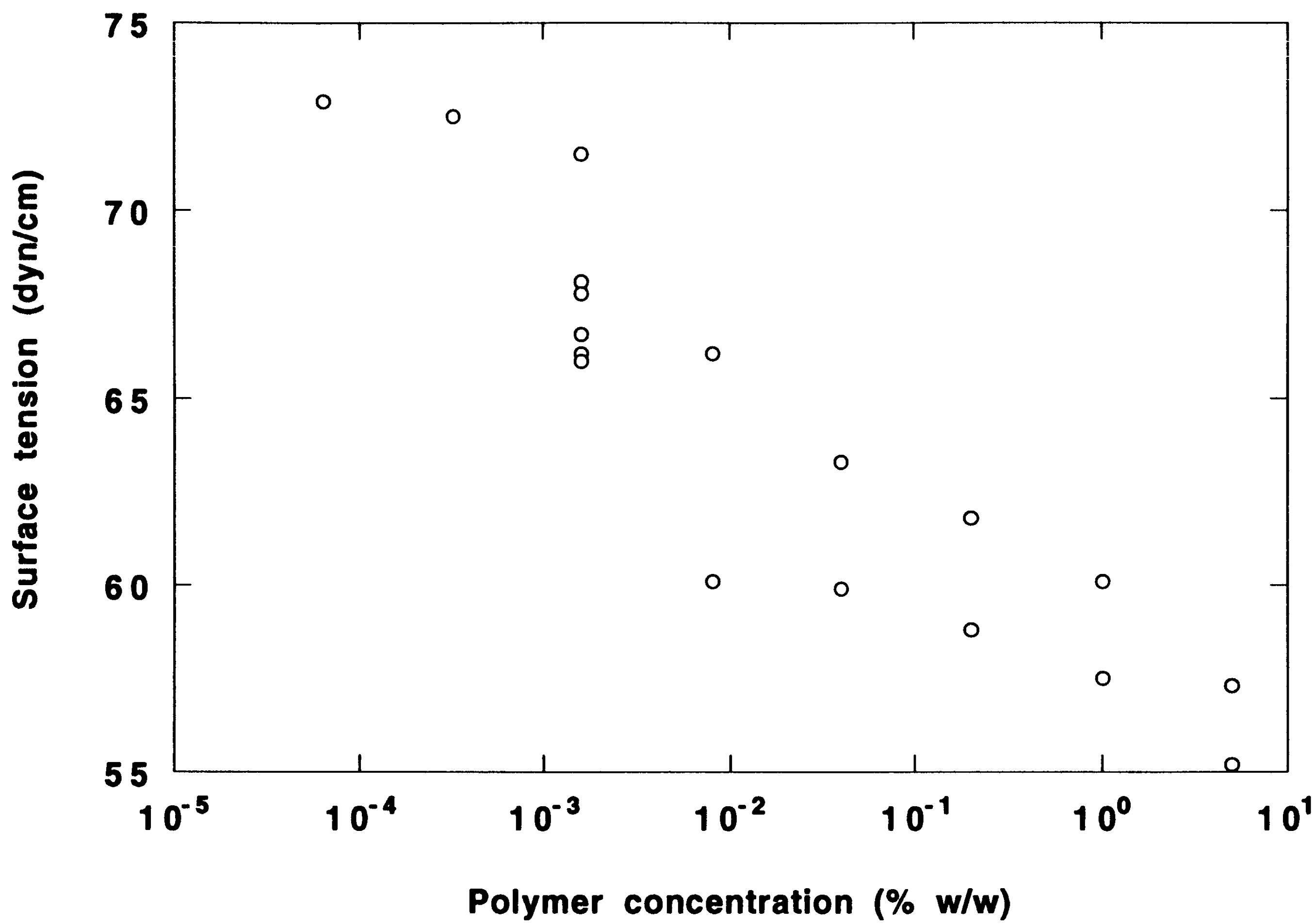

Figure 10.5 Surface tension of triblock Polymer 2 in 0.01M acetate and pH 4.5. At a given concentration, the higher value of the surface tension corresponds to the initial reading, while the lower to the equilibrium reading.